



**US Army Corps  
of Engineers®**  
Engineer Research and  
Development Center

*Monitoring Completed Navigation Projects Program*

## **Shoaling of Aguadilla Harbor, Puerto Rico**

Steven A. Hughes and Lyndell Z. Hales

June 2007



# **Shoaling of Aguadilla Harbor, Puerto Rico**

Steven A. Hughes and Lyndell Z. Hales

*Coastal and Hydraulics Laboratory  
U.S. Army Engineer Research and Development Center  
3909 Halls Ferry Road  
Vicksburg, MS 39180-6199*

Final report

Approved for public release; distribution is unlimited.

Prepared for U.S. Army Corps of Engineers  
Washington, DC 20314-1000

Under MCNP Work Unit 11M19

**Abstract:** During construction of the Aguadilla Harbor, Puerto Rico, breakwater (June 1993 through July 1995), shoaling of the harbor was observed, and excessive wave heights in the harbor caused by refraction/diffraction were much larger than expected. Following construction, additional shoaling occurred even with only limited wave activity, and significantly excessive harbor shoaling occurred. The source of the harbor-shoaling sand was not known with certainty. The quantity of sediment deposited in the harbor was surprising given the relatively minor amount of sand thought to be available within the littoral system.

The following five aspects of the Aguadilla Harbor project were proposed for monitoring under the Monitoring Completed Navigation Projects (MCNP) Program: (a) breakwater armor stability; (b) harbor wave action; (c) physical mechanisms causing harbor shoaling; (d) rates and quantity of harbor sedimentation; and (e) sources of sand causing the harbor shoaling.

A detailed breakwater stone elevation survey by standard topographic surveying techniques was performed. It was observed that a few armor stones had experienced a minimal degree of shakedown settlement during these early years following construction, but no major areas of excessive deterioration were found to exist. Tropical storms (hurricanes) approach from the eastern side of the island, and thus do not directly strike the harbor with full-force wave conditions since the harbor is on the western (leeward) protected side of Puerto Rico.

Surface currents were estimated using dyes and drogues. Apparently, the wave-generated alongshore current has a nodal point to the south of the breakwater. With this decrease in southerly flow, it is hard to conclude that any littoral sand is moving to the beach region south of the harbor project. In other words, sand in the littoral system is not bypassing the harbor.

A contour map of the bottom bathymetry of the region of interest was developed by the Scanning Hydrographic Operational Airborne Lidar Survey (SHOALS) system. A geophysical investigation with side-scan sonar was performed and overlain on the SHOALS contour map that indicated locations of rock/coral and layers of sand. The thickness of the sand layers was then determined by subbottom profiling and seismic reflection, and these data were also overlain on the SHOALS contour map. Hence, areas and thickness of sand layers offshore from Aguadilla Harbor that appears to be sources of sand entering the harbor have been mapped. The predominant waves that arrive from offshore have adequate wave power for such harbor shoaling.

A Sediment Trend Analysis (STA) was performed which concluded that sand transported from the offshore region appeared to be the source of sand shoaling Aguadilla Harbor. Southward directed longshore transport was quite small and was not likely to be a main contributor to harbor shoaling. The southward facing Aguadilla marina appeared to be in a position to act as a sediment trap, blocking the counterclockwise oceanic gyre at the shoreline, and precluding the possibility of a sediment return to the offshore during storm activity.

Harbor and beach profile surveys were conducted in 1997, 1998, 2001, and 2002 for the purpose of quantifying the volume of material that was being transported into the harbor, to provide an indication of the repetitiveness with which the harbor might need to be dredged to maintain navigability.

**DISCLAIMER:** The contents of this report are not to be used for advertising, publication, or promotional purposes. Citation of trade names does not constitute an official endorsement or approval of the use of such commercial products. All product names and trademarks cited are the property of their respective owners. The findings of this report are not to be construed as an official Department of the Army position unless so designated by other authorized documents.

**DESTROY THIS REPORT WHEN NO LONGER NEEDED. DO NOT RETURN IT TO THE ORIGINATOR.**

# Contents

<b>Figures and Tables.....</b>	<b>vi</b>
<b>Preface.....</b>	<b>x</b>
<b>1 Introduction.....</b>	<b>1</b>
Monitoring Completed Navigation Projects (MCNP) Program.....	1
Project location.....	2
Problem.....	4
Predicted design performance .....	4
<i>Breakwater armor stability .....</i>	<i>6</i>
<i>Harbor wave action .....</i>	<i>6</i>
<i>Harbor shoaling.....</i>	<i>8</i>
Observed design performance .....	8
<i>Breakwater armor stability .....</i>	<i>9</i>
<i>Harbor wave action .....</i>	<i>9</i>
<i>Harbor shoaling.....</i>	<i>10</i>
MCNP monitoring plan .....	10
<i>Breakwater armor stability .....</i>	<i>11</i>
<i>Harbor wave action .....</i>	<i>11</i>
<i>Harbor shoaling.....</i>	<i>12</i>
Modified MCNP monitoring plan .....	13
<b>2 Background.....</b>	<b>15</b>
Dominant natural forces .....	15
<i>Winds .....</i>	<i>15</i>
<i>Waves .....</i>	<i>16</i>
<i>Tides.....</i>	<i>20</i>
<i>Currents .....</i>	<i>20</i>
Breakwater design .....	21
<i>Design waves.....</i>	<i>21</i>
<i>Armor stone and side slopes.....</i>	<i>21</i>
<i>Crown width.....</i>	<i>23</i>
Project modifications .....	23
<i>Perceived coastal processes .....</i>	<i>23</i>
<i>Revetment and wave absorber modifications.....</i>	<i>27</i>
<b>3 Breakwater Stability .....</b>	<b>30</b>
<b>4 Estimating Surface Currents at Aguadilla Harbor Using Dyes and Drogues.....</b>	<b>41</b>
Dye and drogue studies .....	41
Estimating currents from dye release .....	42
<i>Dye deployment.....</i>	<i>43</i>

Dye tracking.....	44
Dye recommendations.....	45
Equipment recommendations.....	46
Dye study at Aguadilla Harbor .....	46
Dye release no. 1, north beach .....	48
Dye release no. 2, breakwater elbow.....	48
Dye release no. 3, breakwater midpoint.....	48
Dye release no. 4, breakwater south end.....	50
Estimating currents from drogue release .....	51
Drogue deployment.....	52
Drogue tracking.....	52
Equipment recommendations.....	53
Drogue study at Aguadilla Harbor .....	53
Seaward of the breakwater .....	54
Landward of the breakwater .....	55
Summary .....	57
<b>5 Directional Wave Measurements .....</b>	<b>59</b>
Wave gaging near Aguadilla Harbor .....	59
Wave gage record analyses .....	60
Irregular waves.....	60
Spectral analysis .....	63
Aguadilla wave data .....	64
<b>6 Scanning Hydrographic Operational Airborne Lidar Survey (SHOALS).....</b>	<b>83</b>
SHOALS .....	83
Aguadilla Harbor vicinity lidar survey .....	85
<b>7 Geophysical Investigations .....</b>	<b>88</b>
Bathymetry and geophysical surveys .....	88
Equipment .....	91
Navigation.....	91
Digital data acquisition system .....	91
Side-scan sonar.....	91
Subbottom profiler and seismic reflection systems.....	92
Data post-processing .....	93
Side-scan sonar.....	93
Subbottom profiles and seismic reflection data .....	94
Summary .....	98
<b>8 Sediment Trend Analysis (STA©) at Aguadilla Harbor.....</b>	<b>101</b>
Principles behind Sediment Trend Analysis (STA).....	101
Procedures for a Sediment Trend Analysis .....	103
Uncertainties of Sediment Trend Analysis .....	107
Benefits of Sediment Trend Analysis.....	111
Sediment Trend Analysis, Aguadilla Harbor .....	113
Sediment Trend Analysis sampling plan.....	113

<i>Sediment Trend Analysis results</i> .....	113
<i>Discussion</i> .....	118
<i>Summary and conclusions</i> .....	121
Interpretation of hydrodynamic forcing .....	122
Summary .....	123
<b>9 Aguadilla Harbor and Beach Profile Surveys, 1997 through 2002</b> .....	<b>125</b>
Wave Information Study (WIS) .....	126
Beach profiles.....	128
<b>10 Summary and Conclusions</b> .....	<b>146</b>
Summary .....	146
<i>Problem</i> .....	146
<i>MCNP monitoring plan</i> .....	147
Conclusions .....	147
<i>Breakwater stability</i> .....	147
<i>Estimating surface currents using dyes and drogues</i> .....	148
<i>Directional wave measurements</i> .....	151
<i>Scanning Hydrographic Operational Airborne Lidar Survey (SHOALS)</i> .....	152
<i>Geophysical investigations</i> .....	154
<i>Sediment Trend Analysis (STA) at Aguadilla Harbor</i> .....	155
<i>Aguadilla Harbor and beach profile surveys, 1997 through 1992</i> .....	158
<b>References</b> .....	<b>160</b>
<b>Appendix A: Aerial Photographs, Vicinity of Aguadilla Harbor, Puerto Rico</b> .....	<b>164</b>
<b>Appendix B: Aguadilla Harbor and Beach Profile Surveys; Stations 10 through 20;     Years 1997, 1998, 2001, and 2002</b> .....	<b>171</b>
<b>Report Documentation Page</b>	

# Figures and Tables

## Figures

Figure 1. Location map, Puerto Rico, in northeastern Caribbean Sea. ....	2
Figure 2. Aguadilla, Puerto Rico, MCNP study area. ....	3
Figure 3. Aguadilla Harbor, Puerto Rico, completed July 1995. ....	3
Figure 4. Shoaling of Aguadilla Harbor, Puerto Rico, began during harbor construction June 1993 through July 1995. ....	5
Figure 5. Excessive wave activity in Aguadilla Harbor, Puerto Rico, caused by wave refraction/diffraction around breakwater. ....	5
Figure 6. Excessive shoaling in Aguadilla Harbor, Puerto Rico. ....	6
Figure 7. Erosion of the harbor shoreline. ....	7
Figure 8. Aguadilla Harbor, Puerto Rico, rubble-mound breakwater cross section as built July 1995, station 8+00. ....	24
Figure 9. Aguadilla Harbor, Puerto Rico, breakwater and harbor layout as built July 1995. ....	25
Figure 10. Revetment and wave absorber as-built modifications to Aguadilla Harbor, Puerto Rico, interior region to alleviate harbor shoreline erosion. ....	29
Figure 11. Aguadilla Harbor breakwater survey cross-section elevation data September 2003, with elevations in feet referenced to mean lower low water (mllw). ....	32
Figure 12. Aguadilla Harbor breakwater survey elevation contours September 2003, with elevations in feet referenced to mean lower low water (mllw). ....	33
Figure 13. Aguadilla Harbor, Puerto Rico, breakwater. ....	34
Figure 14. Seaward section of Aguadilla Harbor breakwater. ....	35
Figure 15. Landward section of Aguadilla Harbor breakwater. ....	35
Figure 16. Seaward side of Aguadilla Harbor breakwater, station 3+00 near the landward end of the structure, showing stable armor layer. ....	36
Figure 17. Seaward side of Aguadilla Harbor breakwater, station 5+00, near the middle section of the structure, showing stable armor layer. ....	37
Figure 18. Seaward side of Aguadilla Harbor breakwater, station 8+00, near the seaward end of the structure, showing stable armor layer. ....	38
Figure 19. Harbor side of Aguadilla Harbor breakwater, station 1+00, looking seaward from the landward end of the structure, showing stable armor layer. ....	39
Figure 20. Harbor side of Aguadilla Harbor breakwater, station 8+00, looking landward from the seaward end of the structure, showing stable armor layer. ....	40
Figure 21. Dye release at Shinnecock Inlet. ....	43
Figure 22. Approximate initial dye injection locations, Aguadilla Harbor. ....	47
Figure 23. Approximate path of dye release no. 1, Aguadilla Harbor. ....	49
Figure 24. Approximate path of dye release no. 2, Aguadilla Harbor. ....	49
Figure 25. Approximate path of dye release no. 3, Aguadilla Harbor. ....	50
Figure 26. Approximate path of dye release no. 4, Aguadilla Harbor. ....	51

Figure 27. Measurement locations and average current speed estimated with drogues along the breakwater, Aguadilla Harbor .....	54
Figure 28. Drogue paths within Aguadilla Harbor. ....	56
Figure 29. Corps of Engineers, Coastal and Hydraulics Laboratory, trawler-resistant directional wave gage array and pressure sensor pods. ....	60
Figure 30. Directional wave gage pressure sensor installed on one of the array legs. ....	61
Figure 31. Directional pressure wave gage being deployed by winch from survey vessel. ....	61
Figure 32. Typical representative wave record of actual sea surface measurements. ....	62
Figure 33. Ocean wave spectra showing broad, central peak of local wind seas. ....	64
Figure 34. Aguadilla deepwater wave data offshore of breakwater, November 2001. ....	66
Figure 35. Aguadilla deepwater wave data offshore of breakwater, December 2001. ....	67
Figure 36. Aguadilla deepwater wave data offshore of breakwater, January 2002. ....	68
Figure 37. Aguadilla deepwater wave data offshore of breakwater, February 2002. ....	69
Figure 38. Aguadilla deepwater wave data offshore of breakwater, March 2002. ....	70
Figure 39. Aguadilla deepwater wave data offshore of breakwater, April 2003. ....	71
Figure 40. Aguadilla deepwater wave data offshore of breakwater, May 2003. ....	72
Figure 41. Aguadilla deepwater wave data offshore of breakwater, June 2003. ....	73
Figure 42. Aguadilla deepwater wave data offshore of breakwater, July 2003. ....	74
Figure 43. Aguadilla deepwater wave data offshore of breakwater, August 2003. ....	75
Figure 44. Aguadilla deepwater wave data offshore of breakwater, September 2003. ....	76
Figure 45. Aguadilla deepwater wave data offshore of breakwater, October 2003. ....	77
Figure 46. Aguadilla deepwater wave data offshore of breakwater, November 2003. ....	78
Figure 47. Aguadilla deepwater wave data offshore of breakwater, December 2003. ....	79
Figure 48. Aguadilla deepwater wave data offshore of breakwater, January 2004. ....	80
Figure 49. Aguadilla deepwater wave data offshore of breakwater, February 2004. ....	81
Figure 50. Aguadilla deepwater wave data offshore of breakwater, March 2004. ....	82
Figure 51. deHavilland DHC-6 Twin Otter fixed wing aircraft for SHOALS platform. ....	83
Figure 52. SHOALS bathymetric lidar propagating through the water column .....	84
Figure 53. Scanning Hydrographic Operational Airborne Lidar Survey (SHOALS) bathymetric survey contours of vicinity of Aguadilla Harbor, Puerto Rico. ....	86
Figure 54. Scanning Hydrographic Operational Airborne Lidar Survey (SHOALS) bathymetric survey contours near Aguadilla Harbor breakwater, Puerto Rico. ....	87
Figure 55. Bathymetric contours acquired by the Scanning Hydrographic Operational Airborne Lidar Survey (SHOALS) system near the vicinity of Aguadilla Harbor, Puerto Rico. ....	89
Figure 56. Close-up of the SHOALS bathymetric contours near Aguadilla Harbor, Puerto Rico .....	90
Figure 57. Surficial features delineated by typical representative side-scan sonar data from seafloor off Aguadilla Harbor, Puerto Rico. ....	95
Figure 58. Vector line drawings in red of rock and/or coral in the vicinity of Aguadilla Harbor, Puerto Rico, from side-scan sonar survey. ....	95
Figure 59. Close-up view near of vector line drawings in red of rock and/or coral near Aguadilla Harbor, Puerto Rico, from side-scan sonar survey. ....	96

Figure 60. Depth of sand contours (feet) among rock and coral, as interpreted from sub-bottom profiles and seismic reflection data near the vicinity of Aguadilla Harbor, Puerto Rico .....	97
Figure 61. Close-up of depth of sand contours (feet) among rock and coral off Aguadilla Harbor, as interpreted from subbottom profiles and seismic reflection data .....	97
Figure 62. Overlay plot consisting of SHOALS bathymetric contour data, overlain by color-coded side-scan sonar survey data indicating demarcation between rock/coral shown in red with blank areas being interpreted as sand, and also overlain by delineated sand thickness contour data (feet) derived from the subbottom profiles and seismic reflection data in the vicinity of Aguadilla Harbor, Puerto Rico. ....	99
Figure 63. Close-up of the vicinity of the Aguadilla Harbor, showing sand layer thickness (feet) as determined by subbottom profiling and seismic reflection data. ....	100
Figure 64. Interpretation of X-distribution along sediment pathways. ....	106
Figure 65. Sediment pathways for San Juan Harbor, Puerto Rico, by STA .....	108
Figure 66. Sample locations and place names, Aguadilla Harbor. ....	114
Figure 67. Net sediment transport pathways, Aguadilla Harbor. ....	115
Figure 68. Sediment transport environments (TEs), vicinity of Aguadilla Harbor. ....	116
Figure 69. Sediment trends at Aguadilla Harbor breakwater. ....	117
Figure 70. Aguadilla Harbor, Puerto Rico. ....	125
Figure 71. Location of CHL Wave Information Study (WIS) hindcast wave stations WIS 6 and WIS 7 in deep water off the western and northwestern sides of Puerto Rico. ....	127
Figure 72. Wave Information Study (WIS) hindcast wave data, station WIS 6, located in deep water off western coast of Puerto Rico. ....	129
Figure 73. Wave Information Study (WIS) hindcast wave data, station WIS 6, located in deep water off western coast of Puerto Rico. ....	130
Figure 74. Wave Information Study (WIS) hindcast wave data, station WIS 6, located in deep water off western coast of Puerto Rico. ....	131
Figure 75. Wave Information Study (WIS) hindcast wave data, station WIS 7, located in deep water off western coast of Puerto Rico. ....	132
Figure 76. Wave Information Study (WIS) hindcast wave data, station WIS 7, located in deep water off western coast of Puerto Rico. ....	133
Figure 77. Wave Information Study (WIS) hindcast wave data, station WIS 7, located in deep water off western coast of Puerto Rico. ....	134
Figure 78. Location of survey stations, Aguadilla Harbor and vicinity .....	135
Figure 79. Volume change at each station, 1997 versus 1998, looking eastward. ....	137
Figure 80. Volume change at each station, 1997 versus 2001, looking seaward. ....	138
Figure 81. Volume change at each station, 1997 versus 2002, looking seaward. ....	139
Figure 82. Volume change at each station, 1998 versus 2001, looking seaward. ....	140
Figure 83. Volume change at each station, 1998 versus 2002, looking seaward. ....	141
Figure 84. Volume change at each station, 2001 versus 2002, looking seaward. ....	142
Figure 85. Volume change at each station, looking seaward. ....	143
Figure 86. Volume change at each station inside the harbor behind the breakwater, looking seaward. ....	144
Figure 87. Volume change at each station outside the harbor seaward of the breakwater, looking seaward. ....	145

Figure A1. Mosaic of vicinity of Aguadilla Harbor, Puerto Rico. ....	164
Figure A2. Coastline south of Aguadilla Harbor, Puerto Rico, showing plume of fine sediments exiting the Rio Culebrinas River after heavy rainfall. ....	165
Figure A3. Coastline of Puerto Rico further north than Figure A2, between Rio Culebrinas River and Aguadilla Harbor, showing plume of fine sediments which had exited from the river after heavy rainfall. ....	166
Figure A4. Coastline of Puerto Rico further north than Figure A3 between the Rio Culebrinas River and Aguadilla Harbor, showing how plume of fine sediments from the river are not being detected this far north towards the Harbor.....	167
Figure A5. Coastline of Puerto Rico further north than Figure A4, showing minimal amount of fine sediment discharging to the coast from small stream.....	168
Figure A6. Aguadilla Harbor breakwater and vicinity, coastline of Puerto Rico further north than Figure A5. ....	169
Figure A7. Coastline of Puerto Rico further north than Figure A6. ....	170
Figure B1. Volume change station 10, 1997 through 2002, distance offshore from shoreline inside the harbor.....	172
Figure B2. Volume change station 11, 1997 through 2002, distance offshore from shoreline inside the harbor.....	173
Figure B3. Volume change station 12, 1997 through 2002, distance offshore from shoreline inside the harbor.....	174
Figure B4. Volume change station 13, 1997 through 2002, distance offshore from shoreline inside the harbor.....	175
Figure B5. Volume change station 14, 1997 through 2002, distance offshore from shoreline inside the harbor.....	176
Figure B6. Volume change station 15, 1997 through 2002, distance offshore from shoreline inside the harbor.....	177
Figure B7. Volume change station 16, 1997 through 2002, distance offshore from shoreline inside the harbor.....	178
Figure B8. Volume change station 17, 1997 through 2002, distance offshore from shoreline inside the harbor.....	179
Figure B9. Volume change station 18, 1997 through 2002, distance offshore from shoreline inside the harbor.....	180
Figure B10. Volume change station 19, 1997 through 2002, distance offshore from shoreline inside the harbor.....	181
Figure B11. Volume change station 20, 1997 through 2002, distance offshore from shoreline inside the harbor.....	182

## Tables

Table 1. Drogue measurements seaward of the Breakwater, Aguadilla Harbor, November 2001. ....	55
Table 2. Sediment transport trend based on grain-size distribution.....	103

## Preface

The studies reported herein were conducted as part of the Monitoring Completed Navigation Projects (MCNP) Program (formerly Monitoring Completed Coastal Projects (MCCP) Program. Work was conducted under MCNP Work Unit No. 11M19, “Aguadilla Harbor, Puerto Rico”. Overall program management of the MCNP is provided by Headquarters, U.S. Army Corps of Engineers (HQUSACE). The Coastal and Hydraulics Laboratory (CHL), U.S. Army Engineer Research and Development Center (ERDC), is responsible for technical and data management, and support for HQUSACE review and technology transfer. Program monitors for the MCNP Program at the time of this study were Barry W. Holliday, HQUSACE, and Charles B. Chesnutt, U.S. Army Institute for Water Resources (CEIWR). MCNP program managers during the conduct of this study were Robert R. Bottin, Jr., Harbors, Entrances, and Structures Branch (HN-H), Navigation Division (HN), CHL, and Dr. Lyndell Z. Hales, Technical Programs Office (HV-T), CHL.

This research was conducted during the time period October 2000—September 2004 under the general supervision of Thomas W. Richardson, Director, CHL, and under direct supervision of Dennis G. Markle, former Chief, HN-H, and Jose E. Sanchez, present Chief, HN-H. MCNP District Team Member Thomas D. Smith, U.S. Army Engineer District (USAED), Honolulu, and formerly at USAED, Jacksonville, contributed significantly to the development and execution of this study. MCNP Principal Investigator was Dr. Steven A. Hughes, HN-H. This report was compiled by Dr. Hales.

Appreciation is extended to others who assisted in the conduct of this investigation, including Cynthia B. Perez, Jorge M. Tous, and Alberto Gonzalez, the Jacksonville District. Ed H. Hodgins, the Jacksonville District, provided the beach profiles that were analyzed by Jennifer M. Ramos-Ortiz and Dr. Edward F. Thompson, HN-H. Jeff Lillycrop, U.S. Army Engineer District, Mobile, manages the Joint Airborne Lidar Bathymetry Technical Center of Expertise that provided the SHOALS data. The CHL dive team consisted of Larry Caviness and Ralph Ankeny, Field Data Collection and Analysis Branch (HF-F), Flood and Storm Protection Division (HF), CHL; Timothy L. Welp and Cheryl E. Pollock, Coastal

Engineering Branch (HN-C), HN; and Darryl D. Bishop, Office of the Deputy Director and Chief of Staff (HV-ZB), CHL. Dr. Kevin Redman, Evans-Hamilton Inc., Seattle, WA, performed the geophysical investigations, and Dr. Patrick McLaren, GeoSea Consulting (Canada) Ltd., Brentwood Bay, British Columbia, Canada, conducted the Sediment Trend Analysis (STA<sup>©</sup>) for this Aguadilla Harbor, Puerto Rico, shoaling study.

At the time of publication of this report, COL Richard B. Jenkins, EN, was Commander and Executive Director of ERDC. Dr. James R. Houston was Director.

# 1 Introduction

## Monitoring Completed Navigation Projects (MCNP) Program

The goal of the Monitoring Completed Navigation Projects (MCNP) Program (formerly the Monitoring Completed Coastal Projects (MCCP) Program) is the advancement of coastal and hydraulic engineering technology. The program is designed to determine how well projects are accomplishing their purposes and how well they are resisting attacks by their physical environment. These determinations, combined with concepts and understanding already available, will lead to the creation of more accurate and economical engineering solutions to coastal and hydraulic problems, strengthening and improving design criteria and methodology, improving construction practices and cost-effectiveness, and improving operation and maintenance techniques. Additionally, the monitoring program will identify where current technology is inadequate or where additional research is required.

To develop direction for the program, the U.S. Army Corps of Engineers (USACE) established an ad hoc committee of engineers and scientists. The committee formulated the objectives of the program, developed its operation philosophy, recommended funding levels, and established criteria and procedures for project selection. A significant result of their efforts was a prioritized listing of problem areas to be addressed. This is essentially a listing of the areas of interest of the program.

Corps offices are invited to nominate projects for inclusion in the monitoring program as funds become available. The MCNP Program is governed by Engineer Regulation 1110-2-8151 (Headquarters, U.S. Army Corps of Engineers (HQUSACE) 1997). A selection committee reviews and prioritizes the nominated projects based on criteria established in the regulation. The prioritized list is reviewed by the program monitors at HQUSACE, USACE. Final selection is based on this prioritized list, national priorities, and the availability of funding.

The overall monitoring program is under the management of the Coastal and Hydraulics Laboratory (CHL), U.S. Army Engineer Research and Development Center (ERDC), with guidance from HQUSACE. An individual monitoring project is a cooperative effort between the submitting

District and/or Division office and CHL. Development of monitoring plans and conduct of data collection and analyses are dependent upon the combined resources of CHL and the District and/or Division.

## Project location

The Commonwealth of Puerto Rico is situated in the northeastern Caribbean Sea (Figure 1). It is the smallest and easternmost island of the Greater Antilles chain, measuring about 180 km (112 miles) from west to east, and about 65 km (40 miles) from north to south.



Figure 1. Location map, Puerto Rico, in northeastern Caribbean Sea.

The City of Aguadilla is situated within a natural embayment on the northwest coast of Puerto Rico (Figure 2). Along much of the coast, bluffs extend several hundred meters back from the shoreline and the beaches, if existing, are generally narrow and consist of a thin layer of sand over a rocky shoreline. Aguadilla is sheltered from the largest storm swells that approach Puerto Rico from the north through northeast. However, the Aguadilla coastline is exposed to direct wave attack from the northwest and indirect wave attack resulting from refraction/diffraction of waves around Punta Boringquen. Aguadilla Harbor breakwater (Figure 3) construction was completed in July 1995.



Figure 2. Aguadilla, Puerto Rico, MCNP study area.



Figure 3. Aguadilla Harbor, Puerto Rico, completed July 1995.

## Problem

Prior to construction of Aguadilla Harbor breakwater and channel, there were no protected harbors available for commercial fishermen along the 80-km (50-mile) stretch of coast from Arecibo to Mayaguez. Waves in the bay at Aguadilla were often estimated to exceed 1.2 m (4 ft), especially during winter months. Consequently, commercial fishing was restricted to small, flat-bottomed boats that could be easily hauled up onto the limited beach front for storage and protection from waves. Using small boats 5 to 6 m (16 to 19 ft) in length reduced fishing efficiency, made it impossible at times to negotiate the surf zone, and made fishing a hazardous occupation.

In 1982, the Corps of Engineers was requested by the non-Federal municipality to study the feasibility of providing a protected commercial fishing harbor at Aguadilla. The Corps recommended construction of a 345-m- (1,130-ft-) long breakwater to shelter a 3.8-hectar (9.3-acre) harbor area. The three-layer, rubble-mound breakwater and its associated recreation walkway were completed July 1995.

During construction, shoaling of a segment of the harbor was observed (Figure 4). Excessive wave heights in the harbor (Figure 5) caused by refraction/diffraction necessitated subsequent construction of wave absorber. Following construction, additional shoaling occurred even with only limited wave activity and, over time, significantly harbor shoaling occurred (Figure 6). Erosion of the harbor shoreline required construction of 170 m (560 ft) of rubble-mound revetment to stabilize the shoreline and reduce wave reflection within the harbor (Figure 7).

## Predicted design performance

The Aguadilla Harbor and breakwater were designed according to conventional practice using design guidance provided by documents such as HQUSACE (1977), along with design experience from similar successful projects. The engineering investigation and project design were presented in U.S. Army Engineer District (USAED), Jacksonville (1987).



Figure 4. Shoaling of Aguadilla Harbor, Puerto Rico, began during harbor construction June 1993 through July 1995 (date of photo August 1994).



Figure 5. Excessive wave activity in Aguadilla Harbor, Puerto Rico, caused by wave refraction/diffraction around breakwater (date of photo December 1995).



Figure 6. Excessive shoaling in Aguadilla Harbor, Puerto Rico (date of photo May 2002).

### **Breakwater armor stability**

The required weight of the main armor layer stones was estimated using a modified version of the Iribarren formula as prescribed by the Danish Hydraulics Institute. Design wave heights, wave periods, and water levels associated with severe storms and hurricanes were included in the analyses. A stone weight of 14,500 kg (16 tons) was specified, and this proved to be stable when checked using the Hudson equation given in the HQUSACE (1977). Smaller weight armor (5,900 kg (6.5 tons)) was specified for the section of the breakwater closest to land in shallow water. The breakwater was actually constructed using smaller armor stone ranging between 2,700 and 10,900 kg (3 and 12 tons). Assuming repairs would be initiated whenever the primary armor layer experienced 10 percent damage, breakwater maintenance was projected to be necessary every 14 to 34 years for the Aguadilla wave climatology.

### **Harbor wave action**

The maximum allowable wave height criterion within the harbor was specified as 0.4 to 0.6 m (1.5 to 2 ft) with annual duration between 40 to 100 hr. Wave transmission into the harbor through the breakwater was



Figure 7. Erosion of the harbor shoreline (date of photo December 1995).

calculated using a computer program based on the Madsen and White (1976) formulation for linearized long wave motions. Results from the calculations were used to design the breakwater cross section to meet the harbor wave height criterion for different water depths and armor sizes.

Guidance from the HQUSACE (1977) was used to estimate maximum harbor wave heights arising from diffraction of waves around the tip of the breakwater. For the highest incident wave conditions of 2 to 3 m (7 to 10 ft) with periods of 16 sec, diffracted wave heights in the harbor could reach 0.3 to 0.6 m (1 to 2 ft). Because of potential interaction of diffracted waves with transmitted waves, the design report suggested that physical modeling may be advisable.

### **Harbor shoaling**

The coastline features adjacent to Aguadilla consist of rocky headlands separated by small sandy beaches. Littoral sediment is largely derived from eroding limestone cliffs, coral debris, and shell fragments. Littoral sediment moves in a southerly direction in the Aguadilla embayment, but little data existed for making estimates of the gross or net annual sediment transport rate. Historical photographs and charts of impoundment updrift of a naval pier constructed in the 1940s were used to estimate an annual southerly transport rate of between 3,000 and 4,000 cu m/year (4,000 and 5,000 cu yd/year) as an upper limit at Aguadilla.

It was anticipated that after construction of the breakwater, longshore moving sediment would be impounded north of the breakwater for about 2 years until a stable fillet formed. Once the updrift beach was in an equilibrium configuration, longshore moving sediment would then continue moving south along the outer edge of the breakwater and eventually be deposited in the designed impoundment basin just south of the breakwater head. Periodic maintenance would be necessary as the impoundment area filled in, and it was projected that every 5 years it would be necessary to excavate 15,000 cu m (20,000 cu yd) of beach quality sand and deposit it on the downdrift coastline.

### **Observed design performance**

Construction of the Aguadilla Harbor Federal navigation project altered coastal processes within, and adjacent to, the project area. A site investigation was conducted by a team of engineers from the USAED,

Jacksonville, in March 1998. Problems identified by the team were: (a) wave action inside the harbor; (b) considerable recession of the inner harbor's eastern shoreline; and (c) shoaling along the lee of the breakwater. It was concluded that the project was not fully performing its intended design functions of providing safe navigation and shelter for the local fishing community.

The Jacksonville District developed a Section 111 study of the harbor's problems, and the findings are documented (USAED, Jacksonville, 1998).

### **Breakwater armor stability**

Little mention is made about the condition of the breakwater in the Section 111 study, and subsequent site visits have indicated the breakwater remains virtually undamaged since construction. Some settlement may have occurred, but this was anticipated in design. It may be that the structure has not been subjected to a design wave event since being built; but nevertheless, there is no reason to suspect that breakwater armor stability is in question.

### **Harbor wave action**

Wave action within the harbor was larger than expected. Waves approaching from the northern quadrants are refracted toward the breakwater by the nearshore bottom contours. At the southern tip of the breakwater the waves are diffracted into the harbor with perhaps some additional wave refraction due to local bottom contours. Waves entering the harbor were sufficiently energetic to cause erosion of the shoreline to the north of the parking garage. The parking garage was fronted by a vertical seawall that completely reflected the incident waves back across the harbor toward the breakwater. Interaction between the diffracted and reflected waves formed an interference pattern of confused seas. Waves transmitted through the breakwater may have contributed to the observed wave action.

The Section 111 study recommended that the eastern shoreline be stabilized with a 170-m-(560-ft-) long rubble-mound revetment, and that a 90-m- (300-ft-) long rubble wave absorber be placed in front of the vertical sheet-pile seawall of the parking garage to reduce wave reflection, and thus reduce wave action within the harbor. These remedial steps were implemented with construction completed in the early part of 2001.

### **Harbor shoaling**

During and following construction of the breakwater, shoaling of a shallow segment of the northern harbor was observed. Initial shoaling, assumed to be littoral in nature and caused by wave events, was removed while the contractor was still onsite. Subsequent to completion, additional shoaling has occurred.

The source of the harbor-shoaling sand is not known with certainty. Shoaling may be due to littoral movement from the north, movement of fill sands placed landward behind the revetment, sedimentation due to the erosion of the inner-harbor eastern shoreline, or displacement of material originally placed on the breakwater to facilitate the movement of construction vehicles.

Sedimentation paths identified in the 1998 Section 111 report indicated southward moving material entering the harbor through the breakwater and around the breakwater tip. It was thought that waves reflected from the vertical seawall assisted moving sediment in a northerly direction along the lee of the breakwater. Sediment also moved in a northerly direction along the eastern shoreline of the harbor.

The quantity of sediment deposited in the harbor was surprising given the relatively minor amount of sand thought to be available within the littoral system. The Section 111 report noted that upland erosion may represent a significant source of new sediment that is periodically introduced into the littoral system. Immediately north of Aguadilla Harbor are two streams and numerous storm sewer outlets that drain steep contoured catchment basins. High velocity flows can transport considerable quantities of sediments during flash floods, particularly when ongoing construction work has stripped large areas of natural vegetation.

### **MCNP monitoring plan**

The following five aspects of the Aguadilla Harbor project were originally proposed for monitoring under the MCNP Program:

1. Breakwater armor stability
2. Harbor wave action
3. Harbor shoaling
  - a. Physical mechanisms
  - b. Harbor sedimentation
  - c. Sources of sand

### **Breakwater armor stability**

Although the breakwater appears visually to have suffered no damage, measurements of breakwater cross sections are needed to confirm no damage has occurred, and that post-construction settlement has not been excessive. Selected breakwater survey cross-section profiles would be measured using standard surveying techniques for the above-water portion of the breakwater. These measurements would be conducted yearly over the duration of the project. The purpose of the above-water measurements would be to assess any settlement and to identify any changes from the as-built drawings. Visual inspection of the above-water armor stone would also be conducted to document the stability of the structure and identify any broken or dislodged stones.

### **Harbor wave action**

Prior to construction of the new revetment and rubble wave absorber, wave action within the harbor exceeded design estimates. The new wave absorber should have reduced wave action to acceptable levels. Monitoring was needed to determine whether the remedial action has reduced waves below the established criterion of 0.5 to 0.6 m (1.5 to 2 ft) maximum under storm conditions. Monitoring would also examine wave transmission through the breakwater.

Wave measurements within the harbor would be obtained using self-recording bottom-mounted pressure sensors. One instrument would be deployed directly offshore of the breakwater to record the incident wave condition driving the harbor wave action, and up to three instruments would be placed inside the harbor at locations selected based on visual observations during stormy conditions. Deployment would be over 1 or 2 months during the stormy season to assure capturing at least one wave event approaching design conditions.

Field measurements were needed to determine if sand moving through the porous breakwater contributes significantly to harbor shoaling. The field component would be a short-term deployment of bottom-mounted pressure gage pairs, with one gage at the seaward toe and the other at the leeward toe of the breakwater. Analysis of the recorded sea surface elevation time series would be used to examine the time varying head difference between the ocean and harbor to establish the forcing mechanism for sand transport through the structure. Other components of this task would be velocity measurements on the lee side of the breakwater using an Acoustic Doppler Current Meter, and timing how long it takes dye or dyed tracer to travel through the breakwater.

In addition to addressing questions about effectiveness of the stone revetment and wave absorber, the wave data would be essential for any future physical or numerical modeling of the Aguadilla Harbor hydrodynamics.

### **Harbor shoaling**

#### *Physical mechanisms*

The mechanisms that transport littoral material into the harbor are the forcing functions resulting from both alongshore and wave-induced currents. An understanding of the alongshore current was essentially for estimating bed-load transport into the harbor. Wave-induced velocity components are effective in transporting both bed-load and suspended materials, and should be ascertained to fully quantify both aspects of material transport into the harbor.

#### *Harbor sedimentation*

Monitoring was needed to estimate shoaling rates that might be expected within the harbor. This monitoring would examine assumed major pathways into the harbor. One pathway was assumed to be sediment moving along the front of the breakwater and then around the breakwater tip and into the harbor. A second pathway was assumed to be sand that was transported through the breakwater by wave action.

Periodic surveying of beach profiles of the shoreline north and south of the Aguadilla Harbor would be compared to existing post-project surveys to determine any changes to the shoreline (erosion or accretion), as well as any volumetric changes within the active zone. These measurements

would help determine the local sediment budget, and would provide an indication of how to best deal with long-term maintenance of the harbor. Several beach profiles taken perpendicular to the breakwater center line and extending through the breakwater to the lee side would be used to help assess sand transmission through the structure.

#### *Sources of sand*

An assessment would be made of the sources of sand available in the littoral system. If a significant portion of the littoral sand originates from upland runoff immediately north of the harbor, then management of the harbor would require a plan to deal with periodic influxes of sand introduced into the littoral system from upland rain runoff.

Analysis of sand samples taken from the beach, in the harbor, and in the upland basin would help determine whether a significant portion of the sediment shoaling in the harbor was recently introduced into the littoral system from upland sources. Sharp-edged sand grains would indicate sediment new to the littoral system, whereas rounded grains typify sand that has been in the littoral system for some time.

A second aspect of this task would be a geographical analysis to determine the nearest outfalls where upland sediment could be introduced into the littoral system. Aerial photography of sediment plumes would be acquired immediately after periods of heavy rainfall to assist in this task. Low-level photography would also help in evaluating the overall sedimentation patterns within the littoral cell that includes Aguadilla Harbor.

### **Modified MCNP monitoring plan**

The original monitoring plan included components to examine harbor wave action. However, throughout the time period of monitoring (2001 through 2004), the harbor substantially shoaled, thus making that aspect of the investigation unfeasible.

MCNP Monitoring tasks that were successfully executed include:

- Confirmation of the structural stability of the breakwater, by acquiring and analyzing survey cross-section profiles.
- Investigation of the physical mechanisms that result in harbor shoaling, by acquiring and analyzing surface currents and wave data.

- Determination of local sediment pathways that are active during storms by conducting and evaluating a Sediment Trend Analysis (STA), and performing a geophysical investigation using side-scan sonar, a subbottom profiler, and a seismic reflection system.
- Assessment as to whether southward moving littoral sediment continues to be impounded by the breakwater, by performing Scanning Hydrographic Operational Airborne Lidar Survey (SHOAL) data acquisition, by obtaining current aerial photographs, and by analyzing repetitive beach profile surveys.

The modified monitoring plan included several activities that contributed to one or more of the monitoring tasks.

1. Aerial shoreline photography was obtained simultaneously with detailed bathymetry acquired by the Scanning Hydrographic Operational Airborne Lidar Survey (SHOALS) airborne bathymetric technique.
2. Directional wave data were acquired offshore of the breakwater by a bottom-mounted, internally recording wave gauge.
3. A geophysical seabed sediment survey of the region offshore of the harbor, by side-scan sonar, a subbottom profiler, and a seismic reflection system, provided maps showing composition of the bottom (rock or sand), and depth of sand deposits.
4. Over 250 sand samples collected over a grid offshore of the breakwater were used to develop likely sediment pathways based on the Sediment Trend Analysis (STA) technique. The abundance of beach-sized sand observed offshore, combined with projected sediment pathways indicates that much of the sand shoaling the harbor comes from offshore.
5. Previously acquired beach profiles were analyzed, along with profiles acquired during this MCNP monitoring, to assess changes that have occurred north of the breakwater.
6. Breakwater structural integrity was assessed using traditional survey techniques augmented by diver visual inspection of the seaward breakwater toe.

## 2 Background

On February 8, 1982, the municipality of Aguadilla, Puerto Rico, requested the Corps of Engineers to study the feasibility of providing a commercial fishing project at Aguadilla. The authority to conduct that study was provided by Congress under Section 107 of the 1960 River and Harbor Act, as amended. The receipt of this formal request from the municipality of Aguadilla gave the Chief of Engineers authority to direct the District Engineer to study navigation and related water resource problems in the Aguadilla area and make recommendations regarding the feasibility of Federal navigation improvements consisting of a breakwater and harbor construction. The dominant natural forces that would significantly impact development of a harbor project at Aguadilla include (a) winds, (b) waves, (c) tides, and (d) currents.

(Author's note: From February 8, 1982 until start of the construction contract in June 1993 to build the breakwater and harbor at Aguadilla, extensive environmental, engineering, and socio-economic studies were conducted. Many of those studies are presented in *Aguadilla Harbor, Aguadilla, Puerto Rico: Detailed project report and environmental assessment* (U.S. Army Engineer District, Jacksonville, 1987). Those studies were all performed based on the best available data, information, and knowledge pertaining to that region at that point in time. Since that time, many of those environmental and engineering data (especially those data regarding the natural forces of winds and waves) have been superseded by more recent studies utilizing more advanced analysis techniques. Hence, while the data that were applied to the design and construction of Aguadilla Harbor breakwater may not be entirely appropriate at the present time, those analyses were indeed state of the art at the time those studies and evaluations were conducted.)

### Dominant natural forces<sup>1</sup>

#### Winds

The outstanding feature of the marine weather in this location is the steadiness of the easterly trade winds. Northeast through southeast winds

---

<sup>1</sup> This section is extracted from USAED, Jacksonville (1987).

blow 80 percent of the time year round. Gale force winds are unlikely but can occur with a strong front, thunderstorms, or tropical cyclones. Summer gales usually blow from the east while winter gales are more likely to come from the northeast quadrant. Winds with velocities between 27 and 53 km/hr (17 and 33 mph) blow 30 percent of the time. In the summer, the trades tend to strengthen during the day, and the average wind speeds are highest during this season.

Puerto Rican waters are dominated throughout the entire year by the northeast trade winds. At San Juan, the highest percentage of winds observed are easterly with the frequency of wind occurrences decreasing progressively as they deviate from the east. With the seasonal shift in the location of the Bermuda High, northward in summer and southward in winter, the general direction of winds over Puerto Rico shift from north-northeast in winter to east in summer. Winds are more consistently easterly in summer months attaining a maximum frequency in July when the east winds blow 63 percent of the time. The greatest deviation from the pattern of easterly winds occurs during October, when the east wind blows only 34 percent of the time. The minimum average wind velocities for the year of 13 km/hr (8 mph) are also recorded for October.

Winds generally decrease in strength during the night and gradually build up throughout the day to a peak in the early evening. The passage of fronts interrupts the trade wind flow. As a cold front approaches the study area, winds shift to a more southerly direction. As the front passes, there is a gradual shift through the southwest and northwest quadrants back to northeast. East wave approaches are usually characterized by an east-northeast wind ahead of the waves, with a change to east-southeast following wind passage.

## **Waves**

### *Tropical storms*

Puerto Rico lies in the path of tropical storms and hurricanes. The most active period is from August to mid-October. Tropical storms cross the island from east to west. Waves that reach Aguadilla are, therefore, generated as the storms move away from the island in a westerly direction. Estimated waves from a typical hurricane passing within 80 km (50 miles) of Aguadilla would have periods of about 9 sec and wave heights of around 4 m (13 ft). Because of shorter periods, the wave energy associated with

these events is no greater than for the longer period smaller waves generated from seasonal extratropical storms. In addition to the strong winds and high seas, these storms can bring torrential rains and cause significant flooding in low-lying and poorly drained areas.

#### *Extratropical storms*

Storms associated with winter fronts moving across the Atlantic Ocean generate large long-period waves that move towards Puerto Rico from the north to northwest quadrants. Aguadilla is within the shadow of Punta Borinquen at the northwestern end of the island, and is therefore sheltered from most of the severe wave action that typically hits the northern coast. However, waves in excess of 1.2 to 1.8 m (4 to 6 ft) occur periodically throughout the winter months. Data interpreted from a hindcast wave climate and site-specific measurements indicate that waves as high as 2.5 to 3.7 m (8 to 12 ft) can occur 1 percent of the time. These waves approach the study area obliquely from the northwest. Waves from the west to southwest quadrants have much shorter periods and are generally small to negligible.

Prior to the initiation of this study, no site-specific wave data were available for Aguadilla Harbor. Wave statistics had, however, been computed from 20 years of hindcast deepwater wave data by the U.S. Army Engineer Waterways Experiment Station (WES) for a site due north of San Juan. These data were adjusted to obtain an estimate of the wave climate at Aguadilla. To verify this estimate from the adjusted hindcast data, site-specific wave gage data also were obtained.

#### *Adjusted hindcast data*

The WES wave climate available for a deepwater wave station approximately 185 km (115 miles) north of San Juan was derived from historic records of surface pressure and wind data. Although estimating wind from available pressure data is more difficult in the lower southern latitudes, it was found that the majority of the wave energy that hits Puerto Rico's north coast is generated in the mid- and north-Atlantic as a result of extratropical winter storms, and approaches the island from the northern quadrants.

The hindcast data were considered a reliable estimate of the wave climate on that coast. To obtain a wave climate for Aguadilla, it was assumed that

the wave climate at a point 130 km (80 miles) northwest of San Juan would not be significantly different from that derived for the WES deep-water wave station 185 km (115 miles) north of San Juan. The maximum window of azimuth of wave rays that could reach Aguadilla breakwater site was 230 to 350 deg. It was believed that wave occurrences from other azimuths are blocked by Punta Borinquen and Punta Higuero. Data for only this range of azimuths were extracted from the WES wave climate. Because this information was being used to obtain an estimate of damage rates for potential breakwater designs, wave heights less than 0.5 m (1.5 ft) were not included in the analysis.

It was determined that 2.5 m (8 ft) was the equivalent deepwater wave height which would be exceeded by only 1 percent of all wave occurrences. Periods calculated for 2.5-m (8-ft) wave events range from 7 to 17 sec, with a mean of 12 and a maximum of 17 sec. The 10 percent wave height is 1.1 m (3.5 ft). Deepwater irregular waves with significant wave heights of 2.5 m (8 ft) and peak periods of 16 sec would shoal to a significant wave height of 4.1 m (13.5 ft) as it moves into a water depth of 7.3 m (24 ft).

#### *Wave gage data*

An evaluation of the WES hindcast data shows that, except for tropical disturbances, all significant wave energy occurs during the winter months. To verify the extrapolated adjusted hindcast data, a wave gage was installed in 9.1 m (30 ft) of water seaward of the proposed breakwater site. Data were taken every 4 hr for approximately 73 days from mid-December 1982 through February 1983. During this period, four events of significance were recorded. Spectra were computed for each gage record that compensated for hydrodynamic attenuation according to linear wave theory.

The 73-day wave record is too short, and supportive information such as a visual record of wave observations, is too limited to assert that the wave data are a representative sample of all wave conditions at Aguadilla. Analysis revealed that, as indicated in the WES hindcast climate, there is little wave energy resulting from locally generated short period waves, and the highest waves result from swells that are propagated far from their original generating region. A review of past synoptic weather charts for the Atlantic show that the storms that apparently were responsible for generating the higher waves in the record were not as severe as storms that have occurred periodically throughout past winter seasons. On the basis of

this comparison, it was believed that shallow-water waves are unlikely to occur that are much higher than 2.4 to 2.7 m (8 or 9 ft), except possibly during hurricanes or severe tropical storms.

It is interesting to note that the peak spectral frequencies of waves at Aguadilla do not correspond to estimates of peak frequencies for waves generated by corresponding storms in the Atlantic. In addition, data plotted on synoptic weather charts indicate that wind speed is not likely to have exceeded 30 knots (35 mph) in the appropriate fetch region for potential swell generation. The 11-sec waves recorded at Aguadilla may represent swells whose peak period was increased upon leaving the generation area. The shorter period waves that were dominant in the generation area were able to change direction with the wind as they moved through a changing wind field and into the tradewind belt, whereas the larger period waves continued towards Aguadilla. This explanation is consistent with recently published papers by Gunther et al. (1981) and Allender et al. (1983).

### *Summary*

From an analysis of site-specific records, it was believed that shallow-water waves in excess of 2.4 to 2.7 m (8 to 9 ft) should occur only rarely and be associated with tropical disturbances. The adjusted WES hindcast climate, however, indicates that the 1 percent exceedence significant wave climate is predicted to shoal to a height of 4.1 m (13.5 ft) by the time it reaches 7.3 m (24 ft) of water at the toe of the proposed breakwater. A possible explanation for this apparent discrepancy was discussed by Mattie (1982), where predicted shallow-water wave heights using an enhanced version of Goda's irregular wave technique are compared with field measurements. Results showed that predicted wave heights were on the average about 50 percent greater than the actual values. The technique proved to be conservative, but has the advantage that no predictions were less than the measured prototype data. From a design standpoint, there are insufficient site-specific data available at Aguadilla to verify the existence of a lower wave climate than that which has been derived from the WES hindcast data. Therefore, a design wave derived from the adjusted WES wave climate was used to develop the breakwater design criteria.

## Tides

The periodic astronomical tide at Aguadilla is a mixed dominant semi-diurnal type, with high and low tides generally being about equal in amplitude; however, the periodic tidal range is only about 0.3 m (1 ft). The spring tidal range is about 0.4 m (1.3 ft). Consequently, the actual fluctuations in water level depend upon the winds and other meteorological conditions, especially during the winter months. Thus, along the north and west coast due to winds, successive high and low tides can be quite unequal in amplitude. There are also short periods each month when diurnal components significantly modulate the tidal amplitude. Highest tides occur from October to December, while mean sea level varies from a low in the summer months to a high in October.

There is a marked increase in the high-water and low-water elevations during the winter months, while the tidal range remains constant throughout the remainder of the year. Using techniques of Mitchell (1954) and data from National Ocean Service (1984), it was determined there is a 10 percent probability that the extreme high tide elevation for any month will be twice as high as one-half the mean spring tidal range of 0.2 m (0.65 ft). The 1 percent exceedence value is 0.5 m (1.64 ft). An average tidal elevation of +0.3 m (+1.0 ft) above mean low water was established as the water elevation for breakwater design calculations.

## Currents

The easterly tradewinds set up a steady westerly current off the northern coast of Puerto Rico that increases in velocity during winter storm wave attack. Along the northwestern coast, currents are less predictable. Generally, off the coast the currents flows northerly while nearshore they follow the tidal fluctuations. However, during winter months, waves approaching the shoreline obliquely from the north generate a dominant southerly current. This is also considered to be the dominant direction for longshore sediment transport.

The North Equatorial Current, flowing in a west northwesterly direction, dominates the entire Antilles chain. Close to shore, however, this general current may be deflected, and local currents set up that may be entirely different as a result of influences that prevail along the shore. The coastline is, therefore, marked by currents that flow approximately parallel to the shore, and in some instances these currents may extend out to sea for

many miles. Off the northern coast of Puerto Rico, the coastal current is westerly and is driven by the prevailing northwesterly trade winds and their associated wave energy as waves approach the coast from a westerly direction. The velocity of this current averages 0.2 knots (0.25 mph) and is said to be strongest near the island. The wave action associated with winter months can cause considerable increases in the current velocity.

## **Breakwater design<sup>1</sup>**

The plan selected for construction based on economic analyses would provide a 345-m- (1,130-ft-) long breakwater to shelter a 3.8-hectar (9.3-acre) harbor area. Although initial dredging was not required, the limits of an entrance channel, turning basin, and impoundment area would be marked and designated for periodic maintenance operations.

### **Design waves**

A deepwater wave climate developed by WES from 20 years of hindcast data for a station directly north of San Juan, and 73 winter days of site-specific wave gage data were evaluated to determine the design wave for breakwater construction. The deepwater wave climate was modified to reflect the shadowing effect that the adjacent coastline has on waves at Aguadilla, and the wave climate was shoaled into the breakwater site using a shoaling technique developed for irregular waves. From these calculations, it was determined that equivalent deepwater waves ( $H_o'$ ), with significant wave heights of 2.4 m (8 ft) or greater, would occur less than 1 percent of the time. A 2.4-m (8-ft) wave with a 16-sec period was selected as the design deepwater wave. With an existing bottom slope of 1-on-20, and using techniques developed by HQUSACE (1977), the greatest wave height that could occur along the breakwater as a result of a 2.4-m (8-ft) deepwater waves would be about 4.1 m (13.5 ft) with a 16-sec period, and would occur in 7.3 m (24 ft) of water at the breakwater. Once designed, the breakwater's response to a 20-year tropical storm with 5.2-m (17-ft) wave height and 9-sec period was determined.

### **Armor stone and side slopes**

A three-layer breakwater design was utilized. Criteria set forth by the Danish Hydraulic Institute and HQUSACE (1977) indicate the

---

<sup>1</sup> This section is extracted from USADE, Jacksonville (1987).

armor-stone cover layer should be composed of 14,500 kg (16-ton) stone, with a minimum of two stones thick (approximately 1.9 m (6.4 ft)). Smaller armor stone (5,900 kg (6.5 tons)) was specified for the section of breakwater closest to land in the shallow water. The breakwater cover layer was actually constructed using smaller armor stone of 10,900 kg (12 tons) and 2,700 kg (3 tons) on the deepwater section and shallower-water section, respectively. Because unit costs for local rock do not vary significantly with stone size, for ease of construction of the breakwater, the armor layer was designed to blanket the entire structure.

The second layer was composed of 1,100 kg (1.2-ton) stone, with a minimum of three stones thick. The second layer was composed of stone at least one-tenth the size of the cover layer armor stone to prevent them from passing through the armor layer.

The third layer of core material is generally quarry-run stone with weights ranging between 3 and 54 kg (6 and 120 lb). A minimum of 0.3 m (1 ft) of bedding material would be quarry spalls ranging in size from 0.5 to 23 kg (1 to 50 lb), and would be placed on a filter cloth or gravel layer. Side slopes were set at 1 to 2.5 for both sides of the structure in water deeper than about 2.5 m (8 ft), and 1 to 2.0 for the harbor side in water less than about 2.5 m (8 ft). Toe protection would be the same size as the secondary layer. A stone density of 2,650 kg/cu m (165 lb/cu ft) was used since rock of this density is available from active quarries on the island. A typical breakwater cross section as built is shown in Figure 8, and a plan view of the breakwater and harbor layout is presented in Figure 9.

Meeting the nominal harbor wave climate criteria of 0.4 to 0.6 m (1.5 to 2 ft) during a severe tropical storm cannot normally be justified economically. However, annual equivalent damages associated with these rare events should be considered when determining the armor-stone size. This design would result in an estimated damage rate for the entire breakwater of 0.44 percent per year.

Sand tightening of the breakwater was not considered important due to a lack of available littoral material adjacent to the structure within the pocket beach to the north. While some sediment entered the harbor during construction of the breakwater, no initial dredging of the harbor area was required. Plans for minimal future periodic maintenance were considered.

### **Crown width**

The most efficient procedure for constructing the breakwater would be to use land based equipment and build 15- to 30-m (50- to 100-ft) sections at a time, working from the shore out. Under these circumstances, a crown width of 7 m (23 ft) was determined to be the minimum acceptable for the size crane that would be required to place 10,900 kg (12-ton) armor stone.

### **Project modifications<sup>1</sup>**

Construction of the Aguadilla Harbor Federal navigation project has altered coastal processes within and adjacent to the project area. Wave refraction around the tip of the breakwater into the harbor has resulted in considerable erosion of the inner harbor's eastern shoreline. Also, shoaling along the leeward side of the breakwater has occurred since project implementation. The refracted waves are directed northward along the inner harbor eastern shoreline that causes erosion through the northerly transport of sediment. This erosion would result in damage to the adjacent roadway, utilities, and upland development under the "no action plan." In addition, a portion of the refracted wave energy impinges on a vertical steel sheet pile wall at the entrance to the harbor. Wave reflection off of the sheet pile wall interacts with the refracted waves to exacerbate wave conditions inside the harbor, resulting in adverse impacts to navigation.

### **Perceived coastal processes**

Sediment is transported to the project area from both littoral and upland sources. Littoral sediment sources are limited to material transported along and eroded from the rocky shoreline north of the harbor. Upland sediment sources include storm drains located north, inside, and south of the harbor, and a ravine to the north which discharges directly into the ocean. While the southerly-directed net littoral transport is estimated at only 2,300 cu m/year (3,000 cu yd/year), sediment entering the project area from upland sources may exceed that rate during years of locally heavy rainfall. The unstabilized inner harbor eastern shoreline (immediately north of the parking garage) has eroded severely since initial construction of the project with much of the material being transported further into the harbor.

---

<sup>1</sup> This section is extracted essentially verbatim from USAED, Jacksonville (1998).

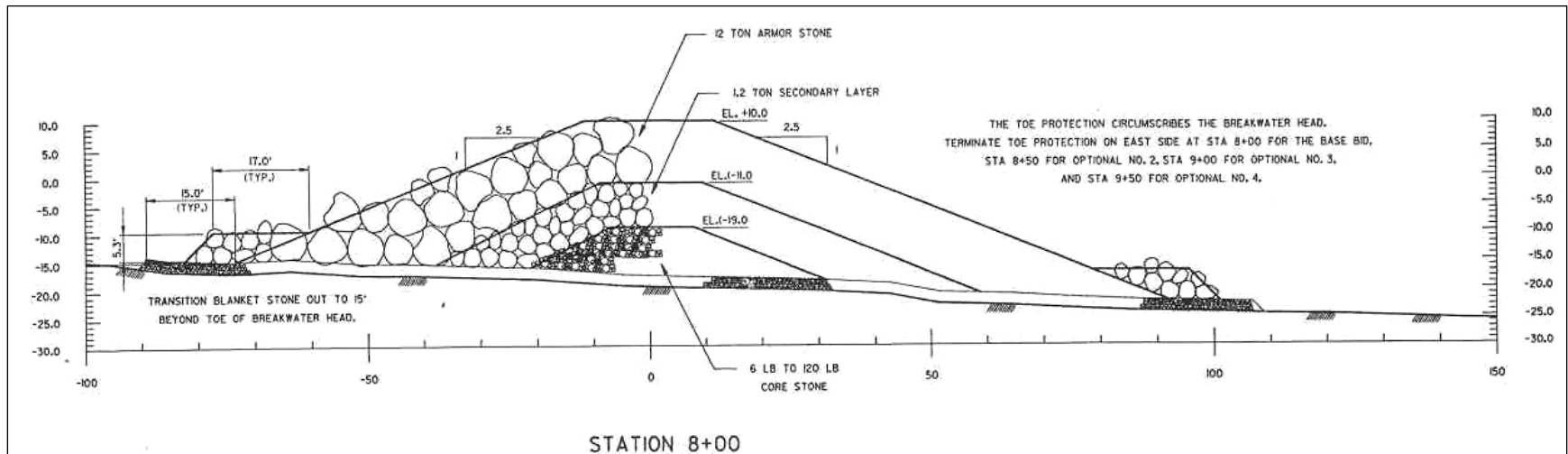
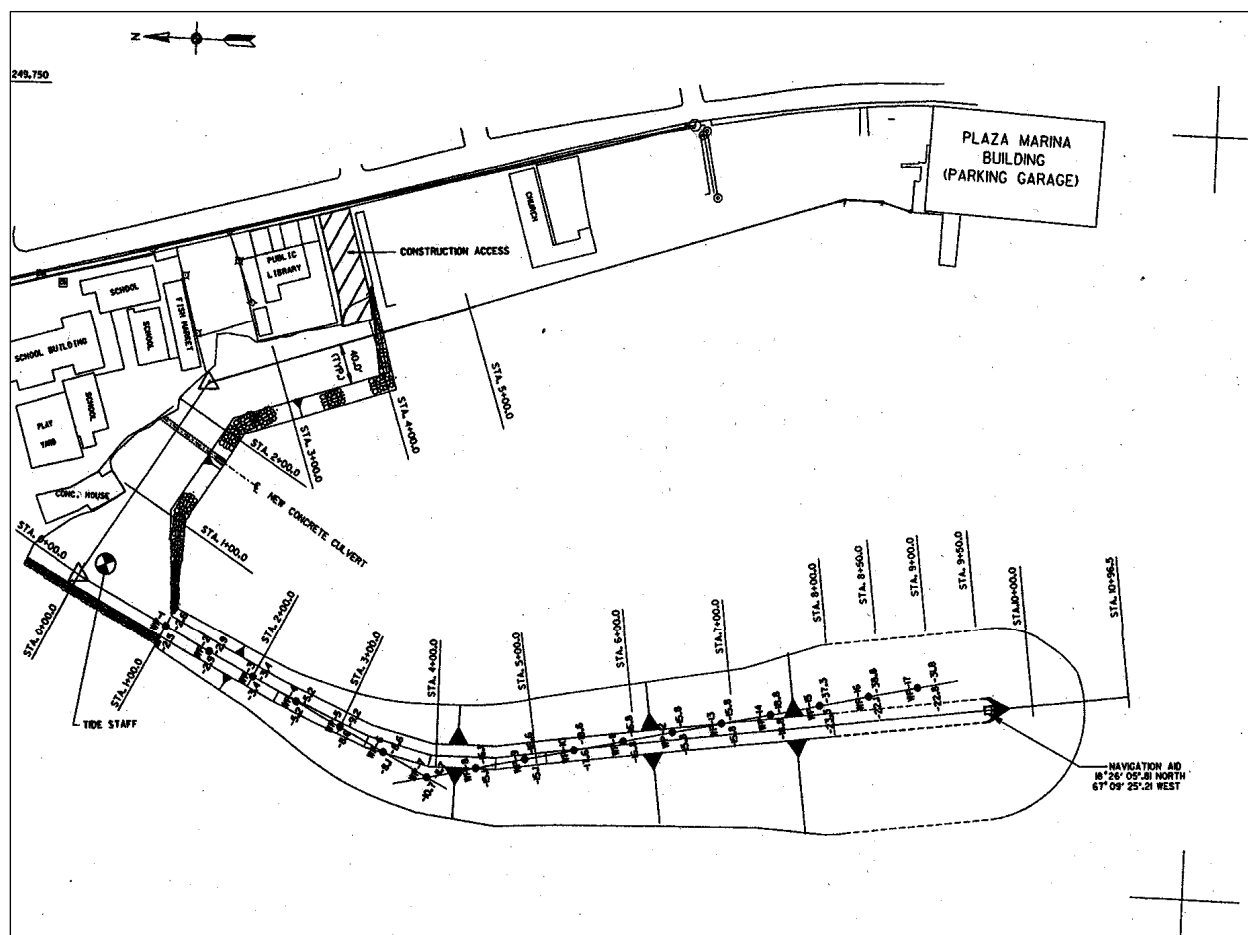


Figure 8. Aguadilla Harbor, Puerto Rico, rubble-mound breakwater cross section as built July 1995, station 8+00.



**Figure 9. Aguadilla Harbor, Puerto Rico, breakwater and harbor layout as built July 1995.**

Construction of the Federal navigation project at Aguadilla, Puerto Rico, began in June 1993 and was completed in July 1995. During the construction process, a shoal formed within the northern end of the harbor. In March 1995, approximately 2,300 cu m (3,000 cu yd) (the majority of this material) was removed from the area and placed within the harbor's eastern shoreline. Shortly after removing the shoal, it began to reform. Significant deposition was occurring even in the summer months when wave activity on this coast is minimal (generally less than 0.3 to 0.6 m (1 to 2 ft)). In addition, a shoal began forming along the first 150 m (500 ft) of the landward side of the breakwater. In addition to shoaling concerns, recession of the inner harbor eastern shoreline has proceeded at a rate of approximately 2.5 m/year (8.0 ft/year) since construction of the project.

The predominant wave direction in the project area is from the northern quadrants (northwest through northeast). The predominant littoral drift is, therefore, from north to south with extremely limited localized

reversals. To the north (updrift of the project area) there are rock headlands with hard bottoms and relatively steep offshore slopes. Downdrift, the coastline is also hardened with vertical bulkheads that intersect rock bottoms. The sediment supply for littoral transport is extremely localized and confined. The active sand sources are two small streams and numerous storm sewer outlets that drain steep contoured catchment basins. High velocity flows can transport a considerable amount of sediment during typical flash floods, especially when ongoing construction work strips large areas of natural vegetation.

Seaward of the breakwater, wave-breaking initiates at the dogleg (station 4+00) and proceeds in both directions along the face of the structure. At the tip of the breakwater, breaking ensues out to the breakwater toe with refraction causing wave crests to bend towards the interior of the harbor. The unrefracted wave crests proceed landward where wave breaking results in near complete dissipation of their energy on the downdrift shore. The refracted wave crests forms arcs that create wave forms appearing to emanate from the tip of the breakwater when viewed from the interior of the harbor.

Inside the harbor, the refracted wave spreads out from the tip of the breakwater. At its southern extent, the refracted wave breaks and dissipates on the eastern interior shoreline fronting the seawall south of the parking garage. The seawall in front of the parking garage reflects nearly 100 percent of the incident wave energy up to the point where waves are large enough to reach the underside of the seawall cap. At times, the uprush of the wave crests compresses underneath the cap, violently spraying water 3 to 4.5 m (10 to 15 ft) into the air. The impact of water wave crests on the underside of the seawall cap dissipates a portion of the waves energy but could potentially result in cap failure.

Wave reflection from the parking garage seawall crisscrosses the incident refracted waves resulting in superposition of wave heights. At the center of the harbor this wave/wave interaction results in a complex surface pattern and periodic unacceptable wave conditions. To the north of the parking garage, the unobstructed portion of the refracted wave breaks on the shoreline. The steep angle of wave breaking along the inner harbor eastern shoreline generates significant sediment transport that moves material towards the inner harbors northern shoreline. Once the reflected waves

travel back across the interior of the harbor, they interact with the refracted waves and break along the landward face of the breakwater.

From updrift to downdrift, sediment moves along the seaward side of the breakwater and around its tip. Sediment is also able to permeate through the breakwater as wave uprush generates a pulsing flow through the structure. Suspended sediment transport through the breakwater appears to be limited while bed-load transport may contribute to the shoaling of the inner harbor. In the lee of the breakwater tip, a stagnation point was evidenced by an accumulation of floating debris. Sediment transport is reinitiated further along the landward portion of the breakwater through the breaking of the convergent refracted and reflected wave crests.

Incident wave crests which pass to the south of the breakwater peel both left and right of a point downdrift of the harbor. A sediment transport node (a point at which sediment transport is directed to both the north and south) appears to be located approximately 150 m (500 ft) south of the harbor. The predominant sediment transport direction is to the south beyond this nodal point. Sediment transport along the pebble beach located just south of the parking garage seems to be primarily onshore and offshore rather than alongshore. Similar conditions occur in front of the parking garage, except that wave induced scour enhances offshore transport. North of the parking garage, sediment is suspended during breaking of the refracted wave. Return flow directed out of the harbor results from the head difference produced by the mass transport of water into the harbor from around and through the breakwater. Based upon the results of drogue studies at the harbor, it was determined that the larger grain size fraction of the suspended sediment is transported further into the harbor while the fines are pulled offshore with the return flow along the channel center line.

### **Revetment and wave absorber modifications**

The recommended alternative modification plan consisted of construction of a rubble-mound revetment along 170 m (560 ft) of shoreline inside the harbor along the existing eroded shoreline. In addition, a rubble-mound wave absorber would be constructed along 90 m (300 ft) of existing steel sheet piling. Wave reflection from the existing vertical steel sheet-pile wall would be reduced by the rubble-mound slope of the wave absorber placed in front of the wall. Construction of the 170-m (560-ft) revetment would further decrease wave reflection inside the harbor, and would reduce

erosion of the sandy shoreline along this portion of the harbor. This erosion will eventually threaten the existing road, and drainage and electrical utilities along the road.

Different cross sections are required for construction of the revetment and for the sheet-pile rubble-mound wave absorber. The revetment will be constructed over the existing (reshaped) beach slope along section 1, whereas no fill or existing underlying slope exists along section 2. Revetment section 1 is more protected from wave attack than section 2 since it is located further inside the harbor, resulting in a smaller median armor-stone size for revetment section 1. A design wave height of 1.2 m (4 ft) was used for section 1, while a design wave height of 2 m (6.5 ft) was used for section 2. These wave heights are based on depth-limited wave conditions and field observations during severe storm events. The most severe wave runup conditions exist when wave periods are 9 sec along section 1, and 11 sec along section 2. These are well within the range of wave periods commonly observed along the west coast of Puerto Rico during large storm swell events with typical wave periods of 8 to 16 sec.

To simulate the most severe conditions for armor-stone size calculation based on depth-limited waves, a 10-year storm surge was added to the water depth at the toe of each revetment section. According to the Federal Emergency Management Agency storm surge values presented in the Aguadilla Harbor Detailed Project Report (U.S. Army Engineer District, Jacksonville, 1987), a 10-year storm surge results in a still-water elevation increase of 0.7 m (2.3 ft) above the mean low water elevation. To minimize wave reflection inside the harbor, a relatively flat revetment slope was used (1 vertical to 3 horizontal). Steeper slopes resulted in excess wave reflection, runup, and overtopping, while flatter slopes required much larger quantities of materials to construct, impacted a larger area of hard bottom, and further reduced the navigable harbor area. Based on these design parameters, median armor sizes of 500 kg (1,100 lb) and 1,650 kg (3,600 lb) were calculated for revetment sections 1 and 2, respectively. A plan layout of the Aguadilla Harbor revetment and wave absorber modifications is shown in Figure 10.

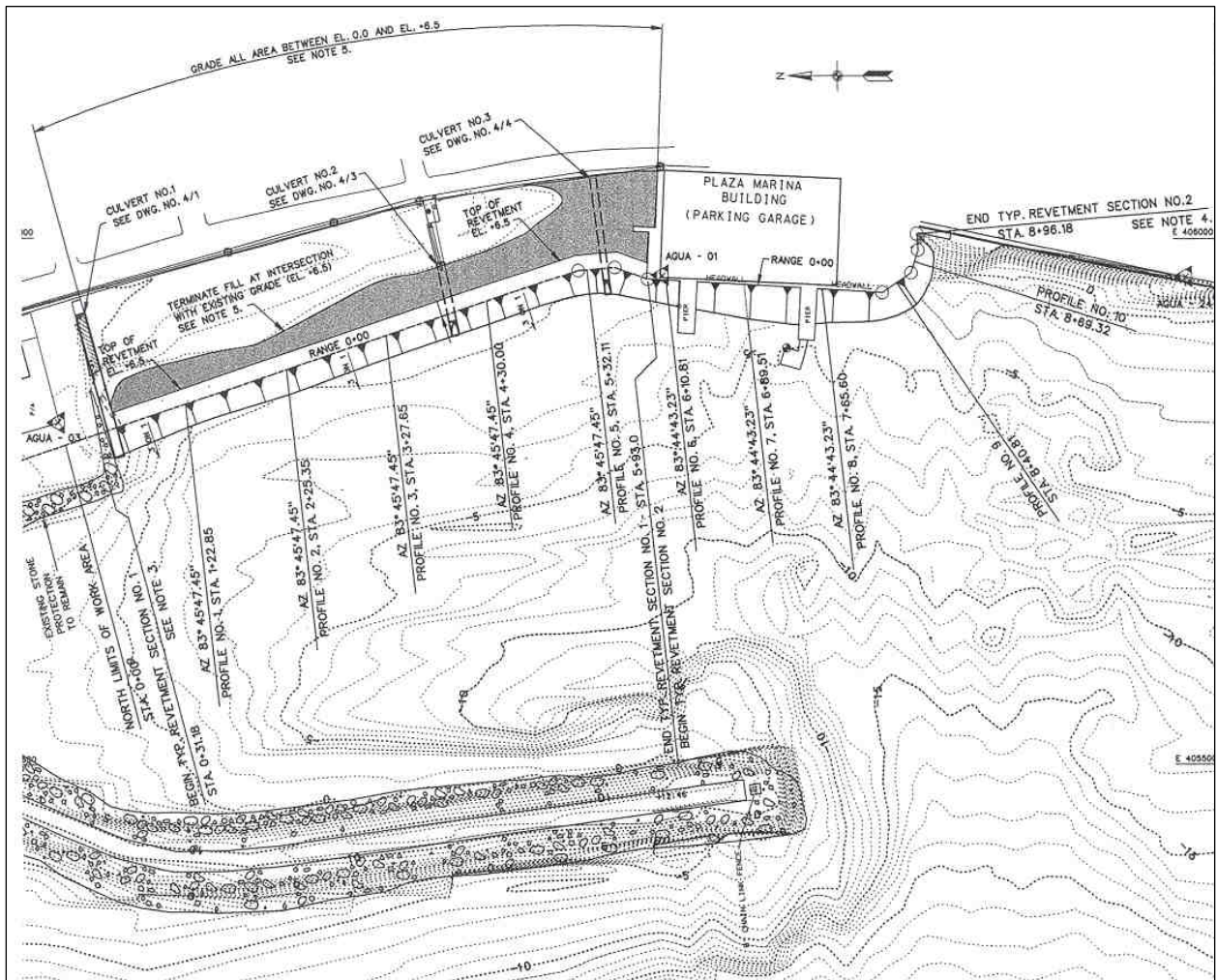


Figure 10. Revetment and wave absorber as-built modifications to Aguadilla Harbor, Puerto Rico, interior region to alleviate harbor shoreline erosion.

### 3 Breakwater Stability

Construction of the Aguadilla Harbor, Puerto Rico, breakwater was completed in July 1995. It was essential to understand how the functional performance of this new structure would be affected by the various environmental parameters (tides, waves, and currents) to which it would be subjected during the early years of its life cycle. The degree to which the structure core and armor stones would settle and lock into place following initial storm exposure would be an indication of the ultimate degree of deterioration to be expected over the design life of the project. This knowledge would provide guidance for operation, maintenance, and rehabilitation planning to ensure that the breakwater would indeed be a functionally stable structure throughout its planned existence.

A detailed breakwater stone elevation survey by standard topographic surveying techniques was commissioned by the Jacksonville District in September 2003. The breakwater survey was performed by Javier E. Bidot and Associates, Caguas, Puerto Rico. Several tropical and extra-tropical storms had occurred between the time of completion of the construction of the breakwater during the summer of 1995 and the time of the breakwater survey in the fall of 2003.

It was observed that a few armor stones had experienced a minimal degree of shakedown settlement during these early years following construction, but no major areas of excessive deterioration were found to exist. The breakwater structure survey cross-section elevation data referenced to mean lower low water (mllw) are shown in Figure 11. A contouring of these specific elevation data points is shown in Figure 12, where the uniformity of the armor-stone elevations can be easily observed. All contours, from the structure design crest elevation of + 3 m (+10 ft) mllw down to the toe elevation of about 0 m (0 ft) mllw on the harbor side and about -1.8 m (-6 ft) mllw on the open-water side, indicate structure settlement is exceedingly uniform or had not taken place by the time of the survey.

A series of ground-level photos of the breakwater are presented in Figures 13 through 20 to illustrate the degree to which the structure has withstood both average waves conditions and severe storm events since its construction in 1995 through 2004. It is pertinent to understand that tropical storms (hurricanes) approach from the eastern side of the island, and thus do not directly strike the harbor with full-force wave conditions since the harbor is on the western (leeward) protected side of Puerto Rico.

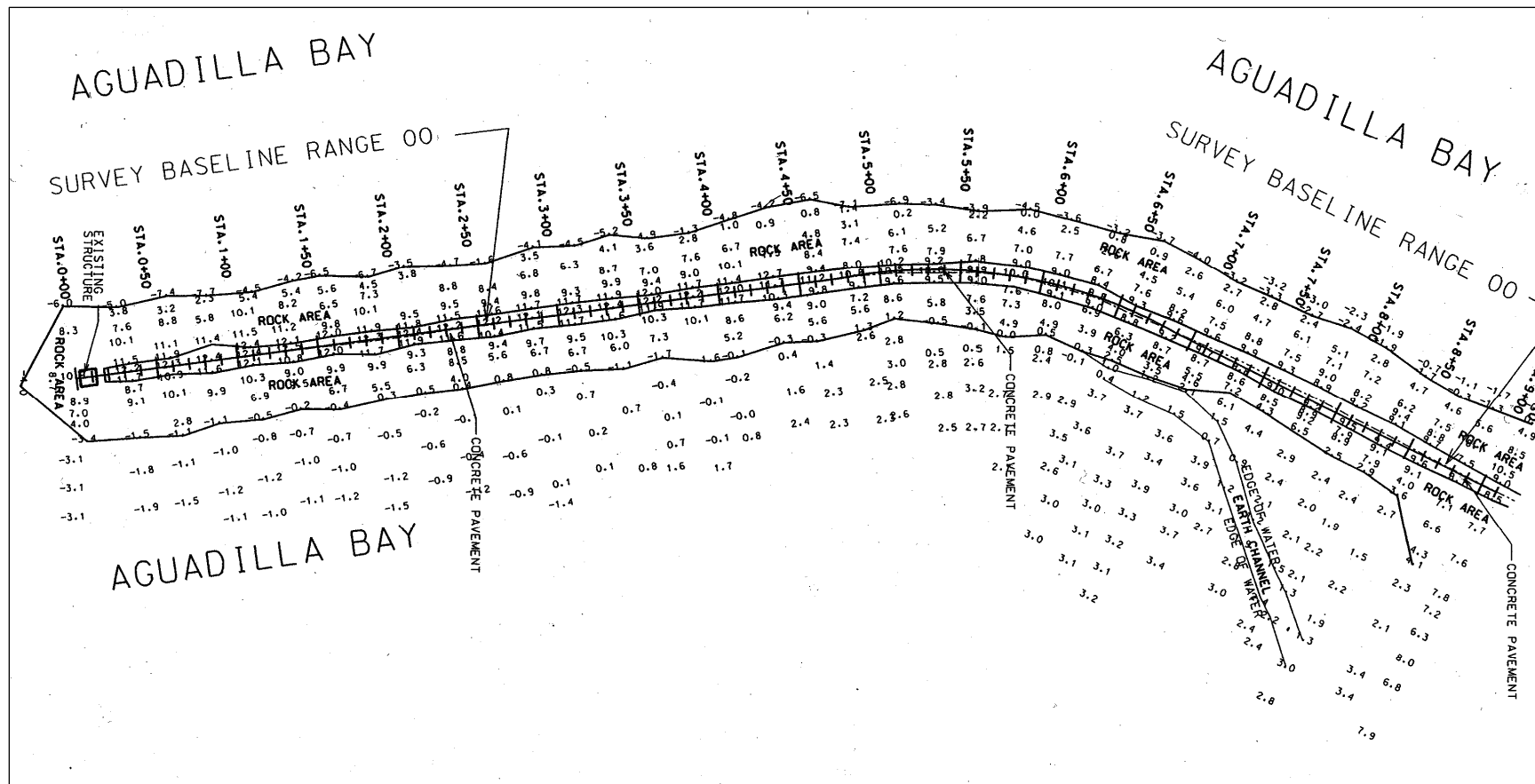


Figure 11. Aguadilla Harbor breakwater survey cross-section elevation data September 2003, with elevations in feet referenced to mean lower low water (mllw) (survey performed by Javier E. Bidot and Associates, Caguas, Puerto Rico, for U.S. Army Engineer District, Jacksonville).

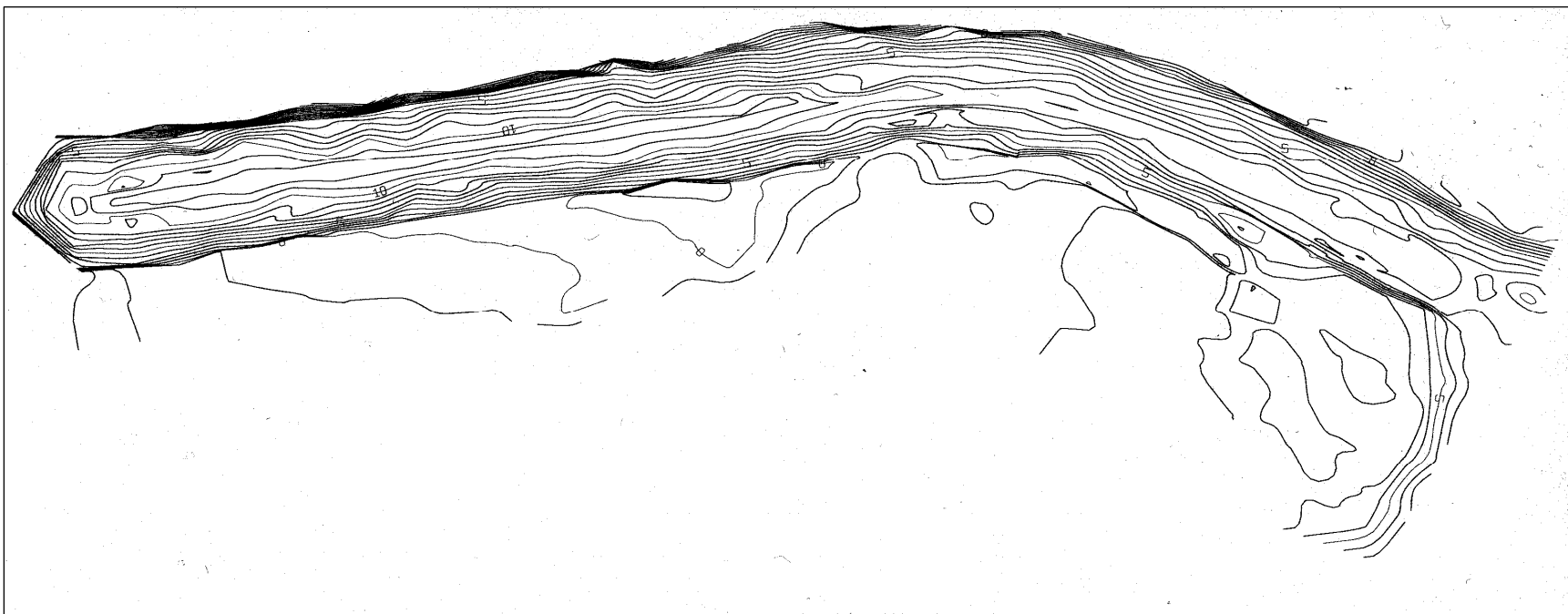


Figure 12. Aguadilla Harbor breakwater survey elevation contours September 2003, with elevations in feet referenced to mean lower low water (mllw) (survey performed by Javier E. Bidot and Associates, Caguas, Puerto Rico, for U.S. Army Engineer District, Jacksonville).



Figure 13. Aguadilla Harbor, Puerto Rico, breakwater.



Figure 14. Seaward section of Aguadilla Harbor breakwater.



Figure 15. Landward section of Aguadilla Harbor breakwater.



Figure 16. Seaward side of Aguadilla Harbor breakwater, station 3+00 near the landward end of the structure, showing stable armor layer.



Figure 17. Seaward side of Aguadilla Harbor breakwater, station 5+00, near the middle section of the structure, showing stable armor layer.



Figure 18. Seaward side of Aguadilla Harbor breakwater, station 8+00, near the seaward end of the structure, showing stable armor layer.



Figure 19. Harbor side of Aguadilla Harbor breakwater, station 1+00, looking seaward from the landward end of the structure, showing stable armor layer.



Figure 20. Harbor side of Aguadilla Harbor breakwater, station 8+00, looking landward from the seaward end of the structure, showing stable armor layer.

## **4 Estimating Surface Currents at Aguadilla Harbor Using Dyes and Drogues<sup>1</sup>**

Two general categories of post-construction monitoring of completed coastal navigation projects are as follows:

- a. Project condition monitoring: Periodic inspections and measurements conducted as part of project maintenance. Information from condition monitoring is used to assess the project state and make decisions about repair and rehabilitation.
- b. Project performance monitoring: Observations and measurements used to assess the actual project performance relative to design objectives.

Onsite observation of environmental conditions (waves, currents, winds, etc.) along with project response, are essential components of both categories of monitoring. However, project performance monitoring typically requires more quantification of environmental parameters to assess how well the project is fulfilling its intended function.

### **Dye and drogue studies**

Techniques for estimating water current magnitude and direction at a navigation project range from simple methods, such as dye and drogue releases, to sophisticated methods, such as suites of in situ instruments or complex numerical models. Dye and drogue studies can provide useful information about surface currents that can then be used to infer sediment pathways in the vicinity of a harbor or other coastal project.

Dye and drogue studies have several advantages including the following:

- a. Inexpensive (minimum equipment requirements).
- b. Low manpower requirements.
- c. Minimum preparation (no calibration or equipment testing).
- d. Flexibility (study plan can be altered or expanded as necessary).

---

<sup>1</sup> This section is extracted essentially verbatim from Hughes (2002).

The major disadvantages of dye and drogue studies include the following:

- a. Limited scope and spatial coverage.
- b. Results apply only to conditions at the time of the study (i.e., no long-term records).
- c. Care must be taken to assure that personnel are not at risk when they are on coastal structures during heavy wave conditions.
- d. Only surface currents are estimated.
- e. Estimation techniques are crude, and consequently, accuracy is less than optimal.

Despite the shortcomings, dye and drogue studies can substantially augment other sources of information, thus providing a broader base on which to make engineering decisions.

Dye and drogue studies are highly visible activities, particularly around navigation structures, harbors, and marinas. Local inhabitants and users of the project may be alarmed when they see patches of water turning bright green, or when they observe strangers throwing objects into the water. They might call local authorities to report such suspicious activity. If the local authorities are aware of the study beforehand, they will have ample time to reassure the concerned citizens and explain what is happening. Appropriate local authorities should be informed of any planned dye or drogue study via official U.S. Army Corps of Engineers letter. Such local authorities might include harbor/marine police, harbor master, local police agencies, and/or local municipalities. The letter needs to state that any dye used in the study is safe for human contact, and safe to the marine environment. It is a good idea to attach a data sheet giving details about the chemical nature of the dye. Hand delivering the letter and giving an oral summary before commencing the study is much better than sending a letter several weeks in advance.

### **Estimating currents from dye release**

Dyes suitable for use in the marine environment are available in liquid, powder, and pellet form. Pellets dissolve in water, resulting in a continuous dye source that is beneficial for showing flow trajectories. Because the pellets usually sink to the bottom, best results for surface currents are obtained where the pellets are affixed to an anchored float so the dye is released on the water surface. Multiple buoy positions give a series of path lines, revealing the principle flow patterns in the vicinity of the structure.

Estimating current velocity from a fixed dye source is performed by tracking the position of the head of the path line as it moves with the current flow. Figure 21 shows an aerial view of a continuous source dye release at Shinnecock Inlet, NY.



Figure 21. Dye release at Shinnecock Inlet (photograph courtesy of Aram Techunian, First Coastal Corp.).

Powdered or liquid dye is usually deployed as a single release at a selected location. At initial release, the dye is concentrated into a small patch that increases in size as it migrates with the flow. The shape of the dye patch can elongate over time indicating stronger flow on one side of the patch, or it may retain a circular shape indicating a more uniform surface current. Current magnitude and direction are estimated by plotting the position of the dye patch centroid as it migrates in time.

### **Dye deployment**

Dye studies achieve best results outside of regions where strong turbulence occurs. For example, dye placed inside the breaker zone quickly dissipates without giving much information about current magnitude. Where vessels can safely navigate, the dye should be deployed from a small boat such as a Zodiac. A small vessel can sequentially inject dye at multiple locations with minimal time lapse between injections. Hand signals, radios, or cell phones can be used to notify shore observers when each dye packet is released so that timing can begin. Number and location of dye

injection points is subjective, and depends to a great extent on the particular project site and the goals of the study.

Launching dye packets from a coastal structure is also a possibility, but placement is much more haphazard. A suggested technique is to wrap about two tablespoons of powered dye in tissue paper, shape it into a ball, and secure it with rubber bands. A powerful slingshot is then used to cast the dye packet into the water. The tissue will dissolve and release the dye as a point injection. This presumes the release occurs near the surface and not after the packet settles to the bottom. Accurate placement of dye packets using this technique requires practice and some experimentation to get the right amount of tissue paper (strong enough to withstand launch forces, but breaks on impact). Tossing packets by hand is another option.

### **Dye tracking**

Most often, movement of dye patches are tracked by shore-based observers who estimate the location of the dye patch centroid and note the time. Estimating distance over water is difficult, and can introduce significant errors in current speed estimation. Depending on the situation, it may be possible to use fixed landmarks in conjunction with dye location estimates. For example, if a dye release is moving along a coastal structure, the observer can note the time when the leading edge of the patch passes through a line perpendicular to a fixed (known) location on the structure. The observer then moves to the next fixed location (if another observer is not already stationed there).

An observer at a fixed location might be able to track the dye movement using a simple compass or surveying instrument to record angle and/or direction to the dye patch at a given time. This also requires a reasonable estimate of distance along the direction radial that becomes more critical as the observation angle becomes more acute. If conditions are favorable, photography is an excellent means for recording dye positions in time. Photography works best if photographs can be taken from an elevated perspective such as a nearby building, or other accessible structure. Reasonable estimates of dye travel distance should be possible without photo rectification provided there is some feature on the photograph from which to estimate the length scale, and the camera lens is not wide-angled.

With Global Positioning System (GPS) resolution now at less than 5 m, another viable option is to track the dye patch using a small vessel situated

within the dye patch or adjacent to the leading edge of the patch. Position of the GPS unit is recorded along with the time of the reading. The accuracy of this method increases with the speed of the dye movement. The GPS resolution is not sufficient for tracking slow moving dye patches.

Each estimate of the location of the dye patch centroid (or leading edge) must be accompanied by the time of observation. Estimates of average dye migration are calculated as the distance traveled between two adjacent observations divided by the time between the two observations. Field recording of dye patch location and time of observation can be made on a notepad showing a plan form sketch of the experiment area along with identifiable landmarks for reference. Sketching the shape of the dye pattern as it evolves may give additional insight into the flow regime. Pencil or indelible ballpoint pens are recommended because they are less likely to run or smear if the notepad gets wet from sea spray. A small voice recorder can be used to give more detailed descriptions of the dye patch movement between estimates of location, but voice recording should not supplant sketches of the dye movement.

### **Dye recommendations**

One of the safest dyes for use in the marine environment is Uranine concentrate dye (Sodium Fluorescein). In powder form Uranine is rusty colored, but when put in water it turns a bright green-yellow color that is easy to see and track. Uranine dye is sensitive to sunlight, and it loses its color over a relatively short time. Several hours after deployment there will be little trace of the dye due to sunlight and dispersion. Uranine dye has no known adverse health effects to either human or marine life.

One source in the United States for Uranine concentrate dye is:

Keystone Aniline Corporation  
2501 W. Fulton Street  
Chicago, IL 60612  
Phone: 1-800-522-4393  
Web: [www.dyes.com](http://www.dyes.com)

Uranine dye costs approximately \$25 per pound (2002 estimate). Normally the dye is sold in barrels, but it is possible to purchase as little as 22.68 kg (50 lb).

About 250 ml (8 oz) of powdered Uranine concentrate is used for each dye injection point. Prepare the dye by pouring about 250 ml (8 oz) of powdered dye into small plastic bottles or other containers that have a good screw-on lid. Latex gloves are recommended for this task. During dye injection, one bottle containing the premeasured amount of dye is opened and poured into the water at each injection location.

### **Equipment recommendations**

The following is a list of recommended and optional equipment needed to perform a simple dye study.

- a. Essential equipment.
  - Dye and containers.
  - Watch or timing device.
  - Notepad and pens/pencils.
  - Map of study area with dye injection points identified.
  - Deployment equipment (vessel, slingshot, etc.).
  - Corps of Engineers identification.
  - Letter describing the study.
- b. Optional equipment.
  - Survey tape to measure distances on land or coastal structures.
  - Communication devices for study team members.
  - Voice recorder.
  - Latex gloves for handling dye.

### **Dye study at Aguadilla Harbor**

Since its construction in 1995, the Corps' harbor project at Aguadilla Harbor has suffered from shoaling by littoral sediment thought to be moving through the more porous sections of the breakwater and around the southern tip of the structure. One aspect of the monitoring program was to investigate the physical mechanisms that result in harbor shoaling and to determine the local sediment pathways that are active during storms.

A dye study was performed at Aguadilla Harbor by ERDC in November 2001. Waves were estimated to have a breaking height of 3 m (10 ft) with periods in the range of 7 to 10 sec. Plunging breakers were mobilizing large quantities of sand along the seaward toe of the breakwater, and as the waves curled, it was evident that sand was suspended throughout the

water column. Sand appeared to be moving from north to south (Figure 22) along the breakwater. At the southern tip of the breakwater, the waves broke across the structure head, and significant quantities of sand were carried by the breaking wave around the head and into the harbor mouth by the diffracted waves.

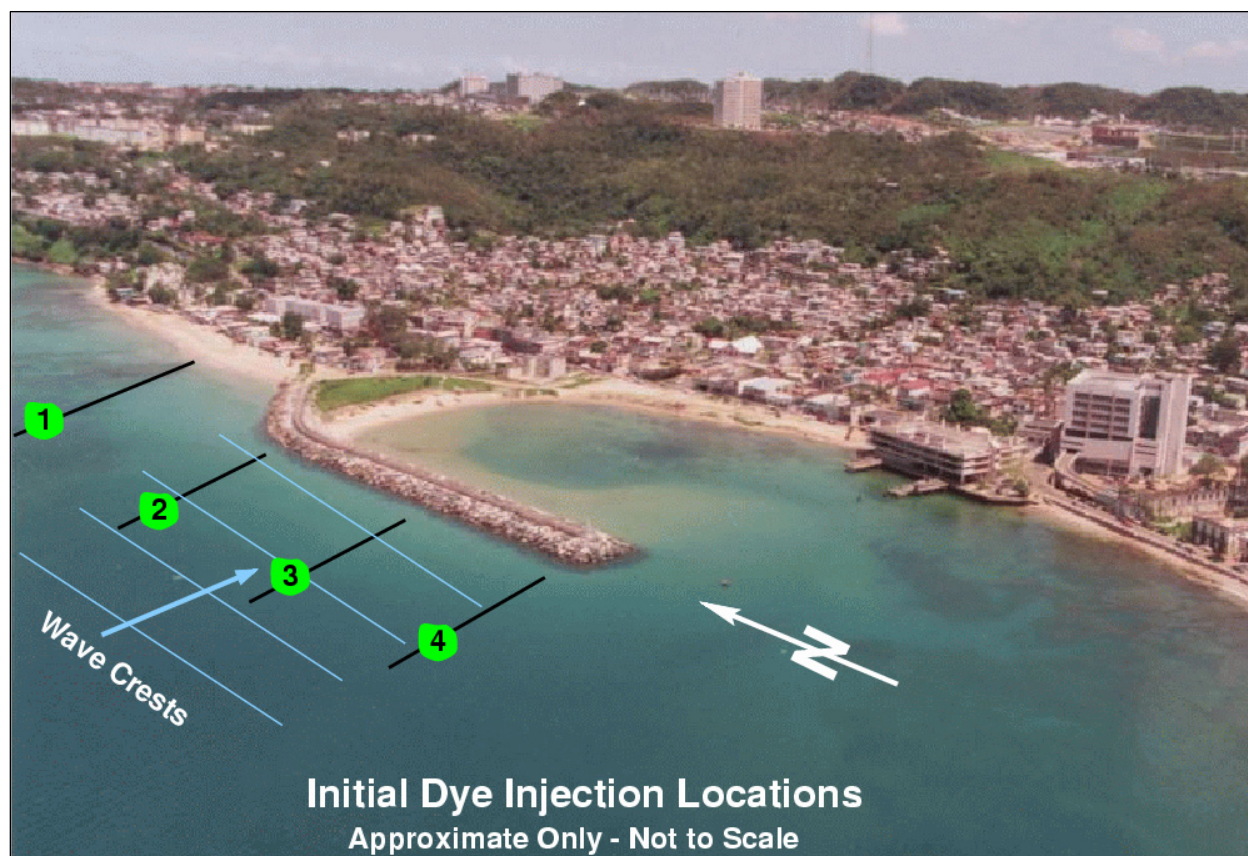


Figure 22. Approximate initial dye injection locations, Aguadilla Harbor.

Four dye releases were made offshore of Aguadilla Harbor in the approximate locations shown in Figure 22. At each location, a volume of approximately 250 ml (8 oz) of Uranine powered dye was released on the water surface from an inflatable Zodiac. The four release points were aligned parallel to the breakwater at an estimated distance 100 m (330 ft) seaward of the breakwater. Large waves breaking seaward of the breakwater and a wide surf zone at the north beach prevented any dye deployments closer to the breakwater.

Sketches illustrating evolution of the dye patterns on the water surface are presented subsequently. These sketches are based on ground-level qualitative observations and, thus, the dye patterns shown are not to scale.

However, the figures do represent the general trends of surface currents during the study period.

#### **Dye release no. 1, north beach**

The dye released seaward of the beach immediately north of the harbor breakwater moved generally south and elongated during the first 20 min as illustrated in Figure 23. The centroid of the dye pattern moved about 100 m (330 ft) during that time, giving an estimated average surface current speed of about 0.08 m/sec (0.3 ft/sec).

During the last 10 min of observation, the dye pattern moved further offshore into a position that was noticeably seaward of the release location for dye packet no. 2. This seaward drift might have been caused by waves reflecting off the breakwater elbow.

#### **Dye release no. 2, breakwater elbow**

The second dye packet was released seaward of the breakwater elbow, where the shore-connected portion of the structure transitions to the main breakwater leg aligned in the north-south direction. Over the span of 35 min, the dye pattern enlarged slightly and moved south along a line generally parallel to the breakwater, as illustrated in Figure 24. Less elongation of the dye pattern was observed compared to dye packet no. 1.

The average speed of the dye centroid as it covered the 100-m distance between the two black lines shown on Figure 24 was estimated to be 0.05 m/sec (0.16 ft/sec). In other words, dye packet no. 2 moved at about half the average speed of dye packet no. 1.

#### **Dye release no. 3, breakwater midpoint**

The most intriguing dye deployment occurred at a location directly seaward of the midpoint of the breakwater's straight section. Figure 25 illustrates the general evolution of this dye deployment. Rather than moving parallel to the breakwater, the dye pattern elongated in a shoreward direction with the shoreward end moving south at a faster rate than the seaward end. The packet also moved at a higher average speed, with the centroid moving at an estimated rate of 0.09 m/sec (0.3 ft/sec) and the shoreward edge moving at about 0.13 m/sec (0.4 ft/sec). The stronger current closer to the breakwater had created a shearing effect that seemed

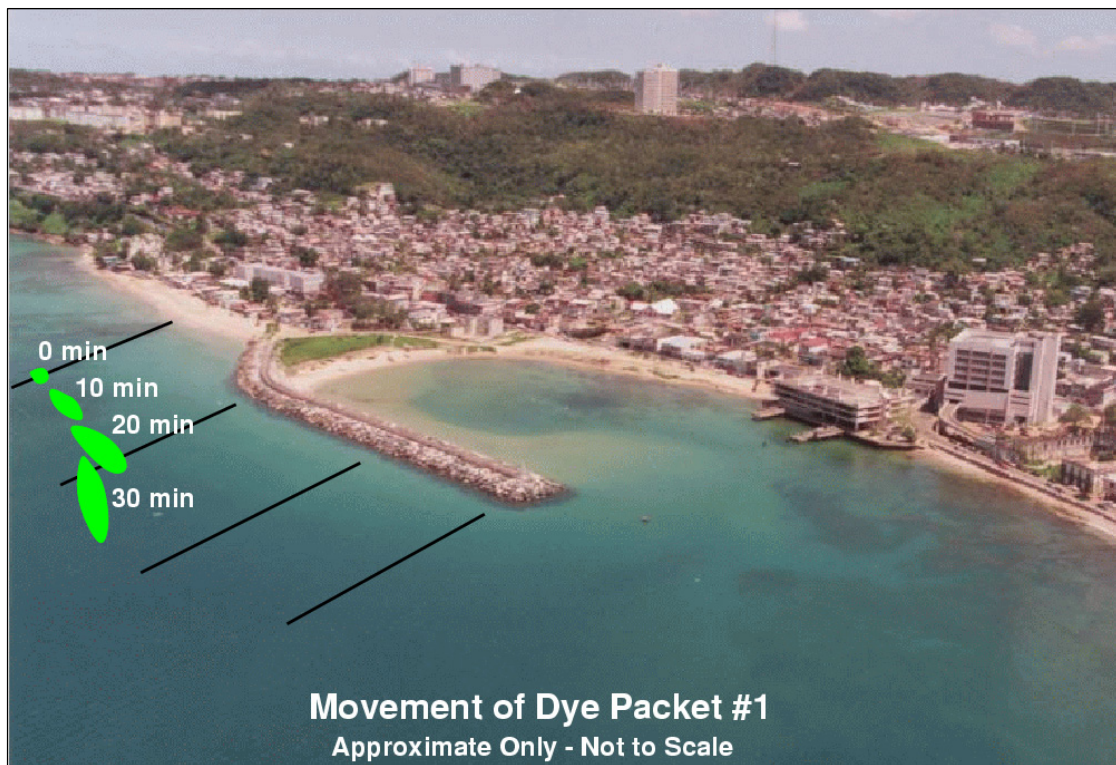


Figure 23. Approximate path of dye release no. 1, Aguadilla Harbor.

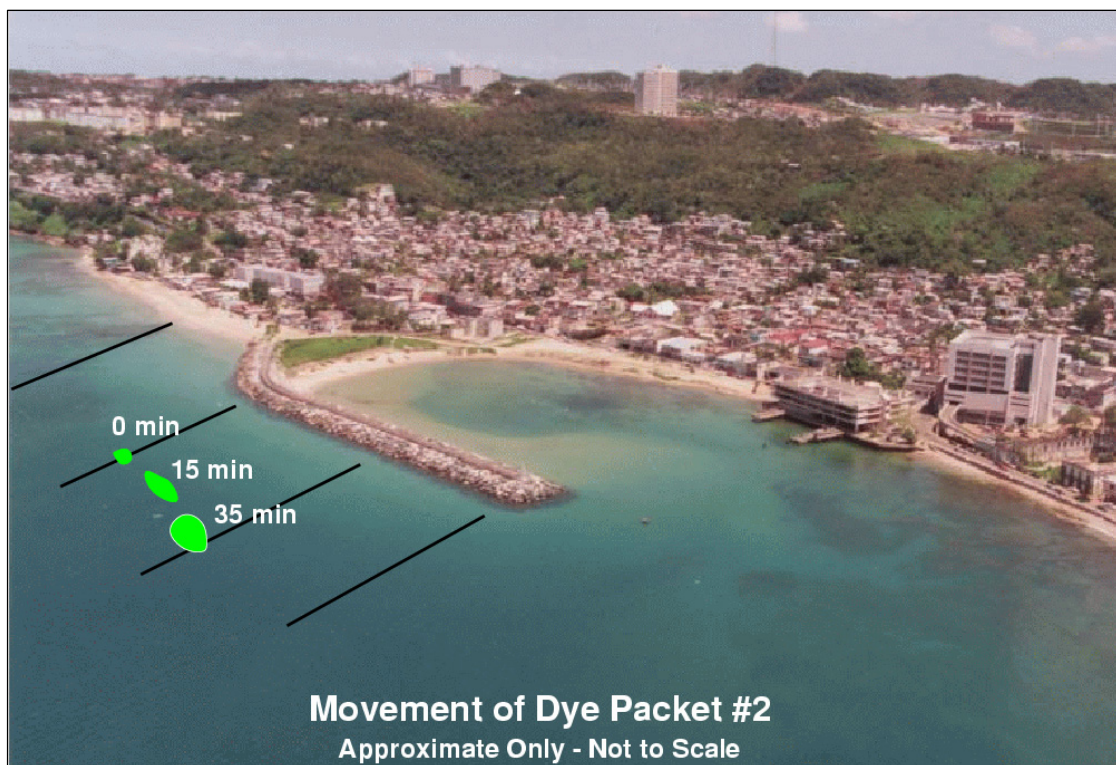


Figure 24. Approximate path of dye release no. 2, Aguadilla Harbor.

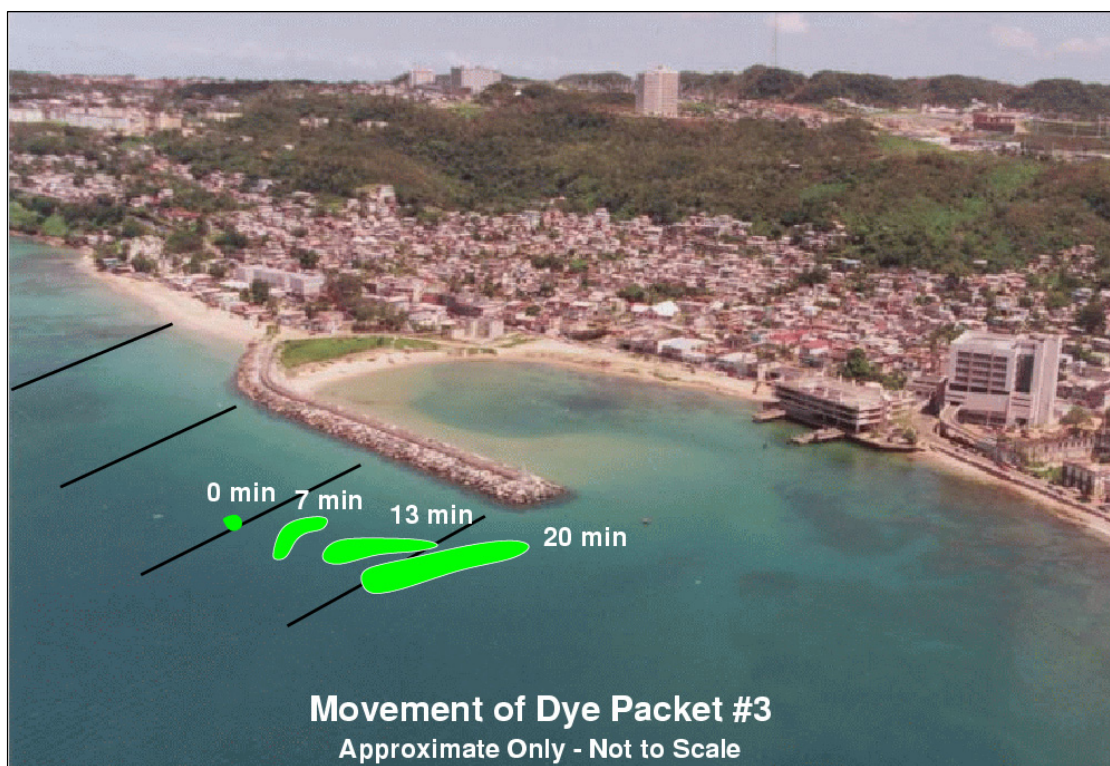


Figure 25. Approximate path of dye release no. 3, Aguadilla Harbor.

to entrain the dye and elongate the pattern. Eventually, the pattern moved beyond the southern end of the breakwater and dissipated.

#### **Dye release no. 4, breakwater south end**

The final dye release was directly offshore of the breakwater's southern tip. As shown in Figure 26, the dye pattern initially moved south as a compact area at an estimated speed of about 0.15 m/sec (0.5 ft/sec). Little elongation or expansion of the pattern was observed. After about 10 min the southerly migration of the dye pattern slowed until it seemed to become stationary at the location labeled "30 min" in Figure 26.

Apparently, the wave-generated alongshore current had a nodal point to the south of the breakwater. This may be an indication that the influence of the breakwater on the alongshore current does not have an effect south of the breakwater. With this decrease in southerly flow as illustrated by dye release no. 4, it is hard to conclude that any littoral sand is moving to the beach region south of the harbor project. In other words, sand in the littoral system is not bypassing the harbor.

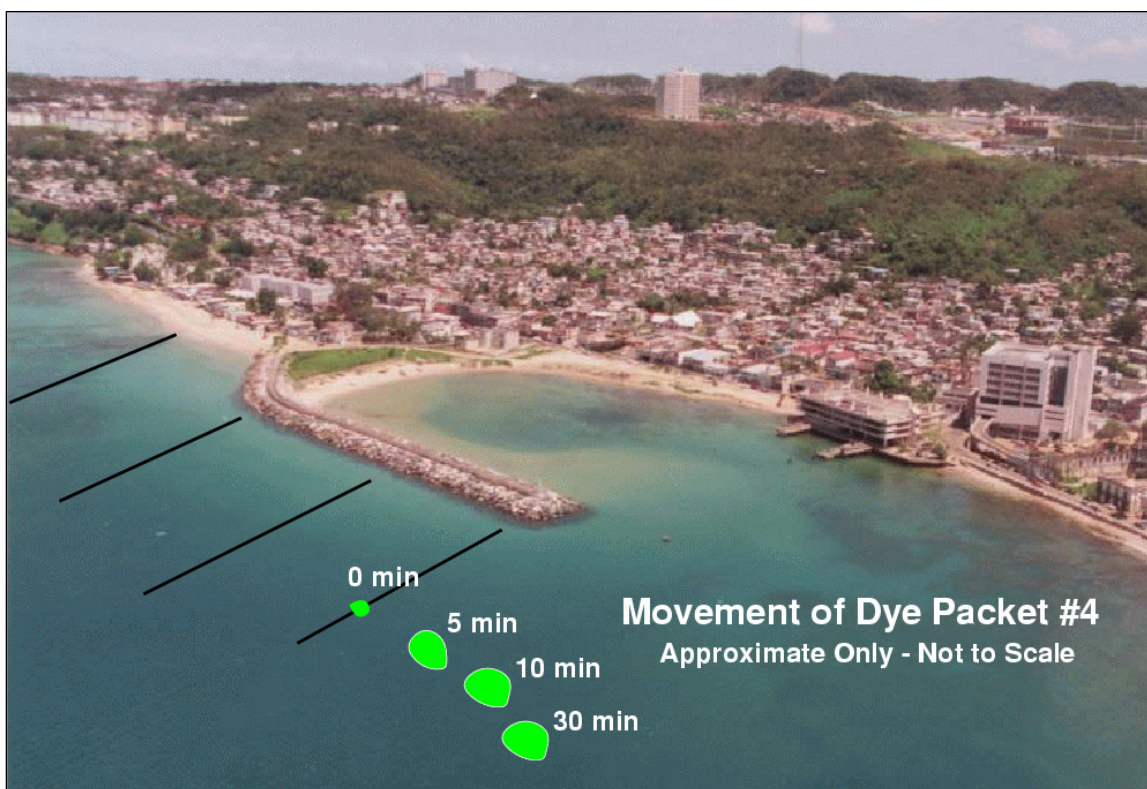


Figure 26. Approximate path of dye release no. 4, Aguadilla Harbor.

## Estimating currents from drogue release

Drogues are objects that float on the surface and move with the surface current. The major assumption is that the drogue moves at nearly the same speed as the current. Drogues with only slightly positive buoyancy are more likely to move at the current speed than lighter drogues. Light drogues such as plastic floats will have a significant freeboard and could be pushed along by wind in addition to water currents.

Drogues can be sophisticated devices complete with electronic instrumentation such as “pingers” that can be tracked from shore stations. These types of drogues are used in more sophisticated studies that cover large areas or studies where the drogues cannot be tracked visually from shore. Typically, deployment and recovery of instrumented drogues requires a vessel. The expense of instrumented drogues is not warranted for estimating currents near coastal structures.

Oranges are a favorite low-cost drogue for estimating currents adjacent to coastal structures. Besides being biodegradable and entirely safe to the environment, oranges are quite easy to see, and they usually float low in

the water. (There is the possibility that a particular variety of orange will not float in fresh water, so testing should be conducted prior to the experiment.) Oranges are locally available at a reasonable cost. Tennis balls also work well as drogues because they are readily seen and do not float too high in the water. The major drawback to using tennis balls as drogues relates to the environment as some means for recovering the tennis balls needs to be incorporated into the study plan. Brightly painted wooden blocks are also suitable drogues.

### **Drogue deployment**

In most cases the drogues (oranges) are thrown into the water from atop a coastal structure. This limits the deployment distance to the capability of the person throwing the orange. However, deployment distance can be estimated reasonably well for each individual by measurement of a few land-based tosses prior to the study. Greater deployment distances can be achieved via vessel deployment or use of some type of “drogue launcher.” Homemade devices such as slingshots, air cannons, or catapults have potential, but testing and safety are important considerations before using these devices in the field. If a launching device is constructed, it should be calibrated for launch distance on dry land.

### **Drogue tracking**

Tracking drogues is similar to tracking dye deployments discussed earlier. A watch is used to time the movement of the drogue between two locations. Distance traveled over the time span needs to be estimated by the observer. This is most easily done where currents are flowing parallel to a coastal structure that can be safely accessed. In this case, simply mark the starting, intermediate, and final positions and step off (measure) the distances between the positions. Establishing and marking timing locations prior to drogue deployment allows the observer to move along the structure with the drogue and note the times when the drogue is perpendicular to the structure at each location.

Estimating travel distances for drogues moving along paths that are neither linear nor structure-parallel is more difficult. Consequently, current speed measurements calculated for this situation must be viewed more qualitatively. Use of photography obtained from a good vantage point can be used to estimate more precise travel distances, provided the drogues can be easily seen and some object of known dimensions is in the

image for scale reference. The example drogue study in the next section illustrates both drogue movement parallel to a structure and drogue movement inside a harbor.

### **Equipment recommendations**

The following is a list of recommended and optional equipment needed to perform a simple drogue study.

- a. Essential equipment.
  - Bag of oranges (or similar drogue).
  - Watch or timing device.
  - Notepad and pens/pencils.
  - Map of study area with drogue insertion points identified.
  - Corps of Engineers identification.
  - Letter describing the study.
- b. Optional equipment.
  - Survey tape to measure distances on land or coastal structures.
  - Drogue launcher (and liability insurance?).
  - Deployment vessel.
  - Communication devices for study team members.
  - Voice recorder.

### **Drogue study at Aguadilla Harbor**

A drogue study was conducted during November 2001 with the purpose of observing and measuring currents near the breakwater and in the harbor during the high-energy wave conditions. Equipment consisted of a bag of 20 small oranges (drogues), a stop watch, and a notepad. Oranges were thrown into the water, and the drift progress was timed between two known points. When possible, the distance between the points was estimated by pacing the distance along the breakwater and assuming each pace was about 0.85 m (2.8 ft). Average surface current was obtained as the distance traveled divided by the time of travel. In all, about 15 oranges were thrown into the water over the course of the study. Some oranges were immediately lost in the white water of the surf zone and could not be tracked. Other oranges were swept onto the rocks of the breakwater by large waves before they traveled any significant lateral distance.

### Seaward of the breakwater

The first drogues (oranges) were thrown into the water from the beach north of the harbor (Figure 27). Here the surf zone was wide, and the oranges could not be thrown far enough offshore to be outside of the breaker zone. When the next wave broke and turned the sea surface white with foam, visual contact with the oranges was lost. However, the oranges did reappear to the south where the beach meets the north leg of the breakwater. The oranges were swept into the swash zone and were unable to move further south.

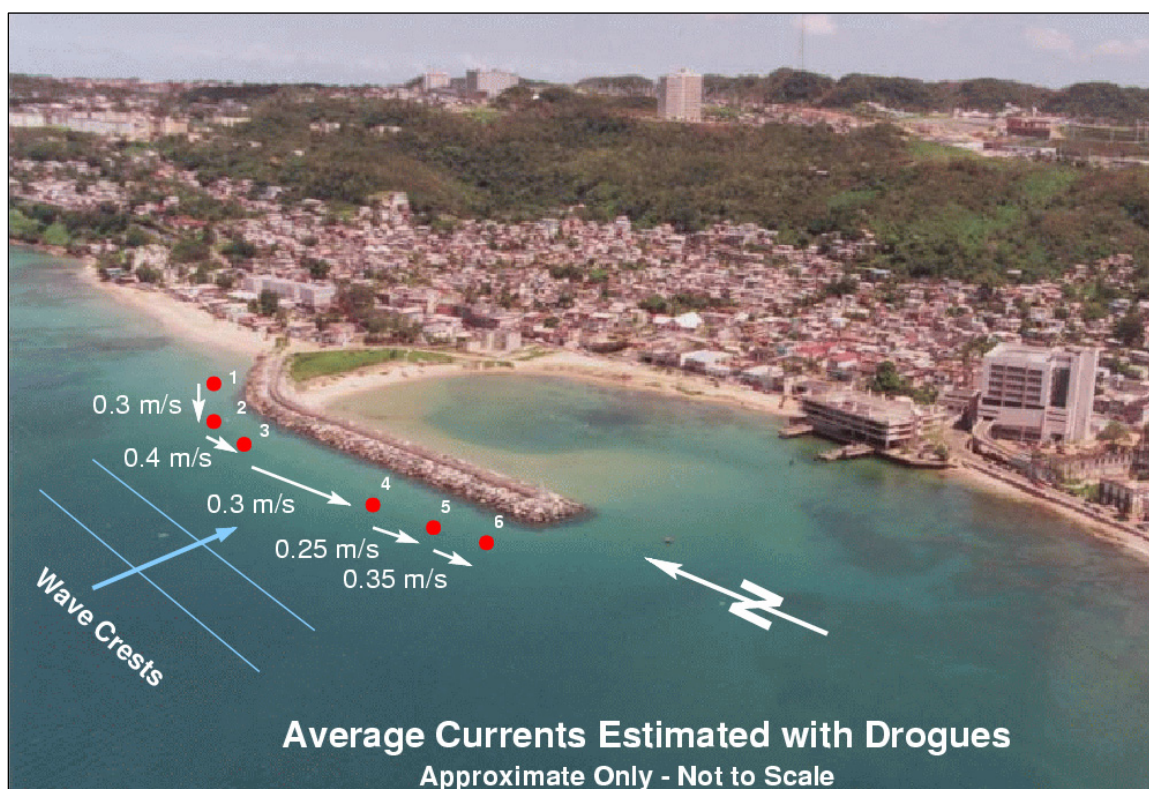


Figure 27. Measurement locations and average current speed estimated with drogues along the breakwater, Aguadilla Harbor.

Successful deployments from the breakwater were obtained over the entire length of the breakwater. Oranges were thrown into the sea a distance estimated to range between 20 and 30 m (65 and 100 ft). Usually, this location was just seaward of the wave breaking point so the onshore/offshore movement of the drogue was primarily oscillatory with most of the translation movement in the longshore direction.

Figure 27 shows the approximate locations of the drogues along the seaward side of the breakwater when times were recorded. Estimated average surface current between the adjacent points is listed for each reach. The measurements are detailed in Table 1. The measurements indicate a relatively constant longshore current of about 0.3 m/sec (1 ft/sec) moving south along the breakwater. Current speed at the seabed would probably be less, but still strong enough to move sediment mobilized into the water column by the breaking waves. Without wave breaking, these current speeds are close to the sediment incipient motion criterion for fine-grained sand. The coarser grain sizes (approximately 0.3 mm) found on the beach north of the breakwater would probably not be transported by this current if the mobilizing action of the waves were absent.

**Table 1. Drogue measurements seaward of the Breakwater, Aguadilla Harbor, November 2001.**

Range	Paces	Distance (m)	Time (sec)	Average Speed (m/sec)
1-2	36	30.6	98	0.3
2-3	35	30.0	73	0.4
3-4	100	85.0	287	0.3
4-5	35	30.0	120	0.25
5-6	30	25.5	73	0.35

### **Landward of the breakwater**

Current patterns in the harbor and at the harbor entrance were examined qualitatively. Because of the drogue movements and difficulty in estimating distance traveled using known reference points, it was not possible to estimate current speeds with any confidence. Five drogues were deployed, and their approximate paths are shown in Figure 28.

#### *Drogue A*

This drogue (orange) was tossed from the southern end of the walking platform on the breakwater into the water about 20 m (65 ft) seaward of the breakwater. The current moved it rapidly past the end of the breakwater in the first minute. The drogue then traveled landward toward the harbor entrance until it moved past the breaking wave point at about 260 sec. Shoreward progress then slowed until it seemed the drogue reached an equilibrium position at the harbor entrance. The drogue maintained this position for the remainder of the observation.

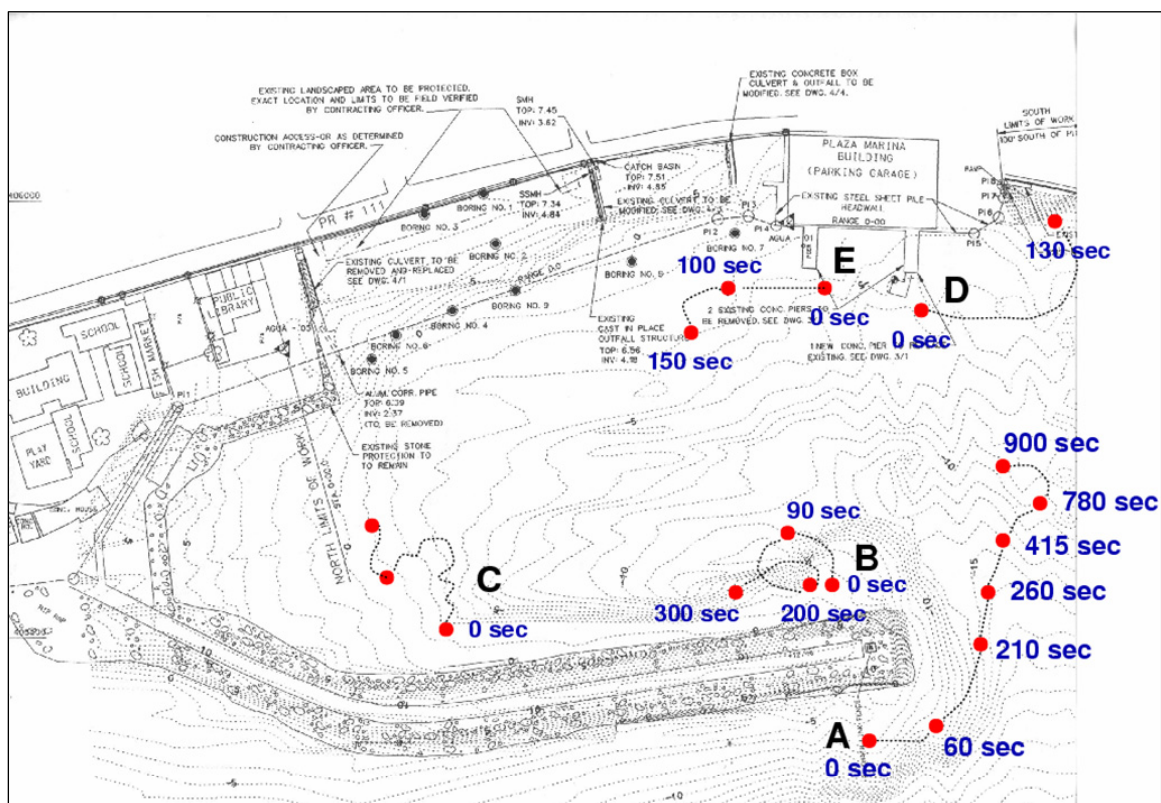


Figure 28. Drogue paths within Aguadilla Harbor.

The track of Drogue A, and eventual stalling, indicated a current nodal point just outside the harbor entrance. This implies that sand moving into the harbor enters close to the breakwater head, and then is carried in by the diffracted waves. Drogue A stayed outside of the diffracted wave influence. This was confirmed by dropping a second orange (not shown) into the water directly south of the breakwater head at the wave breaking point. This drogue was immediately swept well into the harbor by the next breaking wave and was lost from view.

#### *Drogue B*

This drogue was tossed near the leeward breakwater toe from the southern end of the breakwater as shown in Figure 28. From observation of a surfer wading out to the end of the breakwater, water depth at this location was about waist deep. The drogue fell into a circular path resembling a stagnation area in the lee of a flow separation point. This observation is consistent with the accumulation of sand in this area.

*Drogue C*

This drogue was placed into the northern end of the harbor in shallow water near the beach as illustrated in Figure 28. The drogue stayed in the immediate vicinity of the beach as the small waves traveled up the beach face. Because of the general meandering movement, no times were recorded. A member of the dive team spotted an orange at this location 2 days later, and it was most likely the same orange.

*Drogue D*

Visual observation indicated that water was flowing out of the harbor in the region near the parking garage. Drogue D confirmed this observation by moving southward until the orange was trapped in the small pocket beach just to the south of the parking garage. It appeared that the wave pattern would keep the orange in this location indefinitely. A second orange from one of the previous experiments also showed up on this pocket beach. The failure of Drogues A and D to progress any further south provides additional evidence that sand may not be bypassing the harbor project and moving to beaches south of the harbor.

*Drogue E*

This drogue moved slowly into the harbor along the path sketched on Figure 28 by the small spilling waves that had diffracted into the harbor.

**Summary**

Much can be learned about currents in the vicinity of coastal structures using simple dye and drogue techniques. Dye and drogue studies are inexpensive, have minimal manpower requirements, and cause no environmental impact or disruption of navigation. Although the current speed and direction estimates obtained from these studies are not highly accurate, the information is useful when added to other knowledge of the local physical processes at the project site. The main disadvantage of dye and drogue studies is that the acquired information pertains only to the conditions at the time of the study and may not be representative of the average conditions. This is less of a concern where the currents are predominantly tidal and cyclic.

The relative simplicity of performing dye and drogue studies should not overshadow safety concerns. Walking on coastal structures during

energetic wave conditions is hazardous because of the possibility of strong wave overtopping. Always apply common sense on the conservative side when deciding whether or not to venture onto a coastal structure. Finally, when reporting observations and estimates obtained from simple dye and drogue studies, be sure to note sources of potential errors, particularly if travel distances were difficult to ascertain.

## 5 Directional Wave Measurements

Many processes that occur along coastlines result directly from the wave climatology existing in that region. Hence, it is imperative to have good knowledge of waves at a specific site of interest that are both generated locally and that are arriving from some distant source to fully anticipate and understand their potential effects on beaches and infrastructure. Such wave knowledge is ascertained by wave gage measurement programs of the U.S. Army Corps of Engineers and other governmental agencies.

“The measurement of waves at sea is notoriously difficult. They change rapidly, and it is hard to find a place to stand while you measure...” (Kinsman 1965). The problem of finding a place to ‘stand’ has been adequately solved by standing on the ocean floor (i.e., by anchoring a self-recording or transmitting wave gaging device on the sea bottom). This technique, improved by the Corps of Engineers, Coastal and Hydraulics Laboratory (CHL), utilizes an array of pressure gages to determine not only the magnitude of the surface waves which are propagating shoreward, but also calculates the direction from which the waves are approaching. Spectral wave analysis is a powerful frequency domain technique that can identify whether the waves are from one or more predominant storm swells or from local wind seas with broad central spectral peaks.

### Wave gaging near Aguadilla Harbor

All of the valuable information produced by spectral wave analysis is based on a time-series of sea-surface elevations. Although single-point gages such as a wave-riding buoy can effectively measure wave height and period, and can generate an energy spectrum, they cannot be used to determine the direction the waves are traveling. When three or more underwater pressure sensors are placed in close proximity, however, comparison of their measurements does allow direction to be resolved. This is the technique used by CHL in the development of the bottom-mounted pressure sensor arrangement on a trawler-resistant frame that can remain on the seafloor for several years. Raw data can be transmitted to shore in real-time while up to a year’s processed data can be stored in a data processor mounted on the frame (Figure 29).



Figure 29. Corps of Engineers, Coastal and Hydraulics Laboratory, trawler-resistant directional wave gage array and pressure sensor pods (gage and pinger in center of array).

The CHL directional wave gage consists of three pressure sensors, each placed in a separate container on one of the six array legs (Figure 30), and a central electronics and battery module. The batteries are sufficient to enable the gage to sample at a 1-Hz rate and store wave and water level observations for a year or more. The directional wave gage is mounted in a steel hexapod that is pinned to the seafloor by steel pipe pilings. The frame and instruments weigh about 500 kg (1,100 lb). Installation (Figure 31) requires a dive team plus vessel with crew, and takes about a day once the vessel is moored on site. Mild sea states (less than 1 m (3.3 ft) waves) are necessary not only for placing the frame over the side of the vessel but also for positioning it correctly on the bottom, and for safety of the divers.

## Wave gage record analyses<sup>1</sup>

### Irregular waves

There is never a constant progression of identical waves on the open ocean. Instead, the sea surface is composed of waves of varying heights and periods moving in differing directions. When the wind is blowing and the waves are growing in response, the seas tend to be confused: a wide

<sup>1</sup> This section is extracted from Demirbilek and Vincent (2002), and Scripps Institution of Oceanography, Coastal Data Information Program Web site <http://cdip.ucsd.edu>.



Figure 30. Directional wave gage pressure sensor installed on one of the array legs.

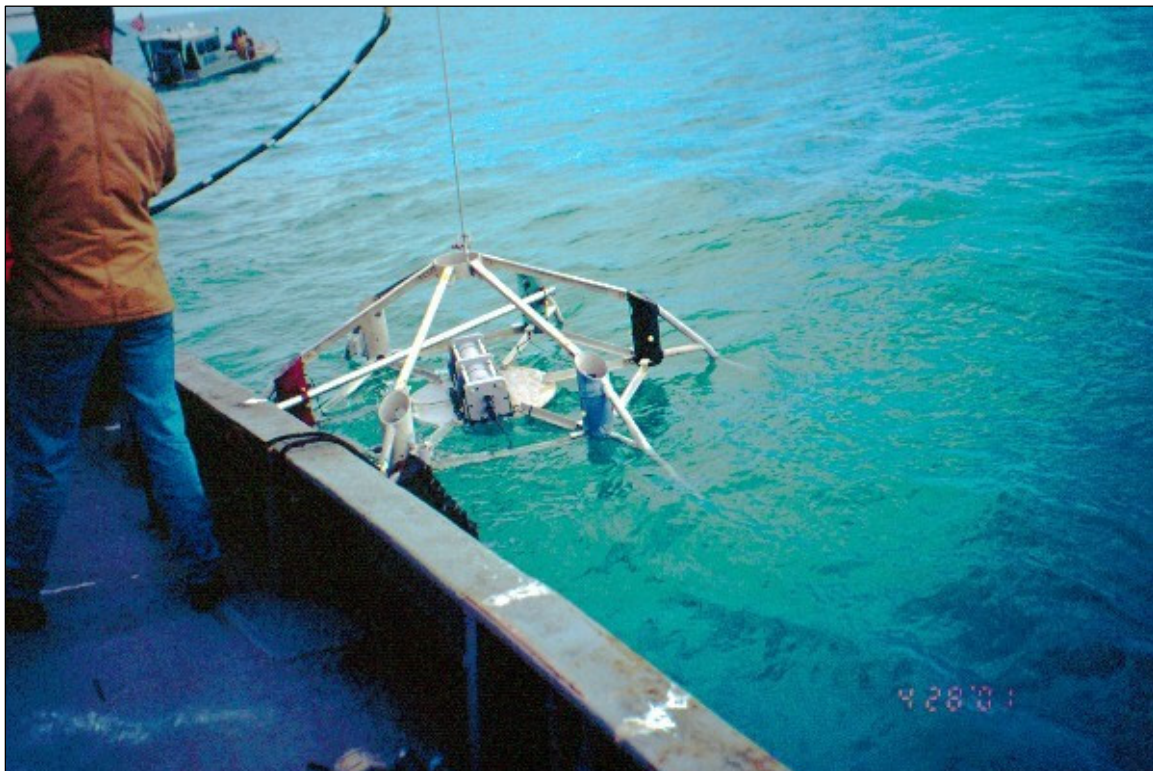


Figure 31. Directional pressure wave gage being deployed by winch from survey vessel.

range of heights and periods is observed. Swell is more regular, but it too is fundamentally irregular in nature, with some variability in height and period. It is necessary to treat the characteristics of such a sea surface in statistical terms. The ocean surface is often a combination of many wave components. These individual components were generated by the wind in different regions of the ocean and have propagated to the region of interest, forming complex waves (Figure 32).

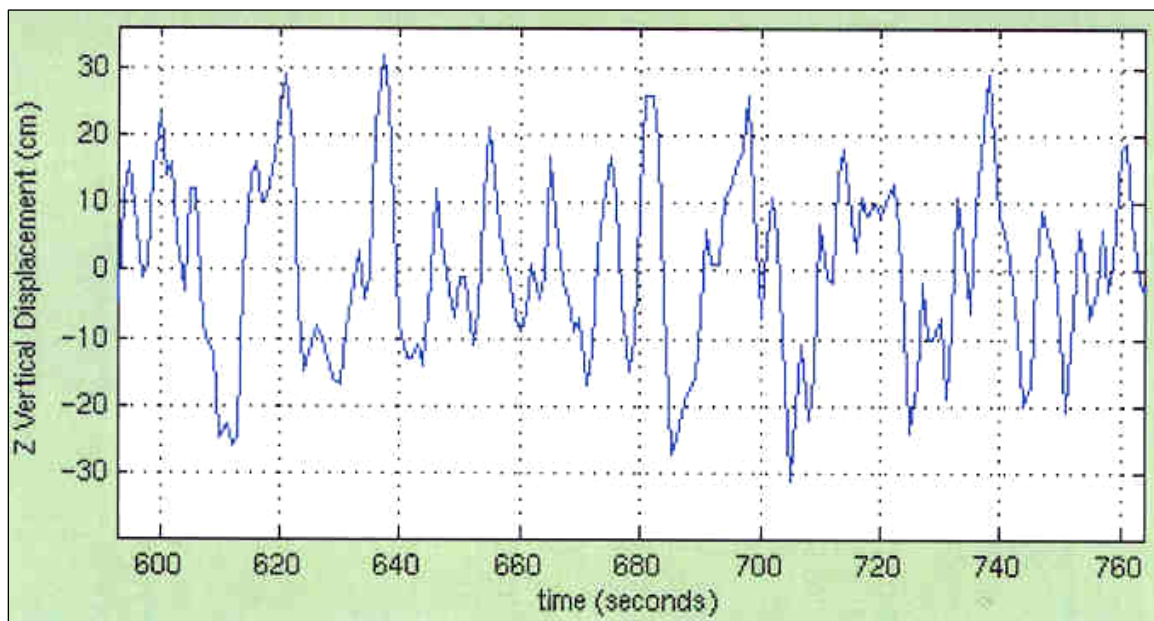


Figure 32. Typical representative wave record of actual sea surface measurements.

By analyzing time-series measurements of a natural sea state, some statistical estimates of simple parameters can be produced. The most important of these parameters is the significant wave height,  $H_s$  (or  $H_{1/3}$ ); it is the mean of the largest one-third (highest 33 percent) of waves recorded during the sampling period. This statistical measure was designed to correspond to the wave height estimates made by experienced observers. (Observers tend to not notice all of the small waves that pass by; instead they focus on the larger, more prominent peaks.)

It is important to remember that the significant wave height is a statistical measure, and is not intended to correspond to any specific wave. During the sampling period there will be many waves smaller than the  $H_s$ , and some that are larger. Statistically, the largest wave in a 1,000-wave sample is likely to be nearly two times (1.86x) the significant wave height.

## Spectral analysis

The more powerful and popular approach for treating complex waves is spectral analysis. Spectral analysis assumes that the sea state can be considered as a linear combination or superposition of a large number of regular sinusoidal wave components with different frequencies, heights, and directions. This is a useful assumption in wave analysis since sea states are in fact composed of waves from a number of different sources, each with its own characteristic height, period, and direction of travel.

Mathematically, spectral analysis is based on the Fourier Transform of the sea surface. The Fourier Transform allows any continuous, zero-mean signal such as a time-series record of the sea surface elevation to be transformed into a summation of simple sine waves. These sine waves are the components of the sea state, each with a distinct height, frequency, and direction. The spectral analysis method determines the distribution of wave energy and average statistics for each wave frequency by converting the time series of the wave record into a wave spectrum. This is essentially a transformation from the time-domain to the frequency-domain, and is accomplished most conveniently using a mathematical tool known as the Fast Fourier Transform (FFT).

The spectral approach indicates those frequencies that have significant energy content, as well as the direction wave energy is moving at each frequency. The energy from all wave directions in a wave spectrum can be readily plotted in a frequency versus energy density graph, which can reveal a great deal of information about a wave sample and ocean conditions. The general shape of the plot, in fact, reveals a great deal: whether seas or swell predominate, the number of distinct swells present, etc. For example, during local wind events, the spectrum tends to have a broad central peak (Figure 33). For swell that has propagated a long distance from the source of generation, on the other hand, waves tend to have a single sharp, low-frequency (long period) peak.

The area under the frequency versus energy density plot is  $H_{mo}$ , the spectral estimate of significant wave height. In deep water  $H_{1/3}$  and  $H_{mo}$  are close in value and are both considered good estimates of  $H_s$ . In fact, all modern wave forecast models report  $H_{mo}$  as the significant wave height. Similarly, the  $H_s$  values reported from wave gauge records is also  $H_{mo}$ . (It is exceedingly important to note, however, that in shallow water  $H_{1/3}$  may be significantly larger than  $H_{mo}$ , especially for low-frequency waves.)

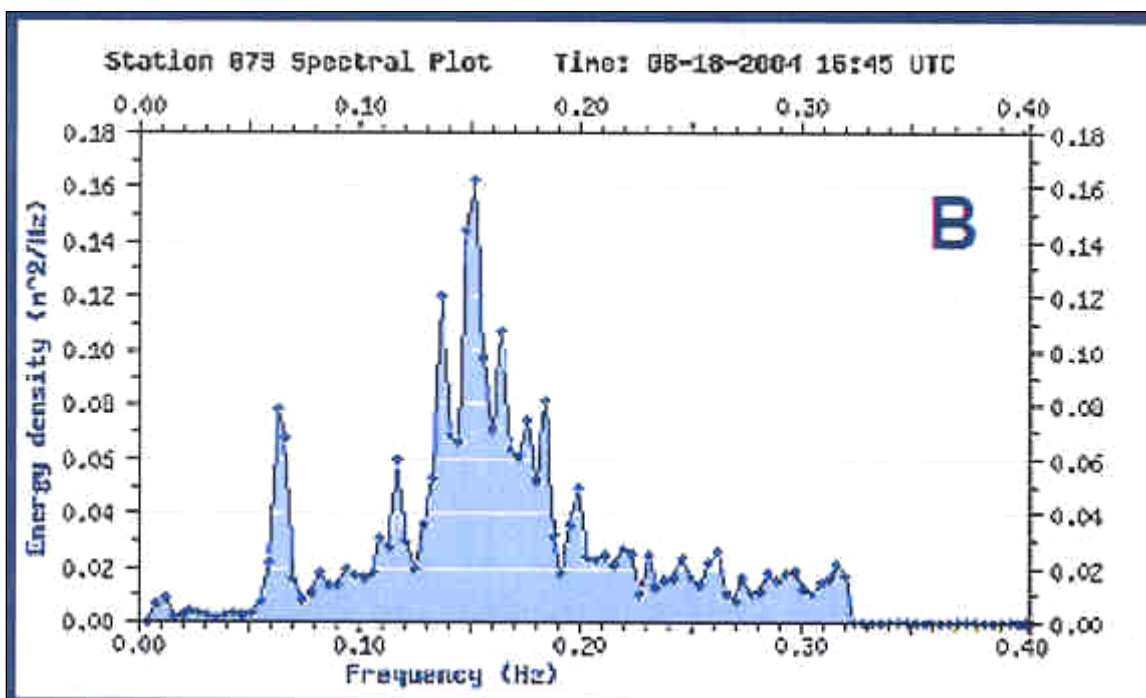


Figure 33. Ocean wave spectra showing broad, central peak of local wind seas.

### Aguadilla wave data

The MCNP Aguadilla Monitoring Plan originally envisioned a self-recording directional wave gage array in deep water directly offshore of the breakwater to record incident wave conditions driving the harbor wave action, and several self-recording wave gages inside the harbor. Wave measurements were needed within the harbor to ascertain whether the recently added revetment and wave absorbed was effective in quelling wave action within the harbor to within acceptable limits. In addition, wave gages on both sides of the breakwater would quantify wave transmission through the breakwater. The gages would be located at positions not affected by wave diffraction around the breakwater tip, or by reflected waves within the harbor. Measured transmitted waves would be compared to prediction based on design guidance provided by the *Coastal Engineering Manual* (U.S. Army Corps of Engineers 2002), and by its predecessor the *Shore Protection Manual* (U.S. Army Corps of Engineers 1984).

Field measurements were needed to determine if sand moving through the porous breakwater contributes significantly to harbor shoaling. The field component would be short-term deployment of bottom-mounted pressure gage pairs, with one gage at the seaward toe and the other at the leeward

toe of the breakwater. Analyses of the recorded sea surface elevation time series would be used to examine the time varying head difference between the ocean and the harbor to establish the forcing mechanisms for sand transport through the structure.

Throughout the time period of monitoring (2001 through 2004), the harbor substantially shoaled, making it impossible to obtain wave measurements within the harbor. However, the deepwater pressure wave gage array was installed in deep water offshore from the breakwater in water approximately 18 m (60 ft) deep, and collected deepwater data for two different time intervals; (a) November 2001 through March 2002, and (b) April 2003 through March 2004). The 1-Hz frequency data were processed by spectral analysis to determine significant deepwater wave height ( $H_{mo}$ ), wave period ( $T_p$ ), and wave direction of approach ( $D_p$ ). These deepwater wave data were used to validate the effectiveness of the project design, and will be a significant contribution to understanding alongshore movement of littoral materials as future harbor dredging must be addressed from the standpoint of remedial measures to reduce harbor shoaling by structural and mechanical means. The Aguadilla offshore gaged wave data are presented in Figures 34 through 50.

Because of the location of the harbor on the northwestern part of Puerto Rico, waves could only approach the harbor from about a west-to-northwest direction (270 to 300 deg azimuth). These gaged wave heights were generally less than about 0.5 m (1.5 ft) high, except for storms when wave heights could exceed 2.0 m (6.6 ft). Normal wave periods were about 6 to 8 sec, with storm wave periods becoming as large as 10 to 12 sec. These wave characteristics are sufficiently adequate for transporting sediment onshore across the surf zone.

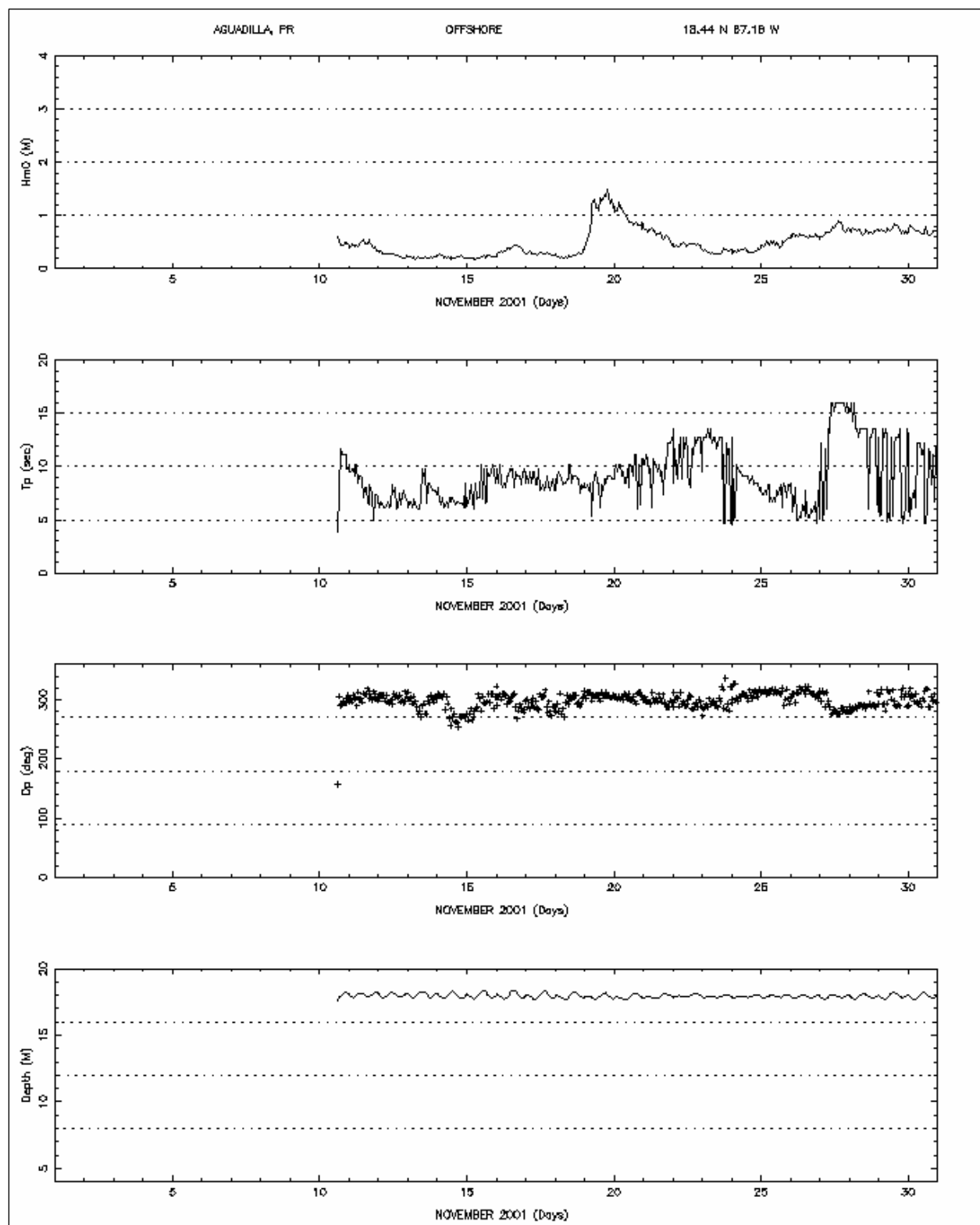


Figure 34. Aguadilla deepwater wave data offshore of breakwater, November 2001.

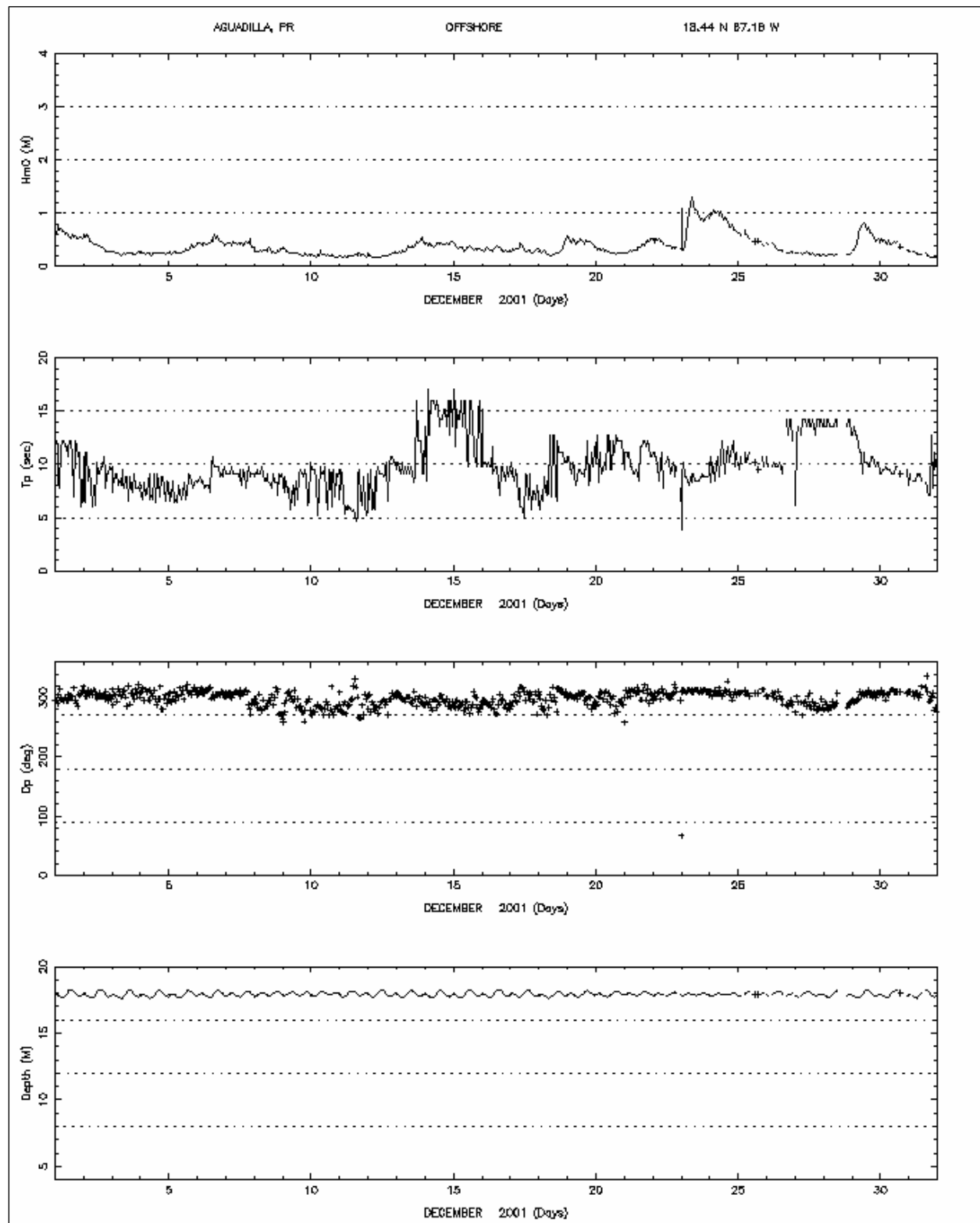


Figure 35. Aguadilla deepwater wave data offshore of breakwater, December 2001.

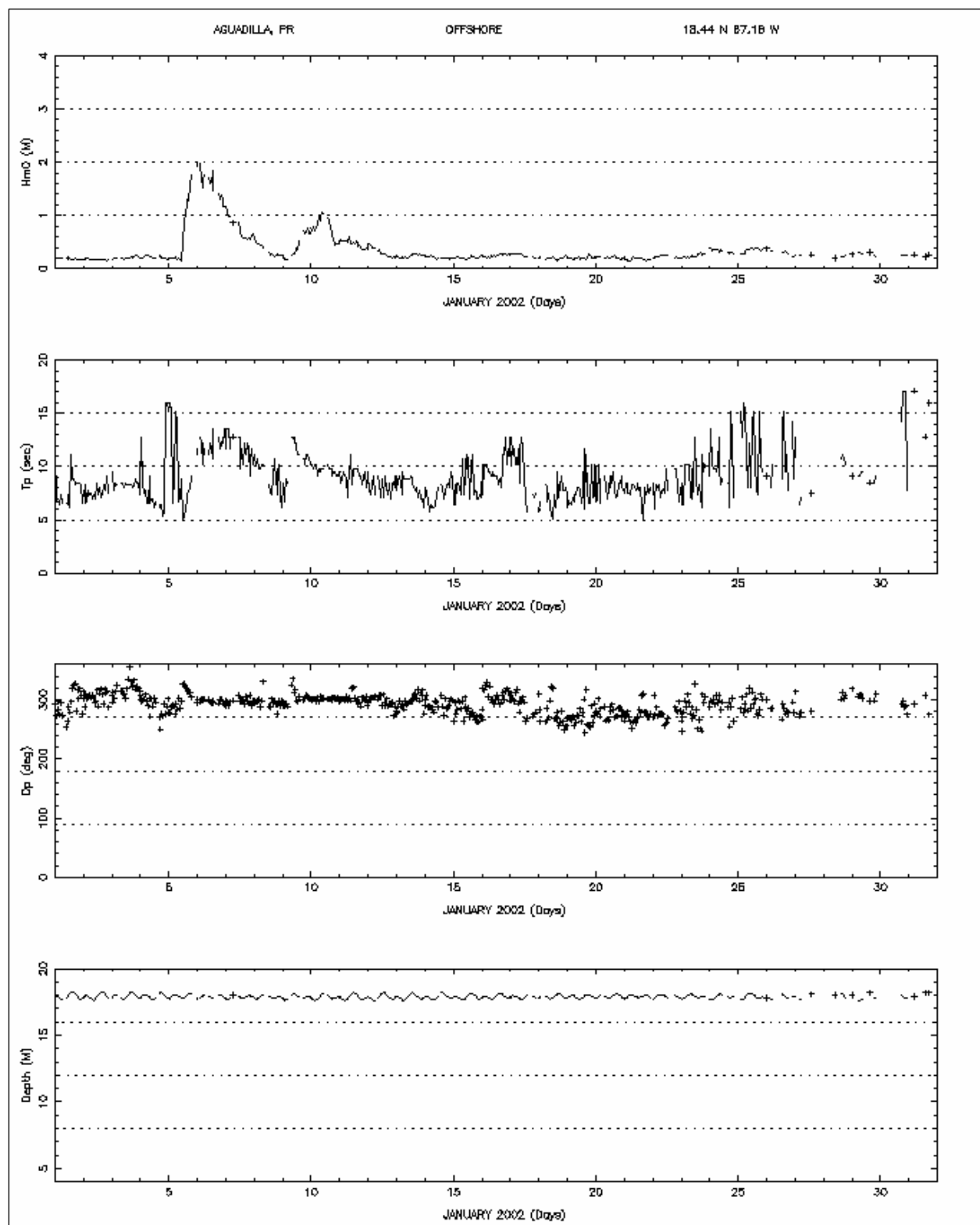


Figure 36. Aguadilla deepwater wave data offshore of breakwater, January 2002.

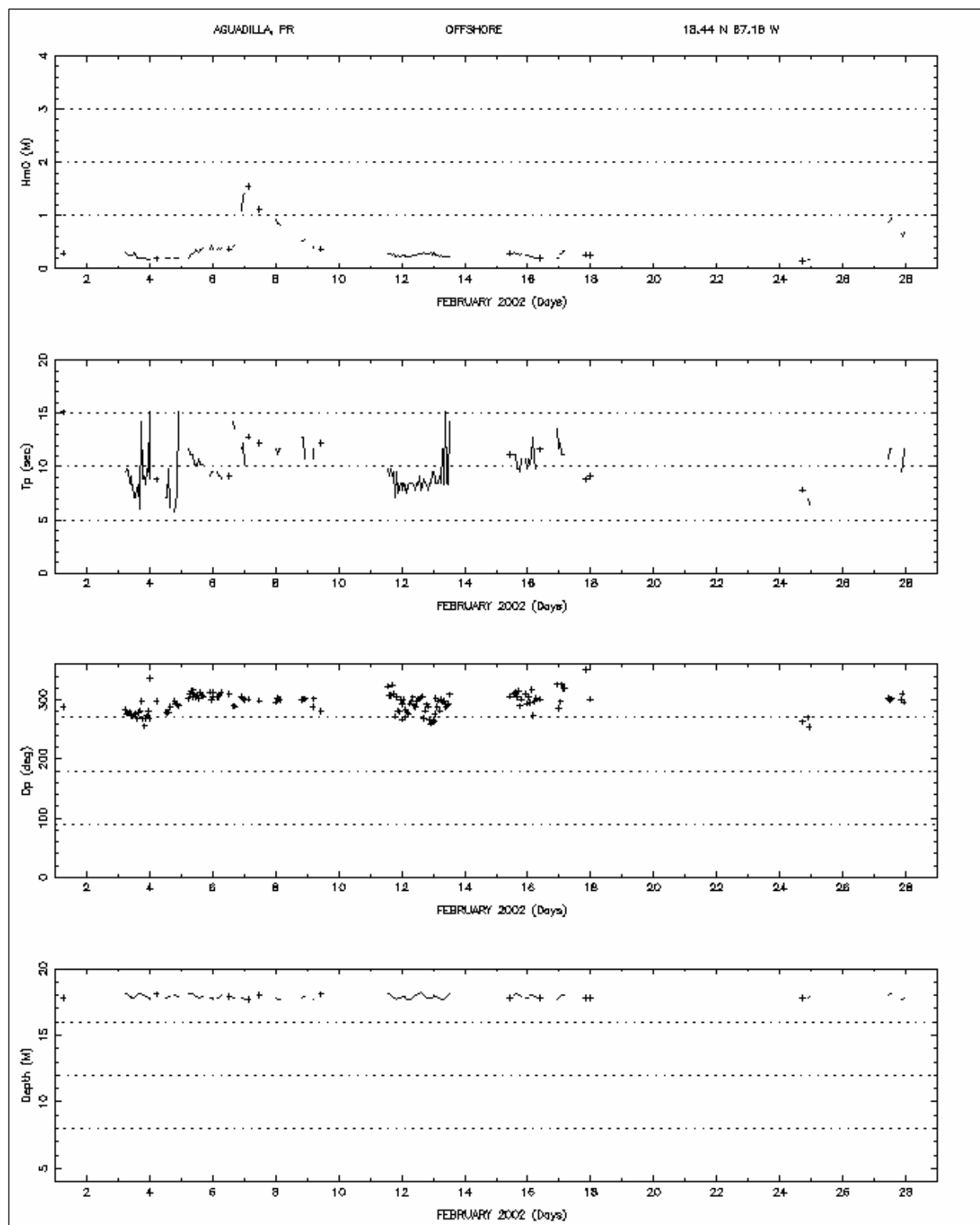


Figure 37. Aguadilla deepwater wave data offshore of breakwater, February 2002.

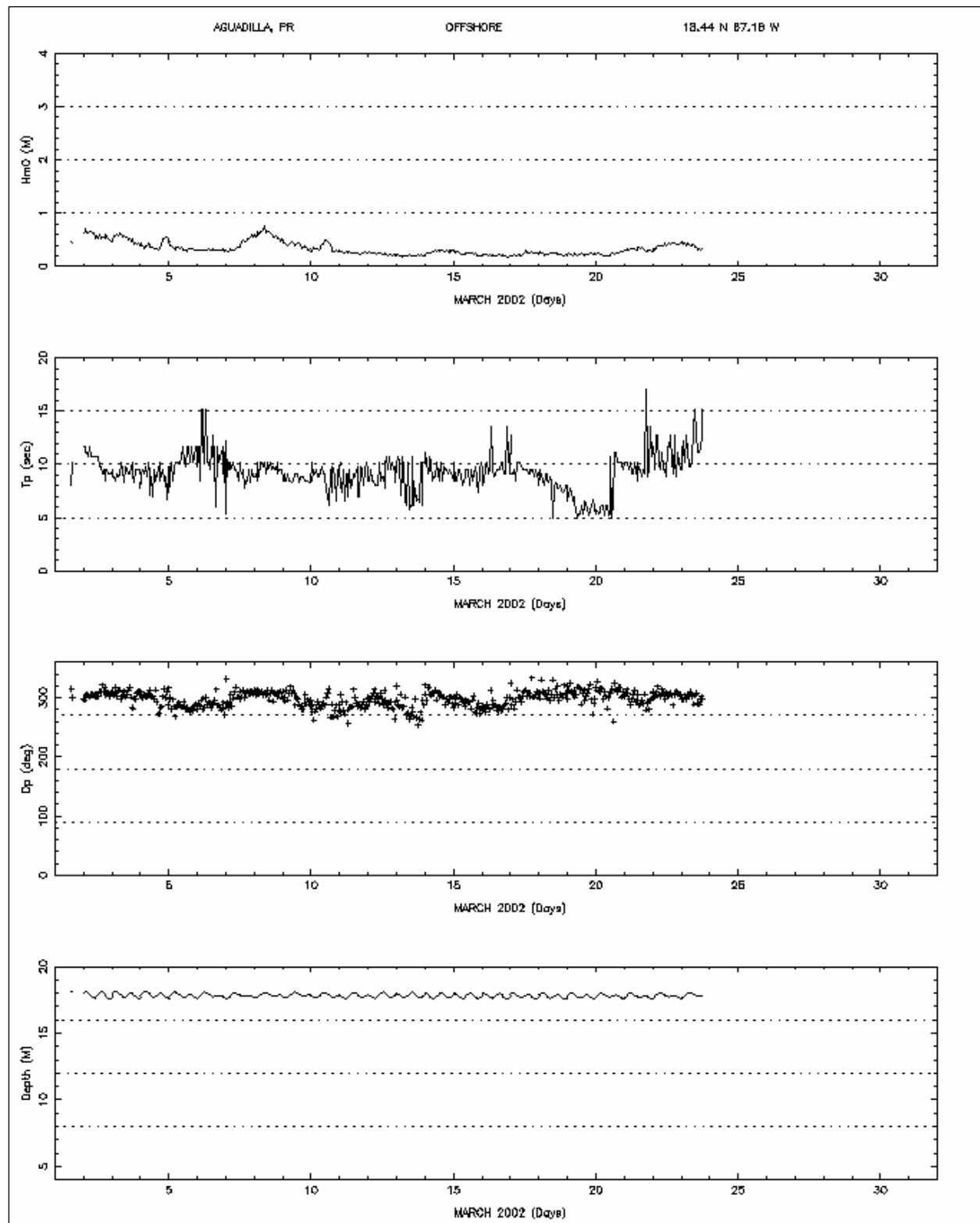


Figure 38. Aguadilla deepwater wave data offshore of breakwater, March 2002.

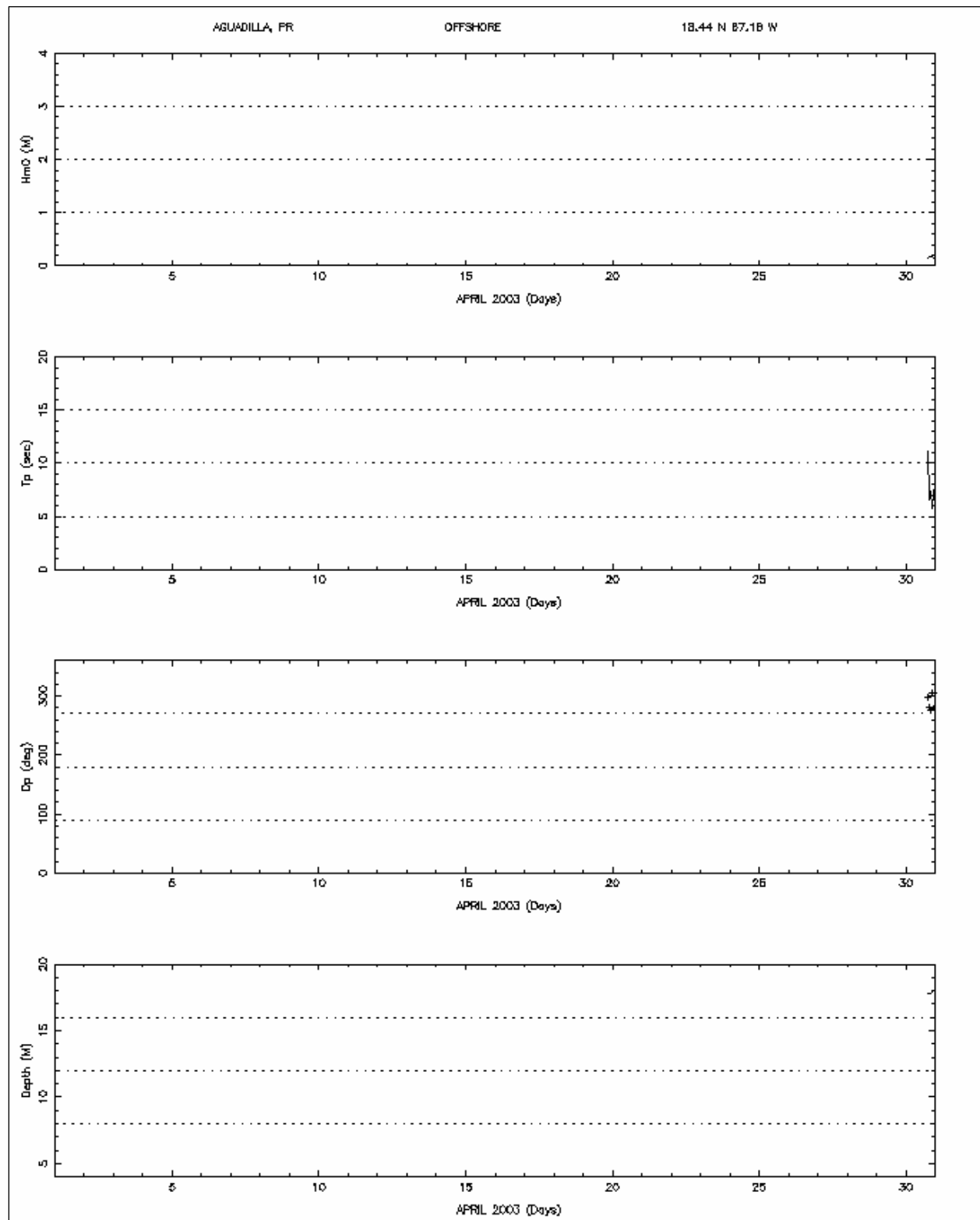


Figure 39. Aguadilla deepwater wave data offshore of breakwater, April 2003.

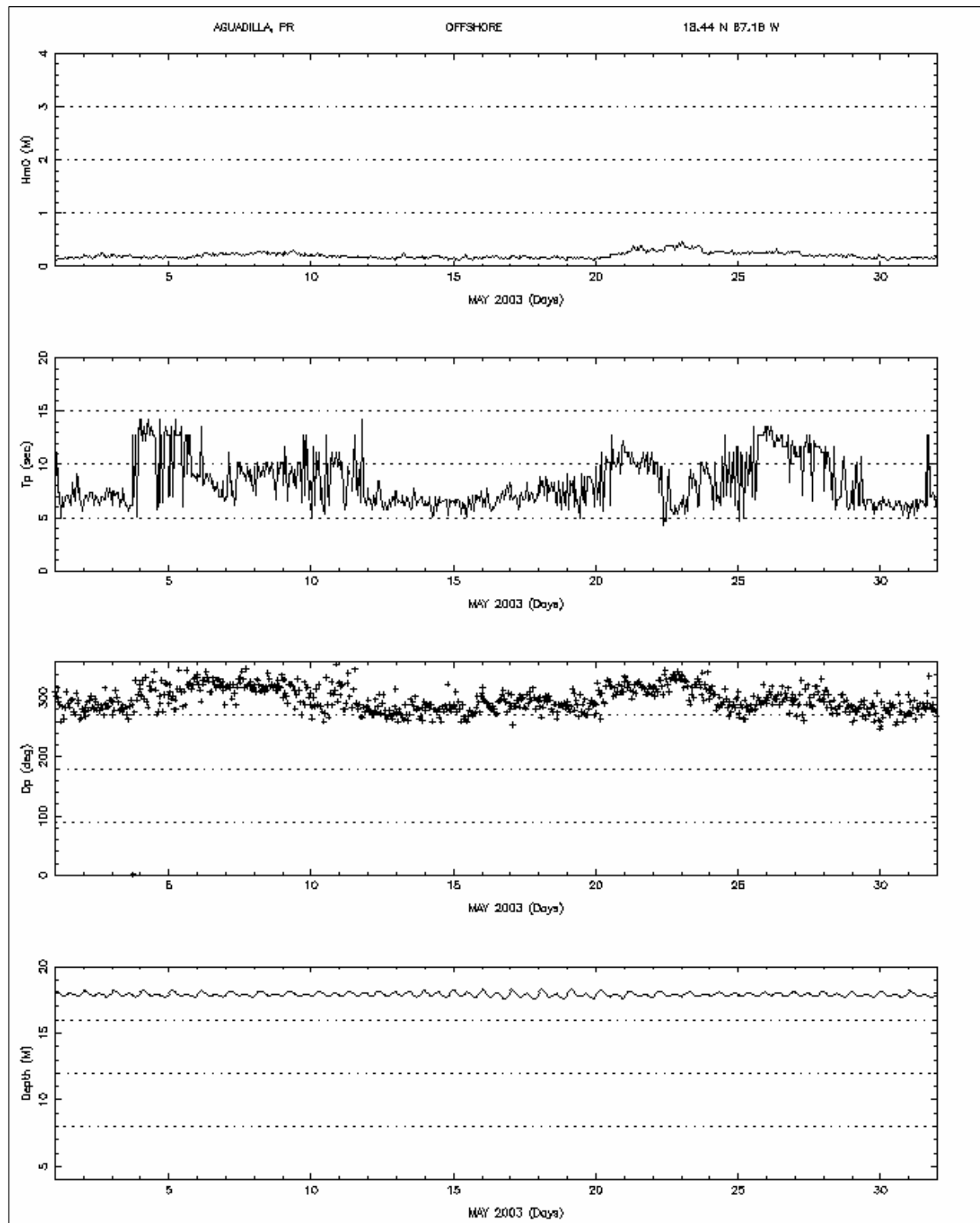


Figure 40. Aguadilla deepwater wave data offshore of breakwater, May 2003.

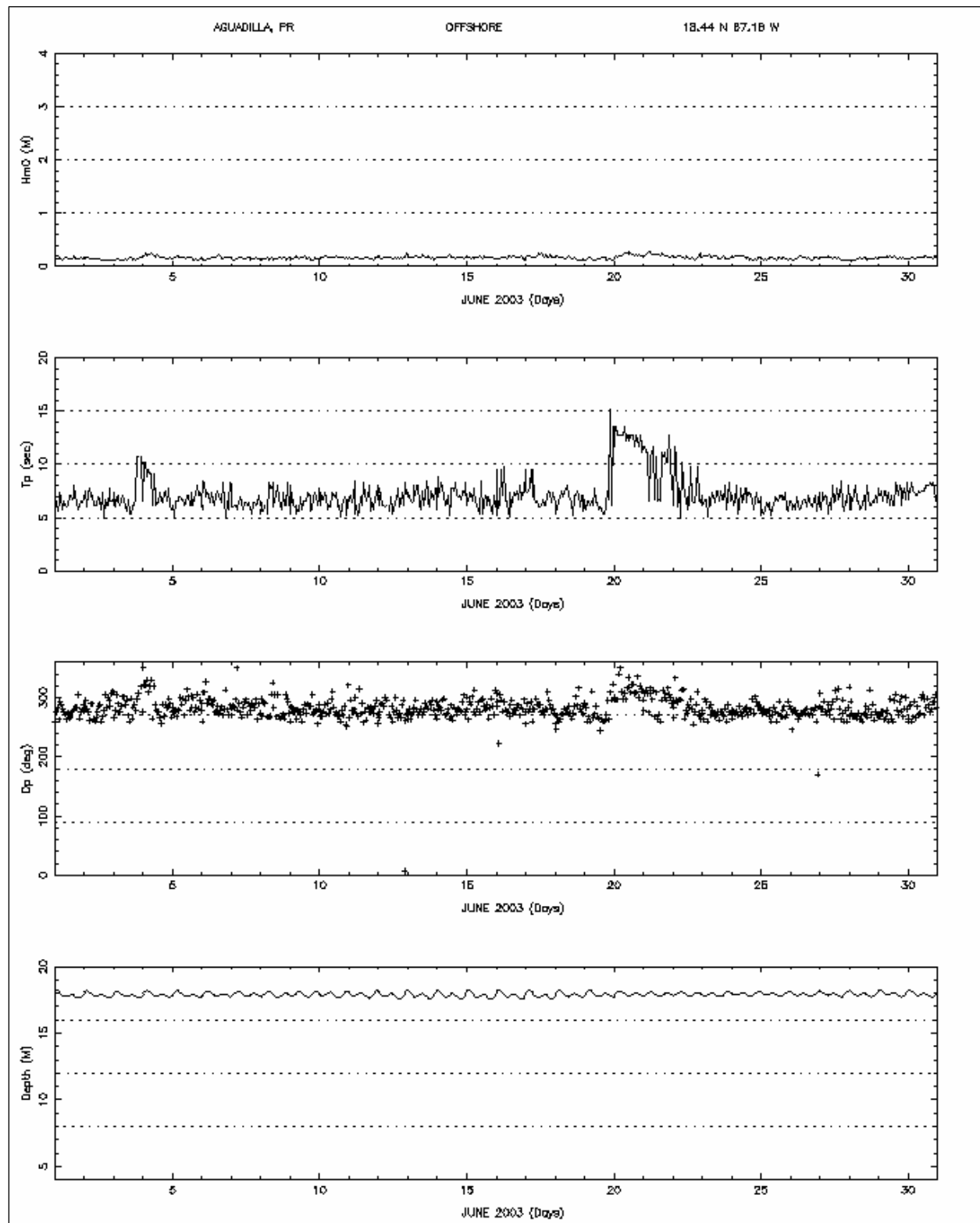


Figure 41. Aguadilla deepwater wave data offshore of breakwater, June 2003.

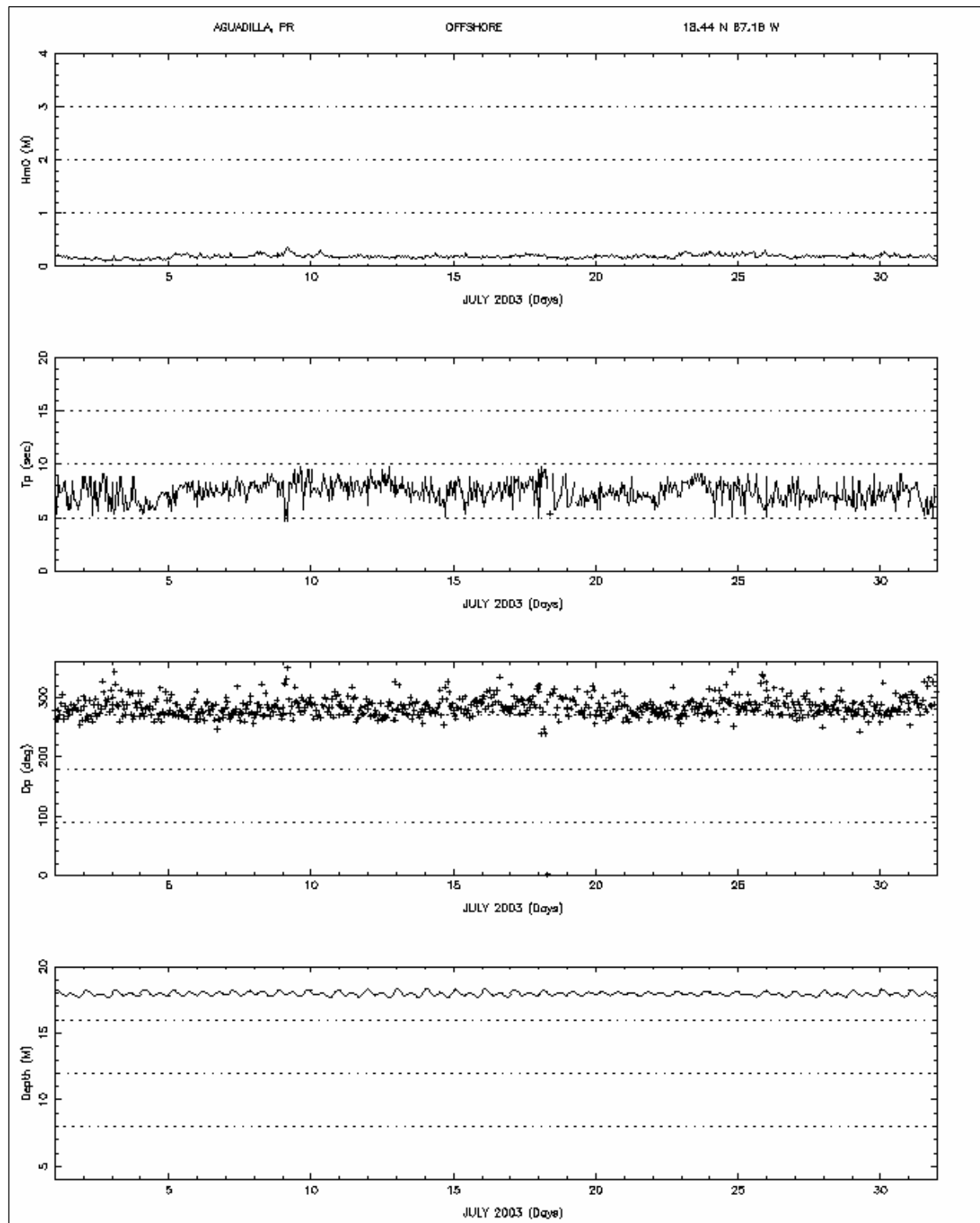


Figure 42. Aguadilla deepwater wave data offshore of breakwater, July 2003.

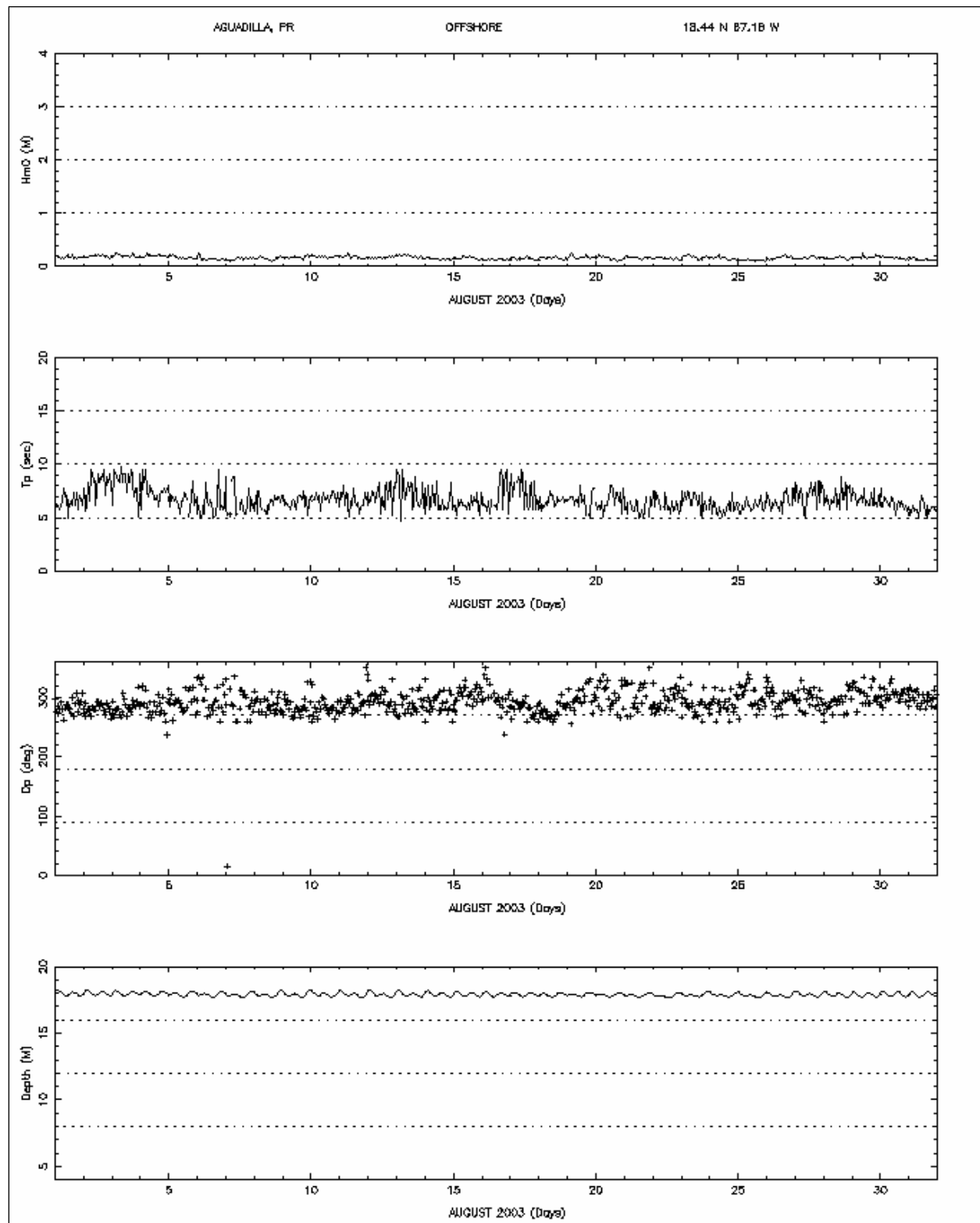


Figure 43. Aguadilla deepwater wave data offshore of breakwater, August 2003.

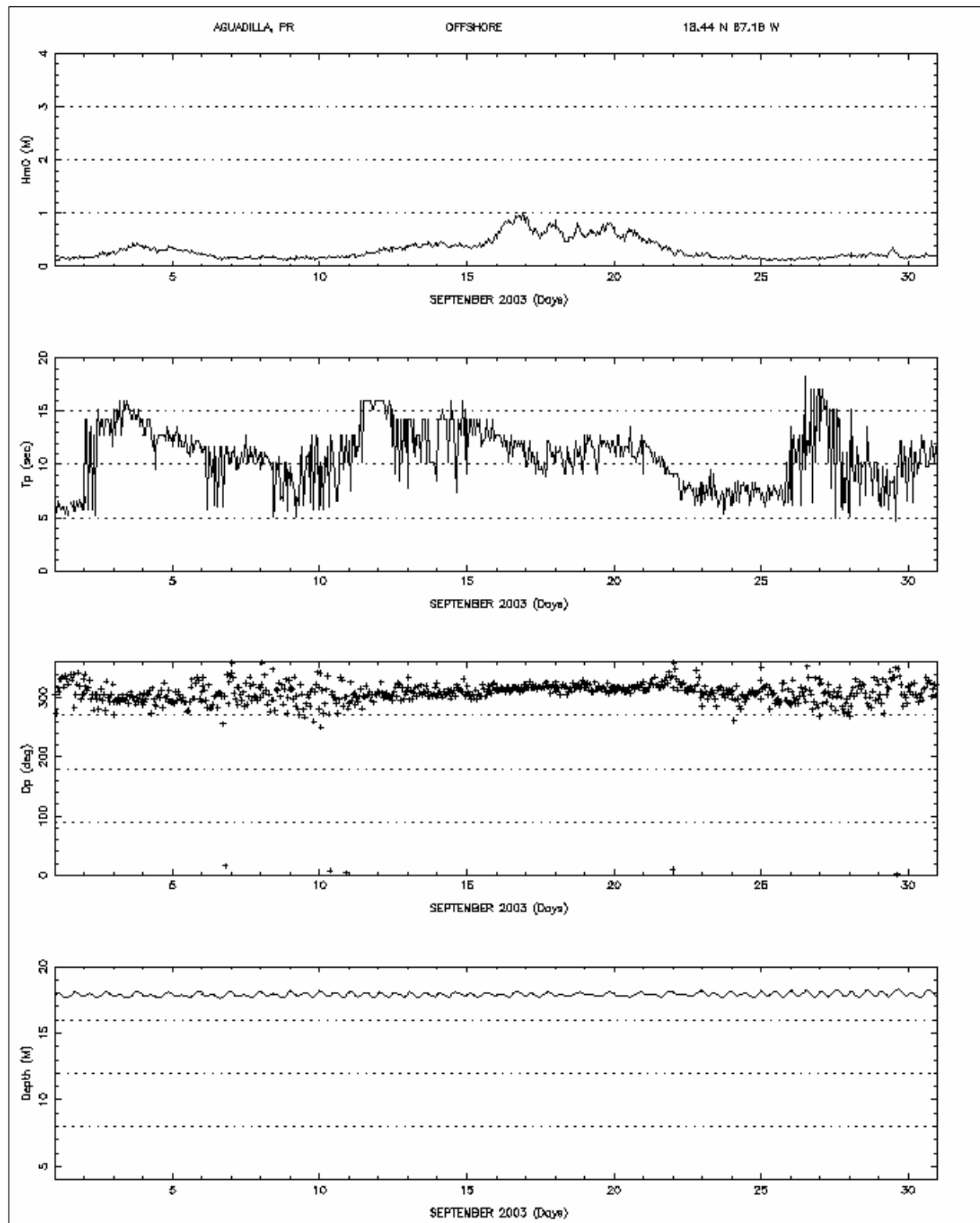


Figure 44. Aguadilla deepwater wave data offshore of breakwater, September 2003.

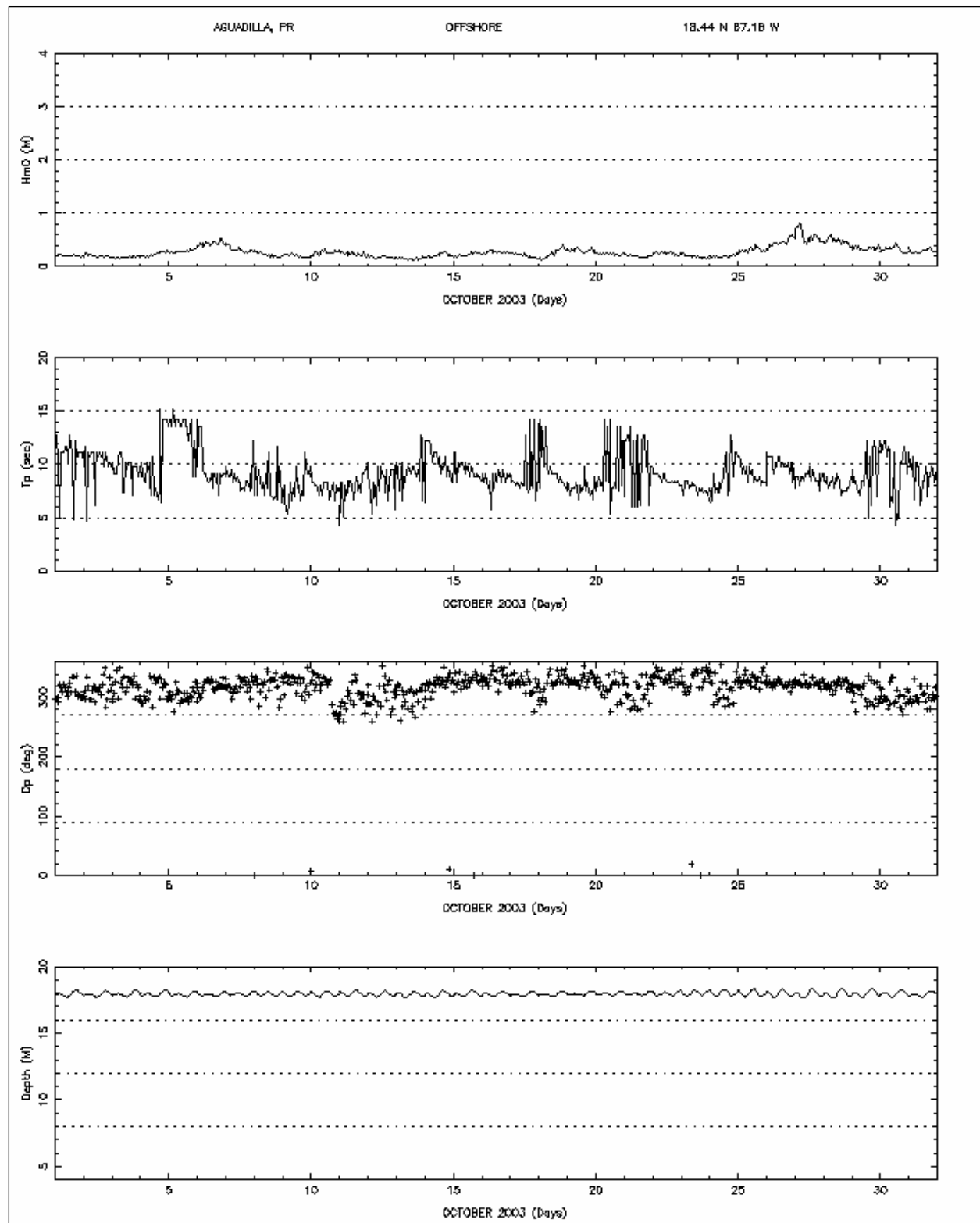


Figure 45. Aguidilla deepwater wave data offshore of breakwater, October 2003.

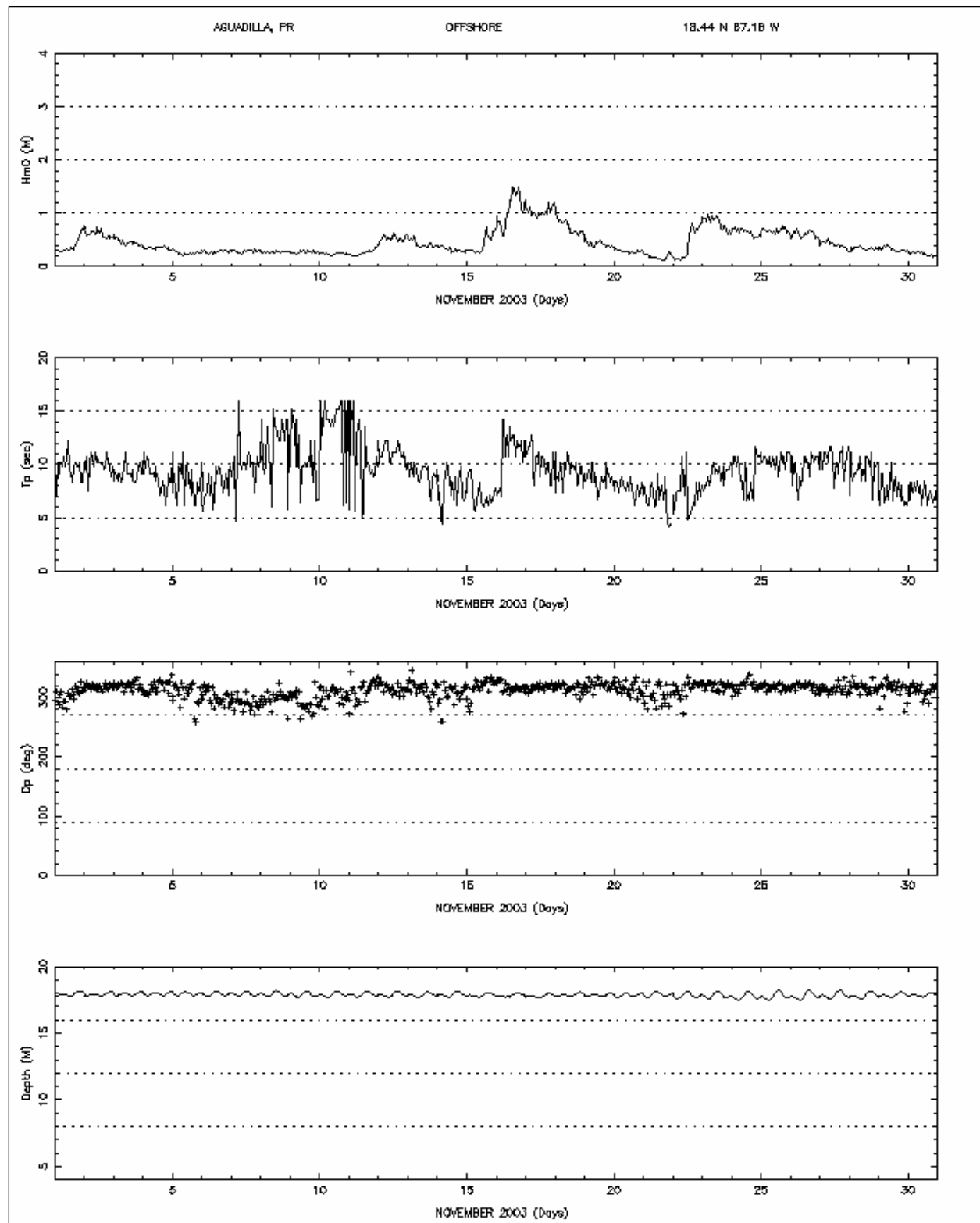


Figure 46. Aguadilla deepwater wave data offshore of breakwater, November 2003.

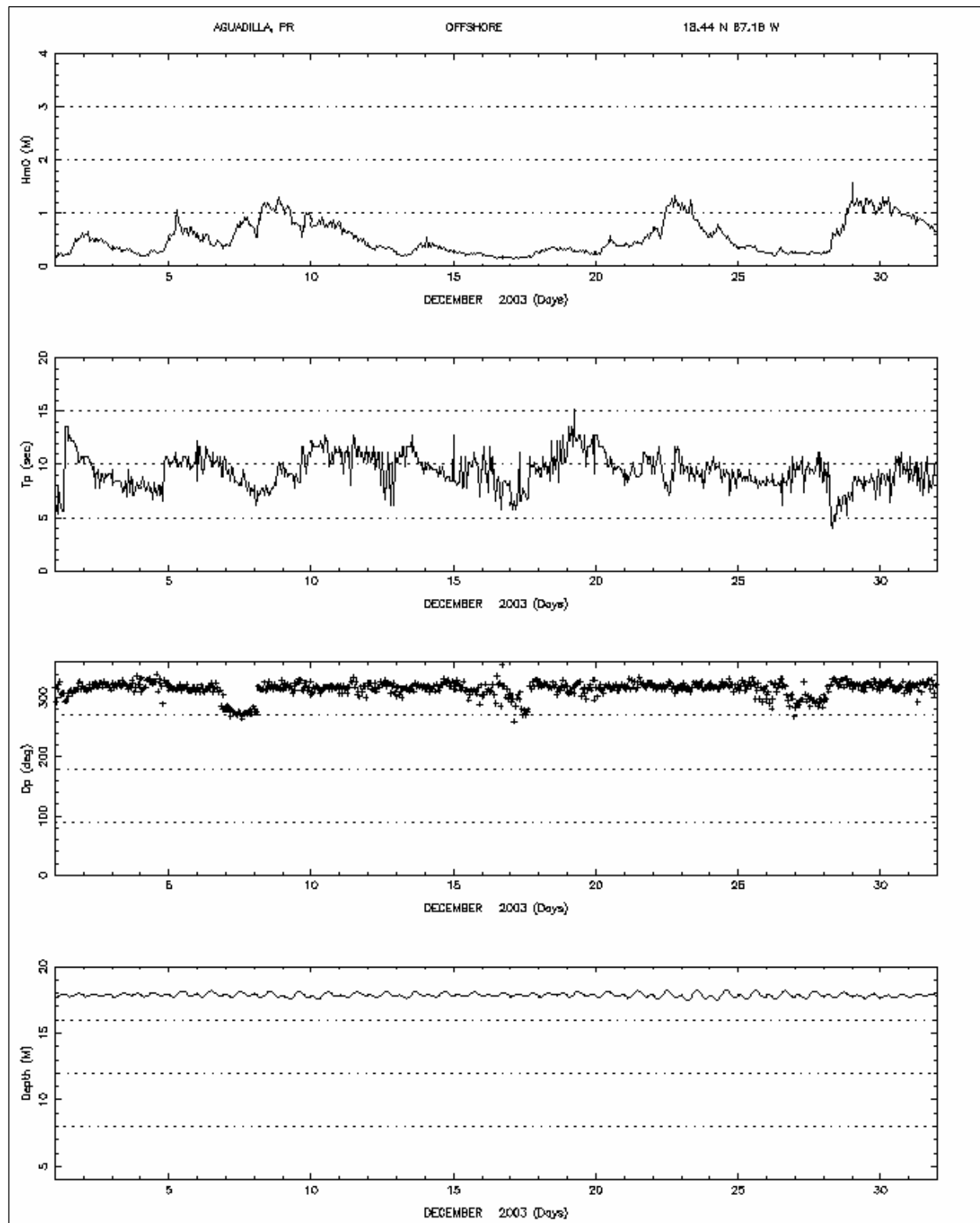


Figure 47. Aguadilla deepwater wave data offshore of breakwater, December 2003.

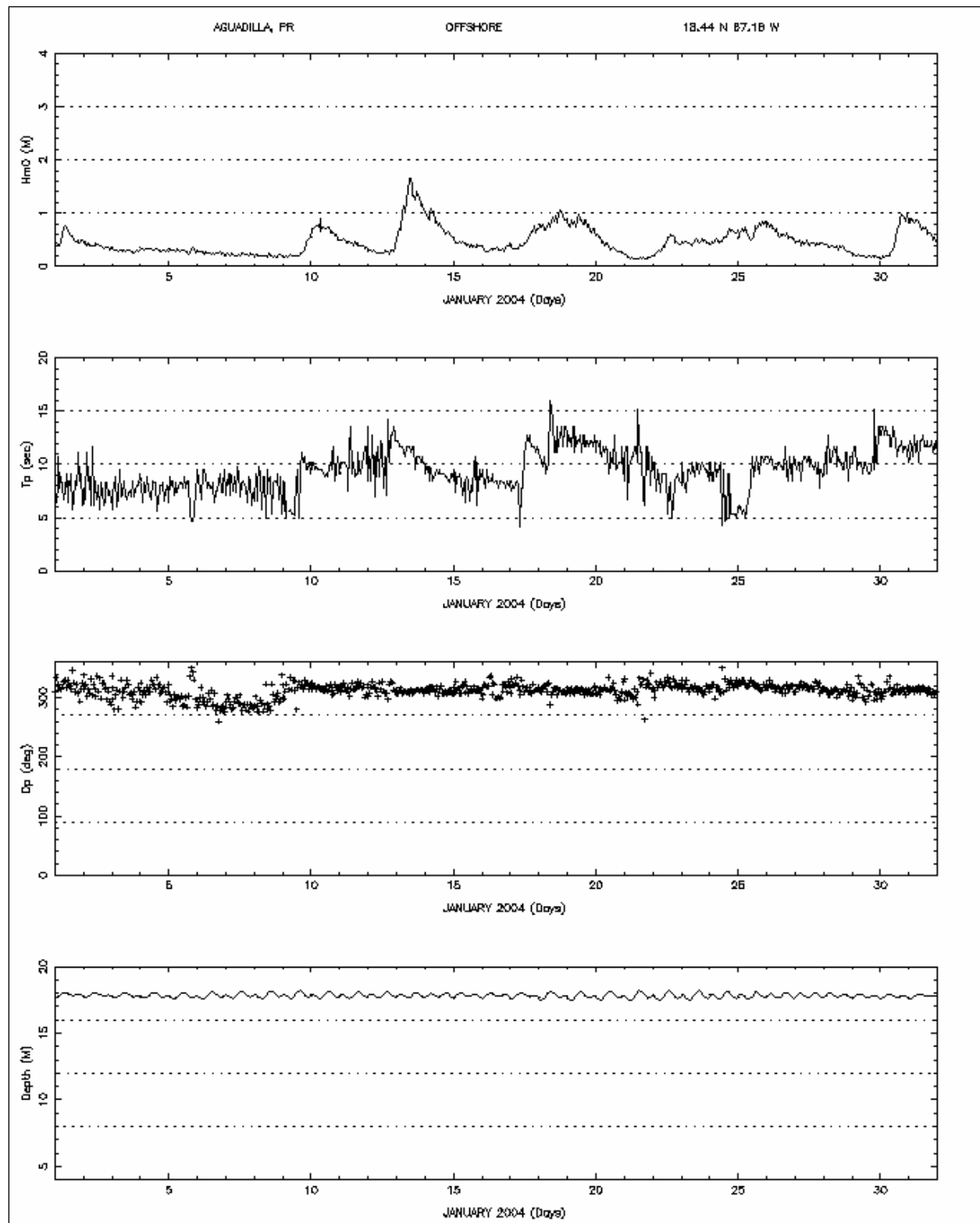


Figure 48. Aguadilla deepwater wave data offshore of breakwater, January 2004.

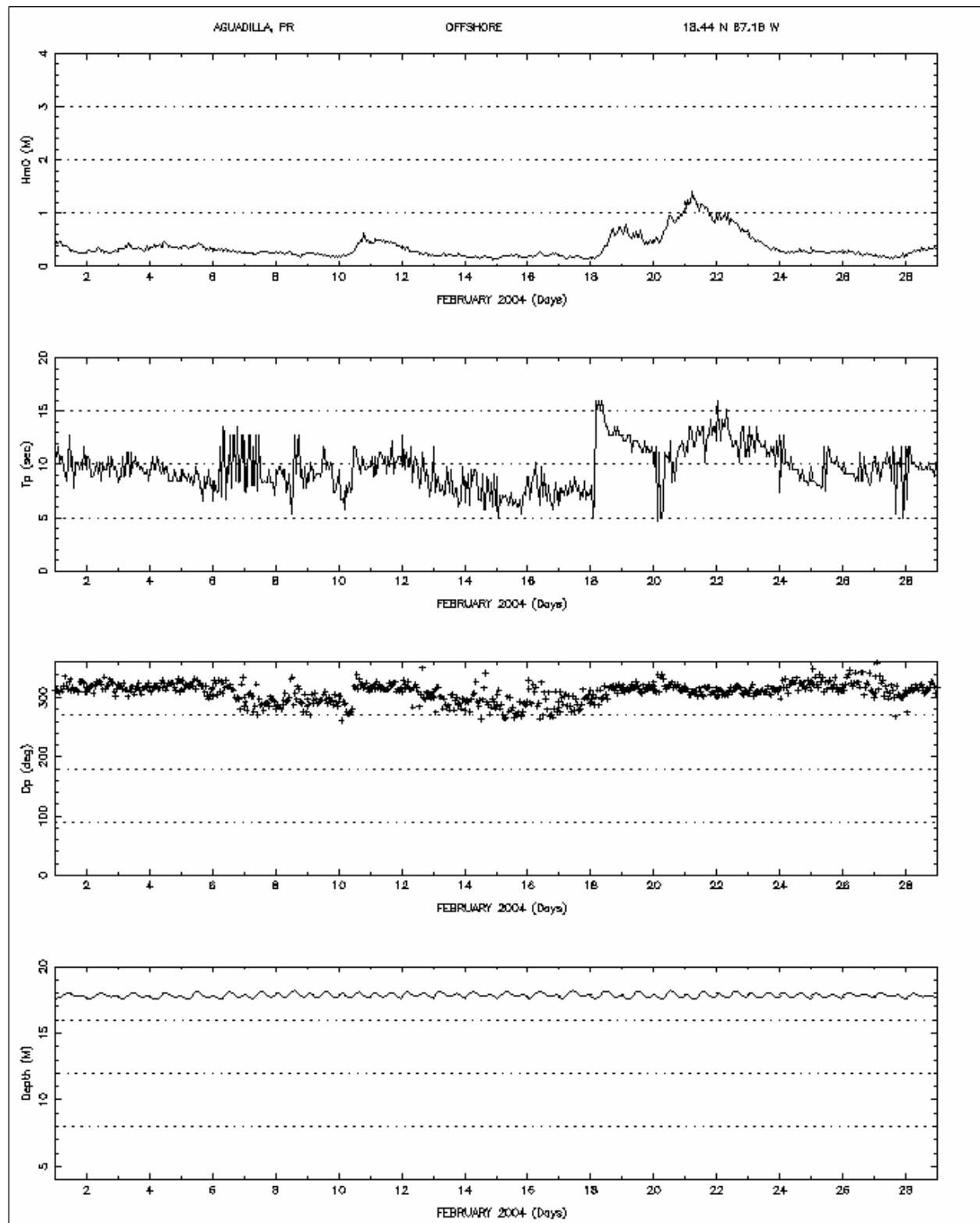


Figure 49. Aguadilla deepwater wave data offshore of breakwater, February 2004.

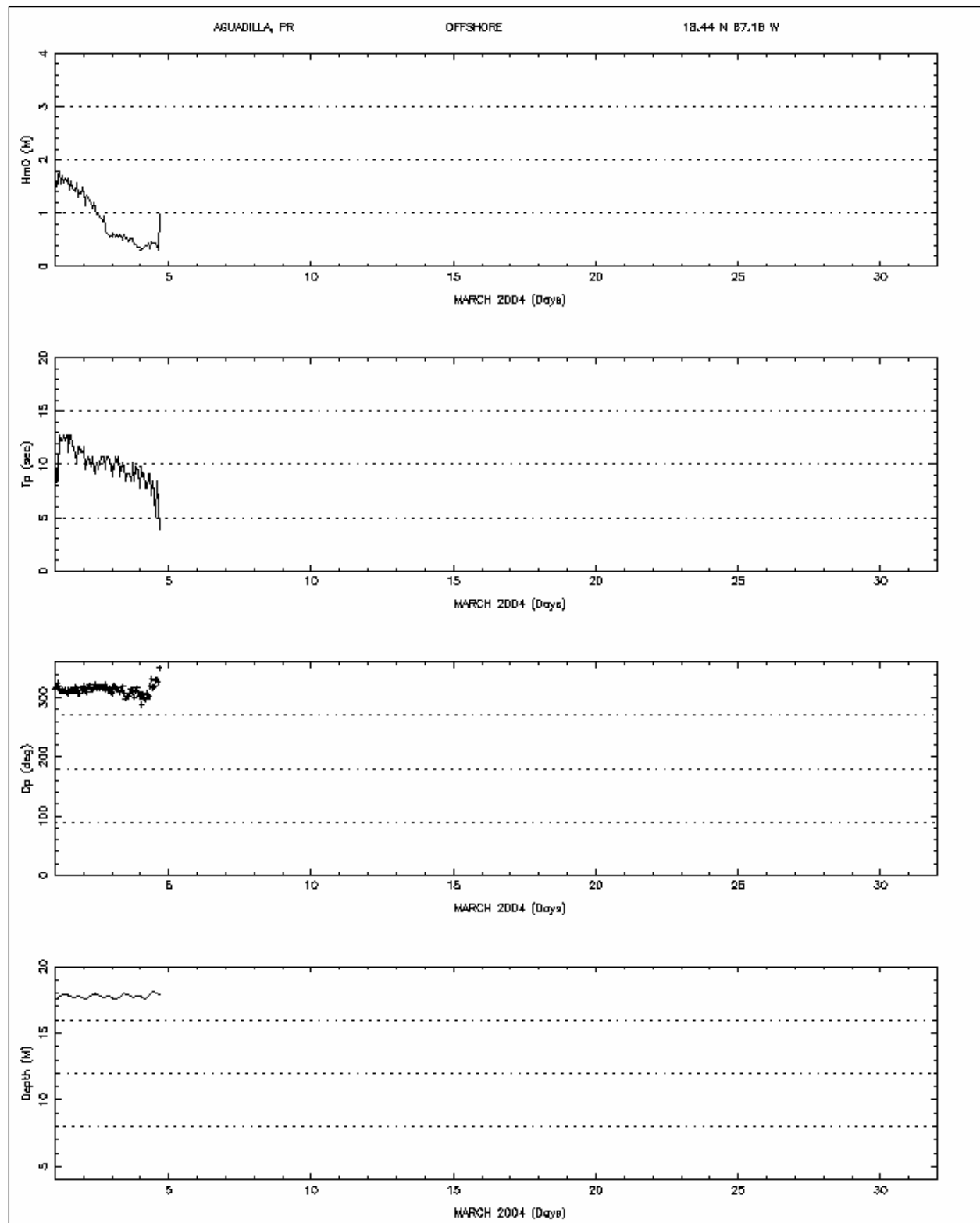


Figure 50. Aguidilla deepwater wave data offshore of breakwater, March 2004.

## 6 Scanning Hydrographic Operational Airborne Lidar Survey (SHOALS)

### SHOALS

The Scanning Hydrographic Operational Airborne Lidar Survey (SHOALS) is an airborne laser system that makes water-depth soundings. The system is mounted on a deHavilland Twin Otter fixed-wing aircraft (Figure 51). The laser is collimated red (1,064 nanometers) and green (532 nanometers) light pulsed at a rate of 400 Hz. A scanning mirror directs each laser pulse toward the sea surface and into the forward flight path of the aircraft. Receivers in the aircraft detect the return of each pulse from the sea surface (specular interface reflection) and seafloor (diffuse bottom reflection and reflected bottom signal) (Figure 52). These returns are analyzed to determine water depth or land elevation for each laser pulse. Each measurement is geopositioned using either pseudo-range or carrier-phase GPS techniques. The result is (x-y-z) data with accuracies of 1 to 3 m (3 to 10 ft) in the horizontal and 0.15 m (0.5 ft) in the vertical (Wozencraft and Millar 2005). Hydrographic lidar data are generally collected at a 3 m by 3 m (10 ft by 10 ft) sounding density with 200 percent coverage, while topographic lidar data are generally collected at a 2 m by 1 m (6 ft by 3 ft) sounding density with 100 percent coverage.



Figure 51. deHavilland DHC-6 Twin Otter fixed wing aircraft for SHOALS platform.

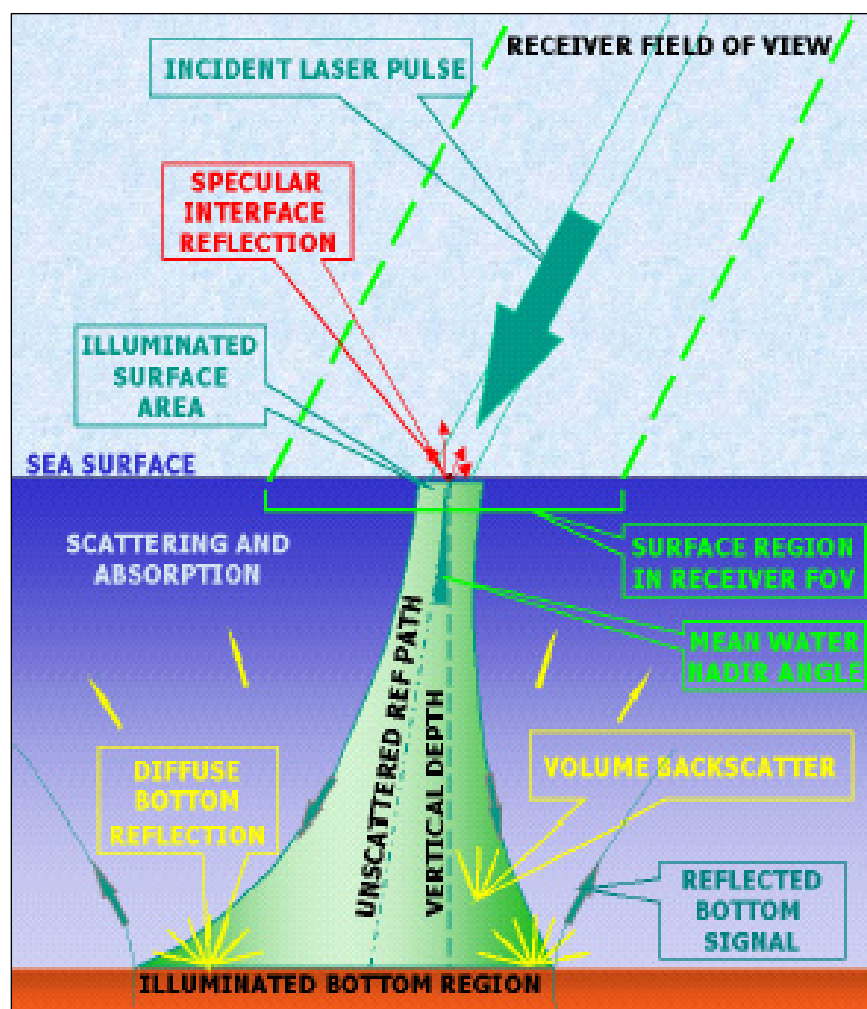


Figure 52. SHOALS bathymetric lidar propagating through the water column (after Wozencraft et al. 2002)

The maximum water depths detectable by SHOALS are limited by water clarity, or the amount of turbidity in the water column. As the laser pulses travel through the water column, several processes occur that limit the amount of light to eventually reflect from the seafloor and return to the receivers in the aircraft. Light energy is lost during refraction and is scattered and absorbed by particles in the water and by water molecules themselves. In practice, SHOALS can see 2 to 3 times the Secchi, or visible water depth. In the clearest coastal waters, the maximum detectable depth is about 60 m (200 ft) (Smith et al. 2000; Lillycrop and Banic 1993).

SHOALS is managed by the Joint Airborne Lidar Bathymetry Technical Center of Expertise (JALBTCX), located at the U.S. Army Engineer District, Mobile ([http://shoals.sam.usace.army.mil/Data/Data\\_Home.asp](http://shoals.sam.usace.army.mil/Data/Data_Home.asp)). Spatial data are being acquired and used to characterize physical and

environmental conditions of the U.S. coastal zones along the Atlantic, Pacific, Gulf of Mexico, Great Lakes, and Puerto Rico. Physical conditions such as elevations, bathymetry, and shoreline position, and environmental resources data such as wetlands, hard bottom sediments, and land use are collected by implementing a program with other agencies to acquire their regional data.

### **Aguadilla Harbor vicinity lidar survey**

JALBTCX was contracted by CHL in September 2001 to conduct a hydrographic survey of the vicinity of Aguadilla Harbor breakwater for an along-shore distance of about 1.6 km (1 mile) north and south of the harbor, and offshore to about a water depth of 30 m (100 ft) or 2,000 m (6,500 ft). The deHavilland Twin Otter flew at altitudes between 200 and 400 m (60 and 120 ft) with a ground speed of about 100 knots (115 mph). The breakwater was covered by a minimum of three passes. SHOALS has previously demonstrated capabilities that meet U.S. Army Corps of Engineers Hydrographic Survey accuracy requirements for Class 1 surveys, and the International Hydrographic Organization nautical charting standards for Order 1.

The SHOALS airborne system acquires a tremendous volume of raw data during a single mission. The lidar data are unique and require a specialized Data Processing System (DPS) for post-processing. The DPS main functions are to (a) import airborne data storage on high density data tape, (b) perform quality control checks on initial depths and horizontal positions, (c) provide display and edit capabilities, (d) calculate depth and position (x-y-z) values for each sounding, and (e) output final positions and depths for each sounding. The processed bathymetric survey charts for the vicinity of Aguadilla Harbor are presented in Figures 53 and 54.

Offshore of Aguadilla Harbor the bathymetry contours are reasonably straight and parallel to shore. There appears to be no particular bathymetry features that would refract waves in such a way to enhance sediment transport in the vicinity of the harbor. However, further south there are two large outcroppings (see Figure 53) that most definitely affect local waves and current patterns.

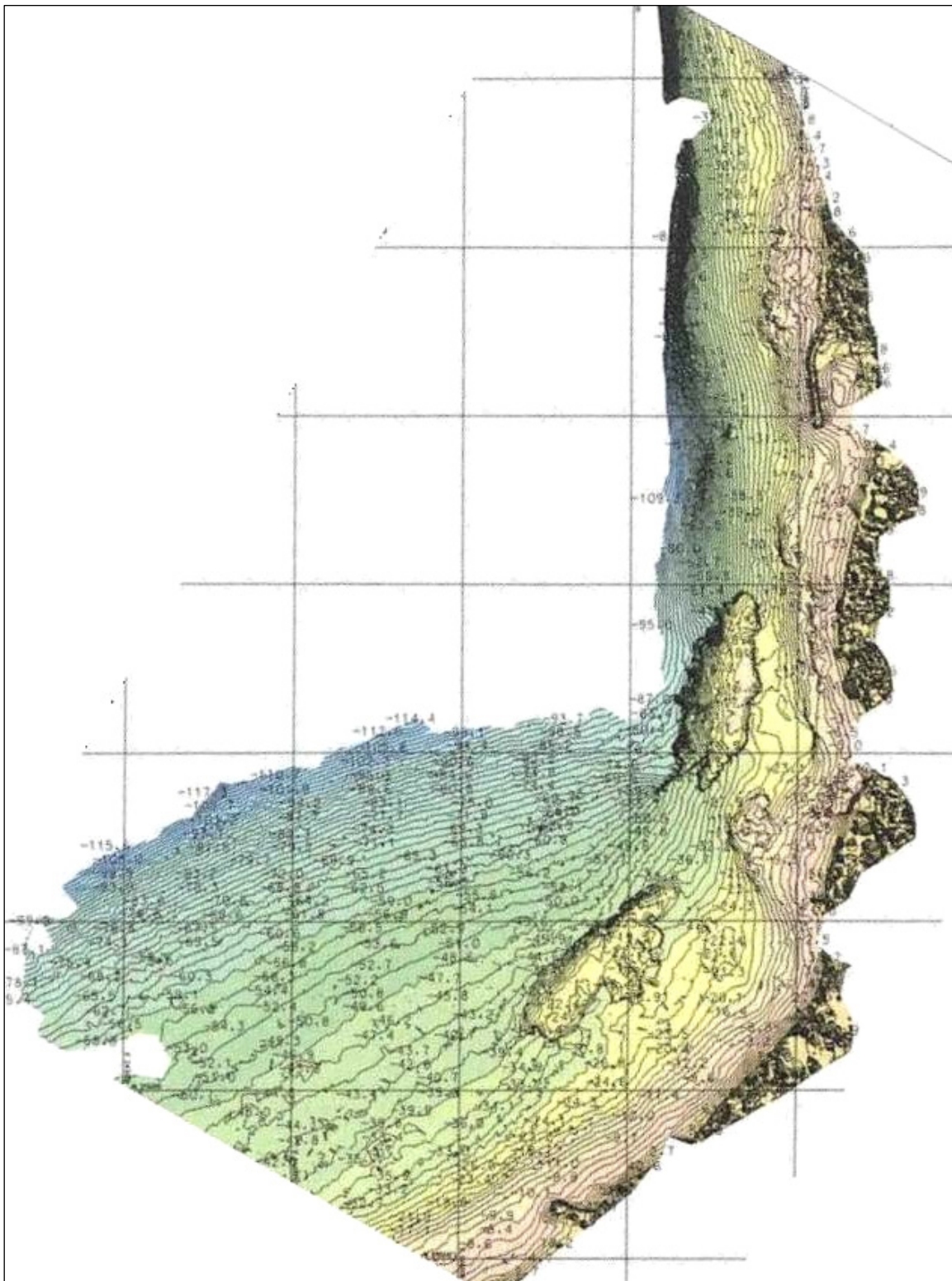


Figure 53. Scanning Hydrographic Operational Airborne Lidar Survey (SHOALS) bathymetric survey contours (feet, mean lower low water) of vicinity of Aguadilla Harbor, Puerto Rico.

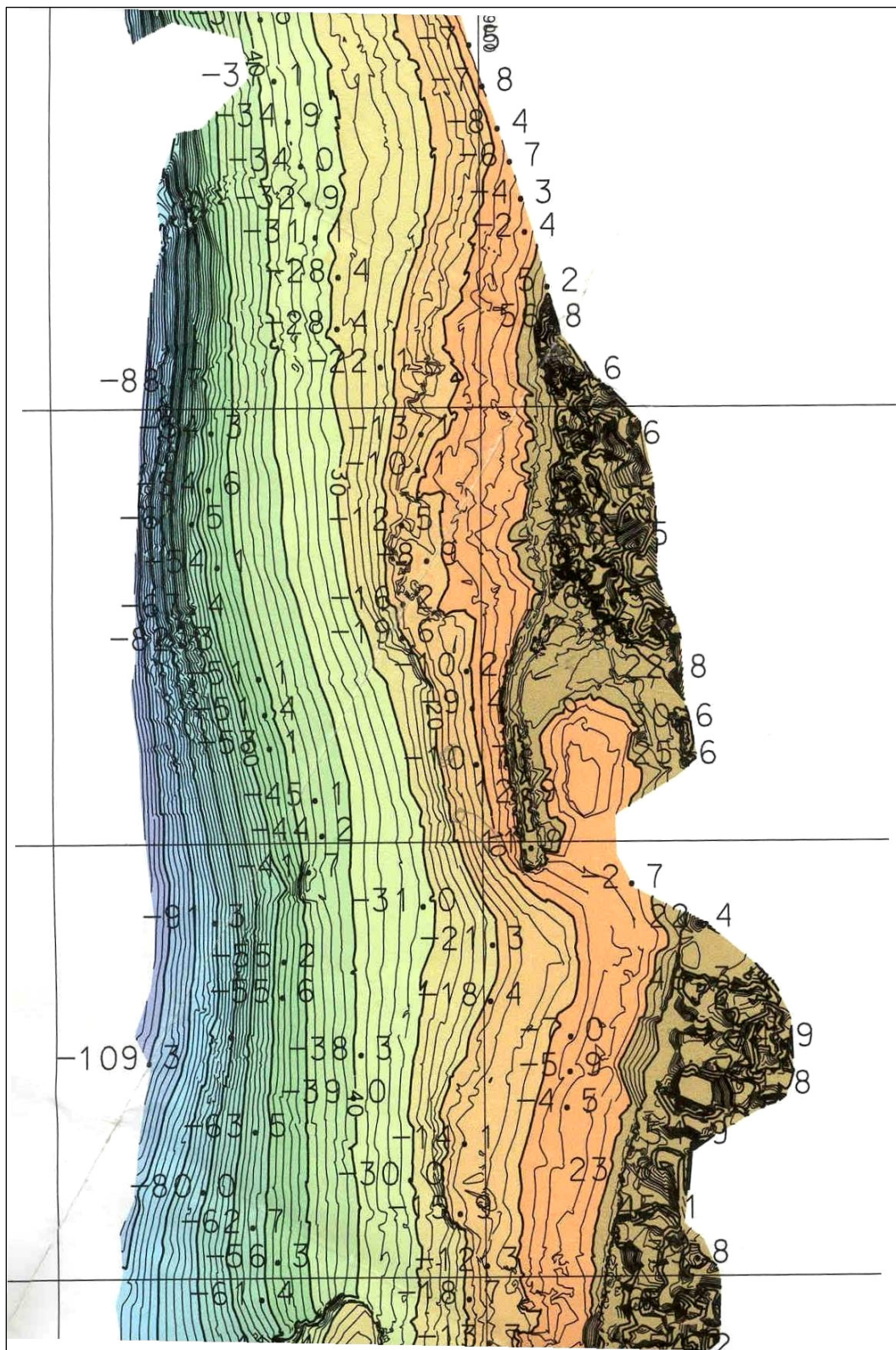


Figure 54. Scanning Hydrographic Operational Airborne Lidar Survey (SHOALS) bathymetric survey contours (feet, mean lower low water) near Aguadilla Harbor breakwater, Puerto Rico.

## 7 Geophysical Investigations<sup>1</sup>

Evans-Hamilton, Inc., Seattle, WA, was contracted by ERDC-CHL in early 2002 to perform a seabed sediment survey of an area immediately off-shore of the Aguadilla Harbor, Puerto Rico, breakwater. The survey area extended north to south for approximately 1.6 km (1 mile) roughly centered on the breakwater; and east to west with the beachfront as the eastern boundary and approximately 18 m (60 ft) of seawater as the western boundary. The purpose of the data collection was to map the extent and depth of sand versus hard bottom in the area. The marine geophysical instruments appropriate for this mapping effort were side-scan sonar (SSS), a subbottom profiler (SBP), and a seismic reflection (SR) system.

### Bathymetry and geophysical surveys

Survey transects were designed by utilizing bathymetric data supplied by CHL. These bathymetric data refer to Scanning Hydrographic Operational Airborne Lidar Survey (SHOALS) Survey No. 01-008 collected June 2001, with coordinates based on Puerto Rico State Plane, North Atlantic Datum 1927. The SHOALS bathymetric charts (previously discussed in Chapter 6) and supplied by CHL to Evans-Hamilton Inc. are shown in Figures 55 and 56. All aspects of the field survey were carried out aboard the University of Puerto Rico (UPR) research vessel *R. V. Sultana* that was contracted for the survey.

The survey commenced 14 May 2002 with loading of equipment and mobilization and testing of the navigation and side-scan sonar systems. This effort was accomplished at the UPR Marine Facility in Mayaguez, Puerto Rico. Following mobilization; the vessel was fueled and made ready for transit to Aguadilla.

The *R. V. Sultana* transited to Aguadilla in the early morning hours of 15 May 2002. Collection of side-scan sonar data commenced at approximately 0700 hr, and was complete by 1700 hr. Subbottom profile and seismic reflection data collection began at approximately 0700 hr on May 16, and were complete by 1500 hr. The equipment was made ready for transit, and the vessel returned to Mayaguez for demobilization.

---

<sup>1</sup> This section is extracted essentially verbatim from Evans-Hamilton Inc. (2002).

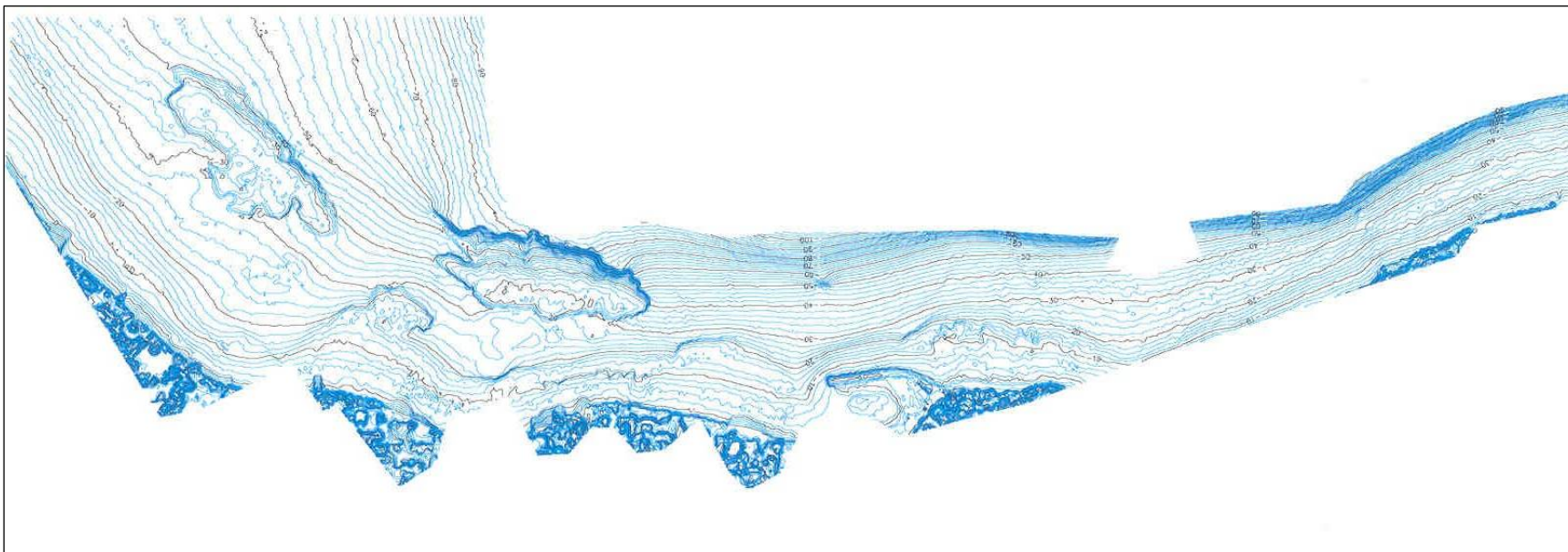


Figure 55. Bathymetric contours (feet, mean lower low water) acquired by the Scanning Hydrographic Operational Airborne Lidar Survey (SHOALS) system near the vicinity of Aguadilla Harbor, Puerto Rico.

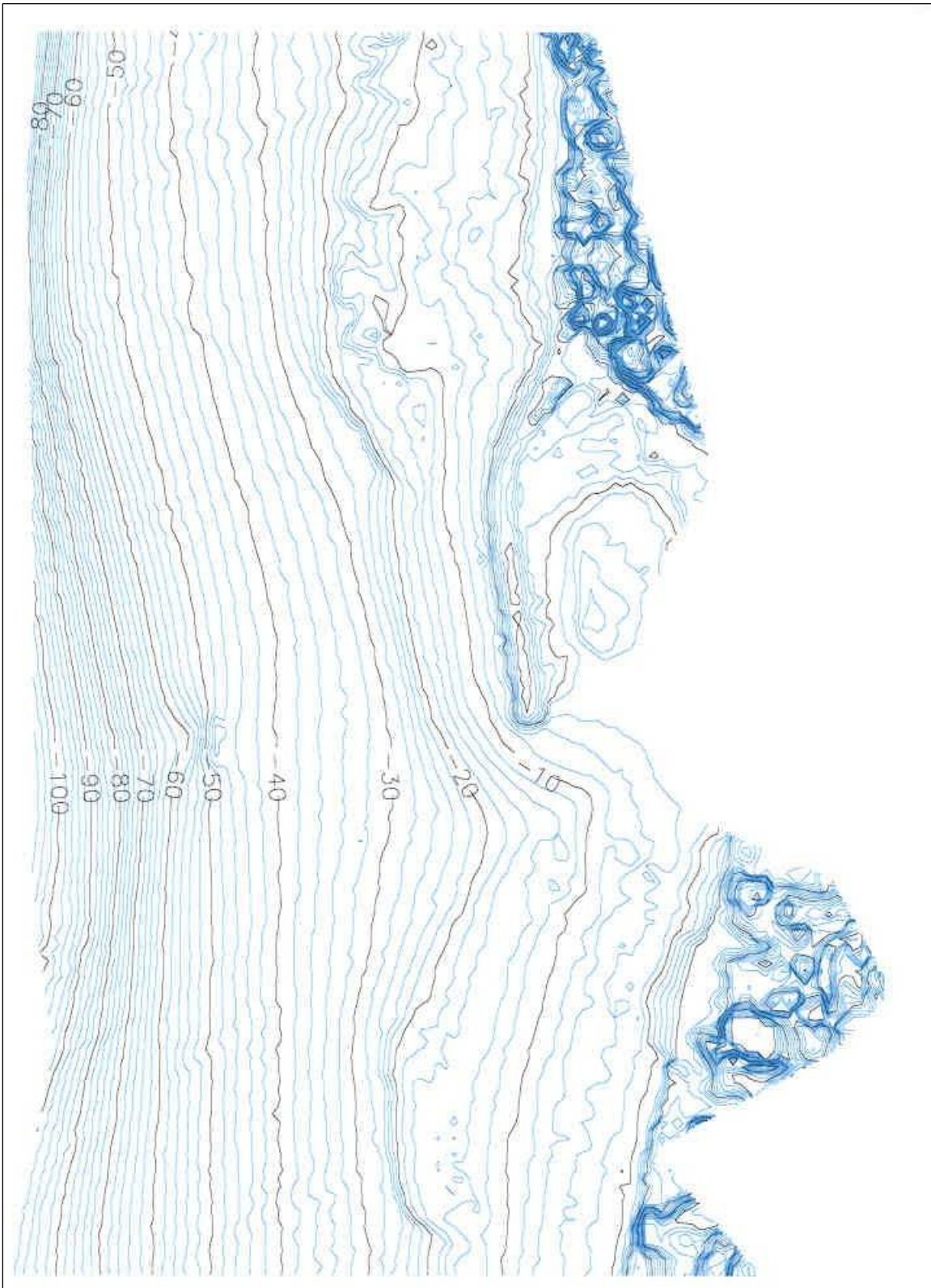


Figure 56. Close-up of the SHOALS bathymetric contours (feet, mean lower low water) near Aguadilla Harbor, Puerto Rico.

## **Equipment**

### **Navigation**

A Trimble Ag-132 Differential Global Positioning System (DGPS) was used for the vessel navigation and positioning. Real-time differential corrections were obtained from the U.S. Coast Guard beacon, Isabela, Puerto Rico.

Survey navigation control, track line generation and recording, and helmsman guidance were accomplished with the HYPACK version 8.9 surveying software package by Coastal Oceanographics Inc. Track lines were designed at 25-m- (82.5-ft-) spacing to allow adequate overlap of side-scan data, and sufficient density of subbottom profiler and seismic reflection data. Track event marks were generated and transmitted to the graphic recorders at 61-m- (200-ft-) intervals for correlation of the paper records to navigation fixes. Vessel heading data were input to the ISIS and HYPACK office data systems via a KVH digital compass, model Azimuth 1000.

### **Digital data acquisition system**

The TritonElics ISIS shipboard data acquisition and image processing system (Version 5.0) was used to acquire, store, and process all sonar data. The ISIS system also acted as an interface between the navigation and sonar systems, providing real-time data geocoding of the imagery. Graphic displays provided real-time quality control of data during acquisition. Side-scan sonar data were recorded at 8 bits per pixel and 1,024 samples per channel. Subbottom profile and seismic reflection data were recorded at 8 bits per pixel and 2,048 samples per channel.

### **Side-scan sonar**

A GeoAcoustics Model SS941 transceiver with Model 159D tow-fish and Model SS942 multiplexer were used in 110-kHz mode to produce imagery of the seafloor. Side-scan sonar data were provided directly to an EPC Model 1086 shipboard graphic recorder to produce a real-time paper record. Analog data were output from the Model SS941 console to the ISIS digital acquisition system for display, slant range correction, and storage.

The side-scan sonar tow fish was deployed from the bow of the survey vessel and was initially lowered approximately 0.6 m (2 ft) beneath the

water surface. As water depth increased, the tow fish was lowered to as much as 4.6 m (15 ft) below the vessel. This mounting scheme proved workable for maintaining the tow fish in undisturbed water (i.e., avoiding propeller wash and wake).

The side-scan sonar was operated at a ping rate of 81 milliseconds. This ping rate produces a range scale of 60.7 m (199.1 ft), and was selected so that imagery data would exceed the center-line stripe (nadir) of each subsequent track line.

### **Subbottom profiler and seismic reflection systems**

The subbottom profiler system consisted of a Datasonics Model 220 transceiver and a single Massa transducer. This system was operated at 5 kHz with a 0.2 milliseconds pulse length.

The seismic reflection system consisted of an Applied Acoustic Engineering Systems Model 300 power supply, operated at 100 joules. Broadband sound sources of this type are generically referred to as boomers, and operate at approximately 300 Hz to 2 kHz. The acoustic output from this system was produced through the discharge plate mounted on an overside pole.

The seismic reflection data were collected with a GeoAcoustics GeoPulse Model 5210A Receiver through a Benthos 3-m (10-ft) hydrophone. The discharge plate was mounted on the aft-port quarter of the *R. V. Sultana* with the hydrophone towed from the starboard bow. This configuration maintained the hydrophone in undisturbed water, and placed the normal reflection point of the data under the navigation antenna at midship.

Both systems were keyed at 0.4 sec and printed at a scan rate of 0.075 sec, utilizing an EPC 1086 graphic recorder. This ping rate was selected for maximum resolution, and was the fastest that the boomer power supply could maintain. Received data of both the SBP and SR systems were input to the ISIS system for geocoding, digital recording, and display.

## Data post-processing

### Side-scan sonar

An ISIS office system (Version 4.0) was used to process the side-scan data for conversion to a GIS compatible format. Processing consisted of the following:

- a. Re-bottom tracking the raw imagery to remove slant-range correction errors that occurred in real-time due to boat heave and water column noise.
- b. Navigation smoothing by using a 25-point running boxcar filter.
- c. Placing imagery data in the smoothed navigation matrix.
- d. Conversion of imagery data from .xtf format to .DDS\_VIF format.
- e. Conversion of DDS\_VIF format to .tif format, with a corresponding .tfw file.

Steps a through d were performed with the ISIS office system. Step e was performed with an additional TritonElcs software product (Delphmap (Version 2.0)).

The processing produced a single TIF file for each line of side-scan data that was collected. During step d the imagery resolution of 0.2 m (0.66 ft) per pixel was selected following an optimization of varying higher and lower pixel resolutions. This was selected as the best resolution that could be produced while maintaining the final TIF files at a workable size of 10 to 25 mb per trackline file.

### *Side-scan sonar data mosaic*

The individual TIF files as described above were imported to AutoCAD for final compiling. This process consisted of the following:

- a. Import of all TIF files.
- b. Arrangement of stacking order of files to produce best mosaic of the available imagery.
- c. Adjustment of individual image file frames to expose best imagery available for seafloor features.

### *Side-scan sonar interpretation*

A typically representative example of the side-scan sonar data display is shown in Figure 57. Analyses of the data delineated sand and rock interfaces, and zones of rock or coral outcrops. Vector line drawings of these analyses are shown in Figures 58, and a close-up of the Aguadilla Harbor vicinity in Figure 59. Areas that remain blank in these figures were interpreted as sand. It is important to note that the side-scan data reveal only surficial features; the operating frequency of the side-scan sonar (110 kHz) produces no subbottom penetration. The objective of this effort was boundary delineation. The exact physical description of sediment type within each zone may be modified in the future, upon receipt of the GeoSea Consulting (Canada) Ltd. Sediment Trend Analysis report discussed subsequently in Chapter 8 (McLauren and Hill 2003).

An additional purpose of this study was to identify the seabed features to individuals not accustomed to side-scan sonar interpretation, and to allow use of the smaller electronic file if GIS importation of the large imagery mosaic file is too cumbersome and timely.

### **Subbottom profiles and seismic reflection data**

These data were processed using the ISIS office system. The desired information from these data was the depth of sand. Therefore, the ISIS subbottom reflector picking routine was used to acquire distance measurements to the seabed first return and the top-of-rock reflector, if overlying sand existed. These reflectors are digitized or “picked” using a cursor to create a series of (x,y,z) points along each horizon (i.e., seabed and rock reflector). The ISIS output of the (x,y,z) data is an ASCII file with .sbp extension. These (x,y,z) points (.sbp file) are then stacked, and processed through two EHI ancillary AutoCAD programs. The final output is an (x,y,z) ASCII file where z represents the difference between the digitized seabed and rock reflectors, in this case the depth of sand. The final (x,y,z) file (isopach\_xyz.dat), which represents the depth of sand, was then processed using an AutoCAD add-on modeling software product named Quicksurf. These data were gridded to a 13.7 by 13.7 m (45 by 45 ft) matrix using a standard curvature with the Delauney triangulation method, and then contoured on the grid, at a 1.5-m (5-ft) interval. The depths of sand among the rock and coral are shown in Figures 60, and a close-up of the Aguadilla Harbor vicinity in Figure 61, from subbottom profiles and seismic reflection data.

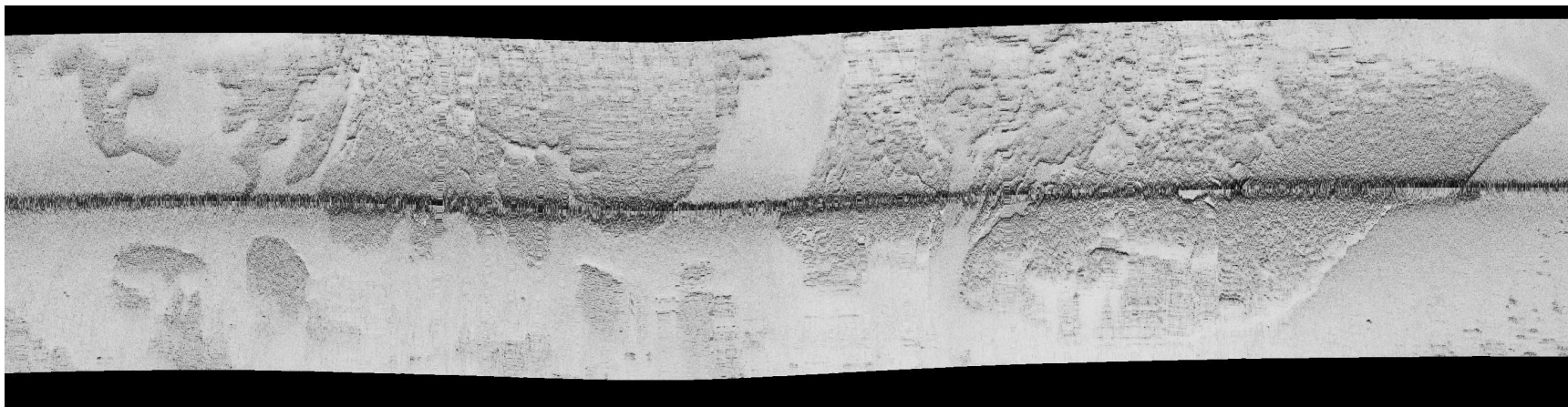


Figure 57. Surficial features delineated by typical representative side-scan sonar data from seafloor off Aguadilla Harbor, Puerto Rico.



Figure 58. Vector line drawings in red of rock and/or coral in the vicinity of Aguadilla Harbor, Puerto Rico, from side-scan sonar survey. Areas not shown in red are interpreted to be sand.



Figure 59. Close-up view near of vector line drawings in red of rock and/or coral near Aguadilla Harbor, Puerto Rico, from side-scan sonar survey. Areas not shown in red are interpreted to be sand.

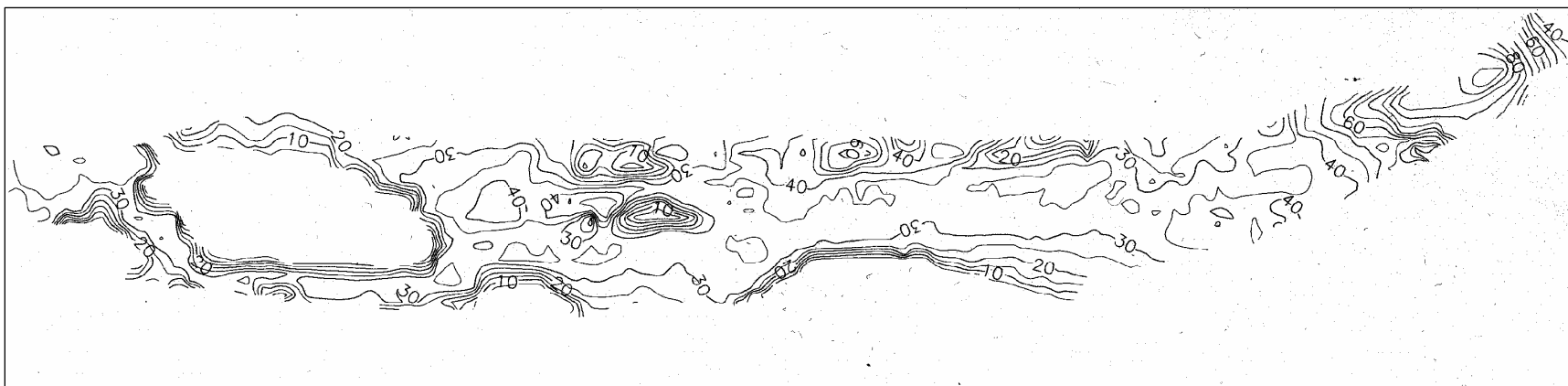


Figure 60. Depth of sand contours (feet) along rock and coral, as interpreted from subbottom profiles and seismic reflection data near the vicinity of Aguadilla Harbor, Puerto Rico.



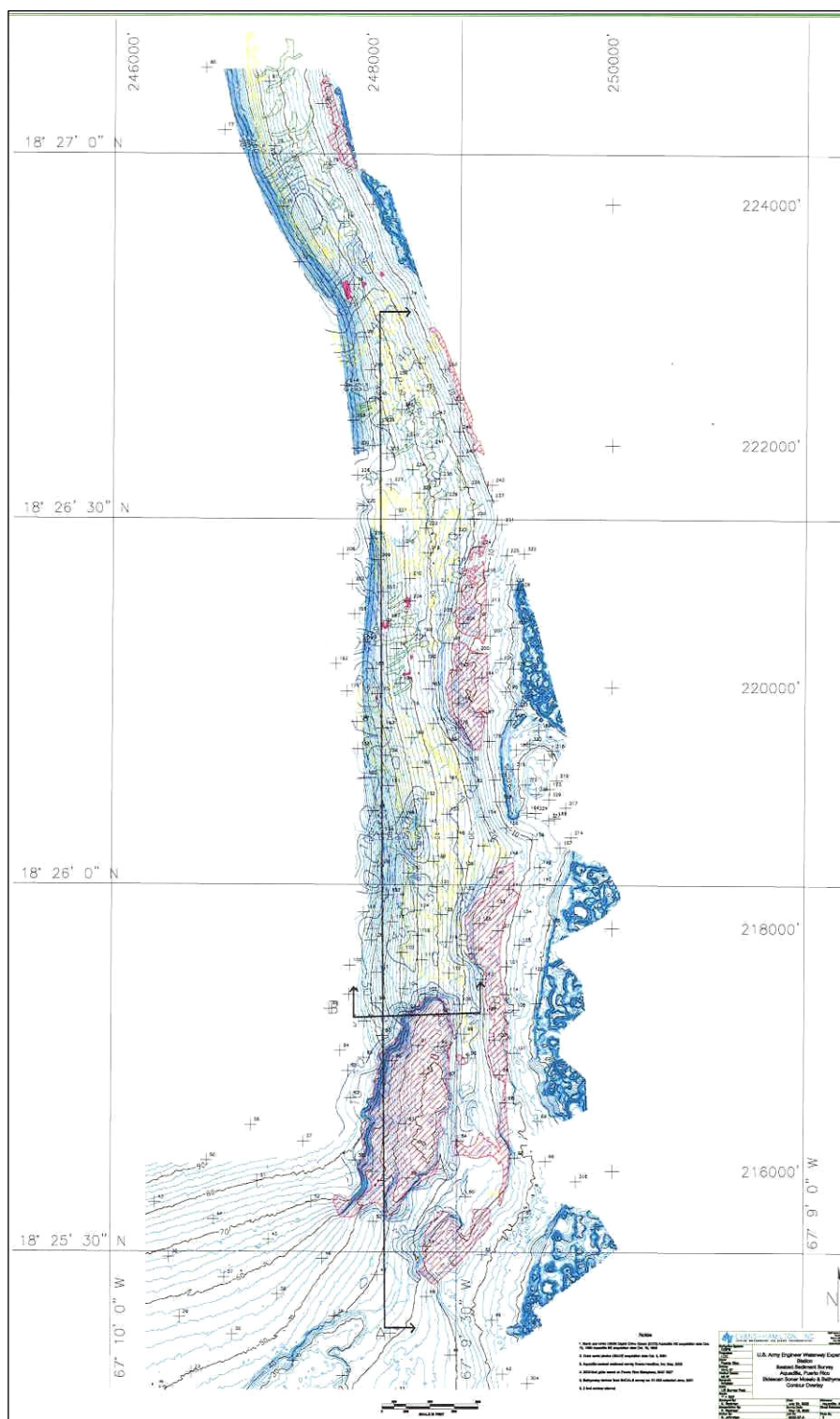
Figure 61. Close-up of depth of sand contours (feet) along rock and coral off Aguadilla Harbor, as interpreted from subbottom profiles and seismic reflection data.

## Summary

The marine geophysical data collected offshore of Aguadilla Harbor, Puerto Rico indicate a complex sand, rock, and coral environment. Side-scan sonar and seismic reflection data have been used to produce multiple illustrations of this regime. The sand thickness varies from 0 m (0 ft) to greater than 12 m (40 ft) while interspersed throughout the numerous rock structures and outcrops. Comparisons of side-scan and reflection data generally produce excellent correlation between the data sets. Areas of rock/coral outcrops however, indicate varying sand depths. Whereas some of the outcrops are products of pinnacles that arise from the lower rock formation, these areas indicate a logical shallower sand depth of approximately 3 m (10 ft), much shallower than the surrounding area. While other outcrops (most likely coral) appear independent of the underlying rock, the sand surrounding and below these outcrops remains at a relatively constant depth of 6 to 9 m (20 to 30 ft).

Figure 62 shows an overlay plot consisting of the SHOALS bathymetric contour data, overlain by the color-coded side-scan sonar survey data indicating the demarcation between the rock/coral shown in red and the blank areas being interpreted as sand. This figure also is overlain by the delineated sand thickness contour data derived from the subbottom profiles and seismic reflection data. Figure 63 is a close-up view of these same three sets of data for the vicinity of the Aguadilla Harbor.

One of the most notable features revealed in these data is the large rock knoll and significant sand bowl to the south of the harbor entrance. This bathymetric feature (rock knoll) may channel and direct a northward water current flow, which provides sand mobility toward the harbor from the nearshore sand bowl. The area immediately offshore of the harbor entrance also provides a significant source of sand available for migration with the predominant wave train, which was from the west-southwest during this survey. Aerial photos taken October 2001 (Appendix A) also reveal a sediment plume, being emitted from the river to the south of Aguadilla, which appears to migrate northward, another possible source of harbor sand. These photos provide correlation of beach and upland features to offshore areas ascertained by the geophysical investigations.



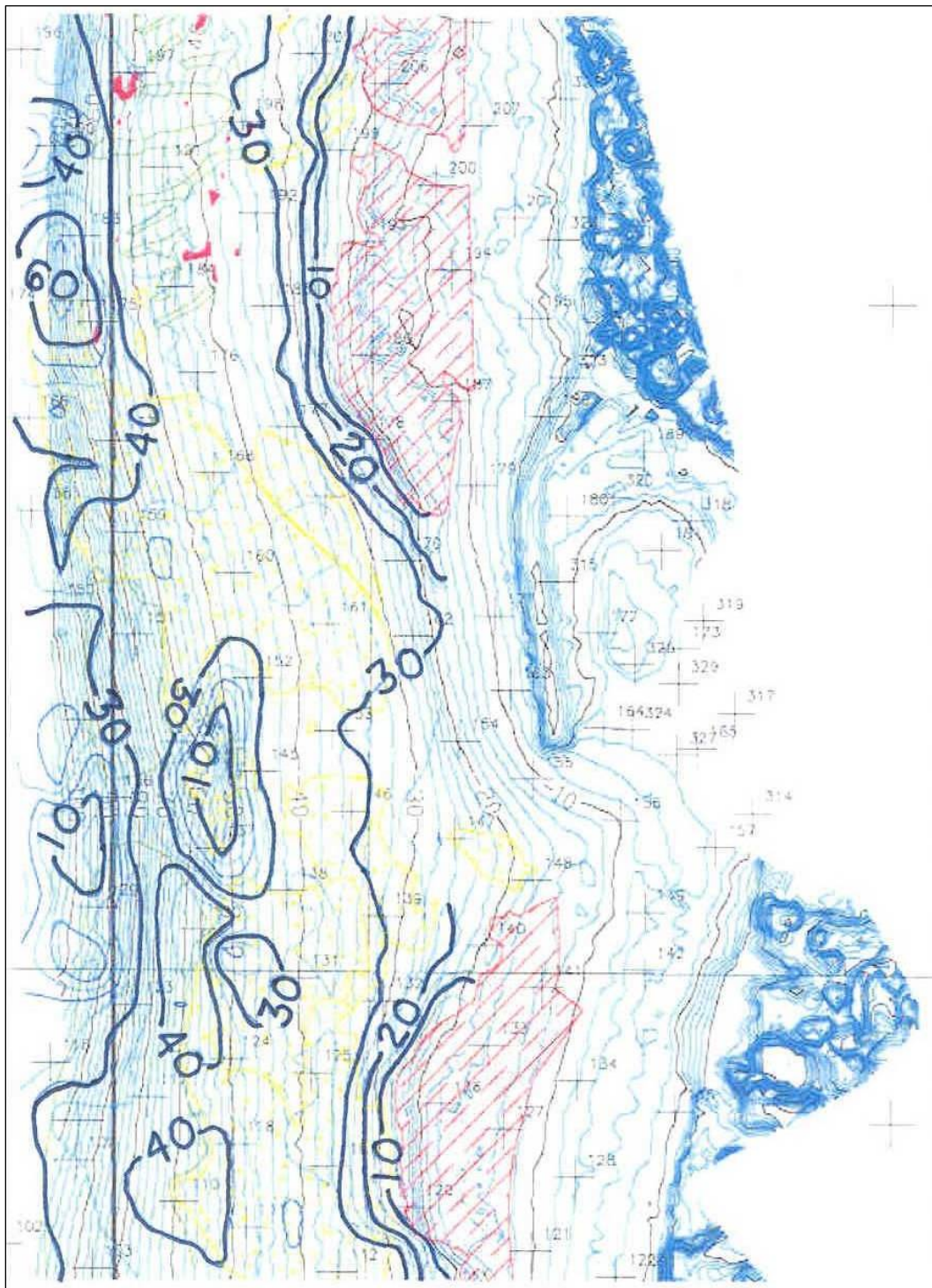


Figure 63. Close-up of the vicinity of the Aguadilla Harbor, showing sand layer thickness (feet) as determined by subbottom profiling and seismic reflection data.

## 8 Sediment Trend Analysis (STA<sup>®</sup>)<sup>1</sup> at Aguadilla Harbor

This phase of the MCNP study utilized the technique of Sediment Trend Analysis (STA<sup>®</sup>) for estimating net sediment pathways in coastal and estuarine environments, and applied this technique of STA to Aguadilla Harbor. The STA technique is based on analyses of sediment samples collected over a uniform grid in the region of interest. STA provides maps indicating sediment pathways, erosion and accretion areas, and areas that are in dynamic equilibrium.

### Principles behind Sediment Trend Analysis (STA)<sup>2</sup>

The STA theory was first published by McLaren and Bowles (1985). In simplest terms, the STA method uses differences in grain-size distributions from bottom sediment samples collected on a regular grid to infer net sediment pathways and regions of erosion, accretion, and dynamic equilibrium. Specifically, sediment samples are collected in the area of interest from the top 10 to 15 cm (4 to 6 in.) of the bottom sediment. The sample grain-size distributions are determined primarily using a laser-based particle-size analyzer. Coarse sediment particles in the size range from 0.7 mm through 4.0 mm in diameter are mechanically sieved, and the results are merged with the majority of the distribution determined by the particle-size analyzer. The STA technique uses the first three central moments from the grain-size distribution; (a) mean, (b) variance (or sorting), and (c) skewness. Other sediment properties such as mineralogy, texture, and shape are not considered in the analysis.

The basic assumption inherent in STA is that differences in sediment grain-size distributions can be due to sediment transport. In other words, the grain-size distribution may change as sediment moves along a pathway, and every deposit is a result of the processes responsible for sediment

---

<sup>1</sup> This study provides a balanced description of the Sediment Trend Analysis (STA<sup>®</sup>) technique and how it may be beneficial to coastal projects. This study should not be considered an official Corps of Engineers endorsement or recommendation of the STA technique or of the private company (GeoSea Consulting (Canada) Ltd., Brentwood Bay, British Columbia, Canada) that performs STA studies.

<sup>2</sup> This section is extracted essentially verbatim from Hughes (2005).

movement. This implies active periods of sediment transport occurring at the site at least part of the time.

McLaren and Bowles (1985) identified three possibilities that can be characterized by relative differences in grain-size distribution parameters (designated as distributions  $d_1$  and  $d_2$ ) between two locations:

- a. **Case A: Lag deposit.** If distribution  $d_2$  has a coarser mean, is better sorted (smaller variance or standard deviation), and more positively skewed than distribution  $d_1$ , then sample  $d_2$  is a lag deposit of sample  $d_1$ , and both distributions were originally the same. In this case no direction of transport can be determined.
- b. **Case B: Fining Sediments.** If distribution  $d_2$  has a finer mean, is better sorted (smaller variance or standard deviation), and more negatively skewed than distribution  $d_1$ , then the transport direction is from sample  $d_1$  to sample  $d_2$ . In this case, the energy regime transporting the sediment is decreasing from  $d_1$  to  $d_2$ , and the coarser grains are not transported as far as the finer grains before depositing.
- c. **Case C: Coarsening Sediments.** If distribution  $d_2$  has a coarser mean, is better sorted, and more positively skewed than distribution  $d_1$ , then the transport direction is from sample  $d_1$  to sample  $d_2$ . In this case, the energy regime is also decreasing from  $d_1$  to  $d_2$ . Initially, this case is counterintuitive because coarse grains are not expected to be transported while finer grains are left behind. A plausible physical explanation is that “armoring” has occurred at location  $d_1$ , effectively trapping the underlying layers of finer material. Thus, the  $d_1$  distribution obtained as a grab sample contains a larger percentage of fine-grained particles that were shielded by the overlying layer of coarser grains. The energy level is such that coarse particles can be transported until they are deposited at site  $d_2$  as the energy level decreases. Finer-grained sediment will continue to be transported past the  $d_2$  location.

Only Cases B and C can be used to infer direction of sediment transport. The other six possible combinations of relative differences in grain-size distribution mean, sorting, and skewness cannot be used to determine a transport direction. Distinguishing between Cases A and C depends on further interpretation of the differences between the energy transfer functions that are constructed based on theoretical considerations. McLaren and Bowles (1985) provide additional theory details. Table 2 summarizes the three pertinent cases.

Table 2. Sediment transport trend based on grain-size distribution.

Case	Relative Change in Parameter from Deposit $d_1$ to Deposit $d_2$	Interpretation
A	Coarser Better sorted More positively skewed	Deposit $d_2$ is a lag deposit of $d_1$ . No direction of transport can be determined.
B	Finer Better sorted More negatively skewed	Transport direction is from $d_1$ to $d_2$ . Energy regime is decreasing. Low energy transfer functions.
C	Coarser Better sorted More positively skewed	Transport direction is from $d_1$ to $d_2$ . Energy regime is decreasing. High energy transfer functions

## Procedures for a Sediment Trend Analysis<sup>1</sup>

Sediment Trend Analysis attempts to determine patterns of sediment transport, or sediment pathways, at any particular site through particle-size analysis of a large number of sediment grab samples collected on a (mostly) uniformly spaced grid. Sample grid spacing must be close enough that it can be safely assumed that sediment transport could conceivably occur between adjacent sample locations. In practice, selection of suitable sample spacing is based on previous experience taking into account (a) the number of sedimentological environments likely to be affecting the area of interest, (b) the spatial scale at which sediment transport trends need to be resolved, and (c) geographic boundaries of the study area. Reducing number of samples and/or increasing the sample spacing may add greater uncertainty to the results.

Several techniques to carry out STA have been developed, a good summary of which is found in Rios et al. (2003). McLaren and Hill (2003) use a vector analysis as an initial guide to source-deposit relationships, followed by the one-dimensional, line-by-line approach whereby selected sample sequences are individually examined for statistically acceptable trends.

After the samples have been collected and the grain-size distributions determined, a computer program is used to examine differences between the grain-size distribution parameters at each location relative to all neighboring sample locations. The goal of the computer program is to recognize statistically significant trends fulfilling the criteria listed in Table 2 for

<sup>1</sup> This section is extracted essentially verbatim from Hughes (2005).

Cases B and C. To infer the direction of sediment transport at a given location,  $d^*$ , a minimum of eight additional samples are needed arranged in a  $3 \times 3$  matrix with sample  $d^*$  located in the center of the matrix. From this matrix a statistical score is calculated for use in establishing sediment pathways. This process continues throughout the entire sampled regime. The minimum number of samples needed to estimate pathways is a  $9 \times 9$  grid containing 81 samples.

The STA analysis steps are as follows:

- a. Assume the direction of sediment transport over an area containing many sample sites.
- b. From this initial assumption, predict the sediment trend that should appear along a particular sequence of samples.
- c. Compare the prediction with the actual trend that is derived from the selected samples.
- d. Modify the assumed transport direction and repeat the comparison until the best fit is achieved.

The important feature of this approach is the use of many sample sites to detect a transport direction. This helps reduce the uncertainty. The principal difficulty is that the number of possible pathways in a given area may be too large to automate the technique, or to test all possibilities. As a result, the choosing of trial transport directions has not been analytically codified. At present, the selection of trial directions is undertaken initially at random; although the term “random” is used loosely as it is not strictly possible to remove the element of human decision-making entirely. For example, a first look at the possible transport pathways may encompass all north-south, or all east-west directions. As familiarity with the data increases, exploration for trends becomes less and less random. In other words, operator input can typically nudge the method toward a viable outcome. The number of trial trends becomes reduced to a manageable level through both experience and the use of additional information (usually the bathymetry and morphology of the area under study). When a final and coherent pattern of transport pathways is obtained that encompasses all or nearly all of the samples, the assumption that the grain-size distributions are a result of sediment transport processes acting along the pathways has been verified, despite the inability to define accurately all the uncertainties that may be present.

Once sediment pathways have been established, the final step is computation and interpretation of what are termed “X-distributions” along the pathways. The X-distribution is defined mathematically as:

$$X(s) = \sum_{i=1}^N \frac{[d_2(s)]_i}{[d_1(s)]_i} \quad (1)$$

This means for each sequential pair of deposits ( $d_1$  and  $d_2$ ) along the sediment pathway, the ratio of the grain-size distributions between deposits  $[d_2(s) / d_1(s)]$  is calculated to provide a new distribution as a function of grain size. After this is completed for all sequential pairs, the composite X-distribution as a function of grain size is determined as the sum of all the individual distributions. Note that along the pathway, deposit  $d_2$  in one pair is often deposit  $d_1$  of an adjacent pair. Composite distributions ( $D_1$ ,  $D_2$ ) composed of all the source deposits ( $d_1$ ) and destination deposits ( $d_2$ ) are also constructed in a similar manner, i.e.:

$$D_1(s) = \sum_{i=1}^N [d_1(s)]_i \quad \text{and} \quad D_2(s) = \sum_{i=1}^N [d_2(s)]_i \quad (2)$$

The  $X(s)$  distribution can be thought of as a function that describes the relative probability of each particle size being removed from deposit  $d_1$  and transported to deposit  $d_2$ . Based on the shape of the X-distribution along the sediment pathway relative to the shapes of the composite distributions  $D_1$  and  $D_2$ , McLaren and Bowles (1985) gave five scenarios for describing what is occurring along the pathway; (a) dynamic equilibrium, (b) net accretion, (c) net erosion, (d) total deposition I, and (e) total deposition II. These five cases are illustrated in Figure 64 and discussed as follows. (Important note: The abscissas on the plots in Figure 64 are in phi units, so finer grain sizes are to the right and coarser grain sizes are to the left.)

- a. **Dynamic equilibrium.** If the shape of  $X(s)$  resembles the  $D_1(s)$  and  $D_2(s)$  distributions (Figure 64a), the probability of a particular grain size being deposited is the same as the probability of that size being transported. The bed is neither eroding nor accreting but, instead, is in dynamic equilibrium.

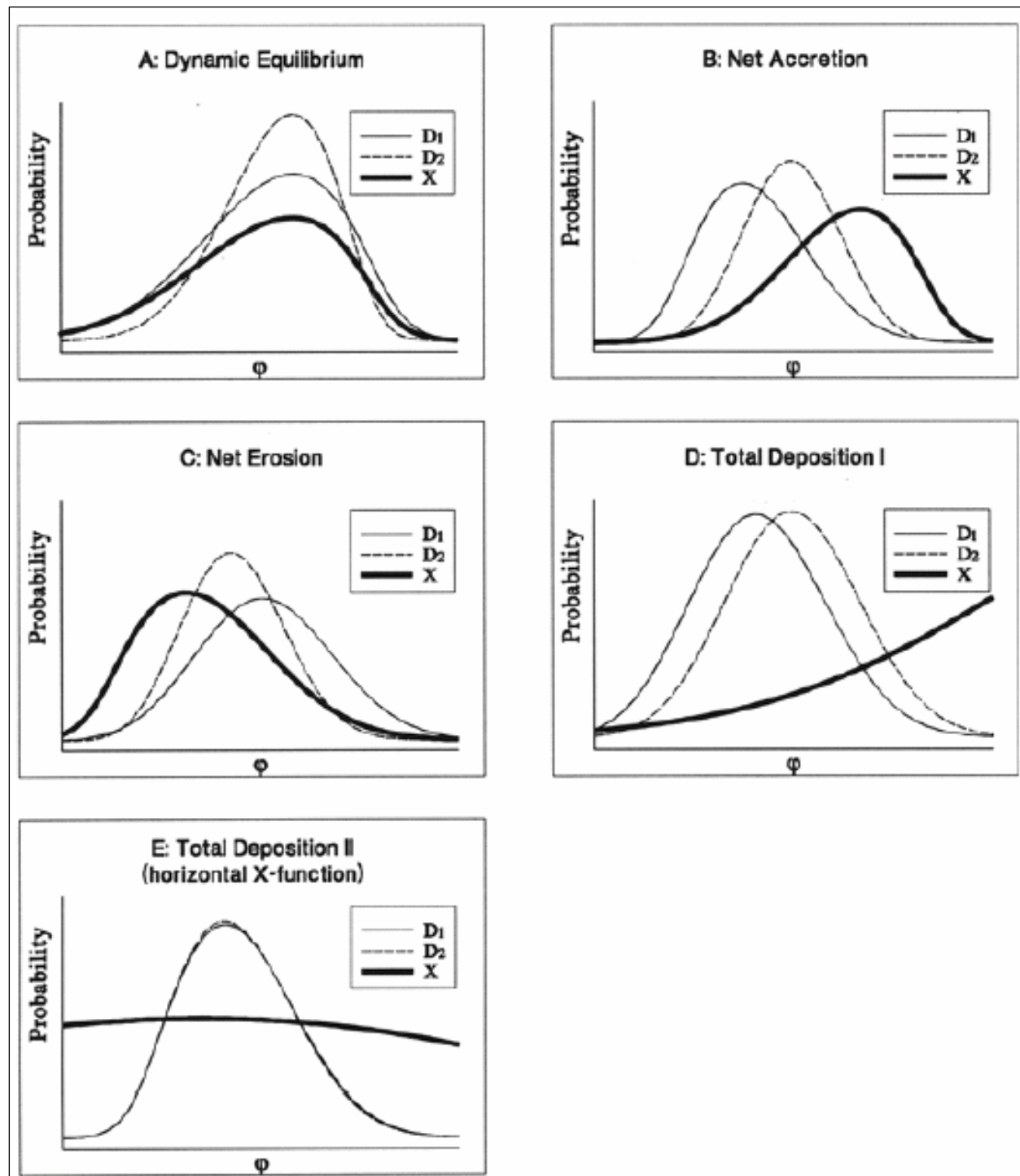


Figure 64. Interpretation of X-distribution along sediment pathways (Note: Abscissas on plots are in phi units so finer grain sizes are to the right, and coarser grains sizes are to the left.) (after McLaren and Hill 2003).

- b. **Net accretion.** If the shapes of the three distributions are similar, but the mode of  $X(s)$  is skewed more toward the finer grain sizes (to the right in Figure 64b), net accretion is occurring. Because the modes of the deposits

- are coarser than  $X(s)$ , finer grained material is being transported and deposited, and this corresponds to Case B transport (fining sediments).
- c. **Net erosion.** If the shapes of the three distributions are similar, but the mode of  $X(s)$  is skewed more toward the coarser grain sizes (to the left in Figure 64c), net erosion is occurring. In this situation the coarser grain sizes are being transported which corresponds to Case C transport (coarsening sediments).
  - d. **Total deposition I.** If the  $X(s)$  distribution increases monotonically from coarse to fine grain sizes over the entire range as shown in Figure 64d, fine grains are being deposited along the sediment pathway (Case B) and are not being remobilized. The shapes of the  $D_1(s)$  and  $D_2(s)$  distributions do not matter in this situation.
  - e. **Total deposition II.** In extremely fine sediments (very fine silt or clay) the  $X(s)$  distribution may be nearly horizontal as shown in Figure 64e, indicating there is an equal probability of all grain sizes being deposited. This situation corresponds to sediments far from the source, and deducing sediment pathways based on changes in grain-size distribution becomes more problematic.

The last step is representing the sediment pathways and perceived sediment transport process graphically by different colored arrows drawn on a map of the project area. As an example, Figure 65 shows results of STA obtained for San Juan Harbor, Puerto Rico. This study was completed in 2002 using 616 sediment samples. The green arrows indicate sand from the littoral system is being moved into the harbor where accretion occurs. Much of the inner harbor remains in dynamic equilibrium.

Although this explanation of Sediment Trend Analysis is lacking in details, it gives an overall impression of how the STA technique is applied. This information may be useful for evaluating the utility of STA for a particular project site.

## Uncertainties of Sediment Trend Analysis<sup>1</sup>

Since its inception, many researchers have applied the concepts of STA to further their understanding of sedimentary environments. A number of authors found their results to agree, either in whole or in part, with a variety of other evidence including direct measurements of processes,

---

<sup>1</sup> This section is extracted essentially verbatim from Hughes (2005).

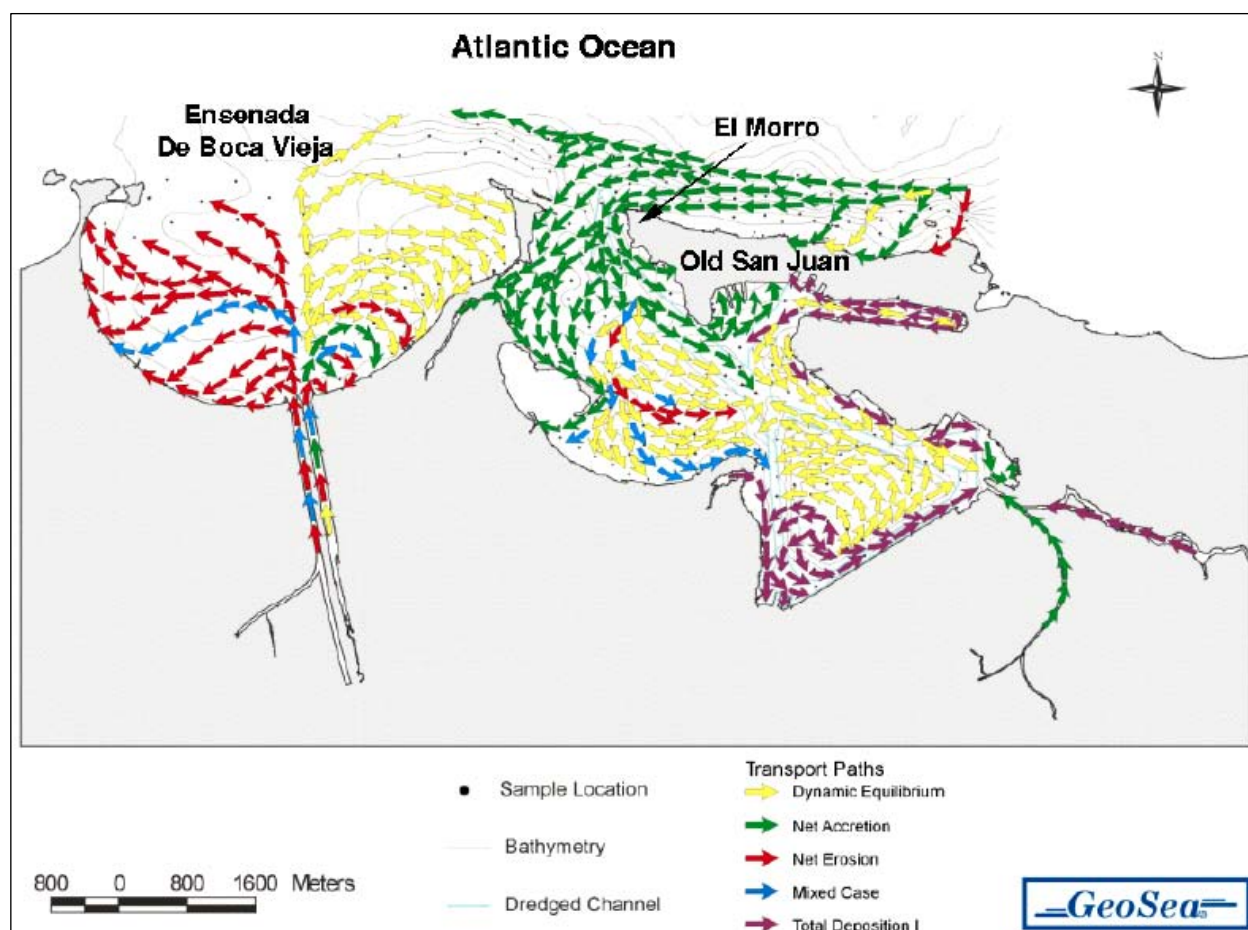


Figure 65. Sediment pathways for San Juan Harbor, Puerto Rico, by STA (after McLaren and Hill 2003).

observations of bed form orientations, and application of numerical modeling (Livingstone 1989; Lanckneus et al. 1992; Van de Kreeke and Robaczewska 1993; Gao and Collins 1994; Gao et al. 1994; Aldridge 1997; Bergemann et al. 1998; Van Der Wal 2000; Mallet et al. 2000; Duck et al. 2001; and Shi et al. 2002). The theory of STA was supported in independent research carried out by the U.S. Army Corps of Engineers (Teeter 1993; and Teeter et al. 2001). Nevertheless, some authors found no agreement between the STA (or various derivatives of the technique) and outside evidence (Flemming 1988; Masselink 1992; and Guillen and Jimenez 1995).

Voiced (but unpublished) criticism of STA methodology stems from specific project application of STA that yielded results different from what other coastal engineering experts believe is occurring in the nearshore sediment transport regime at that particular site. Whether or not the criticism is deserved depends on substantiating evidence for each specific application. It is always important to keep in mind that STA results must

never be used without evaluating the result in the context of all other available information at the project site including hydrodynamics, known sediment transport trends, etc.

Initial development of STA sediment pathway maps such as illustrated in Figure 65 are based strictly on the sediment sample analyses without any consideration of known hydrodynamic conditions that could potentially influence sediment pathways. After the initial pathways are constructed based on statistical tests, knowledge of the local wave and current environment is examined to determine whether the derived sediment pathways make sense in terms of known hydrodynamic forcing. Of course actual construction of the sediment pathways is more involved than the simple description already given, and several additional factors must be considered before finalizing the sediment pathways.

Developers of the STA technique list several uncertainties associated with the methodology including the following:

- a. **Transport model assumptions.** The basic assumption of the transport model used in STA is that smaller grains are more easily transported than larger grains. Under this assumption, it can be shown that transport processes will change the moments of sediments in a predictable way. However, transfer functions obtained from flume experiments demonstrate this assumption is not strictly true. Factors such as shielding whereby the presence of larger grains may impede the transport of smaller grains, increasing cohesion of the finer grains, or the decreasing ability of the eroding process to carry additional fines with increasing load, demonstrate that the transport process is a complicated function related to the sediment distribution and the strength of the erosion process. Furthermore, this basic assumption implicitly dictates that the probability of transport of one particular grain size is independent of the transport of other grain sizes.
- b. **Temporal fluctuations.** Perhaps the most important uncertainty is that sediment pathways and patterns produced by STA are assumed to represent the integration of all physical processes responsible for transport and deposition of sediment at a given location over time. In a coastal regime this could include alongshore sediment movement driven by wave processes, onshore sediment movement during calmer wave climates, offshore sediment movement during storm periods, transport by ocean currents, and sediment carried by river flows and deposited from the

sediment plume in the nearshore region. In other words, sediment samples may comprise the effects of several transport processes. It is assumed that what is sampled is the average of all the transport processes affecting the sample site. The average transport process may not conform to the transport model developed for a single transport process. The possibility also exists that different samples may result from a different suite of transport events. The temporal period for individual physical processes responsible for sediment deposition may vary from several tidal cycles, through the length of a storm season, to several years or more. The STA method cannot distinguish the time associated with the various processes, so while the result might indicate net erosion or deposition, the time scale (rate of erosion or deposition) cannot be determined. In STA, it is assumed that a sample provides a representation of a specific sediment transport type. There is no direct time connotation, nor does the depth to which the sample was taken contain any significance provided that the sample does, in fact, accurately represent the sediment transport type. For example, one sample may represent an accumulation over several tidal cycles, whereas another sample may represent several years of deposition. The trend analysis simply determines if there is a sediment transport relationship between the two sediment types.

- c. **Sample spacing.** Spacing of the sediment-sampling grid must be close enough to assure adjacent samples are likely to be related by transport regime. With increased spacing there is increasing possibility that sediment samples are unrelated by transport mechanism. This could lead to false conclusions about the pathways between samples. Decreasing sample spacing increases the likelihood of adjacent samples being related by transport mechanism, but cost also increases. In practice, determination of an appropriate sampling grid for a specific site will be based on the number of different types of sediment environments thought to be present, e.g., beach sand, river silt deposits, etc.; the desired spatial scale of the sediment trends; and the geographical shape and extent of the study area.
- d. **Sediment size distribution.** Use of the log-normal distribution to characterize the sediment samples may introduce bias in the mean, variance, and skewness which are the key parameters on which the method is based. Other distributions have been proposed and debated in the literature (e.g., Hill and McLaren 2001; Hartmann and Flemming 2002).
- e. **Random environmental and measurement uncertainties.** All samples will be affected by random errors. These may include unpredictable fluctuations in the depositional environment, the effects of

sampling and subsampling a representative sediment population, and random measurement errors.

Considering these listed uncertainties, it is critical that results from any STA be considered tentative until independent observations or analysis of known sediment erosion and deposition trends from the specific study site confirm the general pathways it produced. Usually, a preliminary analysis of likely hydrodynamic forcing supporting the derived pathways is included as part of the STA product, but engineers more versed with the local hydrodynamic processes may have a different interpretation based on their knowledge and observation over many years.

STA is but one interpretation of the sediment transport regime based on the assumption that sediment transport along a pathway results in modification of the grain-size distribution between adjacent sediment samples. The derived patterns of transport are, in effect, an integration of all processes responsible for the transport and deposition of the bottom sediments. To be valid, the STA pathways must generally conform to logical assessments based on past understanding and evidence of the sediment transport regime. In cases where there is substantial variance between the STA result and local knowledge of the transport regime, it is wise to re-examine the basis for the local knowledge before rejecting the STA results.

### **Benefits of Sediment Trend Analysis<sup>1</sup>**

For locations where the sediment pathways are not well understood, STA may provide a tool for better understanding why certain erosion and deposition patterns have occurred. In the best case scenario, the derived pathways will conform to preexisting hypotheses and provide additional detail that can aid in development of engineering solutions to sedimentation problems. In the worst case, the STA results may stimulate debate and reveal what additional site measurements are needed to resolve any conflicts and promote better understanding of the sediment transport regime. The STA results must always be assessed in the context of what is already known at the site. Because STA cannot provide rates of sediment transport, erosion, or deposition, the findings may aid in directing the appropriate inputs into numerical modeling for further quantitative analysis.

---

<sup>1</sup> This section is extracted essentially verbatim from Hughes (2005).

STA does not give sediment pathways associated with single, extreme events unless the sampling is conducted soon after the event occurs, and it can be safely assumed that all collected samples are a direct result of the extreme event. Other methodologies such as numerical and physical models, or site measurements must be used to characterize sediment pathways during severe storms. However, if long-term average trends in sediment erosion and deposition are useful for project development, an STA study has potential benefit in adding to the understanding of the physical regime, potentially avoiding future problems, and perhaps reducing maintenance dredging.

Costs for conducting an STA study are directly related to the number of sediment samples required to cover the study area. Generally, STA studies cost less than comparable sediment tracer studies (which effectively only characterize the sediment pathways over the relatively short duration of the tracer experiment). STA will also be less expensive than most field measurement programs utilizing a suite of sensors, but on the other hand STA does not provide information on transport rates that could be determined from a field measurement program.

The end products from STA include a map delineating the main sediment transport environments within the study area and a map indicating both the sediment pathways and the regions of net erosion, net accretion, dynamic equilibrium, total deposition, and mixed regimes. These are useful for understanding where sediment is moving within the sampled region, and the maps can serve as a predictive tool for initial assessment of what might occur if engineering modifications are made at a project site. However, the STA methodology represents integration over time of all processes acting at a location. So it would not be appropriate to base a prediction of the response of a project to an engineering modification solely on the results of the STA. Other understanding about the site in particular and typical response of the engineering modification in general must be taken into consideration.

STA can be applied to a wide range of sediment types ranging from clay-sized cohesive materials all the way up to gravel deposits. Because the methodology makes no assumptions about the sediment transport mechanisms other than fine grains are more likely to be transported than coarser grains, it can be applied to nearly all hydraulic environments including riverine, estuarine, coastal, and mixed regimes. Finally, the large number

of samples (and analyzed distributions) required to perform STA may be useful as numerical modeling input, remote sensing ground truth (e.g., acoustic mapping, side-scan sonar), habitat studies, and baseline data for documenting future changes in the sediment regime.

## **Sediment Trend Analysis, Aguadilla Harbor<sup>1</sup>**

### **Sediment Trend Analysis sampling plan**

Sampling plans for STA studies are determined by study requirements and the nature of the environment. For the relatively small coastal region delineated for the Aguadilla Harbor study by GeoSea Consulting (Canada) Ltd., Brentwood Bay, British Columbia, Canada (McLaren and Hill 2003), a total of 269 samples were specified as denoted by the circular dots in Figure 66. In the immediate vicinity of the breakwater grid, spacing was 75 m (246 ft). Farther away from the harbor to the north and south, grid spacing was increased to 150 m (492 ft) to establish possible relationships of sediment sources on a more regional scale. During sampling, hard bottom was encountered at 23 locations, so the final number of collected sediment samples was 246. The majority of collected samples (84.2 percent) were classified as sand, followed by muddy sand (12.2 percent) and sandy mud (3.6 percent).

### **Sediment Trend Analysis results**

The major result from the STA of the 246 sediment samples was a map of 51 derived sediment pathways shown in Figure 67. The sampled region exhibited two major transport environment (TE) regimes (Figure 68).

- a. **TE1: Bahia de Aguadilla North.** The first regime (TE1) extended from the northern limit of the study area to about 500 m (1,640 ft) south of the breakwater tip (a location that marks the northern boundary of a hard-ground bottom feature). The STA indicated that TE1 was about 51 percent accretional and 40 percent mixed erosion/accretion. At the offshore limit of TE1, sediment moves in a southerly direction and generally onshore from deeper water. Nearshore, there were indications of transport in a northerly direction with pathways entering the harbor through the entrance. Of particular note is the absence of accretional sediment pathways moving farther south of the harbor into the historically eroding region to the south.

---

<sup>1</sup> This section is extracted essentially verbatim from McLaren and Hill (2003).

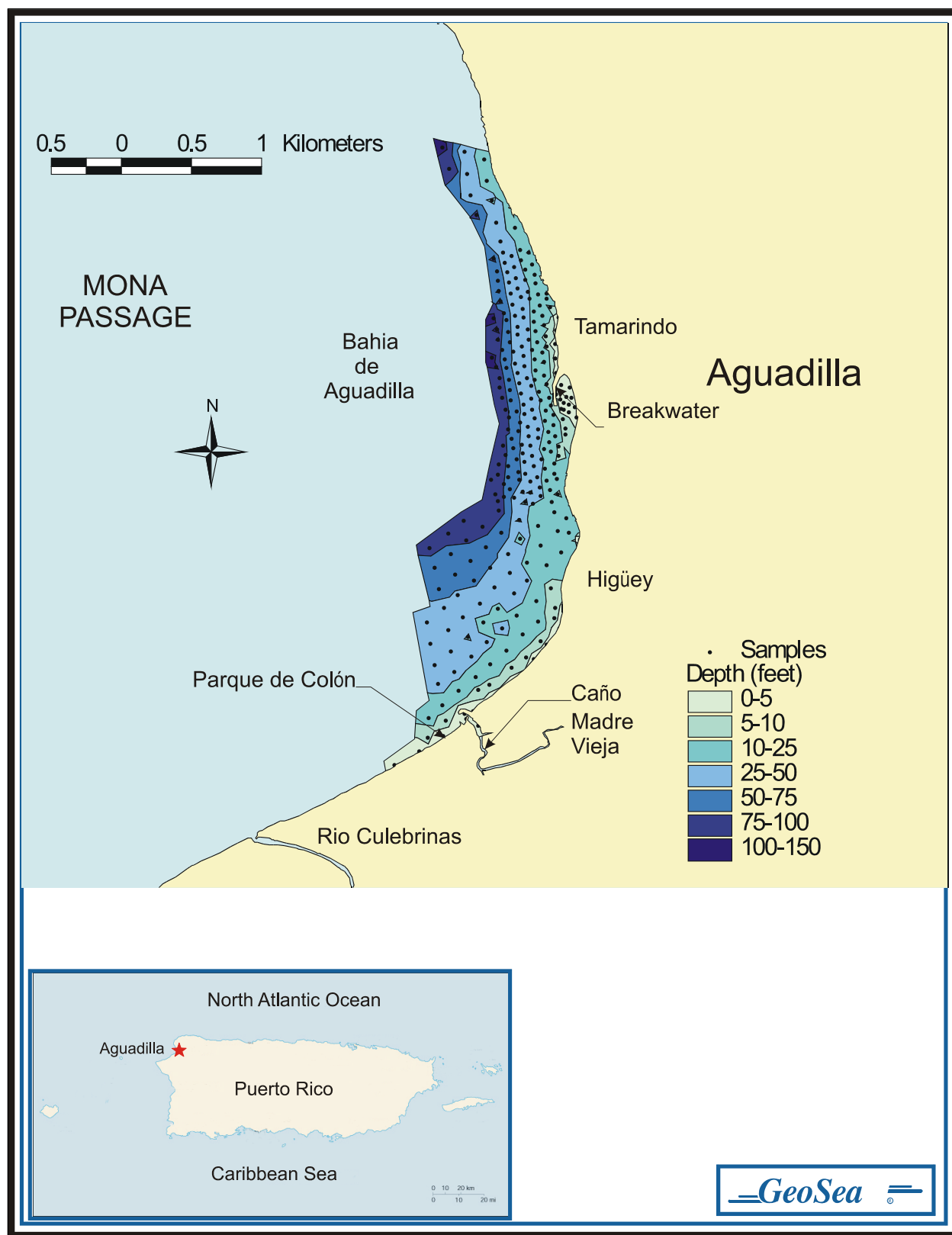


Figure 66. Sample locations and place names, Aguadilla Harbor (after McLaren and Hill 2003).

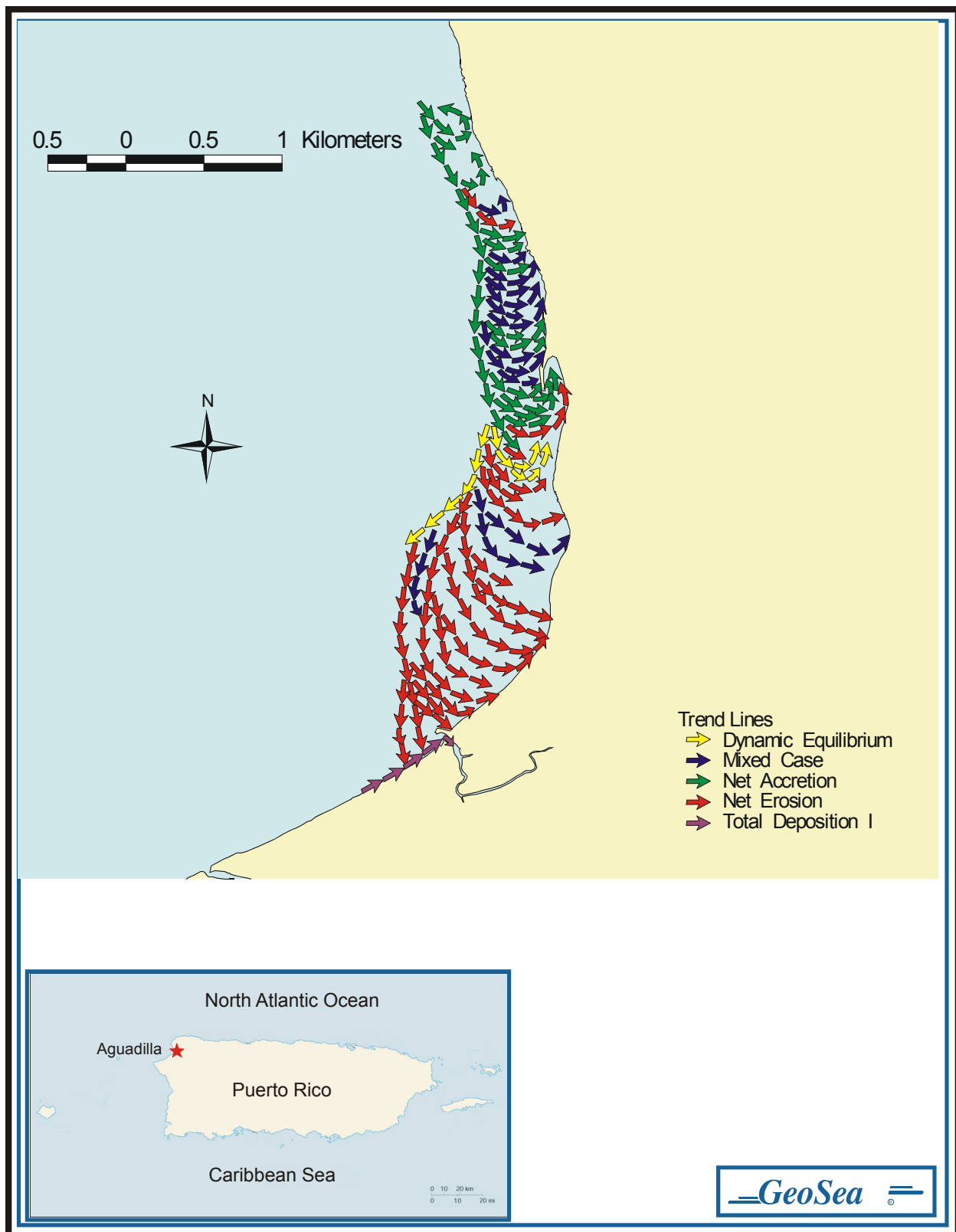


Figure 67. Net sediment transport pathways, Aguadilla Harbor (after McLaren and Hill 2003).

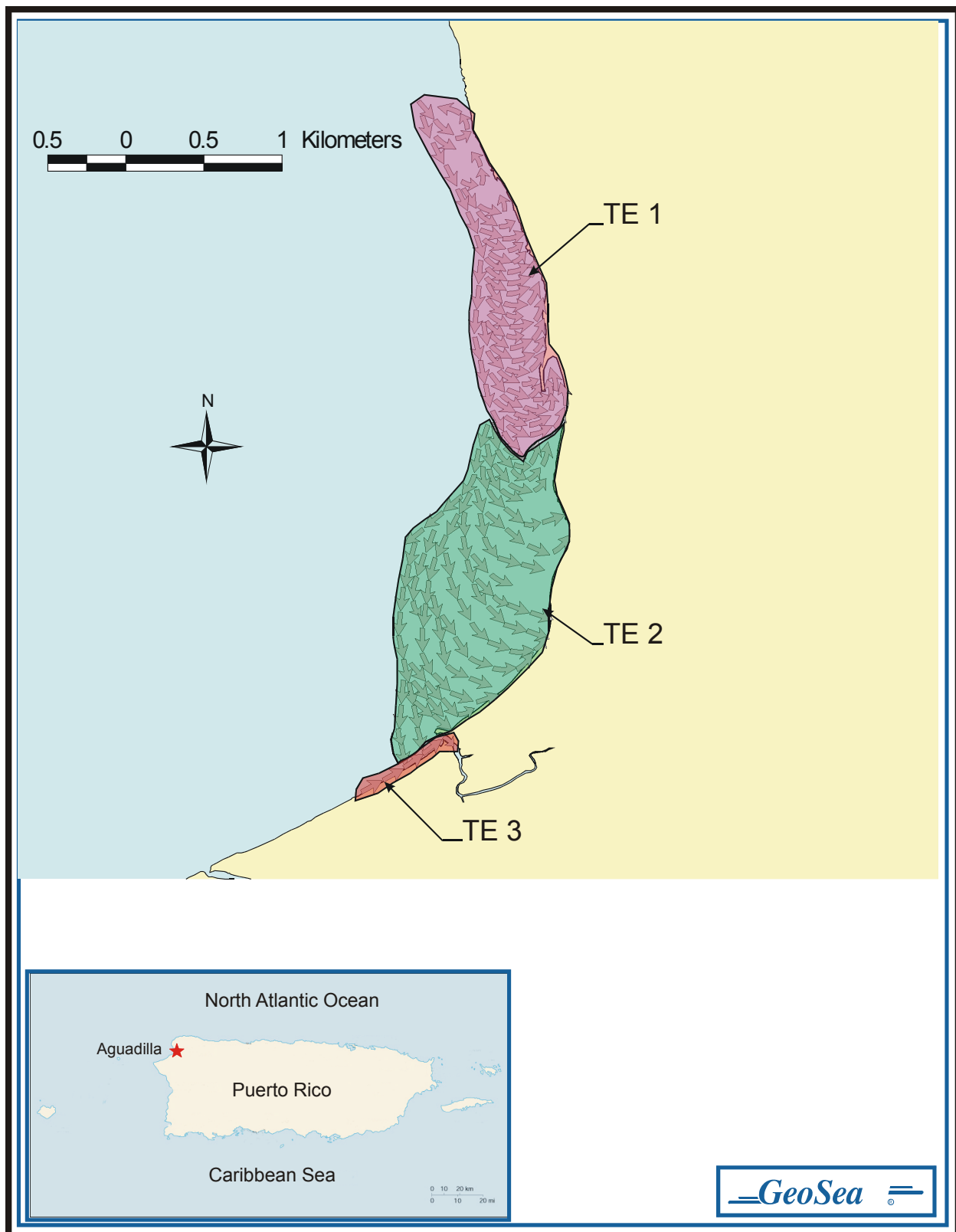


Figure 68. Sediment transport environments (TEs), vicinity of Aguadilla Harbor (after McLaren and Hill 2003).

The group of TE1 lines originates in the offshore portion of the study area and suggests a southerly transport regime at water depths of about 60 ft. Emanating from this southward regime, the pathways move upslope in a counterclockwise gyre to reverse near the shoreline in a northward direction. The majority of the lines produce trends of net accretion, although the accretionary lines are notably clustered inside the breakwater (Figure 69). An exception is a line next to the shoreline, which suggests that erosion may be occurring along the shore at the entrance to the marina.

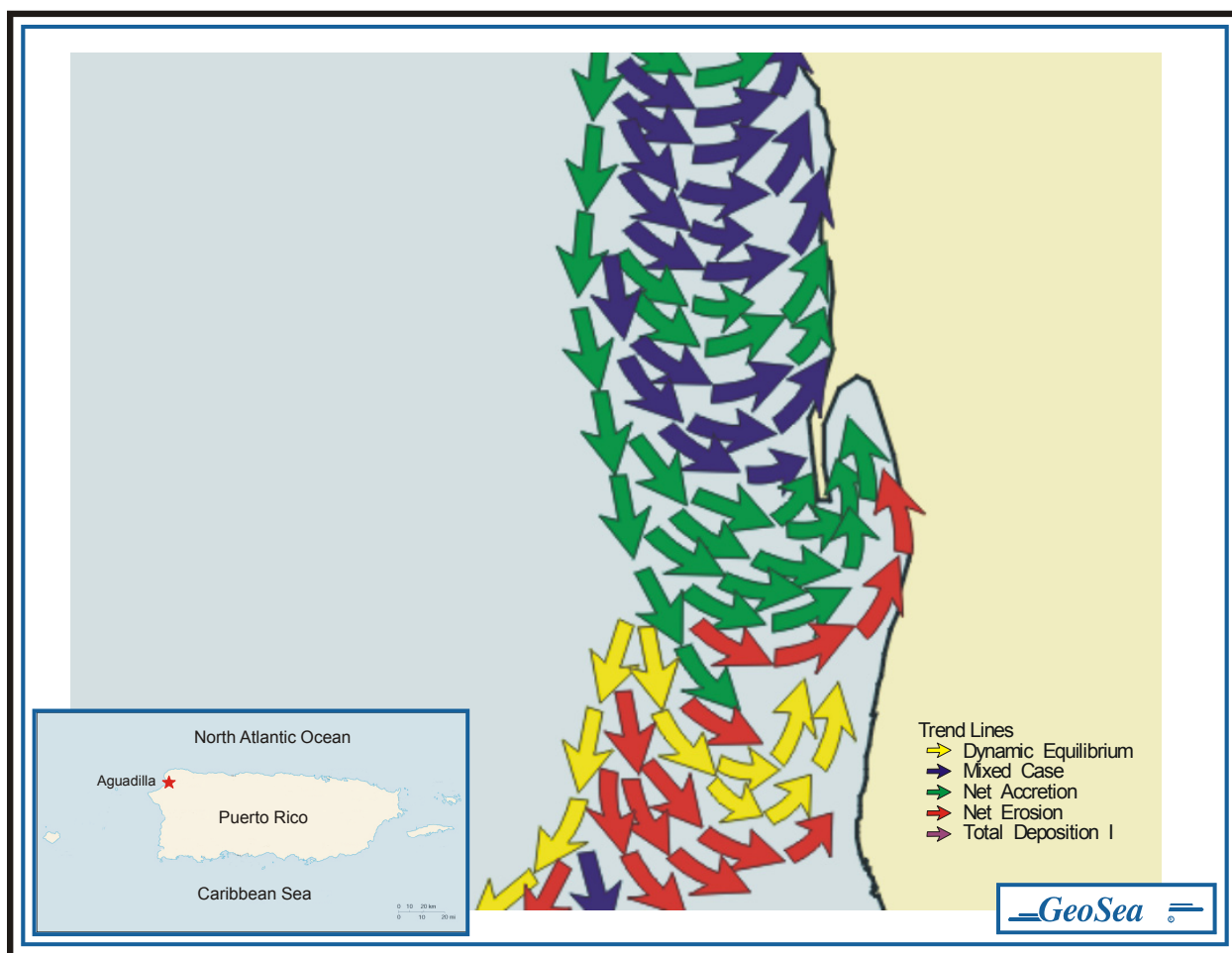


Figure 69. Sediment trends at Aguadilla Harbor breakwater (after McLaren and Hill 2003).

- b. **TE2: Bahia de Aguadilla South.** The second identified transport regime (TE2) extends from about 500 m (1,640 ft) south of the harbor to the southern limit of the study area. Within TE2 the trend is predominately net erosional (73 percent) with some mixed erosion/accretion (27 percent). The shoreward directed erosional arrows in Figure 67 are somewhat misleading, and the explanation is that these pathways are

balanced by seaward transport of sediment by suspension during storm events.

- c. **TE3: Parque de Colon.** This single line of beach samples at Parque de Colón indicates that the mouth of the Caño Madre Vieja is subject to infilling. At the time of sampling, the mouth of the Caño Madre Vieja was nearly completely filled with sand, and the samples collected here could be easily related to the beach sands to the south of the mouth, but not to the offshore samples, nor to the beach sands to the north.

## Discussion

The patterns of transport (Figure 67) indicate that sediment sources for the area under study are in the offshore and from the north. There are not, for example, any land-derived sources in evidence although the Caño Madre Vieja and the Rio Culebrinas (not included in the study area) undoubtedly do provide a supply of sediment to the coast that is dependent on rainfall and the amount of river flow.

The supply of the sand entering the studied area at its north end is consistent with the concept presented by Morelock ([http://geology.uprm.edu/Morelock/GEOLOCN/\\_bchsdWPR.htm](http://geology.uprm.edu/Morelock/GEOLOCN/_bchsdWPR.htm)). He suggests that the westward movement of littoral and shelf sediments along the north coast of Puerto Rico rounds the north-west corner of the island, with much of the material in transport being lost to the littoral zone in the deeper offshore waters. These sediments may then be susceptible to southward movement due, not to waves, but to strong ocean currents moving from north to south through Mona Passage. Tanahara et al. (2002), using a three-dimensional (3-D) Ocean Global Circulation Model, suggest that mean water transport through the Mona Passage is as much as 5.4 Sv (1 sverdrup =  $1.0 \times 10^6$  cu m/sec ( $1.3 \times 10^6$  cu yd/sec)). More importantly, according to direct observations by Johns et al. (1999), currents in the Mona Passage show subsurface maxima directed southwards into the Caribbean together with surface-intensified counterflows along the west coast of Puerto Rico. This observation may be particularly relevant in explaining the patterns of sediment transport derived by the STA. Sediments may be transported southwards by the deep ocean currents, and then moved shoreward and northward in a nearshore counterflow.

This conceptual model of sediment transport suggests that a particle of sand entering the study area from the north may be moved southward and across the shelf to the nearshore, and then transported northwards close

to the shoreline. Likely storm events will tend to re-circulate at least some of the nearshore sediment back into the deeper southward moving transport regime. In this way, sediment may be moved progressively southwards in a series of counterclockwise, elliptical gyres.

At least two observations appear to support this concept. Firstly, the rapidity with which the marina area behind the breakwater infills with sediment makes it unlikely that the sediments are simply a lee deposit trapping only littoral sediments in their movement from the north to south. Deposits in the lee of coastal obstructions are typically small. More likely, the southward opening to the marina causes northward moving sand near the shoreline to be trapped. The breakwater also inhibits storm action from removing the accumulated sediment to recycle with the deeper southward moving transport regime. Secondly, and very important, is the observation that infilling of the marina occurs even during times of limited wave activity (Bottin 2001), a clear indication that wave-driven currents are not necessarily the dominant or only process responsible for the shoaling.

An examination of surface currents using dye and surface markers (oranges) in and around the breakwater (Hughes 2002) showed several interesting features. Nearly all the dye releases outside the breakwater traveled southwards, and none actually entered the harbor. However, the dye patches tended to stop moving once past the breakwater, leading Hughes (2002) to suggest that sand not trapped by the harbor is unlikely to travel farther to feed the beaches to the south. Visual observations made at the time of the dye experiments showed that:

“...plunging breakers were mobilizing large quantities of sand along the breakwater’s seaward toe, and as the wave curled over it was evident that sand was suspended throughout the water column. At the southern tip of the breakwater, the waves broke across the structure head, and significant quantities of sand were carried by the breaking wave around the head and toward the harbor mouth by the diffracted waves.”

As Hughes (2002) pointed out, the actual source of the sediment moving along the breakwater and into the harbor was still unresolved.

Although the tracks followed by the dye do not provide an absolute correlation with the pathways determined by the STA, perhaps the STA has

identified the probable source of the sediments found at the toe of the breakwater. On the regional scale encompassed by the study, the sediments at the toe appear to be clearly related to the deeper water sediments that have come into the area from the north. The surface current just outside the breaker zone will be largely dependent on the angle of the waves approaching the shore, which at the time of dye deployment was slightly favorable to a southward current. Beyond the end of the breakwater, where the surf zone disappears until it is reestablished at the shoreline, the current ceased. There may not, and indeed there need not, be a direct correlation between localized surface currents and the net movement of the sediments on the bottom. The sediment trends do not show specifically that sediments are moving along the toe of the breakwater and round into the harbor, and it is likely that the scale of sampling to achieve such a local detail was inadequate. There were only three or four samples from the toe area of the breakwater, and they produced no preferred direction of transport paralleling it in either direction.

It is possible, therefore, that, superimposed on the regional patterns of transport as derived by the STA, there is some wave-driven littoral transport from north to south aiding in the infilling behind the marina. Beach face sediments, for example, may show local accumulations on the north side of structures such as boat ramps. On the basis of the STA, it is believed that such transport is confined to the dominance of wave activity at the beach face, rather than associated with the northward flowing counter-current in the nearshore.

An important feature of both TE1 and TE2 (Figure 68) is the shoreward transport of sediments from the southward moving offshore transport regime. Such a finding might suggest that the whole coastline is in a state of advancement, which is known not to be the case. In TE1 most of the depositional trends are associated with the marina, which is serving as a trap. North of the marina, only some of the trends are depositional and most of the others are mixed case (i.e., erosion and deposition). In TE2 nearly all the trends are showing net erosion, which may appear as a paradox (i.e., how can sediment be transported shorewards, yet the coast is eroding?). The shoreward directed arrows may be thought of as the bottom half of a conveyor belt, and the sediment samples together with the derived pathways are reflecting only this portion of the belt. The return of sediment (the top half of the conveyor belt) to the offshore occurs during storm events when the bulk of the sediment is carried in suspension back

to the deeper water. If more sediment moves onshore than offshore, depositional trends will result, and the shoreline is likely to be accreting. However, if more sediment moves offshore than is returned (i.e., there is a net sediment loss to the offshore) this will be reflected in the trends showing net erosion. In TE2, this is clearly the case and the derivation of eroding trends is supported by long-term coastal erosion measurements that show that the highest rate of shoreline retreat in all of Puerto Rico is found in this area (3 m/year (10 ft/year)).

### **Summary and conclusions**

- a. Sediment Trend Analysis was performed on 246 samples taken from behind the Aguadilla breakwater and its adjacent waters. An additional 23 sites were visited, but samples were unobtainable due to hard ground conditions (coral reefs).
- b. Most of the samples (77 percent) were pure sand (i.e., < 20 percent of any other size fraction). All the remaining samples were mixtures of sand and mud. There were no samples containing gravel-sized material.
- c. Fifty-one (51) sample sequences were found to describe the sediment transport regime of the area under study. These were divided into three principal Transport Environments (TEs). Two of these comprised the north and south halves of Bahía de Aguadilla, and a third consisted of a single line of beach samples entering the Caño Madre Vieja.
- d. The trends in both the two main transport environments indicated a southward sediment transport regime in the offshore. There appeared to be a counterclockwise gyre emanating from this southward regime driving sediment across the shelf and northwards in the nearshore.
- e. It is suggested that the sediments originate from the littoral drift system on the north coast of Puerto Rico that drives sediment westwards. On rounding into Mona Passage, much of these littoral sediments are lost to the offshore. The present understanding of oceanographic circulation from the Atlantic into the Caribbean indicates that strong southward currents can occur in the Mona Passage combined with return flows in the nearshore along the west coast of Puerto Rico. The presence of these flows correlates well with the patterns of transport derived by the STA.
- f. The southward facing Aguadilla marina appeared to be in a position to act as a sediment trap, blocking the counterclockwise gyre at the shoreline, and precluding the possibility of a sediment return to the offshore during storm activity.
- g. While wave refraction round the breakwater during storms evidently does increase the amount of deposition behind the breakwater, infilling also

occurs during times of limited wave action, lending support to the concept that wave action alone is not entirely responsible.

- h. Both the pathways and the dynamic behavior of the sediments suggest that the sediment trapping effect of the breakwater is unlikely to be playing a major role in the eroding beaches to the south. For this reason, dredging the marina for an economic and renewable source of aggregate material appears to be a desirable option in this particular case, assuming that all other political and environmental issues can be resolved.

### **Interpretation of hydrodynamic forcing<sup>1</sup>**

The two important results of the Sediment Trend Analysis performed by McLaren and Hill (2003) for the Aguadilla Harbor monitoring study include the following:

- a. Sand transported from the offshore region appears to be the source of sand shoaling the Aguadilla Harbor. This result is in agreement with the observation that southward-directed longshore transport at Aguadilla is quite small, and thus, was not likely to be the main contributor to harbor shoaling.
- b. The pathways indicated the sediment-deprived region south of the harbor receives little sediment from the north or from offshore. Thus, the trapping of sediment by the harbor is not contributing to the lack of littoral sediment evident farther south of the harbor. This conclusion is supported by the knowledge that the shoreline in TE2 was deprived of sediment before harbor construction in 1995.

Before accepting the results of a Sediment Trend Analysis, it is imperative that the derived sediment pathways and sedimentation trends be explained in terms of hydrodynamic forcing. Only then can greater credence be given to the STA result. As part of the analysis for Aguadilla Harbor, McLaren and Hill (2003) examined published literature to gain a better understanding of which physical processes were thought to have relevance for forcing sediment transport.

McLaren and Hill (2003) suggested that the primary sediment transport forcing comes from strong southward ocean currents moving through the Mona Passage along the west coast of Puerto Rico. These currents are thought to generate a countercurrent consisting of a shoreward directed

---

<sup>1</sup> This section is extracted essentially verbatim from Hughes (2005).

flow and a northward return flow close to the shoreline. The primary source for sand deposited offshore of Aguadilla is most likely remnants of littoral transport moving westward along the north coast of Puerto Rico and swept southward by the Mona Passage current (although much of the material is lost to deeper water). Thus, it was concluded that the primary forcing mechanism for sediment transport at Aguadilla is oceanic currents rather than wave-induced longshore transport.

Strong currents in the Mona Passage are not thought to be driven by the local wave climate; so according to the STA, sediment deposition in the Aguadilla Harbor should be an ongoing process even during periods of calm waves. Bottin (2001) stated that harbor shoaling occurred during limited wave action, and this supports the STA conclusions. However, observations have also shown that the harbor shoals rapidly during storms; and a dye study by Hughes (2002) during a moderate storm indicated significant quantities of nearshore sand were being mobilized and driven into the harbor around the south tip of the breakwater. Hughes (2002) was unable to identify the source of the shoaling sand other than the fact the sand was available in the nearshore just offshore of the breakwater.

## Summary<sup>1</sup>

The Sediment Trend Analysis for Aguadilla Harbor (McLaren and Hill 2003) identified sediment pathways and erosion/depositional trends that are consistent with observed gross trends at the project site. Earlier observations had tended to rule out southward longshore transport as the source for harbor shoaling material, leaving only onshore moving sediment as a viable source. However, sediment transport by strong nearshore countercurrents associated with the Mona Passage ocean current had not been considered to be the primary forcing mechanism. The derived sediment pathways were consistent with this forcing hypothesis, but field measurements are needed to confirm the existence of currents capable of moving sediment along the prescribed pathways. The STA provided a better understanding of the source and movement of sediment in the Aguadilla Harbor project region. Because the STA conformed to established gross sediment transport trends and could be explained in terms of plausible hydrodynamic forcing, more credence can be given to the result.

---

<sup>1</sup> This section is extracted essentially verbatim from Hughes (2005).

Had the result not conformed to existing knowledge, the STA would have been viewed in a less favorable light. Nevertheless, confirmation of the countercurrent magnitudes with field measurements would have added strength to the STA conclusions.

## 9 Aguadilla Harbor and Beach Profile Surveys, 1997 through 2002

Sediment that has shoaled Aguadilla Harbor (Figure 70), starting at the time of harbor construction (1993-1995), has been transported by wave-induced currents, either alongshore or onshore. Studies indicate the predominant volume of this sediment is arriving onshore from large deposits of sand directly offshore from the harbor and vicinity. To quantify the volume and rate at which sediment was entering Aguadilla Harbor, the U.S. Army Engineer District, Jacksonville, established survey lines (stations) perpendicular to the breakwater, and conducted repetitive surveys for years 1997 through 2002. These surveys extended from the beach line inside the harbor, through the harbor, across the breakwater, and into the open ocean. From these repetitive surveys, volume changes per unit distance along the coastline were ascertained for each station.



Figure 70. Aguadilla Harbor, Puerto Rico (volume change survey stations were established perpendicular to the breakwater and extended through the harbor, across the breakwater, and into the open ocean) (date of photo May 2002).

The MCNP program established a directional self-recording wave gage array in water approximately 18 m (60 ft) deep, directly offshore of the breakwater to record incident wave conditions driving the harbor wave action. These data are displayed in Figures 34 through 50 for time periods (a) November 2001 through March 2002, and (b) April 2003 through March 2004. Here it was seen that, because of the location of the harbor on the northwestern part of Puerto Rico, waves could only approach the harbor from about a west-to-northwest direction (270 to 300 deg azimuth). These gaged wave heights were generally less than about 0.5 m (1.5 ft) high, except for storms when wave heights could exceed 2.0 m (6.6 ft). Normal wave periods were about 6 to 8 sec, with storm wave periods becoming as large as 10 to 12 sec. All these wave characteristics are sufficiently adequate for transporting sediment onshore across the surf zone.

### **Wave Information Study (WIS)**

The CHL Wave Information Study (WIS) has previously established a deepwater wave hindcasting program with hindcast stations located around the coastline of Puerto Rico (Figure 71) in much deeper water than the MCNP wave gage near the breakwater. Hindcast wave data from stations WIS 6 and WIS 7 were correlated with the MCNP wave gage data.

The Wave Information Study (WIS) was authorized in 1976 by Headquarters, U.S. Army Corps of Engineers, to produce wave climate information for U.S. coastal waters. WIS information is generated by numerical simulation of past wind and wave conditions, a process called hindcasting. Knowledge of the wave climate is required to design and maintain the Nation's shore protection and coastal navigation projects such as Aguadilla Harbor, Puerto Rico.

Through the years, hindcasts were added and updated as wave modeling technology advanced and computer power increased. At the end of 1998, hindcasts for all U.S. coasts had been completed; the Atlantic Ocean for two different periods, 1956-1975 and 1976-1995; the Pacific Ocean for 1956-1975; the Gulf of Mexico for 1956-75 and 1976-1995; and the Great Lakes for 1956-1987, and an update of Lake Michigan for 1988-1997.

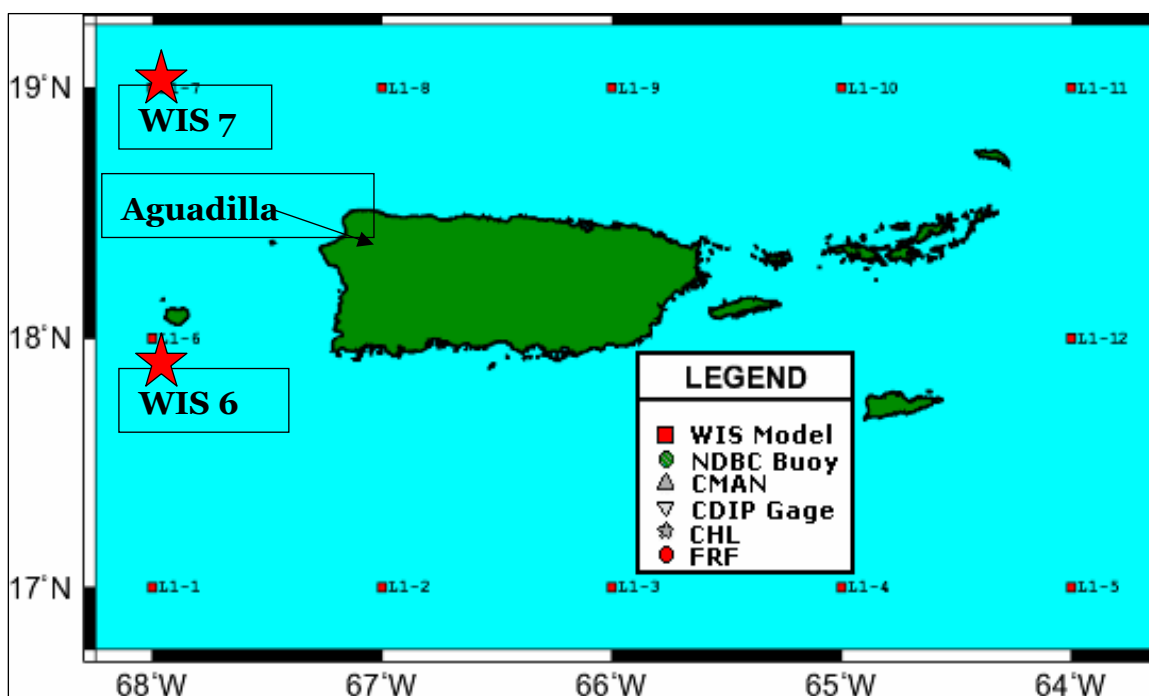


Figure 71. Location of CHL Wave Information Study (WIS) hindcast wave stations WIS 6 and WIS 7 in deep water off the western and northwestern sides of Puerto Rico.

Multiyear time series of bulk wave parameters, significant wave height, period, direction, as well as wind speed and direction, can be viewed and downloaded from the WIS Internet Web site [http://frf.usace.army.mil/cgi-bin/wis/atl/atl\\_main.html](http://frf.usace.army.mil/cgi-bin/wis/atl/atl_main.html). These data are provided at 1-hr intervals. Time series are available for a densely-spaced series of near shore points along the U.S. coastline (in water depths of 15 to 20 m (50 to 65 ft)), and a less-dense series of points in deep water (water depths of 100 m (330 ft) or more). Discrete frequency/directional wave spectra at 3-hr intervals are also available for these same points, but they are not accessible from this site.

The most recent date for which WIS hindcast data are available for stations WIS 6 and WIS 7 off the coast of Puerto Rico is calendar year 1999. The harbor was constructed in years 1993 through 1995, and the MCNP monitoring was conducted during years 2001 through 2004. Hence, for comparison purposes with the MCNP gaged data, WIS hindcast data are presented for years 1997 through 1999. Station WIS 6 data are shown in Figures 72 through 74 for years 1997 through 1999, respectively, and station WIS 7 data are shown in Figures 75 through 77 for years 1997 through 1999, respectively.

A pertinent observation from Figures 72 through 77 is that average daily wave directions are from about a north-to-east direction (0 to 90 deg azimuth), except for storm waves that indeed do approach from a west-to-northwest direction (270 to 300 deg azimuth), analogous to average daily waves recorded by the MCNP wave gage array. The storm waves approaching these WIS stations WIS 6 and WIS 7 from the west-to-northwest direction also have heights of up to 2 m (6.6 ft) with periods up to 10 to 12 sec. Waves with periods in this range begin to disturb material in water as deep as 75 m (250 ft), with a net forward mass sand transport capability.

Uncertainty exists as to whether the onshore movement of sand is predominantly caused by the more moderate daily waves from the west-to-northwest direction as determined by the MCNP wave gage array, or by the more severe storm waves hindcast by WIS that also approach from a west-to-northwest direction. Regardless of the specific wave generation mechanism, both mechanisms result in waves sufficiently adequate to transport sand onshore at the Aguadilla Harbor vicinity where an abundant sand source appears to exist.

## **Beach profiles**

The locations of the beach profile survey lines established by the Jacksonville District are shown in Figure 78, and are identified by stations numbered sequentially from south to north. These survey lines are perpendicular to the breakwater and extend from the shoreline inside the harbor, through the harbor, across the breakwater, and out into the open ocean. The purpose of surveying these beach profile lines was to quantify the volume of material that was being transported into the harbor, to provide an indication of the repetitiveness with which the harbor might need to be dredged to maintain navigability. It was observed during breakwater constructing (June 1993 through July 1995) that sand was accumulating inside the breakwater, with a portion apparently being transmitted through the structure and some being transported around the end of the structure. The beach profile surveys were conducted in years 1997, 1998, 2001, and 2002.

The year 1997 survey was considered the base year survey for subsequent year surveys. The beach profile survey lines were analyzed by a computation of the volume of material per foot of shoreline (cubic yards/foot) that had either accumulated or eroded between two different survey years.

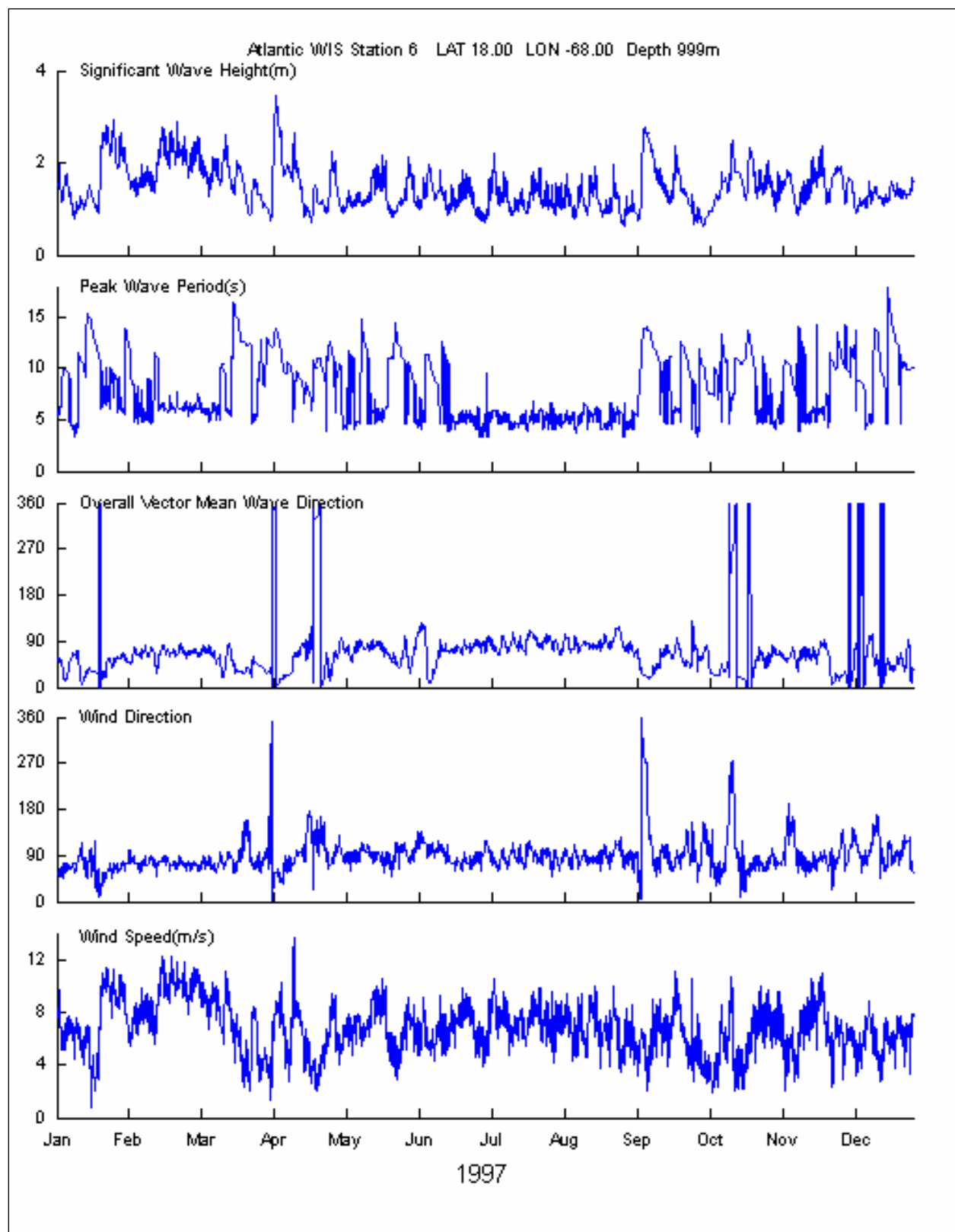


Figure 72. Wave Information Study (WIS) hindcast wave data, station WIS 6, located in deep water off western coast of Puerto Rico (year 1997).

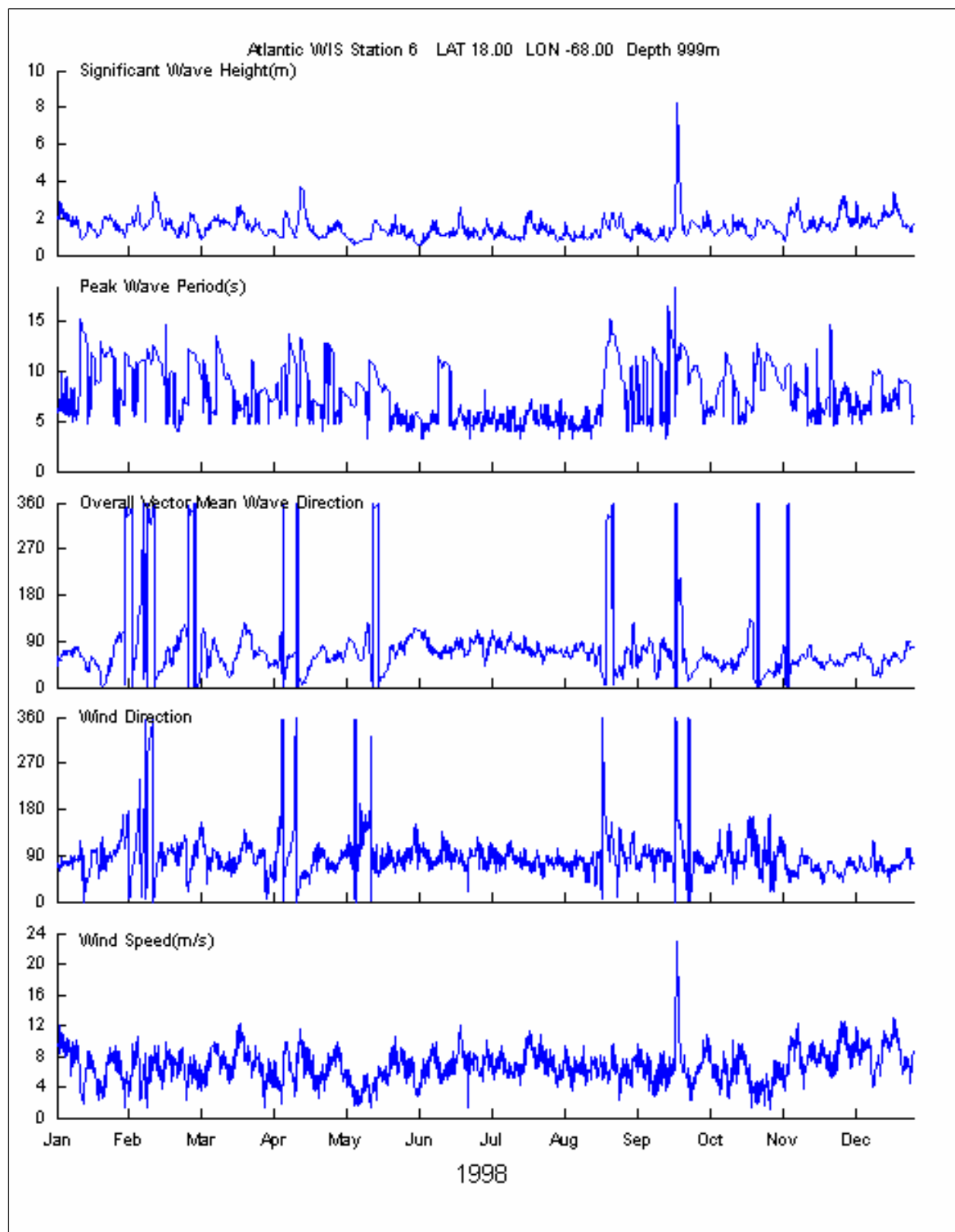


Figure 73. Wave Information Study (WIS) hindcast wave data, station WIS 6, located in deep water off western coast of Puerto Rico (year 1998).

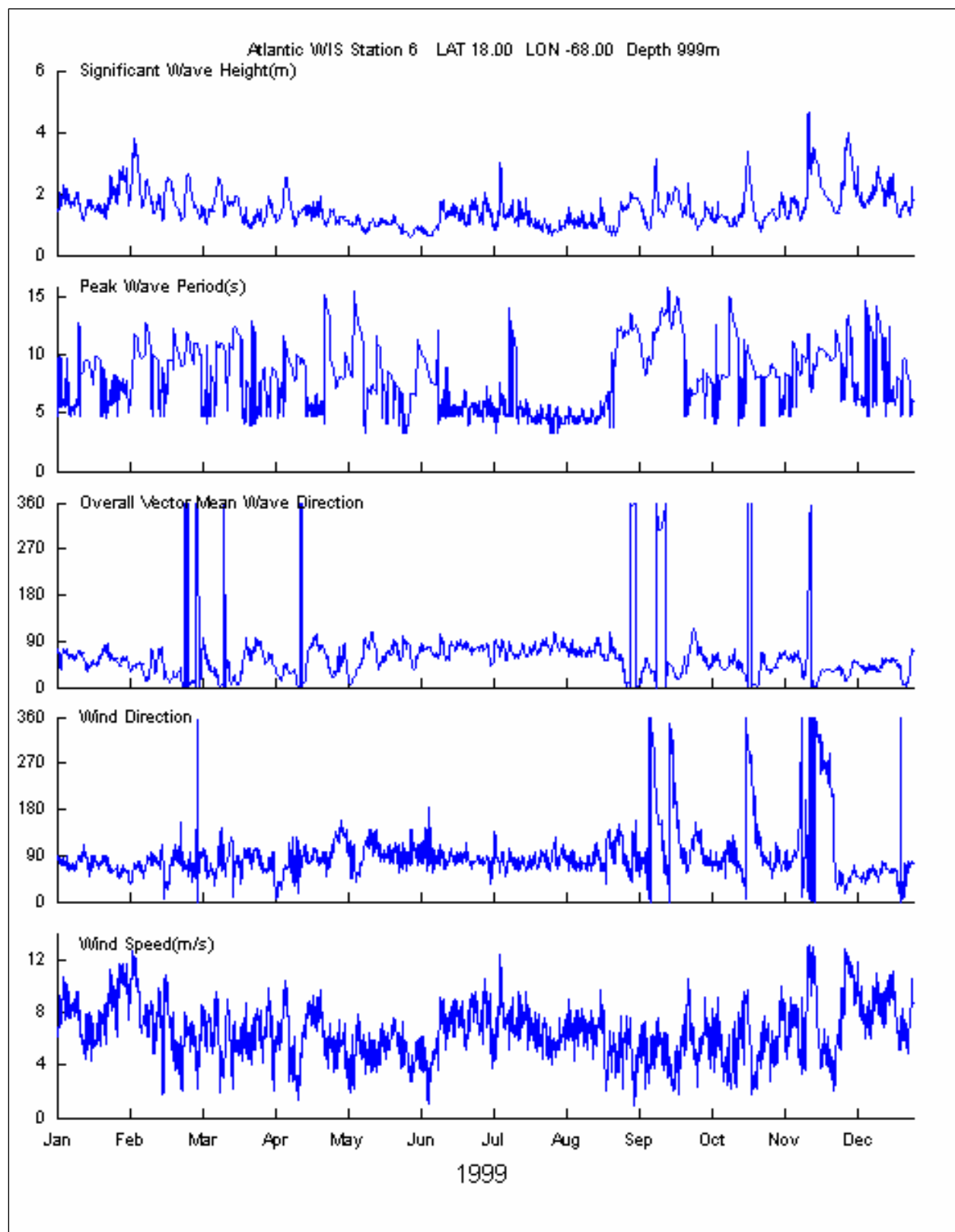


Figure 74. Wave Information Study (WIS) hindcast wave data, station WIS 6, located in deep water off western coast of Puerto Rico (year 1999).

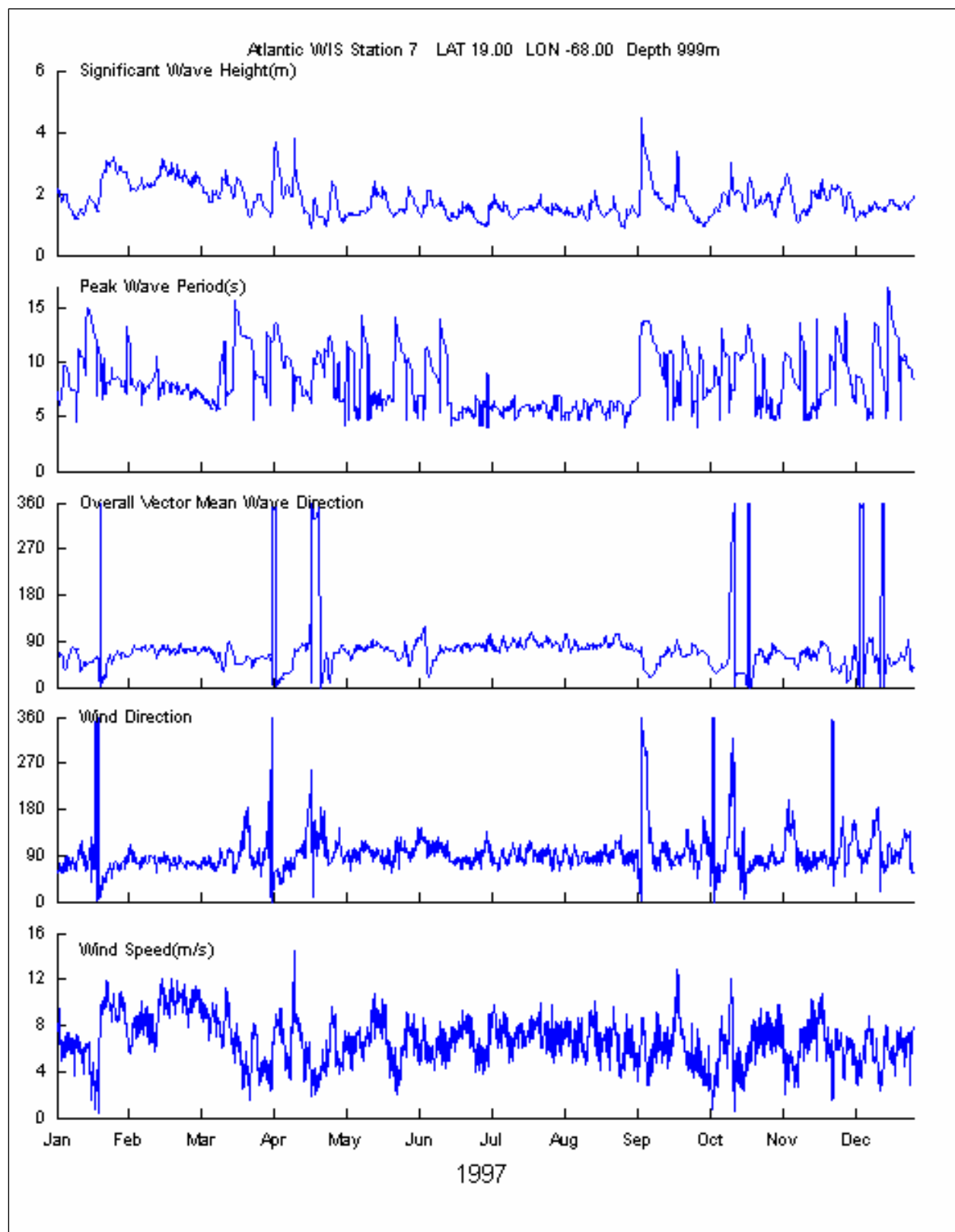


Figure 75. Wave Information Study (WIS) hindcast wave data, station WIS 7, located in deep water off western coast of Puerto Rico (year 1997).

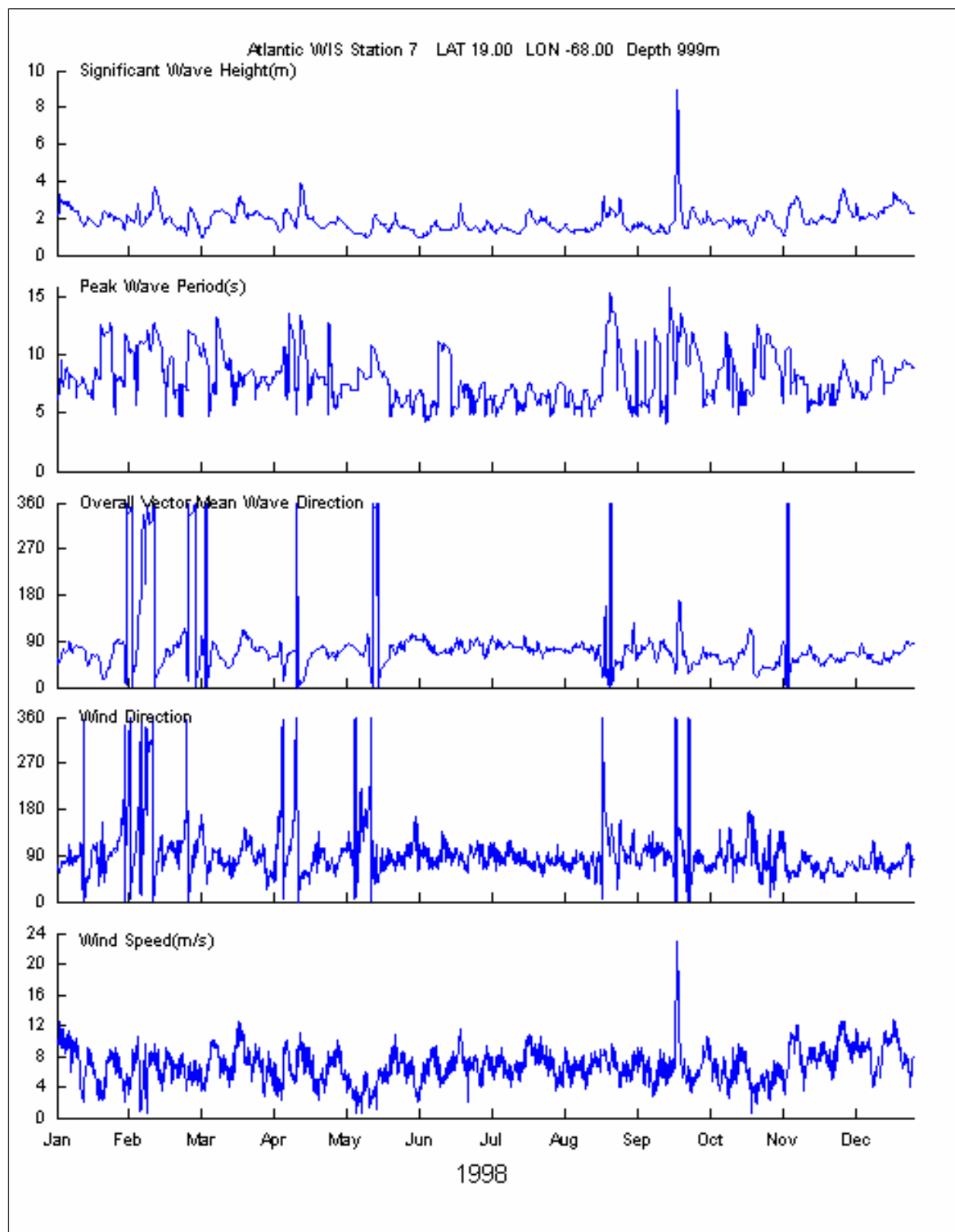


Figure 76. Wave Information Study (WIS) hindcast wave data, station WIS 7, located in deep water off western coast of Puerto Rico (year 1998).

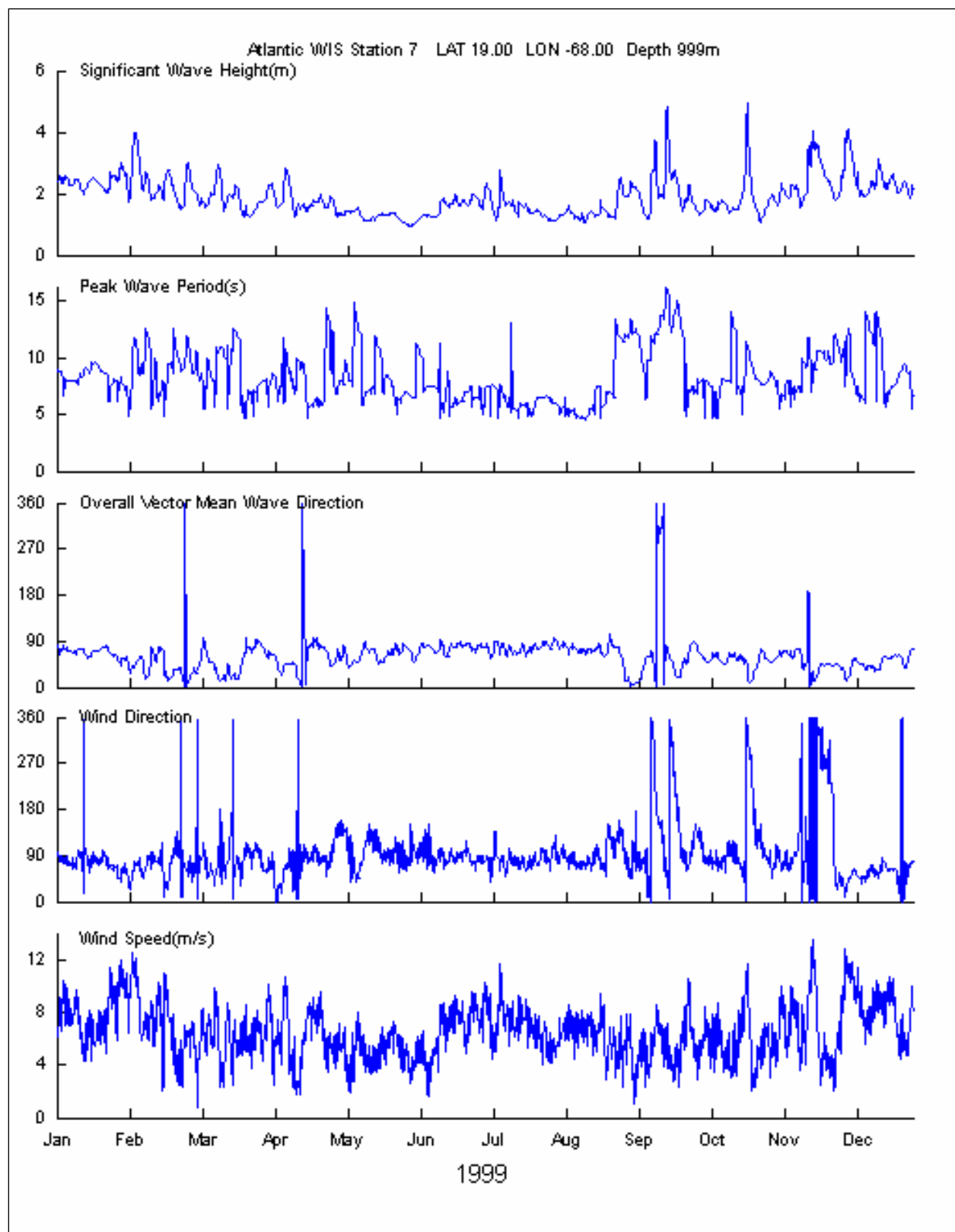


Figure 77. Wave Information Study (WIS) hindcast wave data, station WIS 7, located in deep water off western coast of Puerto Rico (year 1999).

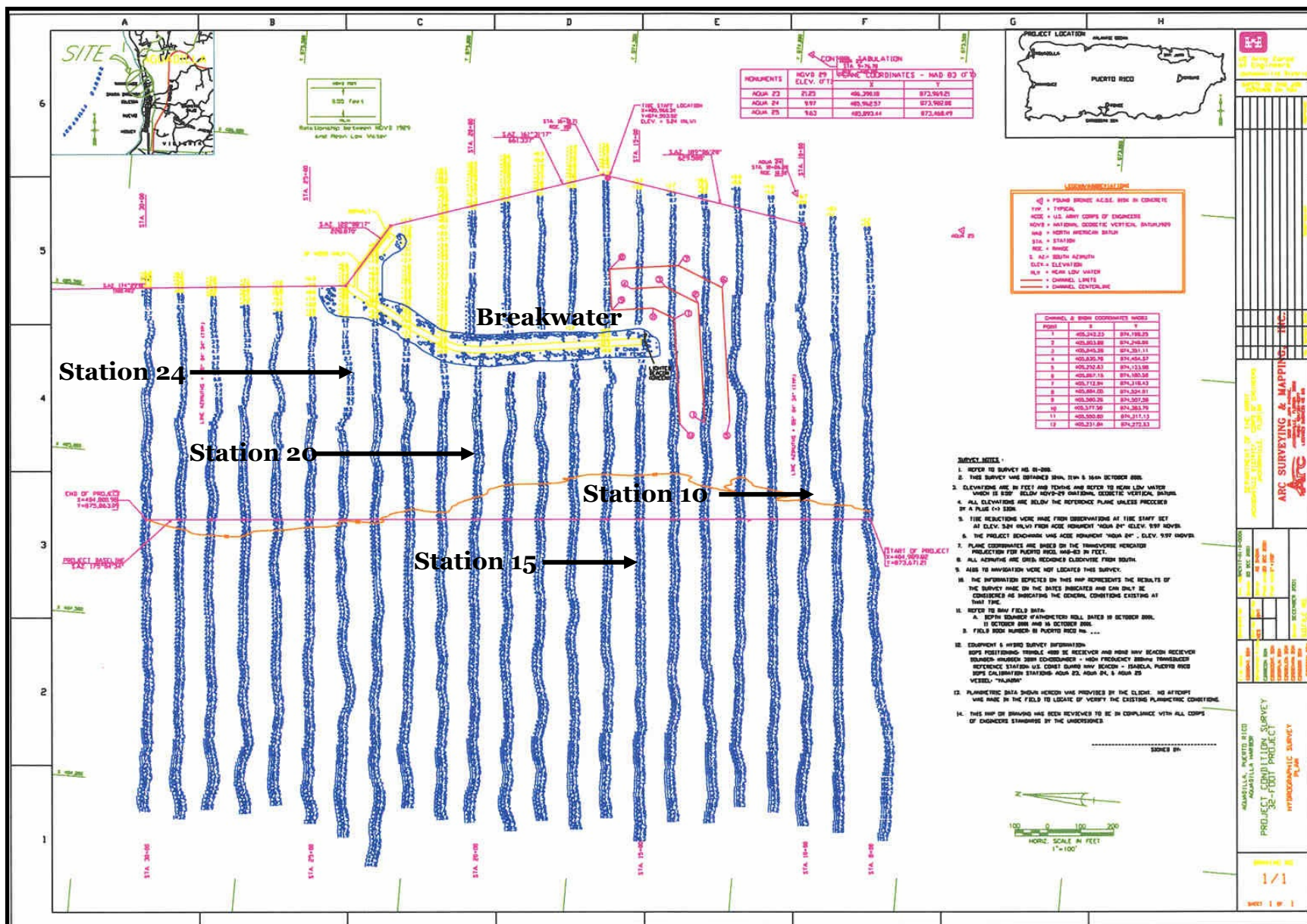


Figure 78. Location of survey stations (survey lines perpendicular to the breakwater), Aguadilla Harbor and vicinity.

Hence, the six volume computational comparisons between two survey years were (a) 1997 versus 1998, (b) 1997 versus 2001, (c) 1997 versus 2002, (d) 1998 versus 2001, (e) 1998 versus 2002, and (f) 2001 versus 2002, for each beach profile survey line. Results of these computations of volume change at each station for the six comparisons are presented in Figures 79 through 84.

These six comparisons are presented in a summation display (Figure 85) that indicates graphically the relationship between each of the six comparisons for each of the beach profile survey station (lines). The same six comparisons are presented in Figure 86 for the volume change at each station inside the harbor (behind the breakwater), and in Figure 87 for the volume change at each station outside the harbor (seaward in front of the breakwater), respectively.

The volume change at each individual beach profile survey station is presented in Appendix B for beach profile survey stations 10 through 20. The region between stations 10 and 20 represents the area where the dominant volume of material accumulation occurred, both inside and outside the breakwater.

Generally, construction of the harbor has resulted in accretion both inside the harbor and immediately seaward of the breakwater during the 4-year interval 1998-2002. However, the rate of change between 2001 and 2002 appears to be less, and that may indicate the nearshore adjustment of the bathymetry due to harbor construction may be nearing equilibrium.

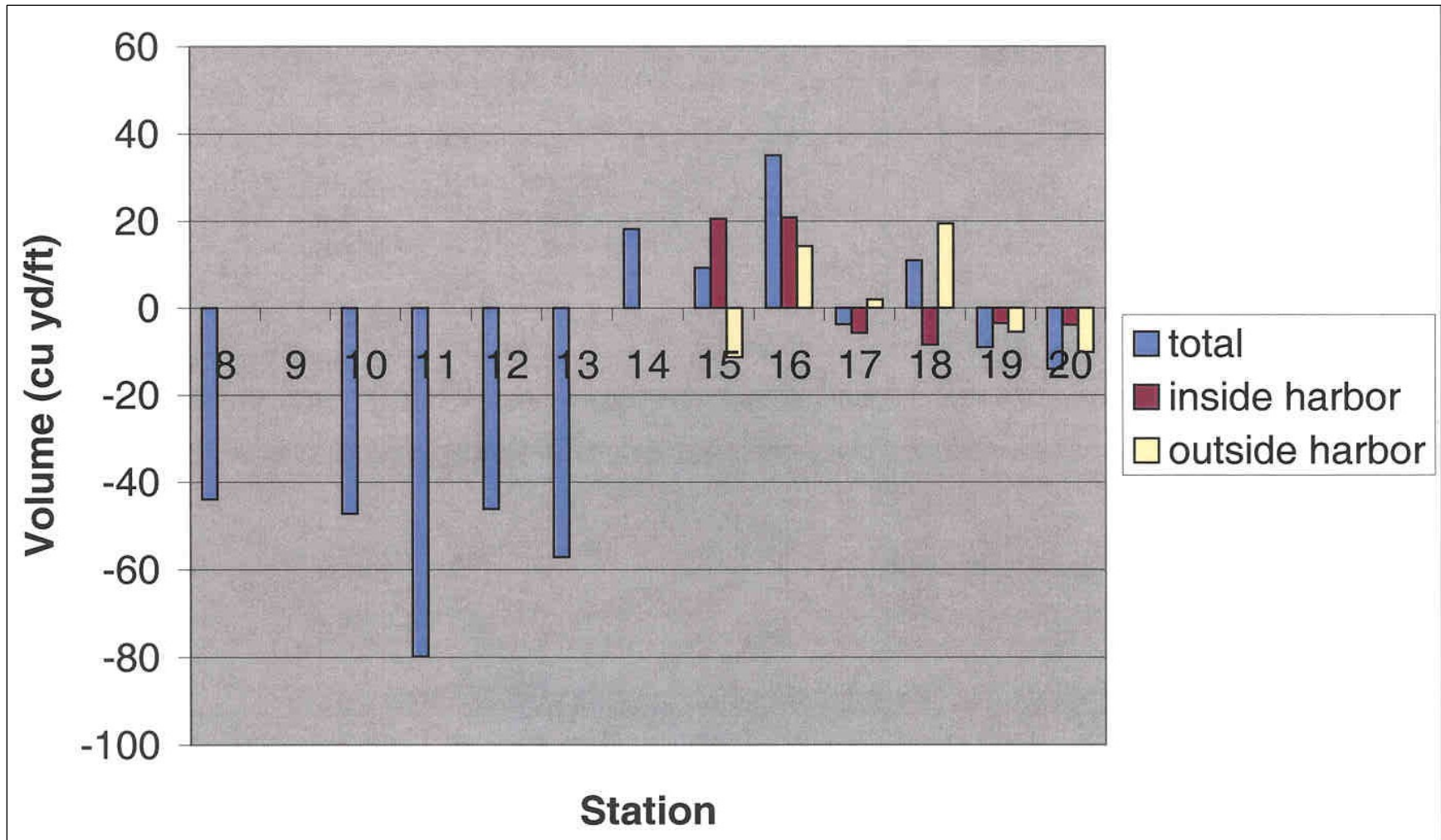


Figure 79. Volume change at each station (cubic yards/foot), 1997 versus 1998, looking eastward.

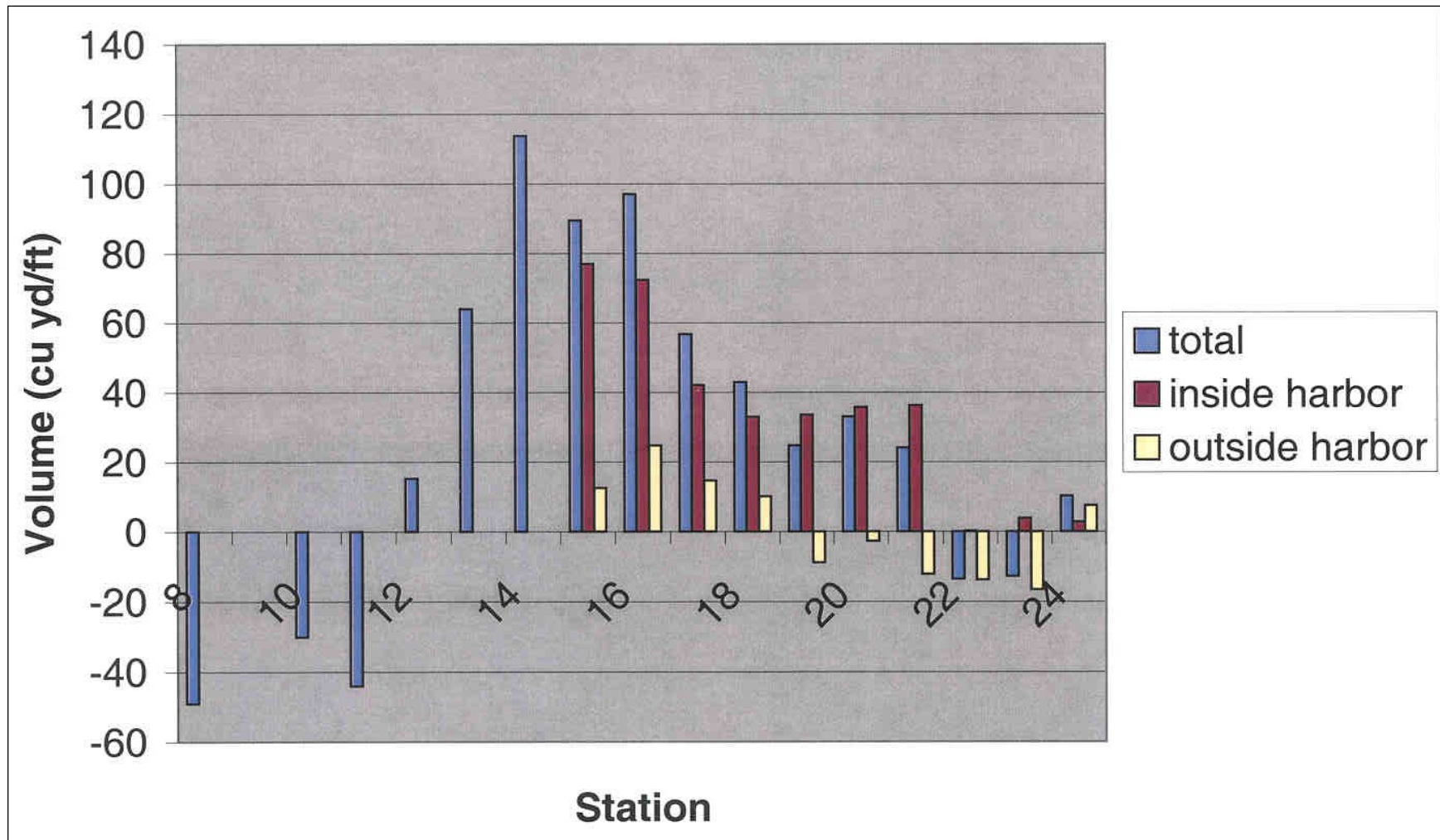


Figure 80. Volume change at each station (cubic yards/foot), 1997 versus 2001, looking seaward.

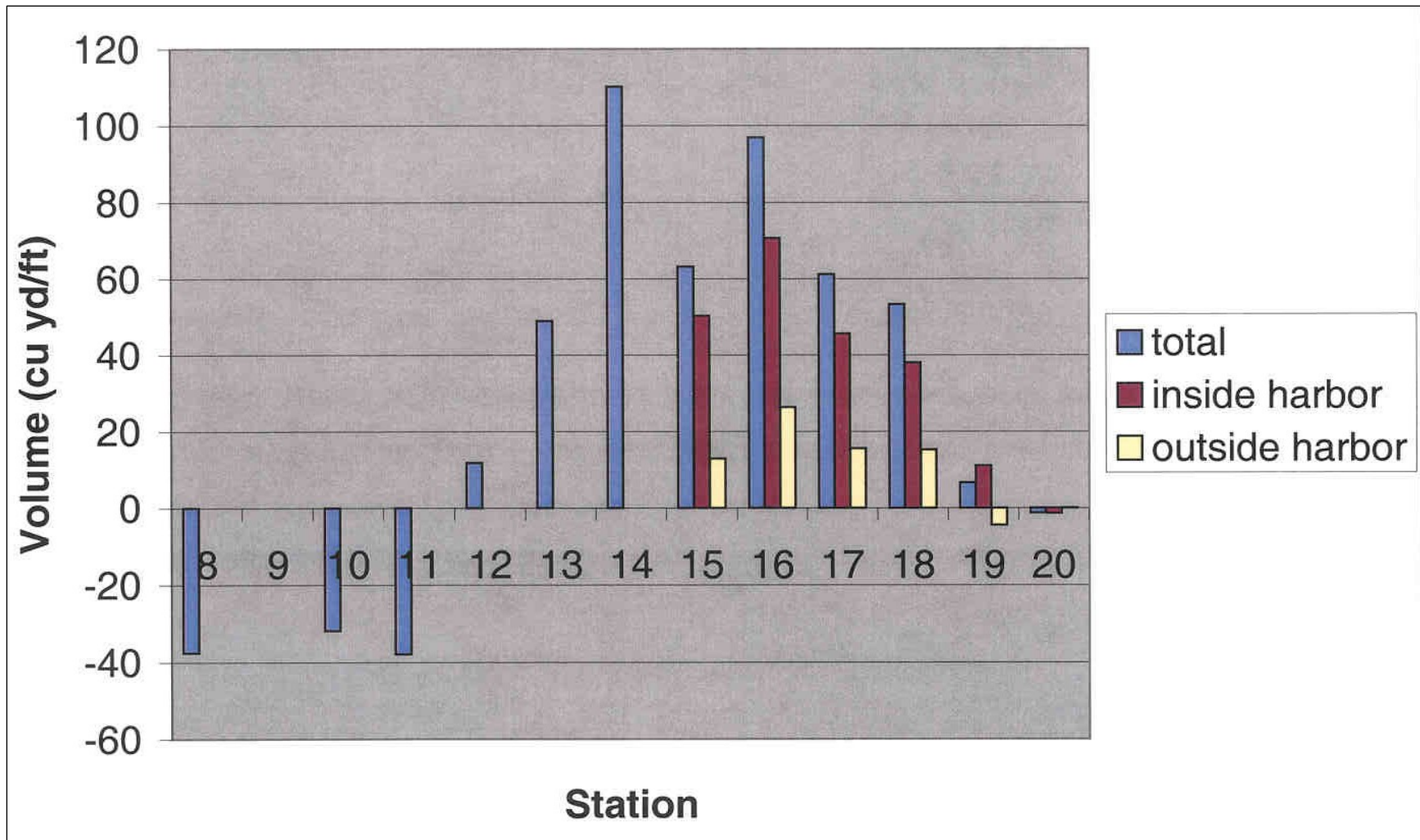


Figure 81. Volume change at each station (cubic yards/foot), 1997 versus 2002, looking seaward.

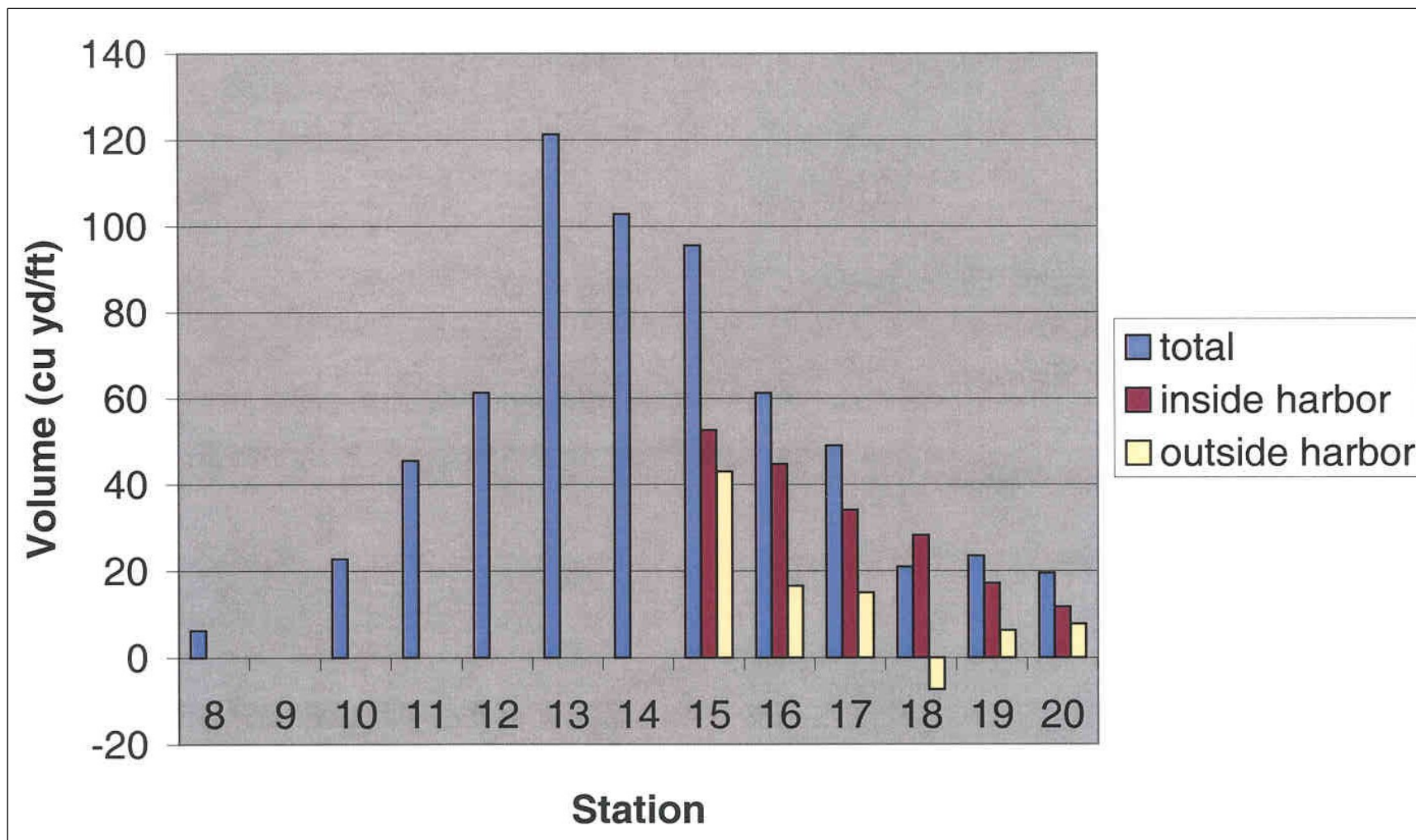


Figure 82. Volume change at each station (cubic yards/foot), 1998 versus 2001, looking seaward.

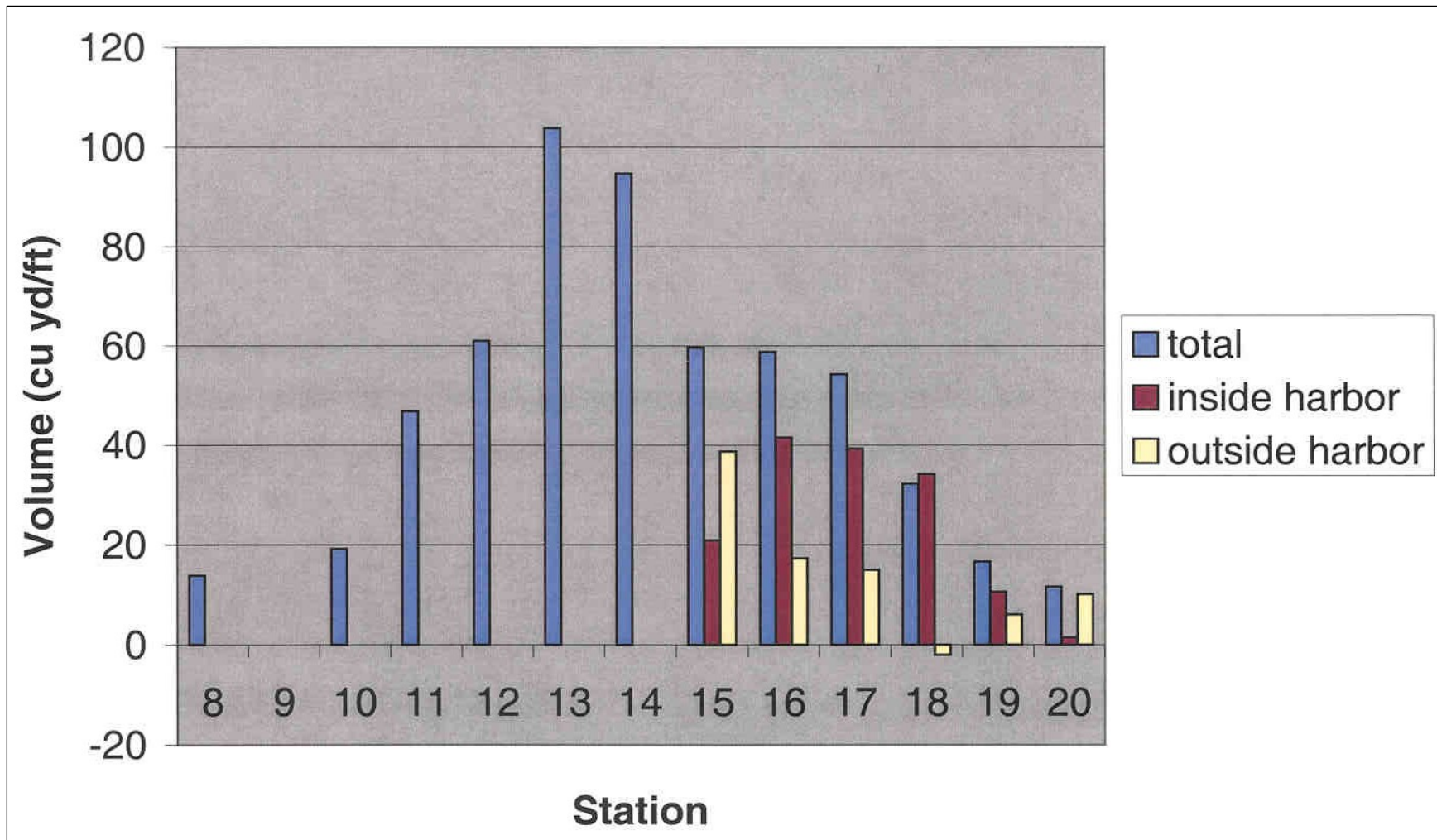


Figure 83. Volume change at each station (cubic yards/foot), 1998 versus 2002, looking seaward.

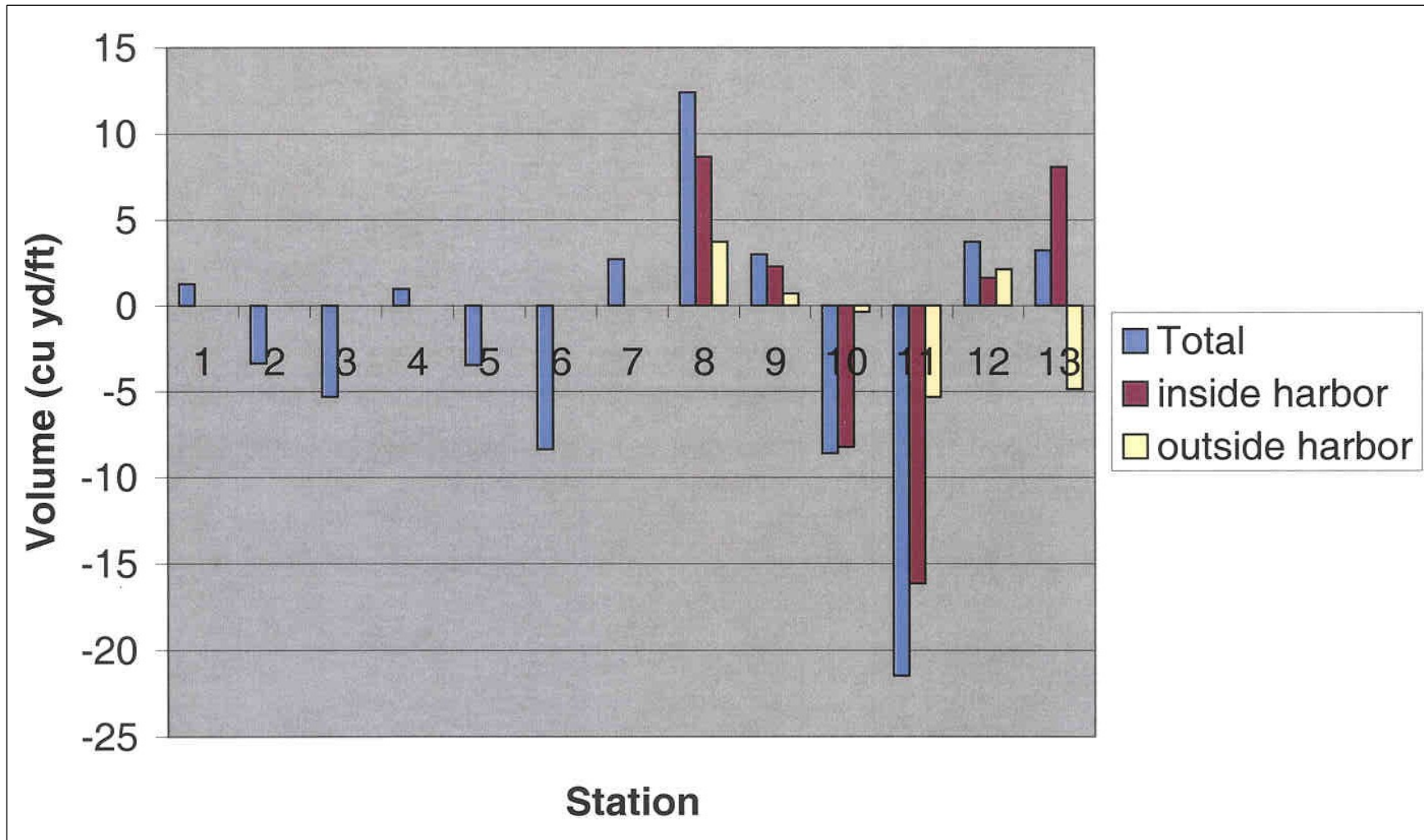


Figure 84. Volume change at each station (cubic yards/foot), 2001 versus 2002, looking seaward.

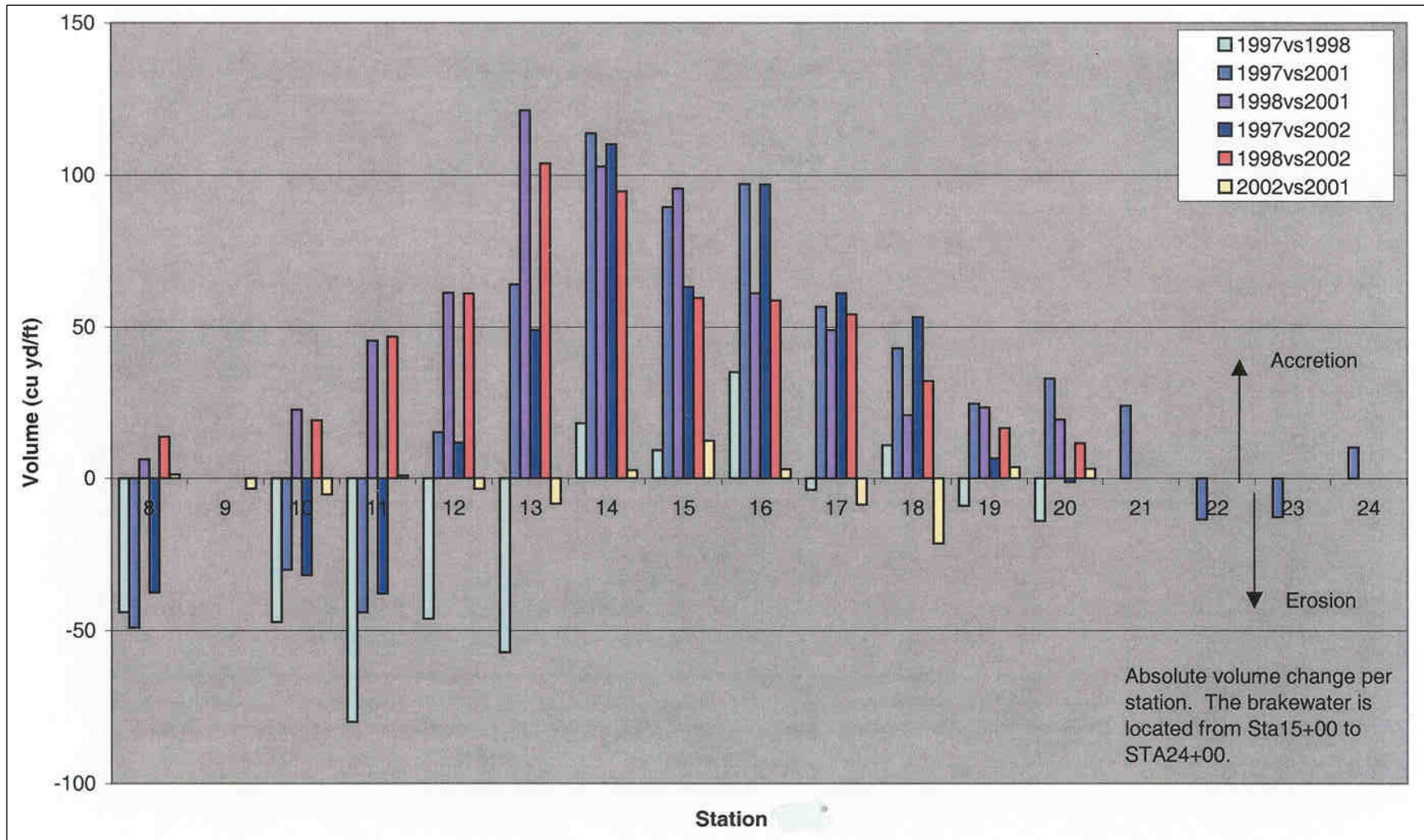


Figure 85. Volume change at each station (cubic yards/foot), looking seaward.

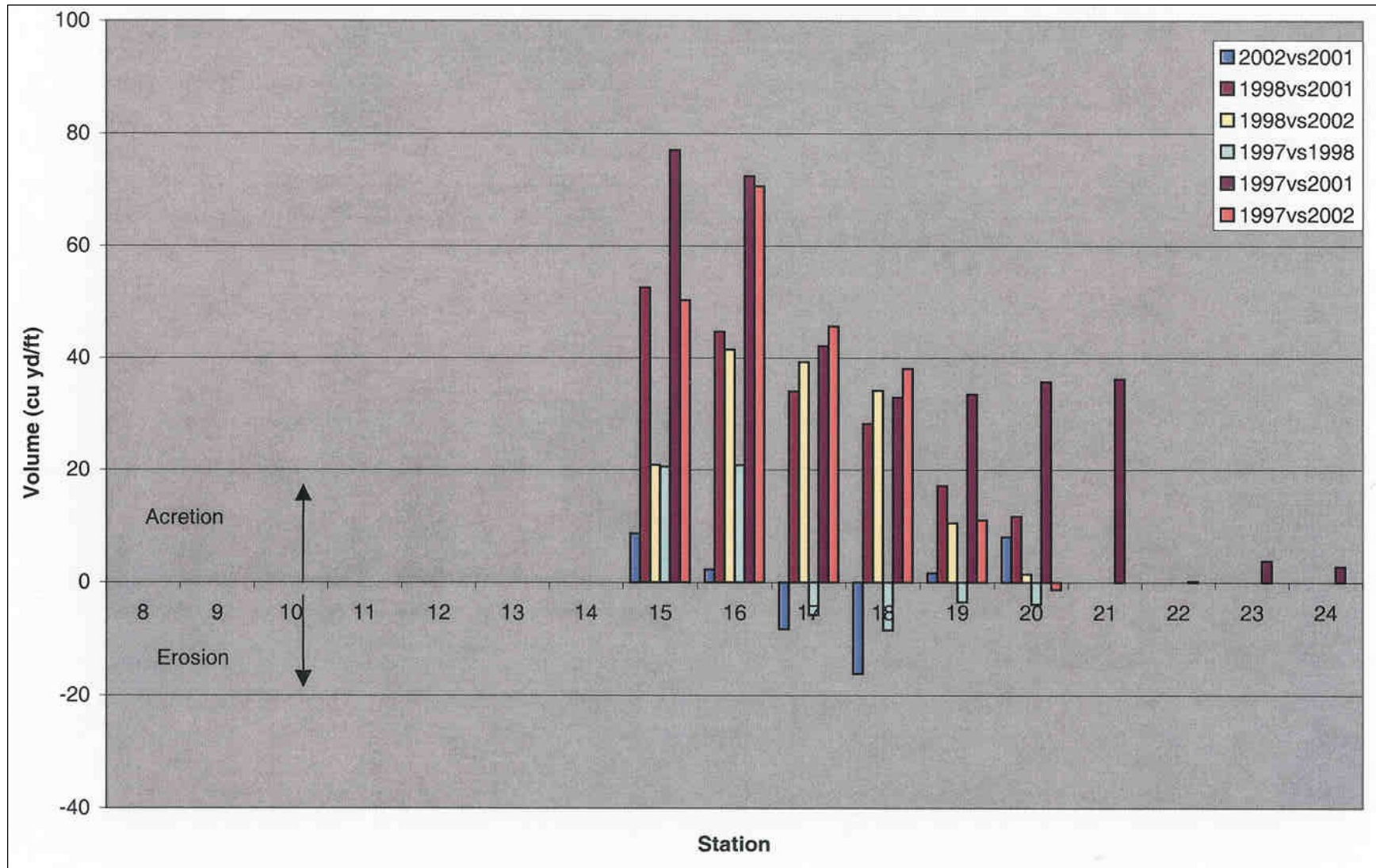


Figure 86. Volume change at each station inside the harbor behind the breakwater (cubic yards/foot), looking seaward.

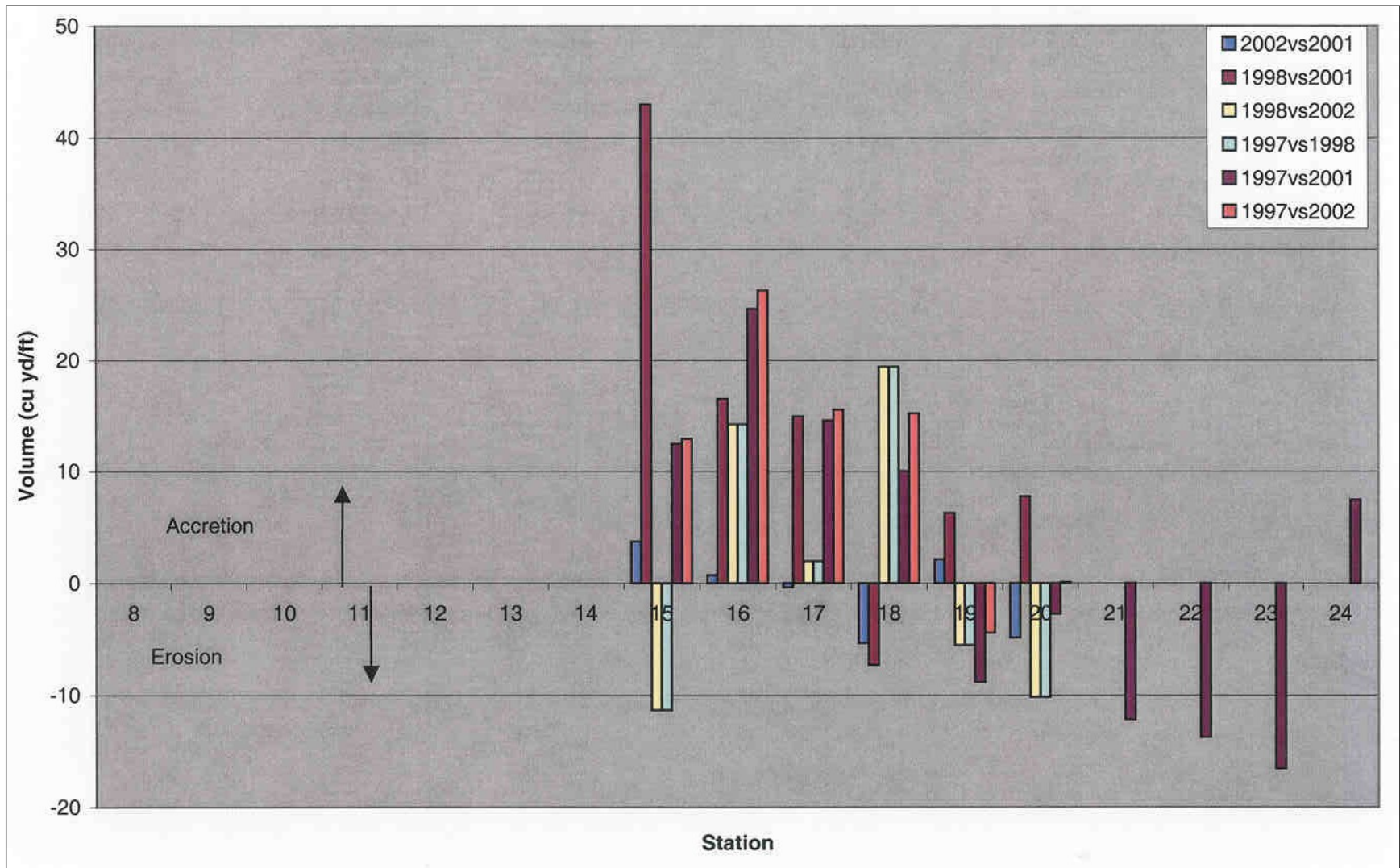


Figure 87. Volume change at each station outside the harbor seaward of the breakwater (cubic yards/foot), looking seaward.

## 10 Summary and Conclusions

### Summary

#### Problem

Prior to construction of Aguadilla Harbor breakwater and channel, there were no protected harbors available for commercial fishermen along the 80-km (50-mile) stretch of coast from Arecibo to Mayaguez. Waves in the bay at Aguadilla were often estimated to exceed 1.2 m (4 ft), especially during winter months. Consequently, commercial fishing was restricted to small, flat-bottomed boats that could be easily hauled up onto the limited beach front for storage and protection from waves. Using small boats 5 to 6 m (16 to 19 ft) in length reduced fishing efficiency, made it impossible at times to negotiate the surf zone, and made fishing a hazardous occupation. In 1982, the Corps of Engineers recommended construction of a 345-m- (1,130-ft-) long breakwater to shelter a 3.8-hectar (9.3-acre) harbor area. The three-layer, rubble-mound breakwater and its associated recreation walkway were completed July 1995.

During construction, shoaling of a segment of the harbor was observed, and excessive wave heights in the harbor caused by refraction/diffraction were much larger than expected, and necessitated subsequent construction of wave absorber. Following construction, additional shoaling occurred within the harbor even with only limited wave activity.

The source of the harbor-shoaling sand was not known. The quantity of sediment deposited in the harbor was surprising given the relatively minor amount of sand thought to be available within the active littoral system. Still, shoaling could possibly have been due to littoral movement from the north. Sedimentation paths identified in a 1998 Section 111 report indicated southward moving material entering the harbor both (a) through the breakwater and (b) around the breakwater tip. It was thought that waves reflected from the vertical seawall assisted moving sediment in a northerly direction along the lee of the breakwater. Sediment also moved in a northerly direction along the eastern shoreline of the harbor.

### **MCNP monitoring plan**

The following five aspects of the Aguadilla Harbor project were proposed for monitoring under the MCNP Program; (a) breakwater armor stability, (b) harbor wave action, (c) physical mechanisms causing harbor shoaling, (d) rates and quantity of harbor sedimentation, and (e) sources of sand causing the harbor shoaling.

Throughout the time period of monitoring (2001 through 2004), the harbor substantially shoaled, thus making the aspects of the monitoring plan pertaining to harbor wave action unfeasible. Other pertinent monitoring tasks were successfully executed. Several activities contributed to one or more of the monitoring tasks, including:

1. Aerial shoreline photography was obtained simultaneously with detailed bathymetry acquired by the Scanning Hydrographic Operational Airborne Lidar Survey (SHOALS) airborne bathymetric technique.
2. Directional wave data were acquired offshore of the breakwater using a bottom-mounted, internally recording wave gauge.
3. A geophysical seabed sediment survey of the region offshore of the harbor, by side-scan sonar, a subbottom profiler, and a seismic reflection system, provided maps showing composition of the bottom (rock or sand), and depth of sand deposits.
4. Over 250 sand samples collected over a grid offshore of the breakwater were used to develop likely sediment pathways based on the Sediment Trend Analysis (STA) technique. The abundance of beach-sized sand observed offshore, combined with projected sediment pathways indicates that much of the sand shoaling the harbor comes from offshore.
5. Previously acquired beach profiles were analyzed, along with profiles acquired during this MCNP monitoring, to assess changes that have occurred north of the breakwater.
6. Breakwater structural integrity was assessed using traditional survey techniques augmented by diver visual inspection of the seaward breakwater toe.

## **Conclusions**

### **Breakwater stability**

A detailed breakwater stone elevation survey by standard topographic surveying techniques was performed by Javier E. Bidot and Associates,

Caguas, Puerto Rico, in September 2003. Several tropical and extra-tropical storms had occurred between the time of completion of the construction of the breakwater during the summer of 1995 and the time of the breakwater survey in the fall of 2003.

It was observed that a few armor stones had experienced a minimal degree of shakedown settlement during these early years following construction, but no major areas of excessive deterioration were found to exist. A contouring of specific elevation data points clearly showed the uniformity of the armor-stone elevations. All contours, from the structure design crest elevation of + 3 m (+10 ft) mllw down to the toe elevation of about 0 m (0 ft) mllw on the harbor side and about -1.8 m (-6 ft) mllw on the open water side, indicate structure settlement is exceedingly uniform or had not taken place by the time of the survey. It can be concluded that parameters used to design the breakwater were correct (or even conservative), and the structure is stable for the expected wave climate.

It is pertinent to understand that tropical storms (hurricanes) approach from the eastern side of the island, and thus do not directly strike the harbor with full-force wave conditions since the harbor is on the western (leeward) protected side of Puerto Rico.

### **Estimating surface currents using dyes and drogues**

#### *Dye study*

Four dye releases were made offshore of Aguadilla Harbor by ERDC in November 2001. Waves were estimated to have a breaking height of 3 m (10 ft) with periods in the range of 7 to 10 sec. Plunging breakers were mobilizing large quantities of sand along the seaward toe of the breakwater, and as the waves curled it was evident that sand was suspended throughout the water column. Sand appeared to be moving from north to south along the breakwater. At the southern tip of the breakwater, the waves broke across the structure head, and significant quantities of sand were carried by the breaking wave around the head and into the harbor mouth by the diffracted waves.

**Dye release no. 1, north beach.** The dye released seaward of the beach immediately north of the harbor breakwater moved generally south and elongated during the first 20 min. The centroid of the dye pattern moved about 100 m (330 ft) during that time, giving an estimated average surface

current speed of about 0.08 m/sec (0.3 ft/sec). During the last 10 min of observation, the dye pattern moved further offshore into a position that was noticeably seaward of the release location for dye packet no. 2. This seaward drift might have been caused by waves reflecting off the breakwater elbow.

**Dye release no. 2, breakwater elbow.** The second dye packet was released seaward of the breakwater elbow, where the shore-connected portion of the structure transitions to the main breakwater leg aligned in the north-south direction. Over a span of 35 min, the dye pattern enlarged slightly and moved south along a line generally parallel to the breakwater. Less elongation of the dye pattern was observed compared to dye packet no. 1. The average speed of the dye centroid as it covered the 100-m distance between the two black lines shown on Figure 24 was estimated to be 0.05 m/sec (0.16 ft/sec). In other words, dye packet no. 2 moved at about half the average speed of dye packet no. 1.

**Dye release no. 3, breakwater midpoint.** The most intriguing dye deployment occurred at a location directly seaward of the midpoint of the breakwater's straight section. Rather than moving parallel to the breakwater, the dye pattern elongated in a shoreward direction with the shoreward end moving south at a faster rate than the seaward end. The packet also moved at a higher average speed, with the centroid moving at an estimated rate of 0.09 m/sec (0.3 ft/sec) and the shoreward edge moving at about 0.13 m/sec (0.4 ft/sec). The stronger current closer to the breakwater had created a shearing effect that seemed to entrain the dye and elongate the pattern. Eventually, the pattern moved beyond the southern end of the breakwater and dissipated.

**Dye release no. 4, breakwater south end.** The final dye release was directly offshore of the breakwater's southern tip. This dye pattern initially moved south as a compact area at an estimated speed of about 0.15 m/sec (0.5 ft/sec). Little elongation or expansion of the pattern was observed. After about 10 min the southerly migration of the dye pattern slowed until it seemed to become stationary. Apparently, the wave-generated along-shore current had a nodal point to the south of the breakwater. This may be an indication that the influence of the breakwater on the alongshore current does not have an effect south of the breakwater. With this decrease in southerly flow, it is hard to conclude that any littoral sand is moving to the beach region south of the harbor project. In other words, sand in the

littoral system is not bypassing the harbor. Prior to harbor construction, the region south of the harbor was already suffering from a lack of sediment, so it would be improper to attribute lack of sand south of the harbor as a direct result of breakwater construction.

#### *Drogue study*

A drogue study was conducted during November 2001 with the purpose of observing and measuring currents near the breakwater and in the harbor during the high-energy wave conditions. Oranges (drogues) were thrown into the water, and the drift progress was timed between two known points. When possible, the distance between the points was estimated by pacing the distance along the breakwater and assuming each pace was about 0.85 m (2.8 ft). Average surface current was obtained as the distance traveled divided by the time of travel.

**Drogue A.** This drogue (orange) was tossed from the southern end of the walking platform on the breakwater into the water about 20 m (65 ft) seaward of the breakwater. The current moved it rapidly past the end of the breakwater in the first minute. The drogue then traveled landward toward the harbor entrance until it moved past the breaking wave point at about 260 sec. Shoreward progress then slowed until it seemed the drogue reached an equilibrium position at the harbor entrance. The drogue maintained this position for the remainder of the observation. The track of Drogue A, and eventual stalling, indicated a current nodal point just outside the harbor entrance. This implies that sand moving into the harbor enters close to the breakwater head, and then is carried in by the diffracted waves.

**Drogue B.** This drogue was tossed near the leeward breakwater toe from the southern end of the breakwater. From observation of a surfer wading out to the end of the breakwater, water depth at this location was about waist deep. The drogue fell into a circular path resembling a stagnation area in the lee of a flow separation point. This observation is consistent with the accumulation of sand in this area.

**Drogue C.** This drogue was placed into the northern end of the harbor in shallow water near the beach. The drogue stayed in the immediate vicinity of the beach as the small waves traveled up the beach face. Because of the general meandering movement, no times were recorded.

**Drogue D.** Visual observation indicated that water was flowing out of the harbor in the region near the parking garage. Drogue D, placed near the parking garage inside the harbor, confirmed this observation by moving southward until the orange was trapped in the small pocket beach just to the south of the parking garage. It appeared that the wave pattern would keep the orange in this location indefinitely. The failure of Drogues A and D to progress any further south provides additional evidence that sand may not be bypassing the harbor project and moving to beaches south of the harbor.

**Drogue E.** This drogue, placed approximately 30 m (100 ft) north of Drogue D near the shoreline inside the harbor, moved slowly into the harbor by the small spilling waves that had diffracted into the harbor.

### **Directional wave measurements**

The monitoring plan initially specified a directional self-recording wave gage array in deep water directly offshore of the breakwater to record incident wave conditions driving the harbor wave action, and a second self-recording wave gage array inside the harbor. Wave measurements were needed within the harbor to ascertain whether the recently added revetment and wave absorbed was effective in quelling wave action within the harbor to within acceptable limits.

The trawler-proof directional gage array consists of three pressure sensors, each placed in a separate container on one of the six array legs, and a central electronics and battery module. The batteries are sufficient to enable the gage to sample at a 1-Hz rate and store wave and water level observations for a year or more. The directional wave gage is mounted in a steel hexapod that is pinned to the seafloor by divers using steel pipe pilings. The frame and instruments weigh about 500 kg (1,100 lb). Installation requires a dive team plus vessel with crew, and takes about a day once the vessel is moored on site. Mild sea states (less than 1 m (3.3 ft) waves) are necessary, not only for placing the frame over the side of the vessel but also for positioning it correctly on the bottom as well as for safety of the divers.

In addition to the directional wave measurements, field measurements were needed to determine if sand moving through the porous breakwater contributes significantly to harbor shoaling. The field component would be short-term deployment of bottom-mounted pressure gage pairs, with one

gage at the seaward toe and the other at the leeward toe of the breakwater. Analyses of the recorded sea surface elevation time series would be used to examine the time varying head difference between the ocean and the harbor to establish the forcing mechanisms for sand transport through the structure. However, throughout the time period of monitoring (2001 through 2004), the harbor substantially shoaled, making it impossible to obtain wave measurements within the harbor.

The deepwater pressure wave gage array was installed in deep water off-shore from the breakwater in water approximately 18 m (60 ft) deep, and collected deepwater data for two different time intervals; (a) November 2001 through March 2002, and (b) April 2003 through March 2004). The 1-Hz frequency data were processed by spectral analysis to determine significant deepwater wave height ( $H_{mo}$ ), wave period ( $T_p$ ), and wave direction of approach ( $D_p$ ).

Because of the location of the harbor on the northwestern part of Puerto Rico, waves could only approach the harbor from about a west-to-northwest direction (270 to 300 deg azimuth). These gaged wave heights were generally less than about 0.5 m (1.5 ft) high, except for storms when wave heights could exceed 2 to 3 m (6.6 to 10 ft). Normal wave periods were about 6 to 8 sec, with storm wave periods becoming as large as 10 to 12 sec. These wave characteristics are sufficiently adequate for transporting sediment onshore from sources in deeper water.

### **Scanning Hydrographic Operational Airborne Lidar Survey (SHOALS)**

#### **SHOALS**

This is an airborne laser system that makes water-depth soundings, and is mounted on a deHavilland Twin Otter fixed-wing aircraft. The laser is collimated red (1,064 nm) and green (532 nm) light pulsed at a rate of 400 Hz. A scanning mirror directs each laser pulse toward the sea surface and into the forward flight path of the aircraft. Receivers in the aircraft detect the return of each pulse from the sea surface (specular interface reflection) and seafloor (diffuse bottom reflection and reflected bottom signal). These returns are analyzed to determine water depth or land elevation for each laser pulse. Each measurement is geopositioned using either pseudo-range or carrier-phase GPS techniques. The result is (x-y-z) data set accuracies of 1 to 3 m (3 to 10 ft) in the horizontal and 0.15 m (0.5 ft) in the vertical. Hydrographic lidar data are generally collected at a

3 m by 3 m (10 ft by 10 ft) sounding density with 200 percent coverage, while topographic lidar data are generally collected at a 2 m by 1 m (6 ft by 3 ft) sounding density with 100 percent coverage.

The maximum water depths detectable by SHOALS are limited by water clarity, or the amount of turbidity in the water column. In practice, SHOALS can see two to three times the Secchi, or visible water depth. In the clearest coastal waters, the maximum detectable depth is about 60 m (200 ft).

#### *Aguadilla Harbor vicinity lidar survey*

The Joint Airborne Lidar Bathymetry Technical Center of Expertise (JALBTCX), located at the U.S. Army Engineer District, Mobile, was contracted in September 2001 to conduct a hydrographic survey, and produce contour maps, of the vicinity of Aguadilla Harbor breakwater for an along-shore distance of about 1.6 km (1 mile) north and south of the harbor, and offshore to about a water depth of 30 m (100 ft) or 2,000 m (6,500 ft). The deHavilland Twin Otter flew at altitudes between 200 and 400 m (60 and 120 ft) with a ground speed of about 100 knots (115 mph). The breakwater was covered by a minimum of three passes. SHOALS has previously demonstrated capabilities that meet USACE Hydrographic Survey accuracy requirements for Class 1 surveys, and the International Hydrographic Organization nautical charting standards for Order 1.

The SHOALS airborne system acquires a tremendous volume of raw data during a single mission. The lidar data are unique and require a specialized Data Processing System (DPS) for post-processing. The DPS main functions are to (a) import airborne data storage on high density data tape, (b) perform quality control checks on initial depths and horizontal positions, (c) provide display and edit capabilities, (d) calculate depth and position (x-y-z) values for each sounding, and (e) output final positions and depths for each sounding. The processed bathymetric survey contour charts for the vicinity of Aguadilla Harbor and vicinity were provided for this MCNP and study tasks. The data were particularly useful for planning operational aspects of the geophysical tasks.

## Geophysical investigations

### *Geophysical survey technique*

Evans-Hamilton, Inc., Seattle, WA, was contracted in early 2002 to perform a seabed sediment survey of an area immediately offshore of the Aguadilla Harbor breakwater. The survey area extended north to south for approximately 1.6 km (1 mile) roughly centered on the breakwater; and east to west with the beachfront as the eastern boundary and approximately 18 m (60 ft) of seawater as the western boundary. The purpose of the data collection was to map the extent and depth of sand versus hard-bottom in the area. The marine geophysical instruments appropriate for this mapping effort were a side-scan sonar system for surficial feature determination, and a subbottom profiler and seismic reflection system for sand layer thickness determination.

Survey transects were designed by utilizing bathymetric contour survey data maps developed by SHOALS. All aspects of the field survey were carried out aboard the University of Puerto Rico (UPR) research vessel *R. V. Sultana*. The survey commenced 14 May 2002 with loading of equipment, and mobilization and testing of the navigation and side-scan sonar systems. Collection of side-scan sonar data commenced at approximately 0700 hr, and was complete by 1700 hr. Subbottom profile and seismic reflection data collection began at approximately 0700 hr on May 16, and were complete by 1500 hr.

### *Surficial features and sand layer thickness*

The marine geophysical data collected offshore of Aguadilla Harbor indicate a complex sand, rock, and coral environment. Side-scan sonar and seismic reflection data were used to produce multiple illustrations of this regime. The sand thickness varies from 0 m (0 ft) to greater than 12 m (40 ft) while interspersed throughout the numerous rock structures and outcrops. Comparisons of side-scan and reflection data generally produce excellent correlation between the data sets. Areas of rock/coral outcrops however, indicate varying sand depths. Whereas some of the outcrops are products of pinnacles that arise from the lower rock formation, these areas indicate a logical shallower sand depth of approximately 3 m (10 ft), much shallower than the surrounding area. While other outcrops (most likely coral) appear independent of the underlying rock, the sand surrounding

and below these outcrops remains at a relatively constant depth of 6 to 9 m (20 to 30 ft).

An overlay plot was developed consisting of the SHOALS bathymetric contour data, overlain by color-coded side-scan sonar survey data indicating the demarcation between the rock/coral shown in color and the blank areas being interpreted as sand. This plot also was overlain by the delineated sand thickness contour data derived from the subbottom profiles and seismic reflection data.

One of the most notable features revealed in these data is the large rock knoll and significant sand bowl to the south of the harbor entrance. This bathymetric feature (rock knoll) may channel and direct a northward water current flow, which provides sand mobility toward the harbor from the nearshore sand bowl. The area immediately offshore of the harbor entrance also provides a significant source of sand available for migration with the predominant wave train, which was from the west-southwest during this survey. Aerial photos taken October 2001 also reveal a sediment plume, being emitted from the river to the south of Aguadilla, which appears to migrate northward, another possible source of harbor sand. These photos provide correlation of beach and upland features to offshore areas ascertained by the geophysical investigations.

It should be noted that these data represent the accumulation and general position of Aguadilla offshore sand in May 2002. The obvious sand migration in this area, as well as any future storm activity, may change both the lateral extent and depth of sand. However, some of the sand deposits are large, so it should be expected that sufficient sediment exists to continually shoal the harbor if routine dredging is implemented.

### **Sediment Trend Analysis (STA) at Aguadilla Harbor**

The STA uses differences in grain-size distributions from bottom sediment samples collected on a regular grid to infer net sediment pathways and regions of erosion, accretion, and dynamic equilibrium. Specifically, sediment samples are collected in the area of interest from the top 10 to 15 cm (4 to 6 in.) of the bottom sediment. The sample grain-size distributions are determined primarily using a laser-based particle-size analyzer. Coarse sediment particles in the size range from 0.7 mm through 4.0 mm in diameter are mechanically sieved, and the results are merged with the majority of the distribution determined by the particle-size analyzer. The

STA technique uses the first three central moments from the grain-size distribution; (a) mean, (b) variance (or sorting), and (c) skewness. Other sediment properties such as mineralogy, texture, and shape are not considered in the analysis.

The basic assumption inherent in STA is that differences in sediment grain-size distributions can be due to sediment transport. In other words, the grain-size distribution may change as sediment moves along a pathway, and every deposit is a result of the processes responsible for sediment movement. This implies active periods of sediment transport occurring at the site at least part of the time.

#### *Hydrodynamic forcing*

The two important results of the STA for the Aguadilla Harbor monitoring study include the following:

1. Sand transported from the offshore region appears to be the source of sand shoaling the Aguadilla Harbor. This result is in agreement with the observation that southward-directed longshore transport at Aguadilla is quite small, and thus, was not likely to be the main contributor to harbor shoaling.
2. The pathways indicated the sediment-deprived region south of the harbor receives little sediment from the north or from offshore. Thus, the trapping of sediment by the harbor is not contributing to the lack of littoral sediment evident farther south of the harbor. This conclusion is supported by the knowledge that the shoreline south of the harbor was deprived of sediment before harbor construction in 1995.

The STA suggested that the primary sediment transport forcing comes from strong southward ocean currents moving through the Mona Passage along the west coast of Puerto Rico. These currents are thought to generate a countercurrent consisting of a shoreward directed flow and a northward return flow close to the shoreline. The primary source for sand deposited offshore of Aguadilla is most likely remnants of littoral transport moving westward along the north coast of Puerto Rico and swept southward by the Mona Passage current (although much of the material is lost to deeper water). Thus, it was concluded that the primary forcing mechanism for sediment transport at Aguadilla is oceanic currents rather than wave-induced longshore transport.

Strong currents in the Mona Passage are not thought to be driven by the local wave climate; so according to the STA, sediment deposition in the Aguadilla Harbor should be an ongoing process even during periods of calm waves. It is well known that harbor shoaling occurred during limited wave action, and this supports the STA conclusions. However, observations have also shown that the harbor shoals rapidly during storms. A dye study during a moderate storm indicated significant quantities of near-shore sand were being mobilized and driven into the harbor around the south tip of the breakwater.

#### *STA conclusions*

1. STA was performed on 246 samples taken from behind the Aguadilla breakwater and its adjacent waters. A further 23 sites were visited but samples were unobtainable due to hard ground conditions (coral reefs).
2. Most of the samples (77 percent) were pure sand (i.e., < 20 percent of any other size fraction). All the remaining samples were mixtures of sand and mud. There were no samples containing gravel-sized material.
3. Fifty-one sample sequences were found to describe the sediment transport regime of the area under study. These were divided into three principal transport environments. Two of these comprised the north and south halves of Bahia de Aguadilla, and a third consisted of a single line of beach samples entering the Caño Madre Vieja.
4. The trends in both the two main transport environments indicated a southward sediment transport regime in the offshore. There appears to be a counterclockwise gyre emanating from this southward regime driving sediment across the shelf and northwards in the nearshore.
5. It was suggested that the sediments originate from the littoral drift system on the north coast of Puerto Rico that drives sediment westwards. On rounding into Mona Passage, much of these littoral sediments are lost to the offshore. The present understanding of oceanographic circulation from the Atlantic into the Caribbean indicates that strong southward currents can occur in the Mona Passage combined with return flows in the near-shore along the west coast of Puerto Rico. The presence of these flows correlates well with the patterns of transport derived by the STA.
6. The southward facing Aguadilla marina appears to be in a position to act as a sediment trap, blocking the counterclockwise gyre at the shoreline, and precluding the possibility of a sediment return to the offshore during storm activity.
7. While wave refraction round the breakwater during storms evidently does increase the amount of deposition behind the breakwater, infilling also

occurs during times of limited wave action, lending support to the concept that wave action alone is not entirely responsible.

8. Both the pathways and the dynamic behavior of the sediments suggest that the sediment trapping effect of the breakwater is unlikely to be playing a major role in the eroding beaches to the south. For this reason, dredging the marina for an economic and renewable source of aggregate material appears to be a plausible option if political, economic, and environmental issues can be resolved.

### **Aguadilla Harbor and beach profile surveys, 1997 through 1992**

#### *Wave Information Study (WIS) and gaged wave data*

Sediments that have shoaled Aguadilla Harbor since the time of harbor construction were transported by wave-induced currents, either along-shore or onshore. Studies indicate the predominant volume of this sediment is arriving onshore from large deposits of sand directly offshore from the harbor and vicinity. To quantify the volume and rate at which sediment was entering Aguadilla Harbor, survey lines (stations) were established perpendicular to the breakwater, and repetitive surveys were conducted for years 1997 through 2002. These surveys extended from the beach line inside the harbor, through the harbor, across the breakwater, and into the open ocean. From these repetitive surveys, volume changes per unit distance along the coastline were ascertained for each station.

A pertinent observation from the Wave Information Study (WIS) hindcast wave stations WIS 6 and WIS 7 is that average daily wave directions are from about a north-to-east direction (0 to 90 deg azimuth), except for storm waves that indeed do approach from a west-to-northwest direction (270 to 300 deg azimuth), analogous to average daily waves recorded by the MCNP wave gage array. The storm waves approaching these WIS stations from the west-to-northwest direction also have heights of up to 2 to 3 m (6 to 10 ft) with periods up to 10 to 12 sec. Waves with periods in this range begin to disturb material in water as deep as 75 m (250 ft), with a net forward mass sand transport capability.

Uncertainty exists as to whether the onshore movement of sand is predominantly caused by the more moderate daily waves from the west-to-northwest direction as determined by the MCNP wave gage array, or by the more severe storm waves hindcast by WIS that also approach from a west-to-northwest direction. Regardless of the specific wave generation

mechanism, both mechanisms result in waves sufficiently adequate to transport sand onshore at the Aguadilla Harbor vicinity where an abundant sand source appears to exist.

#### *Harbor and beach profile surveys*

The locations of the beach profile survey lines are identified by station numbers. These survey lines are perpendicular to the breakwater and extend from the shoreline inside the harbor, through the harbor, across the breakwater, and out into the open ocean. The purpose of surveying these beach profile lines was to quantify the volume of material that was being transported into the harbor, to provide an indication of the repetitiveness with which the harbor might need to be dredged to maintain navigability. The beach profile surveys were conducted in years 1997, 1998, 2001, and 2002.

The year 1997 survey was considered the base year survey for subsequent year surveys. The beach profile survey lines were analyzed by a computation of the volume of material per foot of shoreline (cubic yards/foot) that had either accumulated or eroded between two different survey years. Hence, the six volume computational comparisons between two survey years were (a) 1997 versus 1998, (b) 1997 versus 2001, (c) 1997 versus 2002, (d) 1998 versus 2001, (e) 1998 versus 2002, and (f) 2001 versus 2002, for each beach profile survey line.

These six comparisons are presented in a summation display that indicates graphically the relationship between each of the six comparisons for each of the beach profile survey station (lines). The same six comparisons are presented for the volume change at each station inside the harbor (behind the breakwater), and for the volume change at each station outside the harbor (seaward in front of the breakwater), respectively. The volume change at each individual beach profile survey station also is presented. The region between stations 10 and 20 represents the area where the dominant volume of material accumulation occurred, both inside and outside the breakwater.

## References

- Aldridge, J. 1997. Hydrodynamic model predictions of tidal asymmetry and observed sediment transport paths in Morecambe Bay. *Estuarine, Coastal and Shelf Science* 44: 39-56.
- Allender, J., J. Albrecht, and G. Hamilton. 1983. Observations of directional relaxation of wind sea spectra. *Journal of Physical Oceanography* 13:1519-1525.
- Bergemann, F., G. Lang, and G. Flugge, G. 1998. A particle method for sediment transport modeling in the Jade Estuary. In: M. L. Spaulding and A. F. Blumberg, (ed.), *Proceedings of the 5th International Conference of Estuarine and Coastal Modeling*, Alexandria, VA.
- Bottin, R., Jr. 2001. *Monitoring completed navigation projects program*. Coastal Engineering Technical Note ERDC/CHL CETN-IX-5. Vicksburg, MS: U.S. Army Engineer Research and Development Center.
- Demirbilek, Z., and L. Vincent. 2002. *Water wave mechanics*. In: Z. Demirbilek, *Coastal Engineering Manual*, Coastal Hydrodynamics, Engineer Manual 1110-2-1100, Part II-1. Washington, DC: U.S. Army Corps of Engineers.
- Duck, R., J. Rowan, P. Jenkins, and I. Youngs. 2001. A multi-method study of bedload provenance and transport pathways in an estuarine channel. *Physics and Chemistry of the Earth (B)* 26(9):747-752.
- Evans-Hamilton, Inc. 2002. *Results of seabed sediment survey, Aguadilla, Puerto Rico*. Evans-Hamilton, Inc., Seattle, WA. Report prepared for U.S. Army Engineer Research and Development Center, Vicksburg, MS.
- Flemming, B. 1988. Process and pattern of sediment mixing in a microtidal coastal lagoon along the west coast of South Africa. In: P. L. De Boer, A. Van Gelder, and S. D. Nio, ed., *Tide-influenced sedimentary environments and facies*. D. Reidel Publishing Company, 275-288.
- Gao, S., and M. Collins. 1994. Analysis of grain size trends, for defining sediment transport pathways in marine environments. *Journal of Coastal Research* 10(1):70-78.
- Gao, S., M. Collins, J. Lanckneus, G. De Moor, and V. Van Lancker. 1994. Grain size trends associated with net sediment transport patterns: An example from the Belgian continental shelf. *Marine Geology* 121: 171-185.
- Guillen, J., and J. Jimenez. 1995. Processes behind the longshore variation of the sediment grain size in the Ebro Delta coast. *Journal of Coastal Research* 11(1): 205-218.
- Gunther, H., W. Rosenthal, and M. Dunckel. 1981. The response of surface gravity waves to changing wind direction. *Journal of Physical Oceanography* 11: 718-728.

- Hartmann, D., and B. Flemming. 2002. A comparison between log-hyperbolic and model-independent grain size distributions in sediment trend analysis (STA). *Journal of Coastal Research* 18(3):592-595.
- Headquarters, U.S. Army Corps of Engineers. 1997. *Engineering and design: Monitoring completed navigation projects*. Engineer Regulation 1110-2-8151. Washington, DC: Headquarters, U.S. Army Corps of Engineers.
- Hill, S., and P. McLaren. 2001. A comparison between log-hyperbolic and model-independent grain size distributions in sediment trend analysis (STA). *Journal of Coastal Research* 17(4):931-935.
- Hughes, S. 2002. Estimating surface currents near coastal structures using dye and drogues. Coastal and Hydraulics Engineering Technical Note ERDC/CHL CHETN-VI-37. Vicksburg, MS: U.S. Army Engineer Research and Development Center. (<http://chl.wes.army.mil/library/publications/chetn>).
- Hughes, S. 2005. *Use of sediment trend analysis (STA<sup>®</sup>) for coastal projects*. Coastal and Hydraulic Engineering Technical Note ERDC/CHL CHETN-VI-40. Vicksburg, MS: U.S. Army Engineer Research and Development Center. (<http://chl.wes.army.mil/library/publications/chetn>).
- Johns, E., W. Wilson, and R. Molinari. 1999. Direct observations of velocity and transport in the passages between the Intra-Americas Sea and the Atlantic Ocean, 1984-1996. *Journal of Geophysical Research* 104:25,805-25,820.
- Kinsman, B. 1965. *Wind waves: their generation and propagation on the ocean surface*, Englewood, NJ: Prentice-Hall, Inc.
- Lanckneus, J., G. De Moor, and G. De Schaepmeester. 1992. Residual sediment transport directions on a tidal sand bank: Comparison of the 'McLaren model' with bed-form analysis. *Bulletin de la Societe belge d'Etudes Geographique – SOBEG*. 2:425-446.
- Lillicrop, J., and J. Banic. 1993. Advancements in the U.S. Army Corps of Engineers hydrographic survey capabilities; the SHOALS system. *Marine Geology* 15.
- Livingstone, I. 1989. Temporal trends in grain-size measures on a linear sand dune. *Sedimentology* 26:1017-1022.
- Madsen, O., and S. White. 1976. *Reflection and transmission characteristics of porous rubble-mound breakwaters*. Miscellaneous Report 76-5. Fort Belvoir, VA: U.S. Army Coastal Engineering Research Center.
- Mallet, C., H. Howa, T. Garlan, A. Sottolichio, P. Le Hir, and D. Michel. 2000. Utilization of numerical and statistical techniques to describe sedimentary circulation patterns in the mouth of the Gironde estuary. *Earth and Planetary Sciences* 331:1-7.
- Masselink, G. 1992. Longshore variation of grain size distribution along the coast of the Rhone Delta, Southern France: A test of the 'McLaren model'. *Journal of Coastal Research* 8(2):286-291.

- Mattie, M. 1982. *Empirical guidelines for use of irregular wave model to estimate nearshore wave height*. Technical Report No. 82-1. Fort Belvoir, VA: U.S. Army Coastal Engineering Research Center.
- McLaren, P., and D. Bowles. 1985. The Effects of sediment transport on grain-size distributions. *Journal of Sedimentary Petrology* 55(4):0457-0470.
- McLaren, P., and S. Hill. 2003. *A sediment trend analysis (STA<sup>®</sup>) at Aguadilla, Puerto Rico*. Brentwood Bay, British Columbia, CA (prepared for U.S. Army Engineer Research and Development Center, Vicksburg, MS).
- Mitchell, R. 1954. *A survey of the geology of Puerto Rico*. Paper No. 13. Mayaguez, Puerto Rico: Agricultural Experiment Station, University of Puerto Rico.
- National Ocean Service. 1984. *Tide Tables 1985; High and low water predictions*. Washington, DC: National Oceanic and Atmospheric Administration.
- Rios, F., R. Ulloa, and I. Cerrea. 2003. Determination of net sediment transport patterns in Lirquen Harbor, Chile through grain-size analysis: A test of methods. *Pesquisas em Geociencias* 30(1):65-81.
- Shi X., C. Chen, R. H. Liu, and H. Wang. 2002. Trend analysis of sediment grain size and sedimentary process in the central south Yellow Sea. *Chinese Science Bulletin* 47(14):1202-1207.
- Smith, R., J. Irish, and M. Smith. 2000. Airborne lidar and airborne hyperspectral imagery; a fusion of two proven sensors for improved hydrographic surveying. *Proceedings, Canadian Hydrographic Conference 2000*, Montreal, Canada.
- Tanahara, S., J. Candela, and M. Crepon. 2002. Study of the Yucatan Strait Current with a high resolution numerical model. *Proceedings, 2<sup>nd</sup> Meeting on the Physical Oceanography of Sea Straits, Villefranche*, 219-223.
- Teeter, A. 1993. Size dependence in fine-grained sediment transport. Dredging Research Technical Notes (DRP), 1(11):1-16. Vicksburg, MS: U.S. Army Engineer Waterways Experiment Station.
- Teeter, A., M. Saruff, T. Fagerburg, T. Waller, C. Callegan, and D. Brister. 2001. *Sediment depositional areas of inner Albemarle Sound, NC*. ERDC/CHL unpublished report. Vicksburg, MS: U.S. Army Engineer Research and Development Center. (Prepared for U.S. Environmental Protection Agency, Region 4).
- U.S. Army Corps of Engineers. 1977. *Shore Protection Manual*. Washington, DC: U.S. Army Corps of Engineers (in 3 volumes).
- \_\_\_\_\_. 1984. *Shore Protection Manual*. Washington, DC: U.S. Army Corps of Engineers (in 2 volumes).
- \_\_\_\_\_. 2002. *Coastal Engineering Manual*. Engineer Manual 1110-2-1100, Washington, DC: U.S. Army Corps of Engineers (in 6 volumes).
- U.S. Army Engineer District, Jacksonville. 1987. *Aguadilla Harbor, Aguadilla, Puerto Rico: Detailed project report and environmental assessment*. Jacksonville, FL: U.S. Army Engineer District, Jacksonville.

- U.S. Army Engineer District, Jacksonville. 1998. *Aguadilla Harbor, Aguadilla, Puerto Rico: Section 111 study; Detailed project report with final environmental assessment*. Jacksonville, FL: U.S. Army Engineer District, Jacksonville.
- Wozencraft, J., and D. Millar. 2005. Airborne lidar and integrated technologies for coastal mapping and nautical charting. *Journal of the Marine Technology Society* 39(3):27-35.
- Wozencraft, J., J. Lillycrop, and N. Kraus. 2002. *SHOALS toolbox; software to support visualization and analysis of large high-density data sets*. Coastal and Hydraulics Engineering Technical Notes ERDC/CHL CHETN-IV-43. Vicksburg, MS: U.S. Army Engineer Research and Development Center.
- Van de Kreeke, J., and K. Robaczewska. 1993. Tide-induced residual transport of coarse sediment; application to the Ems Estuary. *Netherlands Journal of Sea Research* 31(3):209-220.
- Van Der Wal, D. 2000. Grain-size-selective aeolian sand transport on a nourished beach. *Journal of Coastal Research* 16(3):896-908.

## Appendix A: Aerial Photographs, Vicinity of Aguadilla Harbor, Puerto Rico

This series of aerial photographs taken October 2001 defines the shoreline in the vicinity of Aguadilla Harbor, Puerto Rico, and shows a plume of fine sediment being delivered to the coast by the Rio Culebrinas River.

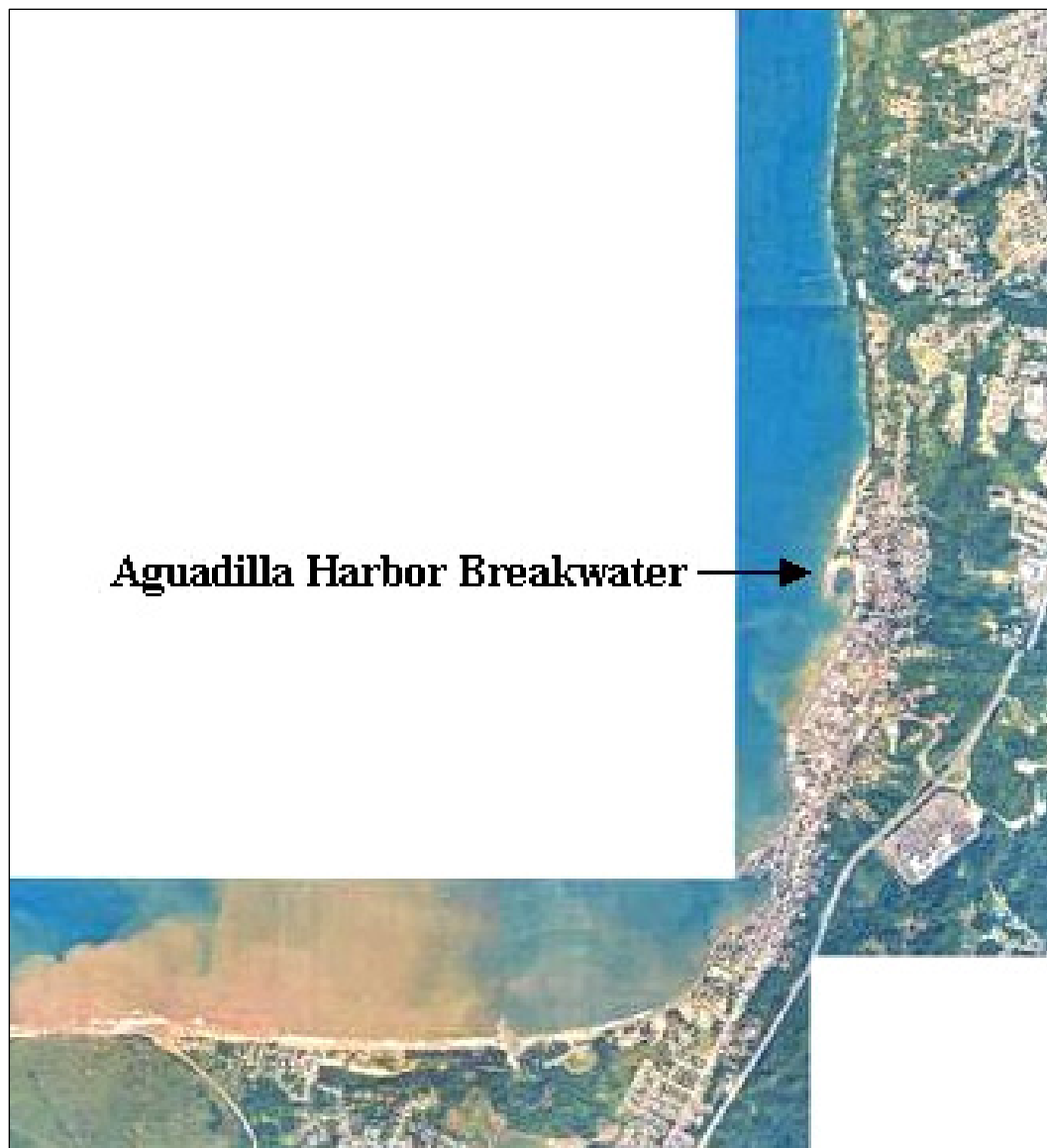


Figure A1. Mosaic of vicinity of Aguadilla Harbor, Puerto Rico (October 2001).



Figure A2. Coastline south of Aguadilla Harbor, Puerto Rico, showing plume of fine sediments exiting the Rio Culebrinas River after heavy rainfall (October 2001).



Figure A3. Coastline of Puerto Rico further north than Figure A2, between Rio Culebrinas River and Aguadilla Harbor, showing plume of fine sediments which had exited from the river after heavy rainfall (October 2001).



Figure A4. Coastline of Puerto Rico further north than Figure A3 between the Rio Culebrinas River and Aguadilla Harbor, showing how plume of fine sediments from the river are not being detected this far north towards the Harbor (October 2001).



Figure A5. Coastline of Puerto Rico further north than Figure A4, showing minimal amount of fine sediment discharging to the coast from small stream (October 2001).

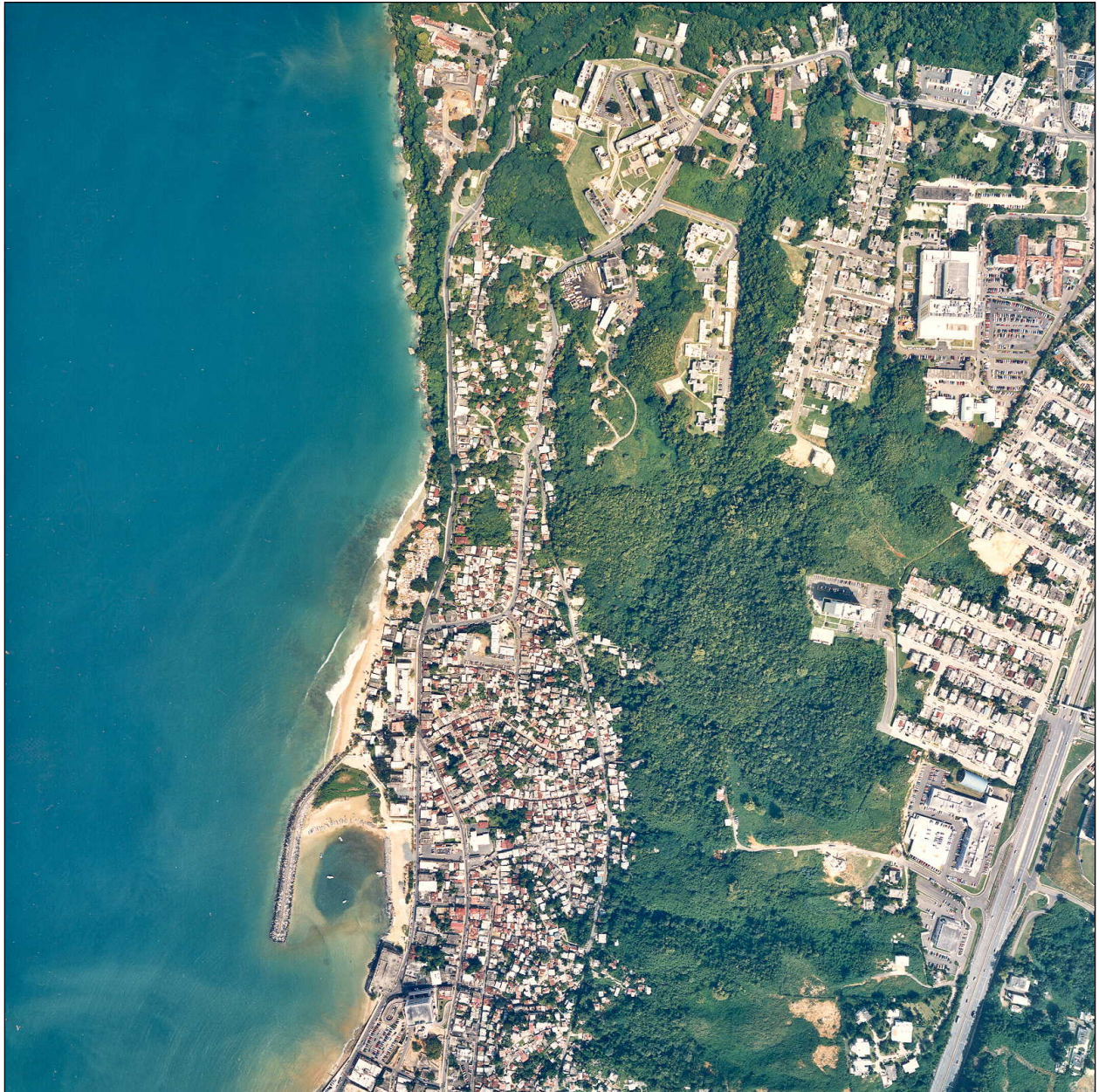


Figure A6. Aguadilla Harbor breakwater and vicinity, coastline of Puerto Rico further north than Figure A5 (October 2001).



Figure A7. Coastline of Puerto Rico further north than Figure A6 (October 2001).

## **Appendix B: Aguadilla Harbor and Beach Profile Surveys; Stations 10 through 20; Years 1997, 1998, 2001, and 2002**

To quantify the volume and rate at which sediment was entering Aguadilla Harbor, the U.S. Army Engineer District, Jacksonville, established survey lines (stations) perpendicular to the breakwater, and conducted repetitive surveys for years 1997, 1998, 2001, and 2002. These surveys extended from the beach line inside the harbor, through the harbor, across the breakwater, and into the open ocean. From these repetitive surveys, volume changes per unit distance along the coastline were ascertained for each station. The locations of the beach profile survey lines (stations) established by the Jacksonville District are shown in Figure 78, and are identified by station numbers. The volume changes (cubic yards/foot) for stations 10 through 20 are presented in Figures B1 through B11, respectively.

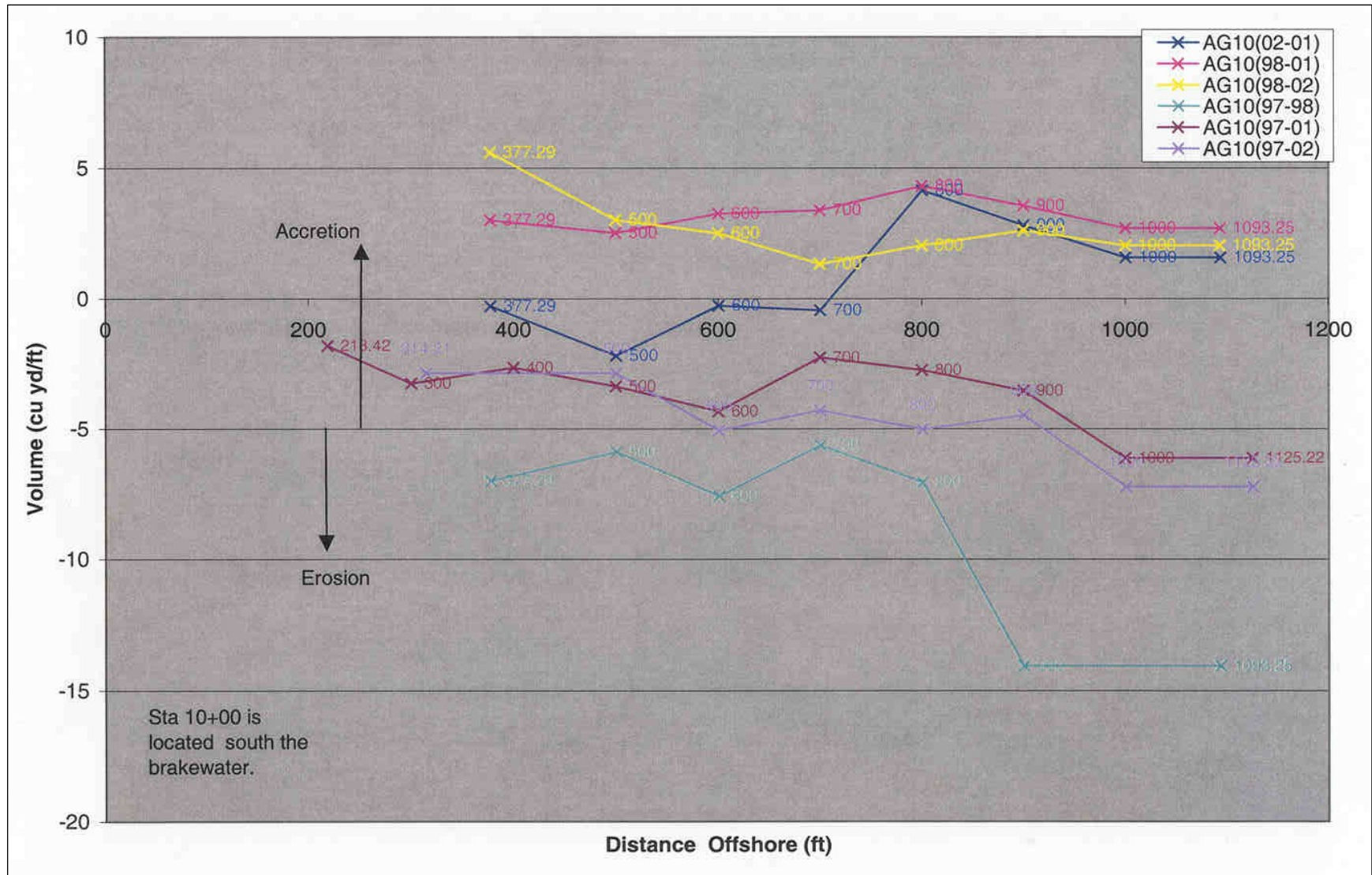


Figure B1. Volume change station 10 (cubic yards/foot), 1997 through 2002, distance offshore from shoreline inside the harbor.

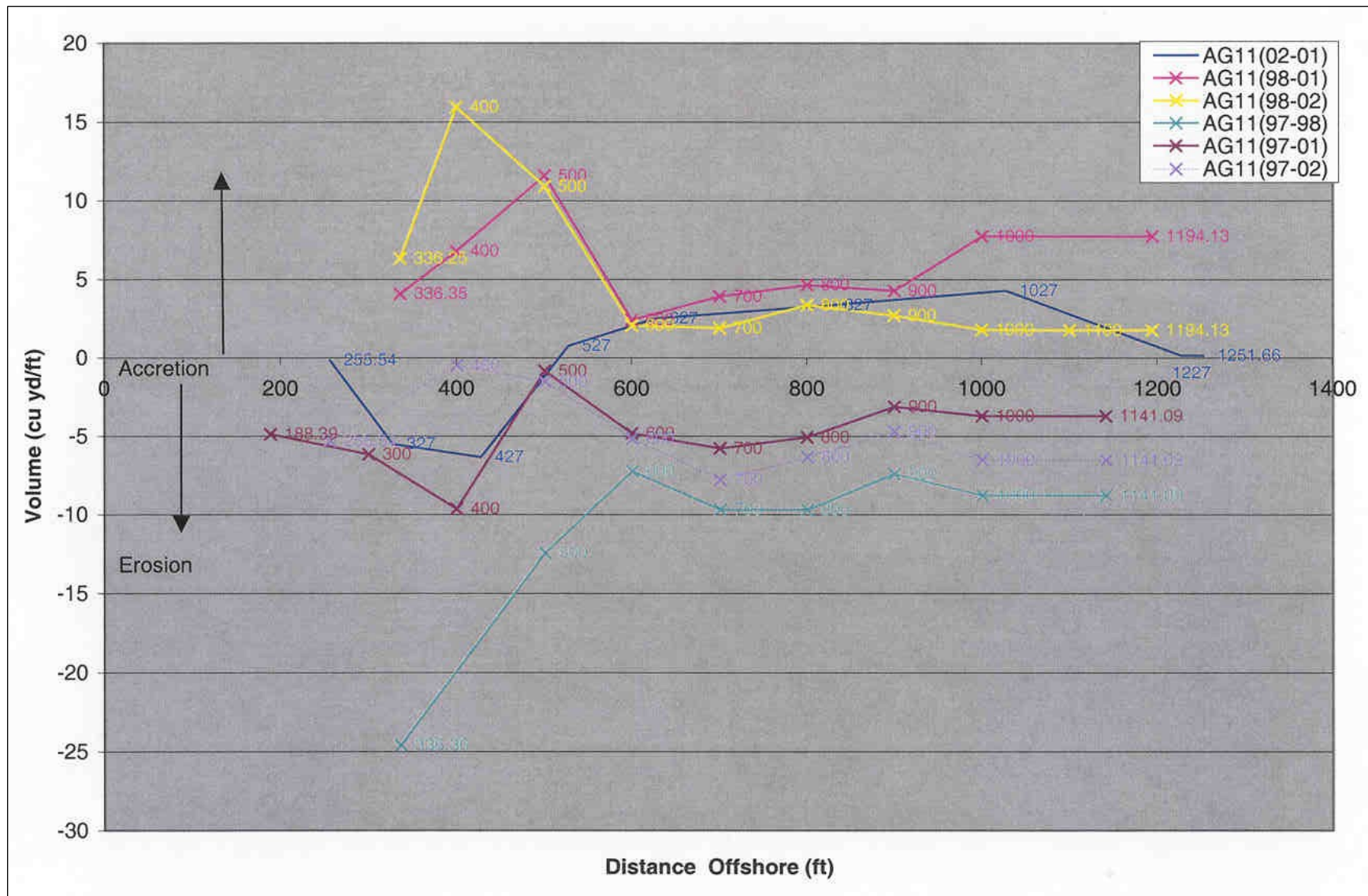


Figure B2. Volume change station 11 (cubic yards/foot), 1997 through 2002, distance offshore from shoreline inside the harbor.

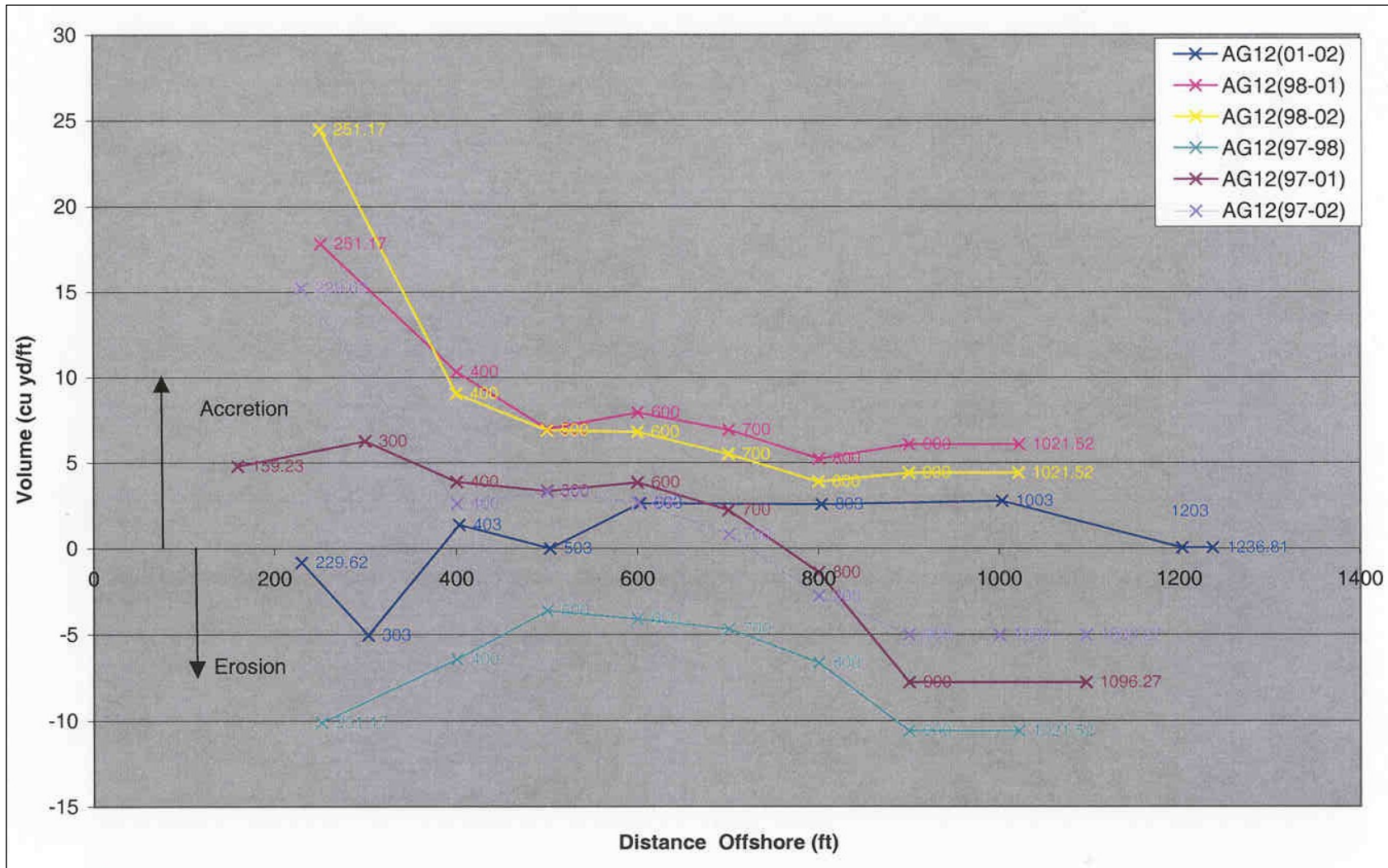


Figure B3. Volume change station 12 (cubic yards/foot), 1997 through 2002, distance offshore from shoreline inside the harbor.

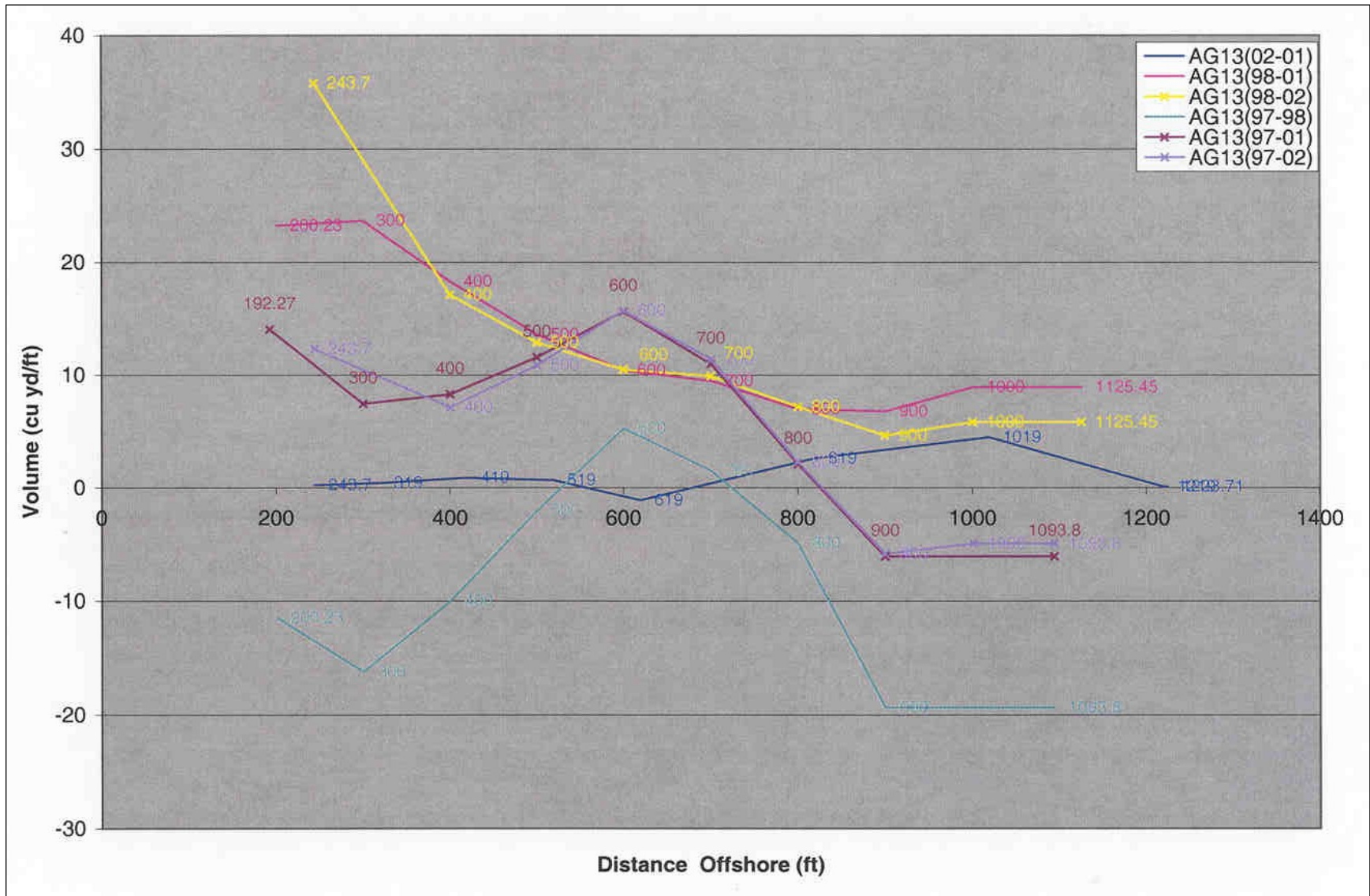


Figure B4. Volume change station 13 (cubic yards/foot), 1997 through 2002, distance offshore from shoreline inside the harbor.

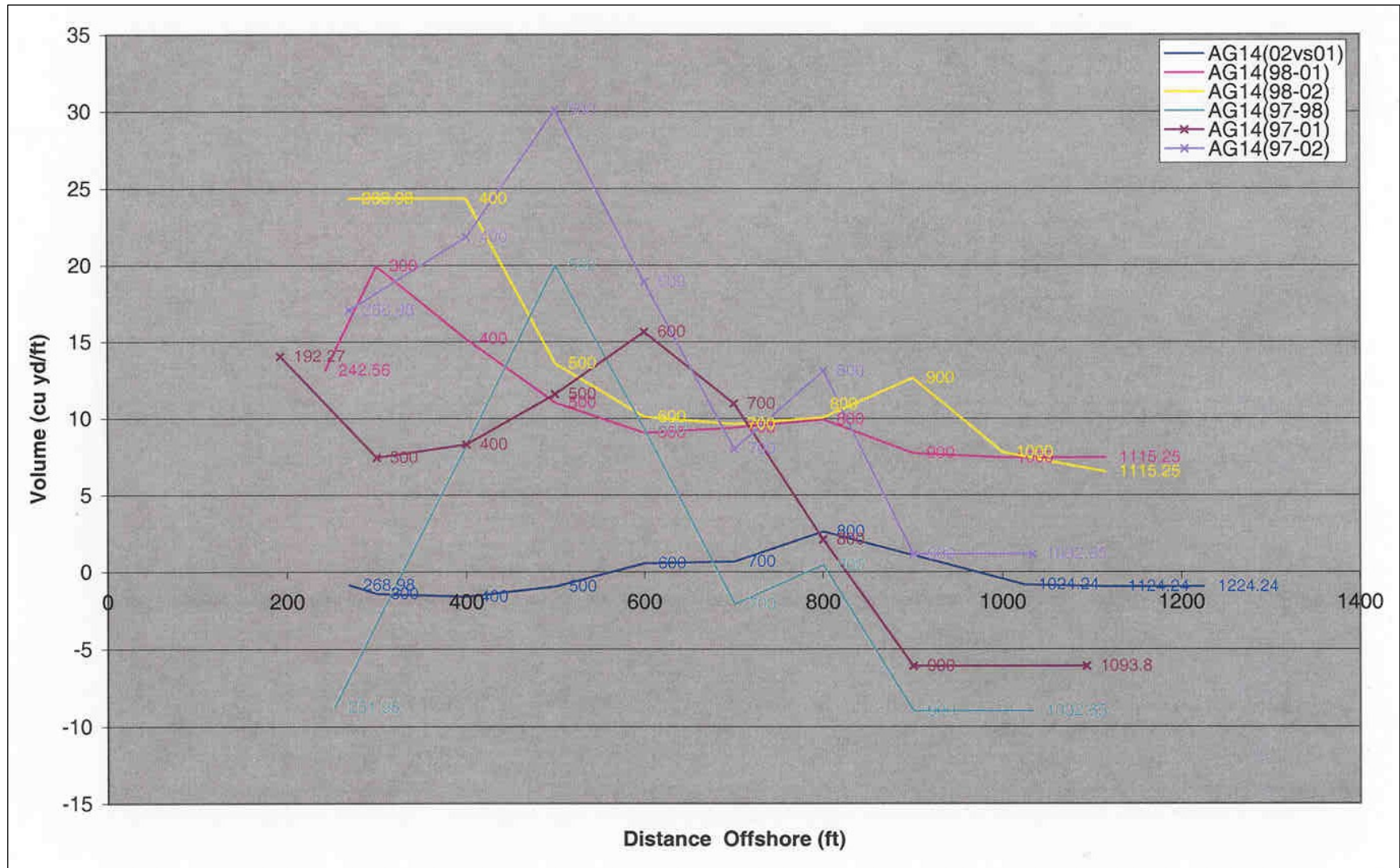


Figure B5. Volume change station 14 (cubic yards/foot), 1997 through 2002, distance offshore from shoreline inside the harbor.

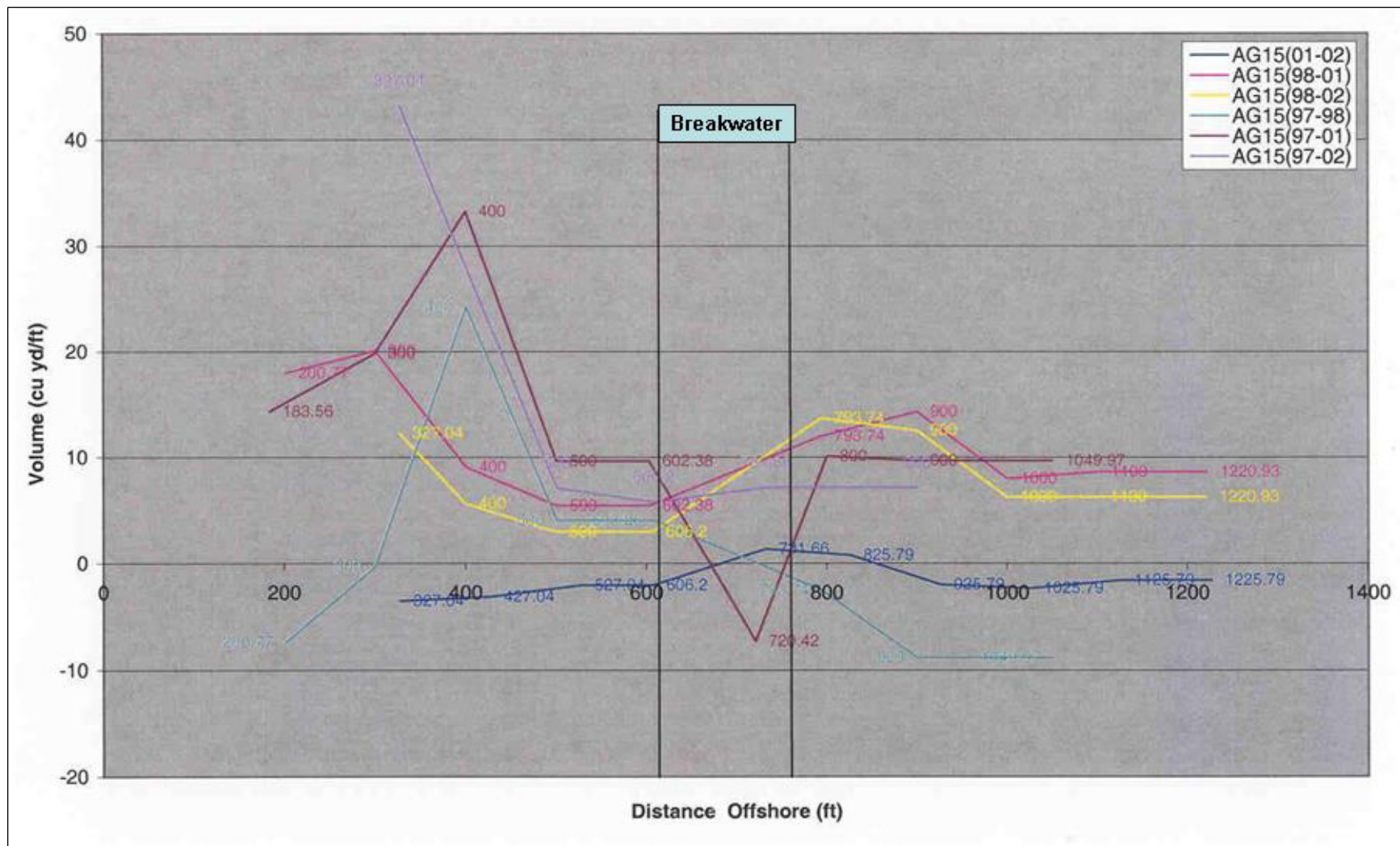


Figure B6. Volume change station 15 (cubic yards/foot), 1997 through 2002, distance offshore from shoreline inside the harbor.

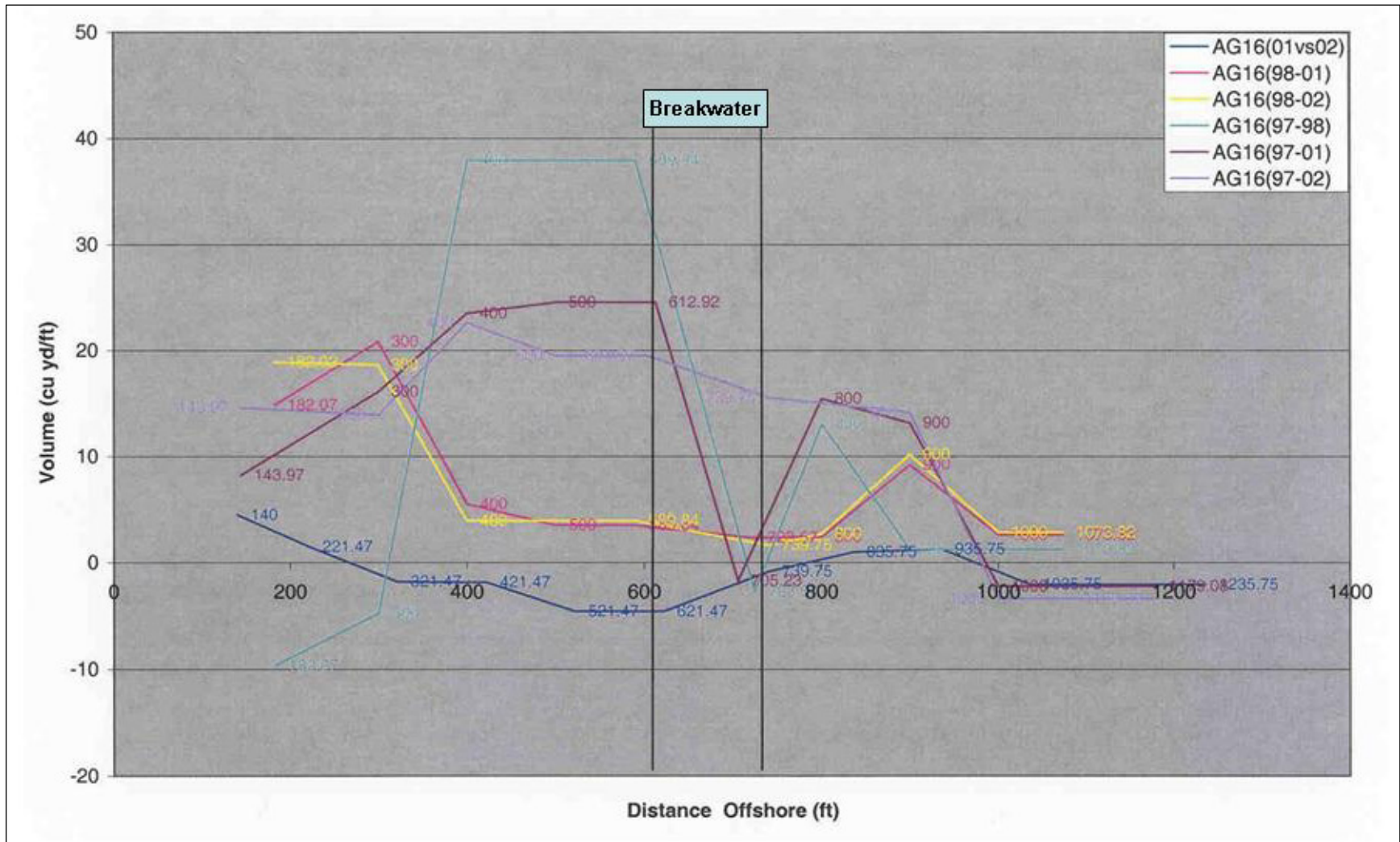


Figure B7. Volume change station 16 (cubic yards/foot), 1997 through 2002, distance offshore from shoreline inside the harbor.

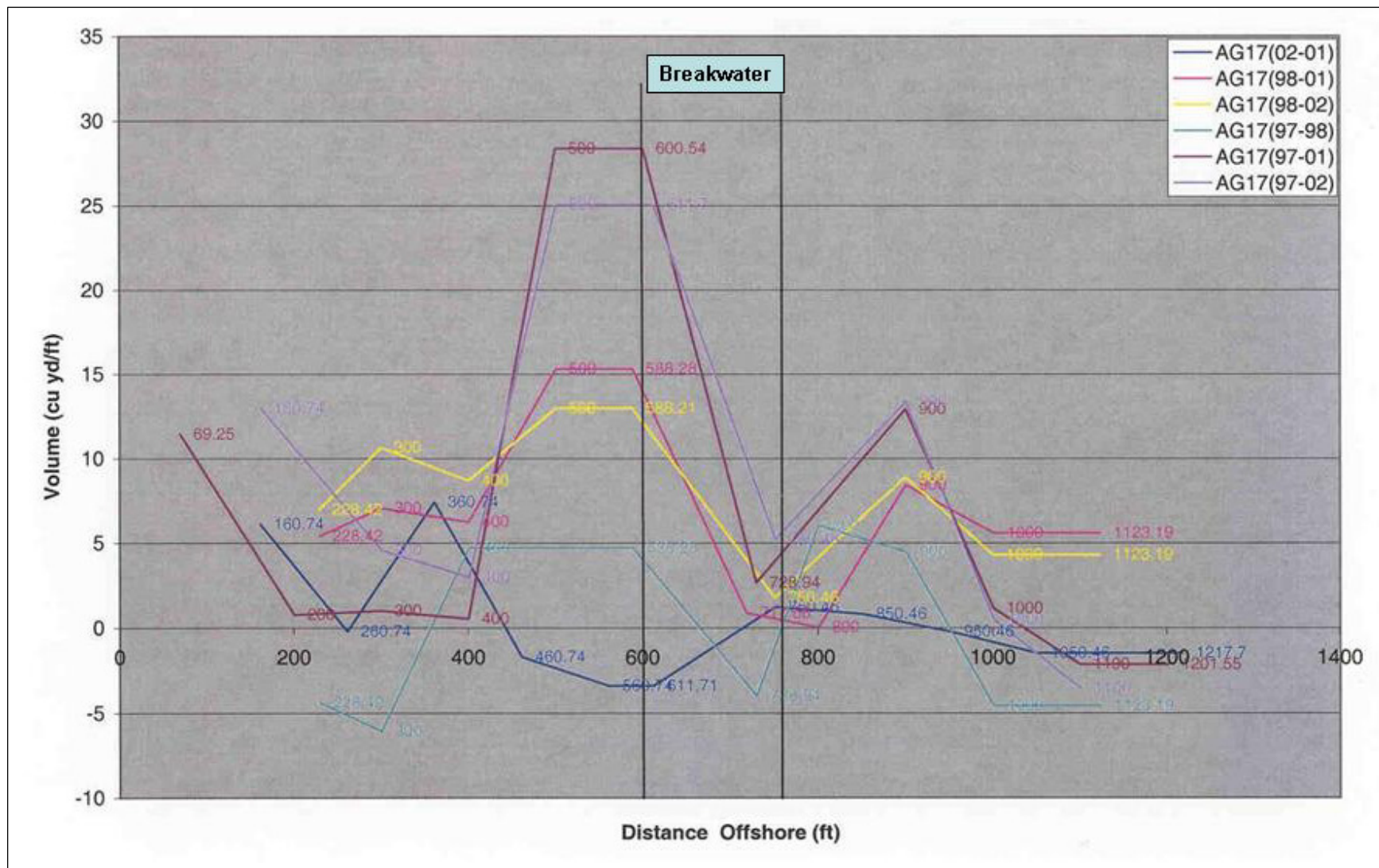


Figure B8. Volume change station 17 (cubic yards/foot), 1997 through 2002, distance offshore from shoreline inside the harbor.

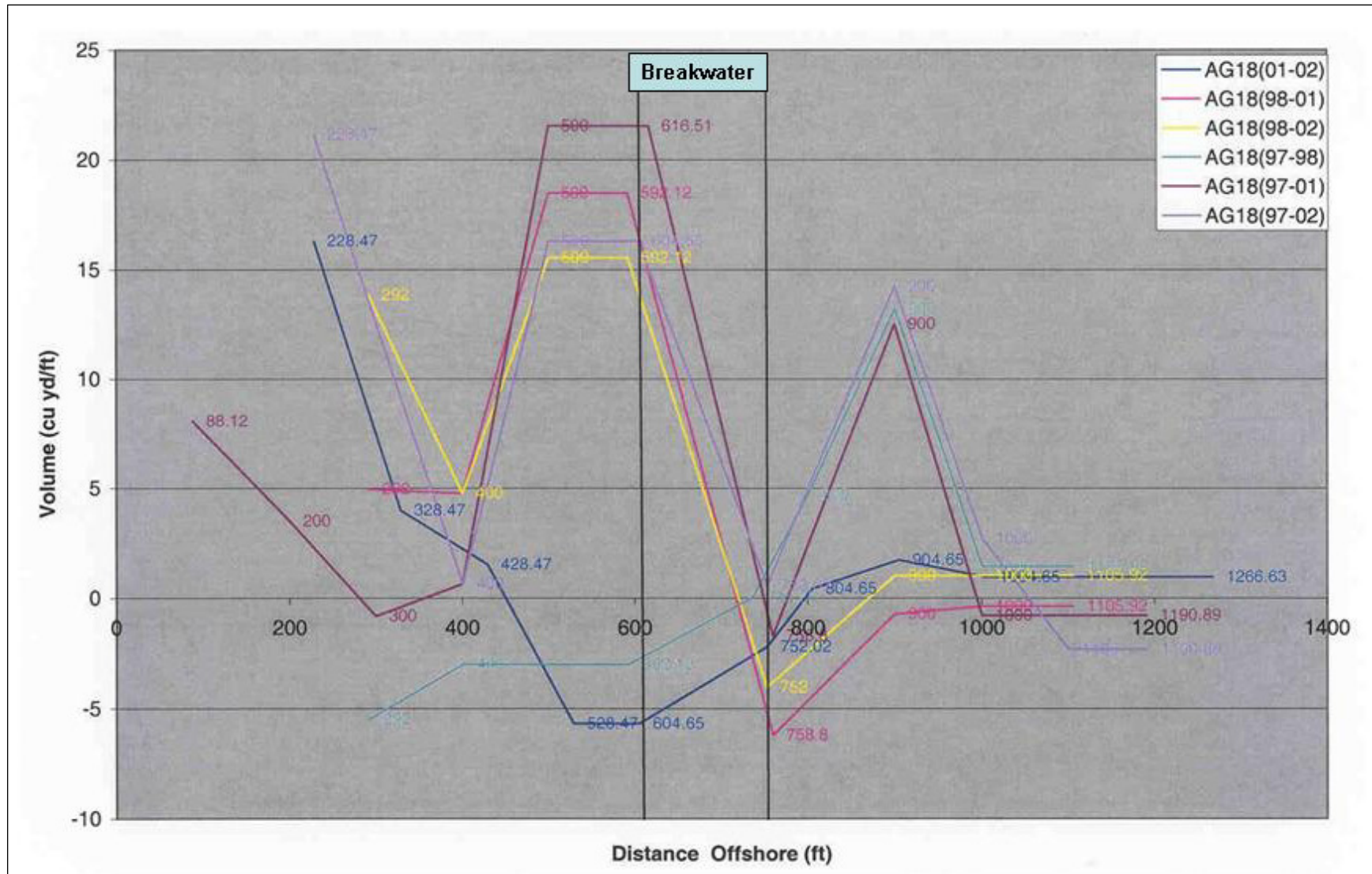


Figure B9. Volume change station 18 (cubic yards/foot), 1997 through 2002, distance offshore from shoreline inside the harbor.

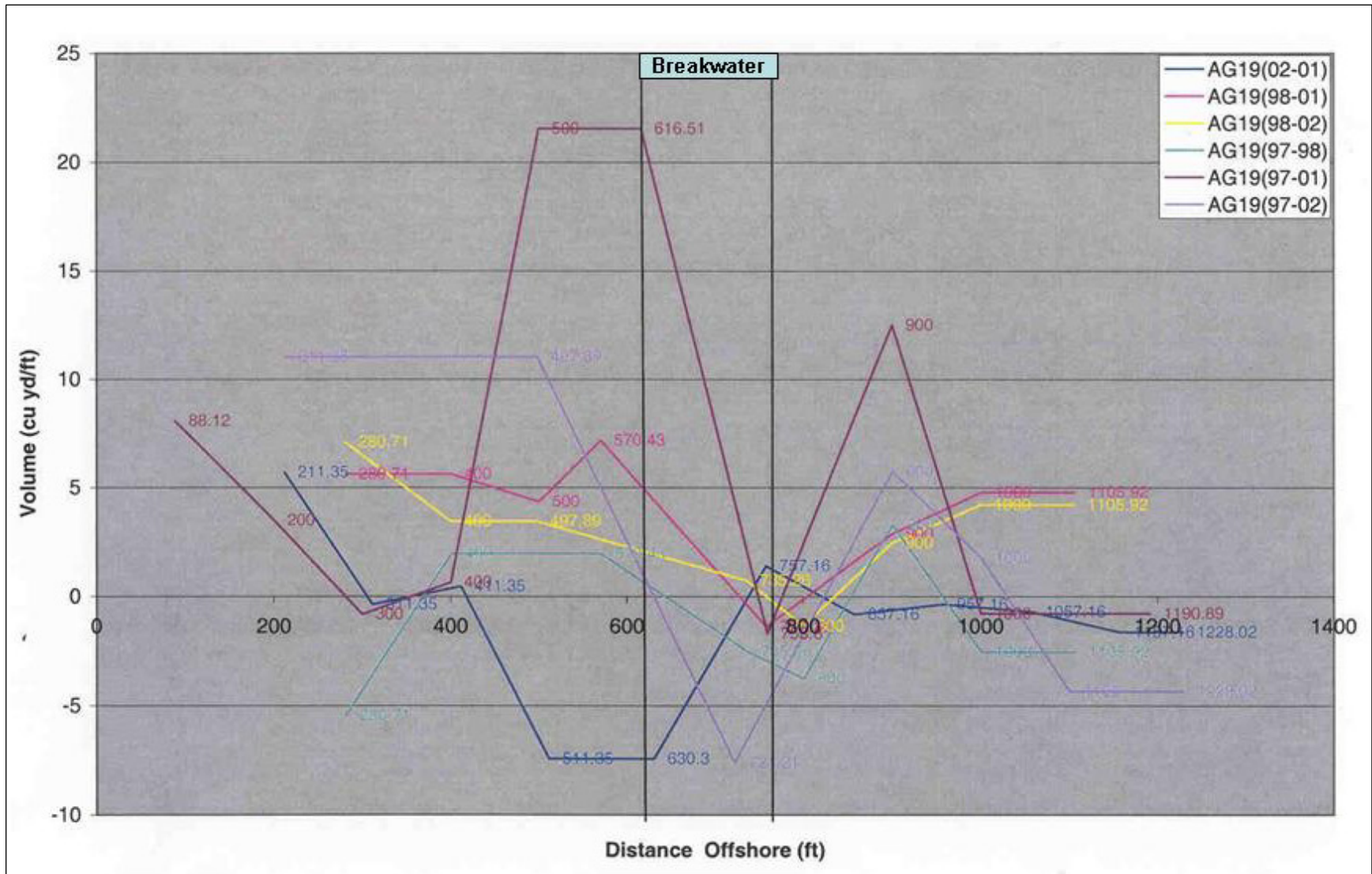


Figure B10. Volume change station 19 (cubic yards/foot), 1997 through 2002, distance offshore from shoreline inside the harbor.

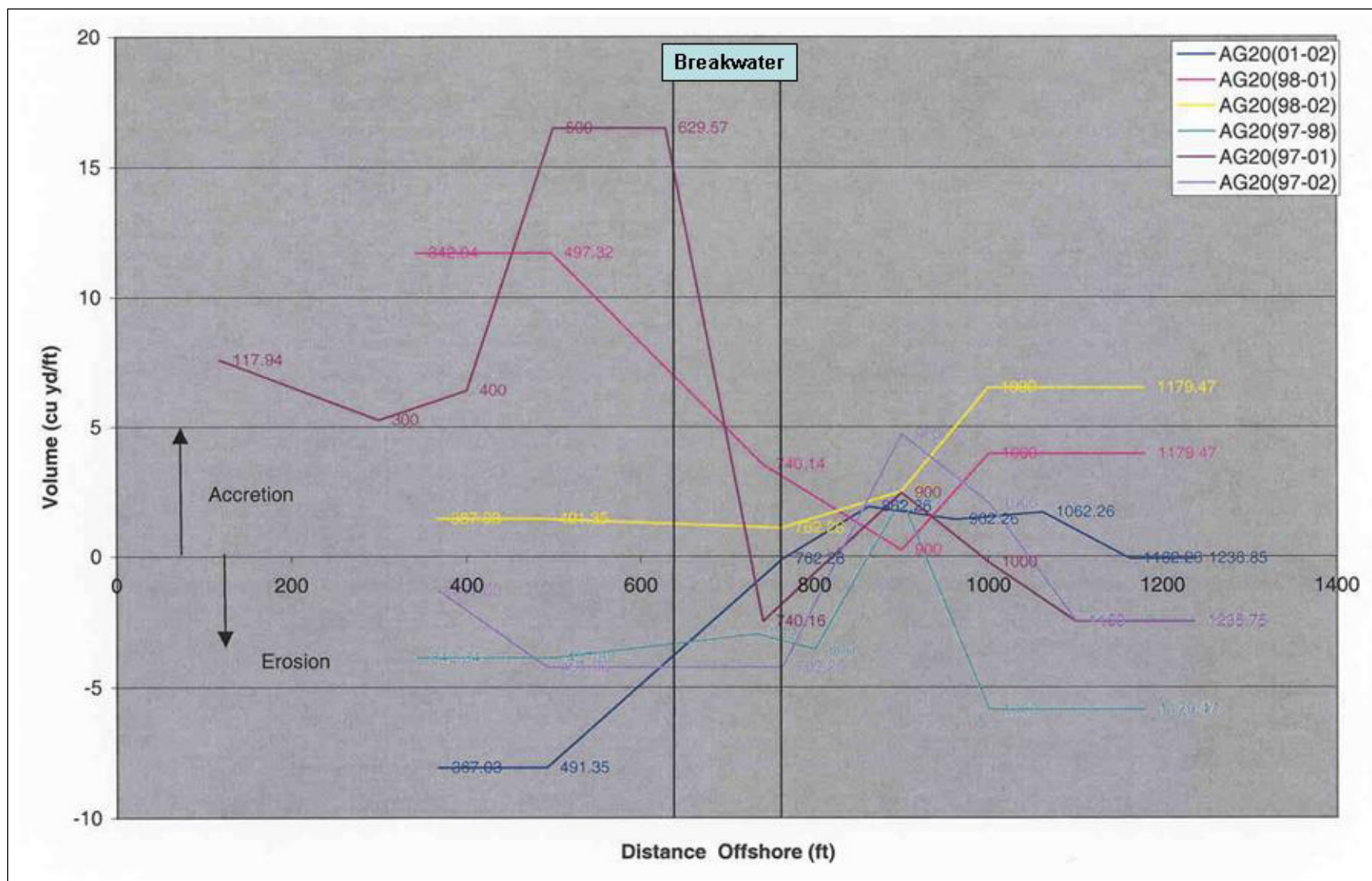


Figure B11. Volume change station 20 (cubic yards/foot), 1997 through 2002, distance offshore from shoreline inside the harbor.

<b>REPORT DOCUMENTATION PAGE</b>				<i>Form Approved</i> <i>OMB No. 0704-0188</i>	
Public reporting burden for this collection of information is estimated to average 1 hour per response, including the time for reviewing instructions, searching existing data sources, gathering and maintaining the data needed, and completing and reviewing this collection of information. Send comments regarding this burden estimate or any other aspect of this collection of information, including suggestions for reducing this burden to Department of Defense, Washington Headquarters Services, Directorate for Information Operations and Reports (0704-0188), 1215 Jefferson Davis Highway, Suite 1204, Arlington, VA 22202-4302. Respondents should be aware that notwithstanding any other provision of law, no person shall be subject to any penalty for failing to comply with a collection of information if it does not display a currently valid OMB control number. <b>PLEASE DO NOT RETURN YOUR FORM TO THE ABOVE ADDRESS.</b>					
<b>1. REPORT DATE (DD-MM-YYYY)</b> June 2007		<b>2. REPORT TYPE</b> Final report		<b>3. DATES COVERED (From - To)</b>	
<b>4. TITLE AND SUBTITLE</b>  Shoaling of Aguadilla Harbor, Puerto Rico				<b>5a. CONTRACT NUMBER</b>	
				<b>5b. GRANT NUMBER</b>	
				<b>5c. PROGRAM ELEMENT NUMBER</b>	
<b>6. AUTHOR(S)</b>  Steven A. Hughes and Lyndell Z. Hales				<b>5d. PROJECT NUMBER</b>	
				<b>5e. TASK NUMBER</b>	
				<b>5f. WORK UNIT NUMBER</b> 11M19	
<b>7. PERFORMING ORGANIZATION NAME(S) AND ADDRESS(ES)</b>  U.S. Army Engineer Research and Development Center Coastal and Hydraulics Laboratory 3909 Halls Ferry Road, Vicksburg, MS 39180-6199; U.S. Army Engineer District, Jacksonville 701 San Marco Blvd., Jacksonville, FL 32207-8175				<b>8. PERFORMING ORGANIZATION REPORT NUMBER</b>  ERDC/CHL TR-07-2	
<b>9. SPONSORING / MONITORING AGENCY NAME(S) AND ADDRESS(ES)</b>  U.S. Army Corps of Engineers Washington, DC 20314-1000				<b>10. SPONSOR/MONITOR'S ACRONYM(S)</b>	
				<b>11. SPONSOR/MONITOR'S REPORT NUMBER(S)</b>	
<b>12. DISTRIBUTION / AVAILABILITY STATEMENT</b>  Approved for public release; distribution is unlimited.					
<b>13. SUPPLEMENTARY NOTES</b>					
<b>14. ABSTRACT</b> <p>During construction of the Aguadilla Harbor, Puerto Rico, breakwater (June 1993 through July 1995), shoaling of the harbor was observed, and excessive wave heights in the harbor caused by refraction/diffraction were much larger than expected. Following construction, additional shoaling occurred even with only limited wave activity, and significantly excessive harbor shoaling occurred. The source of the harbor-shoaling sand was not known with certainty. The quantity of sediment deposited in the harbor was surprising given the relatively minor amount of sand thought to be available within the littoral system.</p> <p>The following five aspects of the Aguadilla Harbor project were proposed for monitoring under the Monitoring Completed Navigation Projects (MCNP) Program: (a) breakwater armor stability; (b) harbor wave action; (c) physical mechanisms causing harbor shoaling; (d) rates and quantity of harbor sedimentation; and (e) sources of sand causing the harbor shoaling.</p> <p>A detailed breakwater stone elevation survey by standard topographic surveying techniques was performed. It was observed that a few armor stones had experienced a minimal degree of shakedown settlement during these early years following construction, but no major areas of excessive deterioration were found to exist. Tropical storms (hurricanes) approach from the eastern side of the island, and thus do not directly strike the harbor with full-force wave conditions since the harbor is on the western (leeward) protected side of Puerto Rico.</p> <p style="text-align: right;">(Continued)</p>					
<b>15. SUBJECT TERMS</b>		Breakwater Harbor shoaling Longshore sediment transport		Wave climate Sand layers Sedimentation	
Aguadilla Harbor, Puerto Rico				Sediment Trend Analysis SHOALS	
Beach profiles					
<b>16. SECURITY CLASSIFICATION OF:</b>			<b>17. LIMITATION OF ABSTRACT</b>	<b>18. NUMBER OF PAGES</b>	<b>19a. NAME OF RESPONSIBLE PERSON</b>
<b>a. REPORT</b>  UNCLASSIFIED	<b>b. ABSTRACT</b>  UNCLASSIFIED	<b>c. THIS PAGE</b>  UNCLASSIFIED			<b>19b. TELEPHONE NUMBER</b> (include area code)

#### 14. (Continued)

Surface currents were estimated using dyes and drogues. Apparently, the wave-generated alongshore current has a nodal point to the south of the breakwater. With this decrease in southerly flow, it is hard to conclude that any littoral sand is moving to the beach region south of the harbor project. In other words, sand in the littoral system is not bypassing the harbor.

A contour map of the bottom bathymetry of the region of interest was developed by the Scanning Hydrographic Operational Airborne Lidar Survey (SHOALS) system. A geophysical investigation with side-scan sonar was performed and overlain on the SHOALS contour map that indicated locations of rock/coral and layers of sand. The thickness of the sand layers was then determined by subbottom profiling and seismic reflection, and these data were also overlain on the SHOALS contour map. Hence, areas and thickness of sand layers offshore from Aguadilla Harbor that appears to be sources of sand entering the harbor have been mapped. The predominant waves that arrive from offshore have adequate wave power for such harbor shoaling.

A Sediment Trend Analysis (STA) was performed which concluded that sand transported from the offshore region appeared to be the source of sand shoaling Aguadilla Harbor. Southward directed longshore transport was quite small and was not likely to be a main contributor to harbor shoaling. The southward facing Aguadilla marina appeared to be in a position to act as a sediment trap, blocking the counterclockwise oceanic gyre at the shoreline, and precluding the possibility of a sediment return to the offshore during storm activity.

Harbor and beach profile surveys were conducted in 1997, 1998, 2001, and 2002 for the purpose of quantifying the volume of material that was being transported into the harbor, to provide an indication of the repetitiveness with which the harbor might need to be dredged to maintain navigability.